UNIVERSITE DE LAUSANNE
FACULTE DES SCIENCES

Institut de Géologie et Paléontologie

Geology, correlations, and geodynamic evolution of the Biga Peninsula (NW Turkey)

Thèse de doctorat

présentée à la

Faculté des Sciences de
l'Université de Lausanne

par

Laurent Beccaletto

Diplômé en Géologie
Université de Montpellier (France)

Jury

Prof. Gervais Chapuis, Président
Prof. Gérard M. Stampfli, Directeur de thèse
Prof. Aral I. Okay, Expert
Prof. Laurent Jolivet, Expert
Dr. Olivier Monod, Expert
Prof. Jean Hernandez, Expert

UNIVERSITE DE LAUSANNE

Faculté des sciences

Imprimatur

Vu le rapport présenté par le jury d'examen, composé de

Président	Monsieur Prof.	Gervais **Chapuis**
Directeur de thèse	Monsieur Prof.	Gérard **Stampfli**
Rapporteur		
Experts	Monsieur Prof.	Jean **Hernandez**
	Monsieur Prof.	Laurent **Jolivet**
	Monsieur Prof.	Aral I. **Okay**
	Monsieur Dr	Olivier **Monod**

le Conseil de Faculté autorise l'impression de la thèse de

Monsieur Laurent Beccaletto

Géologue diplômé de l'Université de Montpellier, France

intitulée

Geology, correlations, and geodynamic evolution of the Biga Peninsula (NW Turkey)

Lausanne, le 14 juillet 2003

pour Le Doyen de la Faculté des Sciences

Prof. Gervais Chapuis

A Marie et Auriane

A ma mère

TABLE OF CONTENTS

- CHAPTER 4 -

- CHAPTER 5 -

- REMERCIEMENTS (AKNOWLEDGEMENTS) -

Je tiens tout d'abord à remercier chaleureusement mon directeur de thèse le professeur Gérard Stampfli, de l'Institut de Géologie et de Paléontologie de l'Université de Lausanne. Je lui sais gré de m'avoir permis de continuer dans la voie de la recherche en géologie, en me faisant confiance pour mener à bien ce travail de thèse. J'ai tout autant apprécié son approche globale (i.e. geodynamique) des problèmes géologiques, que profité de ses vastes connaissances de la géologie téthysienne.

J'exprime toute ma gratitude envers le Professeur Aral. I. Okay de l'Université Technique d'Istanbul, qui a été mon contact en Turquie lors de mes missions de terrain successives; je le remercie pour son aide et sa disponibilité, ainsi que pour la mise à disposition de son matériel géologique. Il est de plus le découvreur du mélange de Çetmi, sujet central de cette thèse; son travail de pionnier sur la géologie de la Péninsule de Biga a servi de base à l'ensemble de mon travail de recherche.

Je remercie le Professeur Laurent Jolivet de l'Université Paris VI d'avoir accepté de juger ce travail, ainsi que d'avoir pu me recevoir lors de mes trop rares visites à Paris VI. C'est en partie à la suite d'une de ses missions en Grèce, à laquelle j'ai pu me joindre, que j'ai décidé de développer le chapitre sur l'extension Tertiaire.

Je remercie le Docteur Olivier Monod, chargé de recherche au C.N.R.S. à l'Université d'Orléans, et grand spécialiste de la géologie turque, d'avoir accepté de faire partie de ce jury de thèse.

Je sais gré au Professeur Jean Hernandez de l'Institut de Minéralogie et de Géochimie de l'Université de Lausanne d'avoir accepté de juger ce travail; son expérience pétrographique et géochimique dont j'ai pu largement bénéficier m'a été fort utile.

Les travaux micro-paléontologiques ont été réalisés par le Docteur A-C Bartolini (Université Paris VI, radiolaires), le Professeur L. Zaninetti et le Docteur R. Martini (Université de Genève, foraminifères du Trias), le Docteur H. Kozur (Budapest, conodontes du Trias), le Docteur C. Jenny (Université de Lausanne, foraminifères du Permien), le professeur M. Caron (Université de Fribourg, foraminifères du Crétacé), le Docteur P. Hochuli (ETH Zürich, palynologie). Je remercie vivement toutes ces personnes pour leur indispensable travail de détermination.

Le séjour au laboratoire du Docteur Nicolai Bonev, de l'Université de Sofia, a été déterminant quant aux corrélations de la Péninsule de Biga avec le Massif du Rhodope; je le remercie vivement pour son aide.

Jean-Claude Lavanchy et Laurent Nicod ont effectué respectivement l'ensemble de mes analyses géochimiques et l'ensemble de mes lames minces; Philippe Thélin et Liliane Dufresne ont déterminé par RX l'illite; à tous les quatre j'adresse mes remerciements sincères.

Ces quelques années passées à l'Université de Lausanne auraient été plus ternes sans les

membres de l'équipe de géologie téthysienne; j'adresse en particulier toutes mes amitiés à Christian Steiner, Gilles Borel, Laurent Langhi et François Rosselet.

Je remercie également Anna-Chiara Bartolini, Sébastien Bruchez, Philippe Montjoie, Micha Schlup, Piercarlo Gabriele, Andreas Mulch, Jean-Claude Vannay et Sébastien Pilet de m'avoir donné apporté une aide appréciable à l'occasion.

Un salut amical à Elisabeth Carrupt, Benita Putlitz, David Giorgis, Olivier Ferrari, ainsi qu'à l'ensemble des assistants de la section des Sciences de la Terre.

Je remercie mes amis Tarık O. Eke et Burak Yıkılmaz de m'avoir fait découvrir ce pays magnifique qu'est la Turquie et ses habitants simples et chaleureux (çok teşekkür ederim !). Merci à Tarık, ainsi qu'à Hüseyin Ekiz, de m'avoir assisté sur le terrain.

J'ai profité occasionnellement des conseils avisés des professeurs F. Boudier (Montpellier), G. Gorin (Genève), J-M. Jaquet (Genève), A. Poisson (Paris), ainsi que de N. Lyberis (Paris); merci à eux.

Ce travail de recherche a été financé par le Fond National de la Recherche Scientifique Suisse (fond n° 2049114-96 et n° 2061885-00).

Je remercie très chaleureusement les professeurs Jean-Paul Cadet (Université de Paris VI) et Jean-Jacques Lagasquie (Université de Pau) d'avoir été présents aux bons moments ! Merci à eux d'avoir accepté de m'accompagner sur le terrain, et pour les intéressantes discussions que nous avons eues. Remerciement spécial à JJL pour les conseils à la rédaction en fin de thèse...

- ABSTRACT -

The purpose of this study is to unravel the geodynamic evolution of the Biga Peninsula (NW Turkey) through the detailed study of two poorly known areas, the Çetmi mélange and the Ezine zone (i.e. the Ezine Group and the Denizgören ophiolite). The methodology was based on a detailed field work and a multidisciplinary approach.

• The accretion-related **Çetmi mélange** is mainly cropping out north and south of the Biga Peninsula; the main results of its study can be summarized as follows:
-Its present-day structural aspect (type of contacts, tectonic organisation) is largely inherited from the Tertiary extensional regime in the region.
-It is made of blocks of various natures: Han Bulog limestones with a Scythian to Ladinian age, common carbonate ramp Norian-Rhaetian limestones (biggest blocks of the mélange), red radolarite with a Bajocian to Aptian age; the most common lithology of the mélange is made by block/slices of spilitic magmatic rocks (basalt to andesite); they have volcanic arc or within plate basalt geochemical signatures.
-The matrix of the mélange is made of a greywacke-shale association of Early-Middle Albian age.
- The mélange stopped its activity before the Cenomanian (no younger blocks than the matrix, and Cenomanian unconformity).
- If compared to the regional geology, the Çetmi mélange shares some characteristics with the Izmir-Ankara mélanges (less), and with the mélanges from allochthonous nappes found in eastern Rhodope (more); it appears finally that its emplacement is related to a Balkanic logic (ante-Cenomanian northward thrusting).

• The **Ezine Group** and the overlying **Denizgören ophiolite** are cropping out in the western part of the Biga Peninsula. The Ezine Group is a thick sedimentary sequence interpreted as a syn-rift deposit of Middle Permian-Early Triassic age. It represents a part of the south Rhodopian passive margin, following the opening of the Maliac/Meliata oceanic domain.
The Denizgören ophiolite has been emplaced northward on the Ezine Group in the Barremian (125 Ma, age of the amphibolitic sole); this age is unique in the Aegean domain, but here again, it may be related to a Balkan logic.

• All the previous units (Çetmi mélange, Ezine Group and Denizgören ophiolite) have passively suffered two extensional regimes during the Tertiary. In the Ezine and northern Çetmi mélange area, the underlying HP Çamlıca micaschists were exhumed before the Middle Eocene. As for the southern mélange, it was strongly eroded following the Late Oligocene to Quaternary uplift of the underlying Kazdağ Massif. This uplift was characterized by the development of a low-angle detachment fault controlling a part of the exhumation, as well as the development of a supra-detachment basin.

• Based on the previous results, and on the data from the regional geology, one can propose a scenario for the geodynamic evolution of the Biga Peninsula. Its key points are:
- The Biga Peninsula is belonging to the Rhodope margin.
- The Ezine Group is a remnant of the northern Maliac/Meliata passive margin.

- Both the Denizgören ophiolite and the Çetmi mélange have been emplaced northward on the previous margin, respectively in the Barremian and in the Late Albian-Early Cenomanian times.
- The preservation of the remnants of the Rhodope margin, as well as the absence of metamorphism in the lower plate suggest a strong strike-slip component during the emplacements.
- All the previous events are (at least) partly obliterated by the Tertiary extensional regime.

- RÉSUMÉ -

L'objectif de ce travail de recherche était de décrypter l'évolution géodynamique de la Péninsule de Biga (Turquie du N-O), à travers l'analyse de deux régions géologiques peu connues, le mélange de Çetmi et la zone d'Ezine (i.e. le Groupe d'Ezine et l'ophiolite de Denizgören). Une étude complète et détaillée de terrain (cartographie et échantillonnage) ainsi qu'une approche multidisciplinaire (sédimentologie de faciès, pétrographie sédimentaire et magmatique, micropaléontologie, datations absolues, géochimie sur roche totale, cristallinité de l'illite) ont permis d'obtenir de nouveaux éléments d'information sur la région considérée.

• Le mélange de Çetmi, de type mélange d'accrétion, affleure au nord et au sud de la Péninsule de Biga ; les principaux résultats de son étude peuvent se résumer comme suit:

- Son aspect structural actuel (nature des contacts, organisation tectonique) est principalement dû au régime extensif Tertiaire présent dans la région.
- Il est constitué de blocs de différentes natures : rares calcaires Scythien-Ladinien dans le faciès Han Bulog, blocs hectométriques de calcaires d'âge Norien-Rhaetien de rampe carbonatée, nombreux blocs décamétriques de radiolarites rouges d'âge Bajocien-Aptien, blocs/écailles de roches magmatiques de type spilites (basaltes à andésite), ayant des signatures géochimiques d'arcs ou intra-plaques.
- La matrice du mélange est constituée d'une association greywacke-argilites dont l'âge Albien inférieur à moyen a été déterminé par palynologie.
- L'activité du mélange s'est terminée avant le Cénomanien (discordance Cénomanienne au sommet du mélange, pas de bloc plus jeune que la matrice).
- Du point de vue de ses corrélations latérales, le mélange de Çetmi partage plus de traits communs avec les mélanges se trouvant dans les nappes allochtones du Rhodope (nord de la Grèce et sud-ouest de la Bulgarie) qu'avec ceux de la suture Izmir-Ankara (Turquie); il apparaît finalement que sa mise en place s'est faite dans une logique balkanique (chevauchements vers le nord d'âge anté-Cénomanien).

• Le Groupe d'Ezine et l'ophiolite sus-jacente de Denizgören affleurent dans la partie ouest de la Péninsule de Biga. Le Groupe d'Ezine est une épaisse séquence sédimentaire continue (3000 m), subdivisée en trois formations, caractérisée chacune par un type de sédimentation spécifique, relatif à un environnement de dépôt particulier. De par ses caractéristiques (grande épaisseur, variations latérales de faciès et d'épaisseur dans les formations, érosion de matériel provenant de l'amont du bassin), le groupe d'Ezine est interprétée comme un dépôt syn-rift d'âge Permien moyen-Trias inférieur. Il pourrait représenter une partie de la future marge passive sud Rhodopienne à la suite de l'ouverture de l'océan Maliac/Méliata.

L'ophiolite de Denizgören sus-jacente repose sur le Groupe d'Ezine par l'intermédiaire d'une semelle métamorphique à gradient inverse, du faciès amphibolite à schiste vert. L'âge du faciès amphibolite suggère une initiation de l'obduction au Barrémien (125 Ma, âge Ar/Ar); cet âge est unique dans le domaine égéen, mais il peut là aussi être relié à une logique balkanique, sur la base de comparaison avec le domaine Rhodopien.

• Toutes les unités précédentes (mélange de Çetmi, Groupe d'Ezine et ophiolite de

Denizgören) ont passivement subi trois phases extensives pendant le Tertiaire. Dans la région d'Ezine et du mélange nord, les micaschistes HP sous-jacents ont été exhumés avant l'Eocène moyen. Dans le cas du mélange sud, cette exhumation Eocene est en partie enregistrée dans les mylonites séparant le mélange du dôme métamorphique sous-jacent du Kazdağ.

Le mélange sud est dans tous les cas fortement érodé à la suite de la double surrection du dôme du Kazdağ, près de la lim ite Oligocène/Miocene et pendant le Plio-Quaternaire. Dans le premier cas, ce soulèvement est caractérisé par le développement d'une faille de détachement à faible pendage, qui contrôle à la fois l'exhumation du massif, et la formation d'un bassin sédimentaire syntectonique, de type bassin supra-détachement; quant à la phase extensive la plus récente, elle est contrôlée par le jeu de failles normales à forts pendages qui remanient l'ensemble des structures héritées, et dictent la géomorphologie actuelle de la région.

• Il est possible de proposer un scénario pour l'évolution géodynamique de la Péninsule de Biga, basé sur l'ensemble des résultats précédents et sur les données de la géologie régionale ; ses points principaux sont:

- La Péninsule de Biga fait partie de la marge Rhodopienne.
- Le Groupe d'Ezine est un témoin de la marge passive nord Maliac/Méliata.
- L'ophiolite de Denizgören et le mélange de Çetmi ont été mis en place tous deux vers le nord sur la marge précédente, respectivement au Barrémien et à l'Albien terminal-Cénomanien inférieur.
- Une forte composante décrochante durant l'emplacement est suggérée par la préservation de fragments de la marge passive et l'absence de métamorphisme dans la plaque inférieure.
- Tous les évènements précédents ont été largement affectés par le régime d'extension Tertiaire.

- RÉSUMÉ GRAND PUBLIC -

Le géologue est comme un «historien» de la Terre, qui porte un intérêt particulier à l'étude du passé de notre planète; ce dernier, très ancien, se mesure en dizaines ou centaines de millions d'années (Ma). Or le visage de la terre a constamment évolué au cours des ces millions d'années écoulés, car les plaques (continentales et océaniques) qui composent son enveloppe superficielle ne restent pas immobiles, mais se déplacent continuellement à sa surface, à une vitesse de l'ordre du cm/an (théorie de la tectonique des plaques); c'est ainsi, par exemple, que des océans naissent, grandissent, puis finissent par se refermer.

On appelle sutures océaniques, les zones, aujourd'hui sur la terre ferme, où l'on retrouve les restes d'océans disparus. Ces sutures sont caractérisées par deux associations distinctes de roches, que l'on appelle les mélanges et les ophiolites; ces mélanges et ophiolites sont donc les témoins de l'activité passée d'un océan aujourd'hui refermé.

L'équipe de recherche dans laquelle ce travail à été réalisé s'intéresse à un vaste domaine océanique fossile: l'océan Néotéthys. Cet océan, de plusieurs milliers de kilomètres de large, séparait alors l'Europe et l'Asie au nord, de l'Afrique, l'Inde et l'Australie au sud. De cet océan, il n'en subsiste aujourd'hui qu'une infime partie, qui se confond avec notre mer Méditerranée actuelle.

Or, tout comme l'océan Pacifique est bordé de mers plus étroites (Mer de Chine, du Japon, etc…), l'océan Néotéthys était bordé au nord de mers marginales. C'est dans ce cadre que s'est inscrit mon travail de thèse, puisqu'il a consisté en l'étude d'une suture océanique (mélange plus ophiolite), témoin d'une des mers qui bordait l'océan Néotéthys sur sa marge nord. L'objectif était de préciser de quelle suture il s'agissait, puis de déterminer quand et comment elle avait fonctionné (i.e son évolution géologique).

Les roches qui composent cette suture affleurent aujourd'hui en Turquie nord occidentale dans la Péninsule de Biga. Au nord et au sud de la péninsule se trouvent les zones géologique du mélange de Çetmi, et à l'ouest, le Groupe d'Ezine et l'ophiolite sus-jacente, dite ophiolite de Denizgören.

Une étude complète et détaillée de terrain (cartographie, échantillonnage), suivie de diverses analyses en laboratoire (détermination de leur âge, de leur condition de formation, etc…), ont permis d'aboutir aux principaux résultats suivants :

- Mise en évidence dans le mélange de Çetmi des témoins (1) de l'océan Lycien disparu (ancienne mer marginale de la Néotéthys), et (2) de la marge continentale qui le bordait au nord.
- Fin de l'activité du mélange de Çetmi il y a environ 105 Ma (Albien).
- Le mélange de Çetmi est difficilement corrélable dans le temps avec les unités semblables affleurant dans la région d'étude (unicité du mélange), ce qui implique des conditions particulière de formation.
- L'ophiolite de Denizgören est un morceau d'océan Lycien posé sur un reste préservé de sa marge continentale nord.
- Cette dernière est représentée sur le terrain par une succession de roches caractéristiques, le Groupe d'Ezine. Celui-ci est lui-même un témoin de l'ouverture d'un océan marginal de la Néotethys antérieur au Lycien, l'océan Maliac, qui s'est ouvert il y a 245 Ma (Permien-Trias).

- La mise en place de l'ophiolite de Denizgören sur le Groupe d'Ezine (125 Ma, Barrémien) est antérieure à la mise en place du mélange de Çetmi.

- Il apparaît que ces deux mises en place sont contemporaines de la formation de la chaîne des Balkans, terminée avant le Cénomanien (100 Ma).

- L'évolution dans le temps des objets précédents (océans, marges continentales) montre de grands mouvements latéraux est-ouest entre ces objets (translation). Ce qui implique que les roches que l'on retrouve aujourd'hui sur un transect nord-sud ne l'étaient pas nécessairement auparavant.

- Enfin, il s'avère que le mélange de Çetmi, l'ophiolite de Denizgören, et le Groupe d'Ezine ont subi par la suite des déformations extensives importantes qui ont considérablement perturbé le schéma post-mise en place.

- FOREWORD -

This Ph-D is the result of a four years research project carried out at the Institute of Geology and Paleontology at Lausanne University.

It comes in the continuity of several studies in the Tethyan realm (Ph-D and Master theses), and particularly in the eastern Mediterranean domain; all these works, as well of the thesis, were done within the framework of what may be called the Tethyan plate tectonics "school of Lausanne", instigated by the Pr. Stampfli fifteen years ago: these studies are often based on a multidisciplinary approach (from micropaleontology to geochemistry through sedimentology, tectonics and geochronology), following detailed field work. Their purpose is to replace chosen critical geological objects in a paleotectonic and paleogeographic perspective, giving them a geodynamic significance. This has led, with time, to a more accurate idea of the jigsaw puzzle of the eastern Mediterranean geology.

The present work deals with the geology and geodynamic evolution of the Biga Peninsula of northwest Turkey, with a special focus on two poorly known areas, the Çetmi mélange and the Ezine area. The main goals of the thesis may be summarized as follow:
-To connect the poorly known Çetmi mélange to the regional geology.
-To give a satisfactory solution for the genesis of the Ezine area (Denizgören ophiolite and Ezine Group).
-To refine the exhumation history of the Kazdağ Core Complex, and thus the Tertiary exhumation processes in the Biga Peninsula.
-Following the previous points, to propose a geodynamic scenario for the paleotectonic and paleogeographic evolution of the Çetmi mélange, Ezine area and adjacent regions.

The different areas visited were:

-The Çetmi mélange between Küçükkuyu and Bayramiç (southern mélange), west of Karabiga (northern mélange) and north of Şarkoÿ (Gelibolu Peninsula).

-The Ezine Group and the overlying Denizgören ophiolite north of Ezine.

-The Bozcaada Island, west of Biga Peninsula, not described here.

- The Abant Complex from the Intra-Pontide suture near Abant Lake.

Chapter 1 gives the geological frame of the thesis, by presenting the main features of the eastern Mediterranean domain/Aegean region (sutures, related continental blocks and oceans); it introduces, at the same time, the terms and concepts that will be used all along the thesis. It ends with a focus on the Geology of the Biga Peninsula leading to the main issues of the thesis.

Chapter 2 is devoted to the Çetmi mélange; after a short introduction to the concept of mélange in geology, its geological features are presented (structural observations, nature of the blocks and the matrix). The chapter ends with an attempt to correlate the Çetmi mélange with already known geological units in the north-Aegean region.

Chapter 3 deals with the relationships between the sedimentary sequence of the Ezine Group and the overlying Denizgören ophiolite; it gives their description, their interpretation and their possible correlations.

Chapter 4 focusses on the Tertiary evolution of the Biga Peninsula through the case study of the Kazdağ Massif. The latter, which structurally lies under the Çetmi mélange, is a good example the genesis of a core complex within the frame of the Aegean extensional regime.

Chapter 5 plays the role of the concluding chapter, by integrating all the previous results, plus additional data from the regional geology, in a geodynamic scenario presenting the paleotectonic evolution of the Biga Peninsula (the Çetmi mélange, the Ezine Group and the Denizgören ophiolite) and adjacent areas. This scenario is based on some basic concepts presented at the beginning of the chapter.

LIST OF FIGURES AND TABLES

- CHAPTER 1 -

- CHAPTER 2 -

- CHAPTER 3 -

- CHAPTER 4 -

- CHAPTER 5 -

- CHAPTER 1 -

THE GEOLOGY OF TURKEY AND AEGEAN DOMAIN IN THE FRAMEWORK OF TETHYAN GEOLOGY

This first chapter deals with the geological frame of the thesis. After an introduction to the Tethys concept, the main geological features of the Aegean domain (mainly oceanic sutures and related continental blocks and oceans) are reviewed. It is also the opportunity to introduce the geological and paleogeographical terms and concepts that will be used all along the thesis. The chapter is concluded by an outline of the geology of the Biga Peninsula leading to the main thesis issues.

1.1. The Tethyan realm

The existence of a former "seaway" (*Centrales Mittlemeer*, with a paleo-biogeographic meaning, Figure 1.1) south of Eurasia has been first conceived by the German stratigrapher Melchior Neumayr (1885). Neumayr's father-in-law Eduard Suess attached a tectonic signification to this concept and renamed it as *Tethys* after the sister and consort of Okeanos (!), the Greek god of the ocean (1893). Suess was considering the Tethys Ocean as the mother of the Alpine-Himalayan range. He envisaged the Tethys mainly as a Mesozoic phenomenon, but with possible extensions down to the Paleozoic and up to the present (according to him, the Mediterranean was a remnant of the original Tethys).

Following Neumayr and Suess's initial works, the notion of Tethys has become one of the most important concept of modern geology. For a detailed review of the history of the Tethys concept and its evolution, the reader is referred to Şengör (1984, 1989).

Figure 1.1. Neumayr's Central Mediterranean, the paleogeographic predecessor of the Tethys concept (1885).

About seventy years later, following the onset of plate tectonics, the Tethys ocean appears for the first time on the continental fit of Bullard et al. (1965), regardless of the data from regional geology. But this reconstruction and the following ones were implying a single oceanic domain along the Alpine-Himalayan belt from the Late Carboniferous onward, whereas field data were showing that no ocean could be older than Middle Triassic. This was called later the "Tethyan paradox" (Şengör et al., 1984; Stöcklin, 1984). The solution came from new field evidences which show that the original Tethys, responsible for the Alpine-Himalayan orogeny, actually represents two distinct major tethyan oceans, namely the Paleotethys and the Neotethys (Stöcklin, 1974; Şengör, 1979). Finally the Paleotethys correspond broadly to the Tethys of Bullard et al. (mostly a Paleozoic Tethys), whereas Neotethys is closer to the original Tethys concept of Suess.

The occurrence of two successive and partly contemporaneous tethyan oceans, the northerly older Paleotethys and the southerly younger Neotethys, has currently reached a consensus, as well as their genetic link: the disappearance of Paleotethys and the coeval generation of Neotethys are considered to be the consequence of the rifting from the northern margin of Gondwana of a continental strip (the Cimmerian Continent, Şengör, 1979) which drifted anticlockwise until its collision with the southern margin of Laurasia (Cimmerian orogen); the closure of the Neotethys led to final collision of the Gondwana margin with the Cimmerian southern margin of Laurasia (Alpine orogen). On the other hand, the tectonic scenarios and the driving mechanisms responsible for the tethyan evolution through space and time are still debated (e.g. Şengör, 1985; Stampfli et al., 1991; Dercourt et al., 1993; Ricou, 1994; Robertson et al., 1996).

As proposed by Stampfli (2000), the terms Paleotethys and Neotethys are used in this way: the Paleotethys was the ocean that separated the Variscan domain from the Cimmerian blocks, and the Neotethys was the ocean that separated the Cimmerian blocks from Gondwana. Paleotethys opened during Late Ordovician-Early Silurian times and closed in the Triassic by northward subduction under the southern Laurasian margin. As for Neotethys, various convergent data imply an opening in the Early Permian due to the slab pull effect of Paleotethys, and a closure in the Early Tertiary (excepted the eastern Mediterranean domain still subducting today (Spakman et al., 1993; Wortel and Spakman, 2000). Paleotethys, Neotethys, and the Alpine Tethys (Favre and Stampfli, 1992), plus numerous marginal basins which developed mainly along the Eurasian margin during Permian to Cenozoic times (see part 1.2.2), form the Tethyan domain s.l. that extended from Morocco to the Far-East (Şengör, 1984).

1.2. Geology of the eastern Mediterranean domain/Aegean region

From the last two decades, the eastern Mediterranean domain (or Aegean region if the geology of eastern and south-eastern Turkey is excluded) has become a leading case study for who wants to understand the tethyan evolution (Hsü, 1977; Bonneau, 1984; Mart and Woodside, 1994; Robertson, 1994); it is most probably in the whole tethyan realm the place where the most important amount of data has been gathered by geologists.

First and foremost, the onland geology of this area is characterized from a tectonic point of view by some oceanic sutures delineating several zones or blocks, interpreted in term of terranes (Schermer et al., 1984; Howell, 1985). One of the favourite focus of tethyan geologists is to recognize, interpret, and then correlate these sutures, to finally propose a

spatio-temporal scenario for the evolution of the oceanic domains and associated margins leading to the present day situation.

After a brief introduction to the history of geology in Turkey and Greece, this part presents a review of the sutures, associated oceanic basins and continental margins, both in Western Turkey and Greece (Aegean domain s.s.). Some of the key-points later debated in the thesis are also reported.

1.2.1. Outline of the history of geology in Turkey and Greece

1.2.1.1 Geology of Turkey

Publishing the observations made during his travel through Anatolia, De Tchihatcheff initiated the age of "modern" geological descriptions of Turkey (1867/69). The end of the 19th century is marked by specific geological investigations, mainly made by Austrian geologists, like Neumayr (the father of the *Centrales Mittlemeer*, see 1.1). During the first decades of the 20th century, the geologists came mainly from Germany (e.g. Frech, 1916; for further references see Brinkmann, 1976). In addition to these foreigners, Turkish geologists began to take part in the investigations; this led to the founding of the University of Istanbul in 1915 and of the geological survey (M.T.A.) in Ankara in 1935. The first complete geological map of Turkey, at the scale of 1/800'000, has been published in 1942. An important step for the understanding of the geology of Turkey has been made by Ketin, who proposed in 1966 the first subdivision of Anatolia, into the Pontides (Laurasian realm), the Anatolides, the Taurides, and the Border Folds (Gondwana realm). At the same period of time, syntheses on the geology of Turkey were published (Paréjas, 1940; Egeran, 1947 and Figure 1.2; Brinkmann, 1966; 1976). Finally, following the advent of the theory of plate tectonics, the geology of Turkey has become a major case study for the understanding of the western tethyan evolution (Şengör and Yılmaz, 1981).

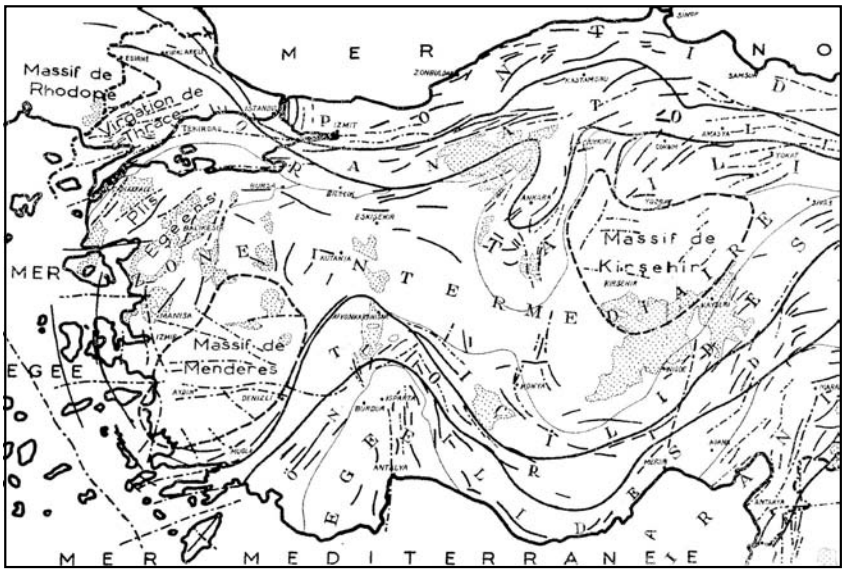

Figure 1.2. Tectonic map of Turkey of Egeran (western part, 1947).

Following Ketin's proposal, many geological subdivisions of Turkey based on paleogeography have been proposed following the concept of plate tectonics. As it is beyond the scope of this work to review each of them, the recent view of Okay and Tüysüz (1999) is followed here (Figure 1.3), on Bozkurt and Mittwede's advice (2001). Their definition of the sutures and microcontinents is more and more used, and does not differ radically from other propositions (e.g. Göncüoğlu et al., 1996-1997). It will therefore be used as a base along the Turkish transect in the part dedicated to the geological features of the sutures, corresponding oceanic domains, and blocks of the Aegean region.

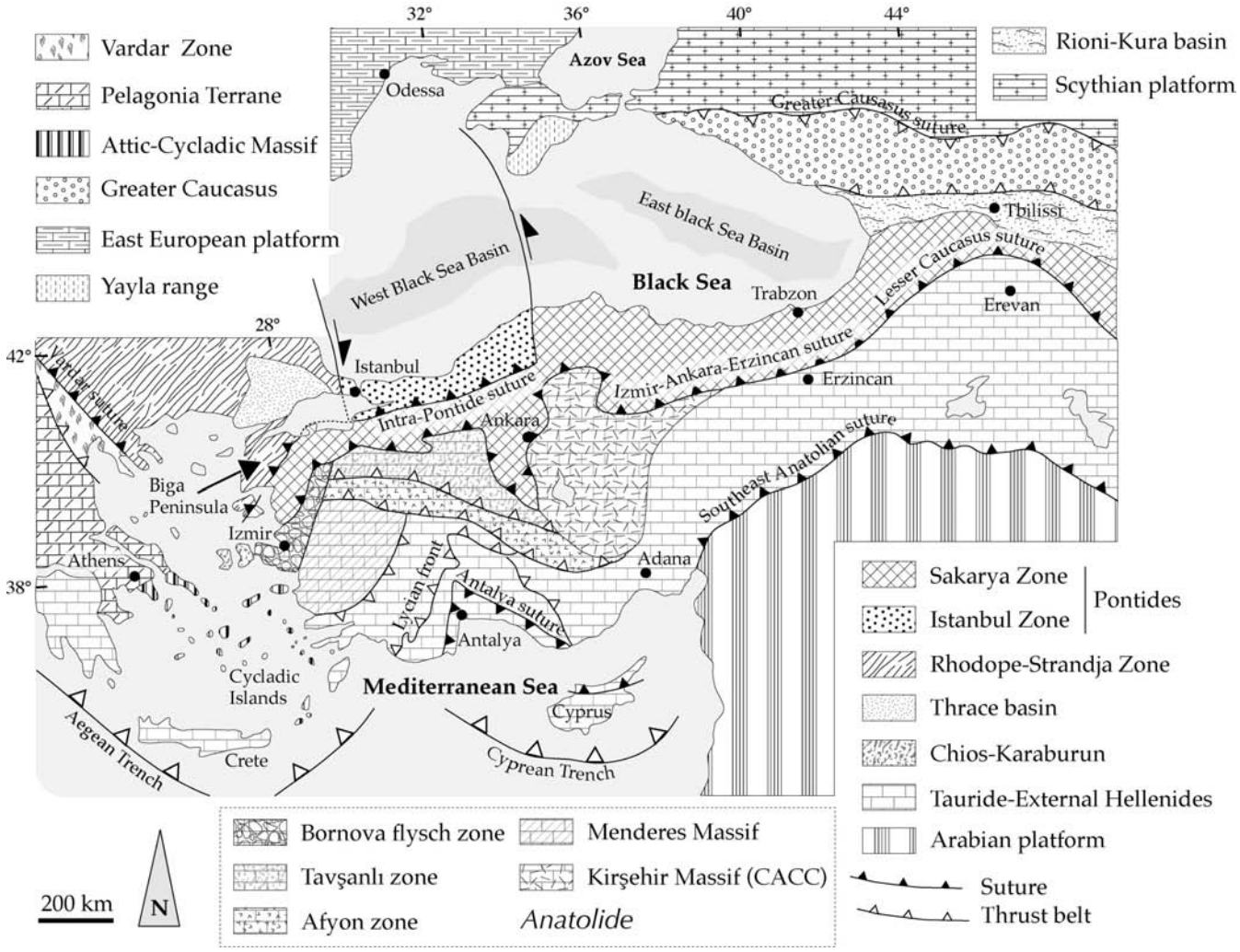

Figure 1.3. Simplified tectonic map of Turkey and surrounding areas; modified from Bozkurt and Mittwede (2001); Okay et al. (2001).

1.2.1.2 Geology of Greece

The systematic study of the geology of Greece started in 1829 with the "French Scientific Expedition of Peloponnesus", whose results have been published in 1833. Many French, German and Austrian geologists followed until the major work of Philippson (1898), who

described the main tectonostratigraphic systems of Greece. For the 20th century, a major reference is the pioneer work of Renz who published two synthesis of Greek geology (Renz, 1940; 1955). The term Hellenides, describing the Greek mountain chains and their geological units, was coined by Kober (1929).

The Hellenides are now considered as the result of a multiphase orogenic belt with nappe structure. The present position of the different structural units is due to the Eohellenic (Middle Jurassic to Early Cretaceous) and the Alpine orogenic phases (or Mesohellenic phase, Eocene to Miocene). In a general way, the boundaries of the thrust nappes respect those of the main paleogeographic domains: the most external ones (to the west) are found at the base of the nappe pile and the most internal ones (to the east) at the top. Out-of-sequence thrusts and Miocene extension complicate this simple pattern.

As in Turkey, the paleogeographic organisation of the Hellenides is still the subject of several interpretations, mainly about the major ophiolite zones. In the next part, the widely accepted subdivision of Papanikolaou is followed (1989, 1996-1997), with some modifications concerning the nature and original position of certain units (De Bono, 1998; Vavassis, 2001, and Figure 1.4).

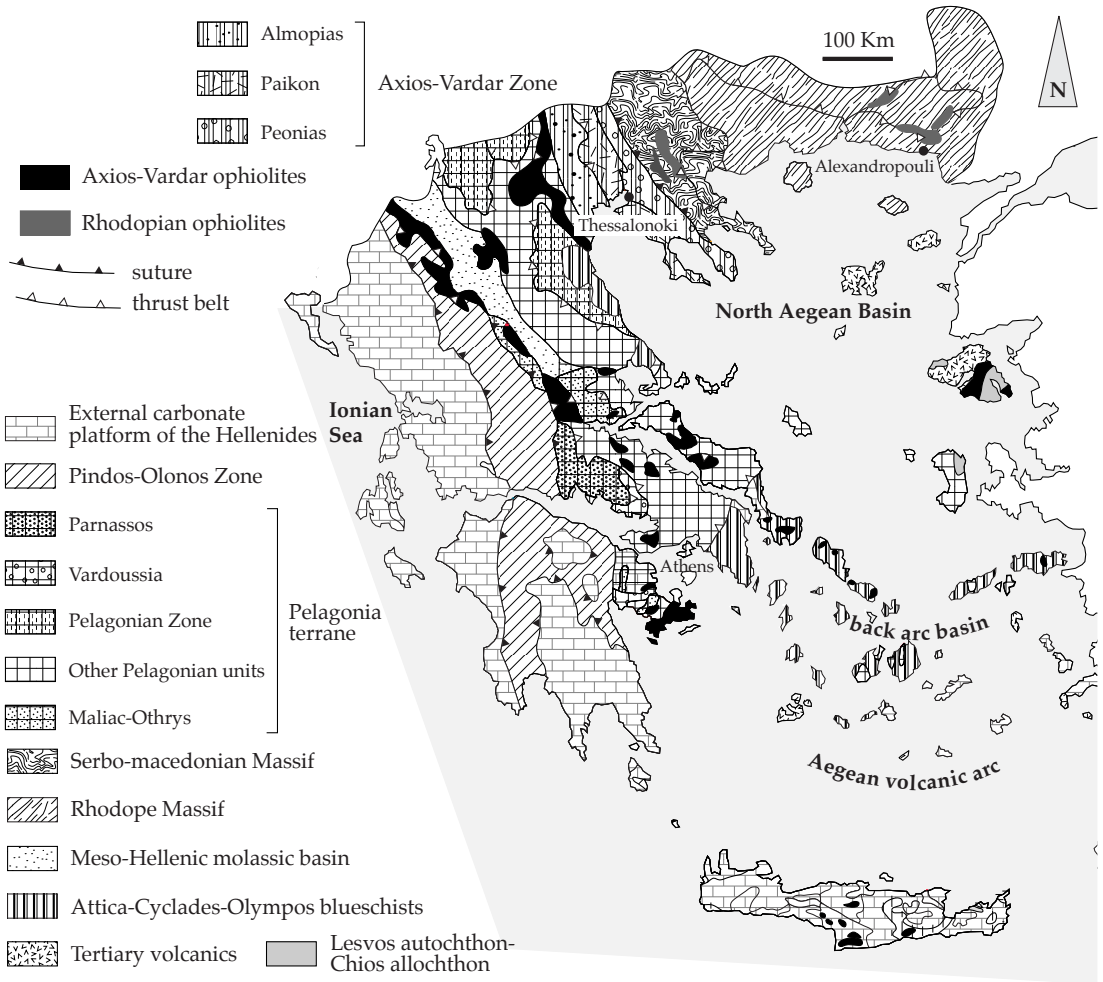

Figure 1.4. Simplified tectonic map of Greece, redrawn from Papanikolaou (1989, 1996-1997); modified by Stampfli and Vavassis (Vavassis, 2001).

1.2.2. Sutures, associated oceanic domain and terranes of the Aegean region

The main geological features of the Aegean domain are presented here, following their palaeogeographic and palaeotectonic affinities; three domains are thus differenciated: the Laurasian margin, the complex domain of the oceanic sutures and associated oceanic basins, and the Gondwana margin, represented by the Cimmerian continents.

1.2.2.1. Laurasian margin

The Serbo-Macedonian Massif and the Rhodope Massif (Greece, southern and eastern Bulgaria, Turkey)

The Serbo-Macedonian Massif of northern Greece is the continuation of the metamorphic rocks cropping out in south-western Bulgaria (Figure 1.4). It is made of medium- to high-grade metasedimentary and magmatic rocks (Kerdylia and Vertiskos respectively), plus metamorphic Mesozoic ophiolites (Kockel and Walther, 1965; Mercier, 1966; 1968; Dixon and Dimitriadis, 1984). The Serbo-Macedonian Massif seems to have been tectonised and metamorphosed both during the Variscan event (e.g. Borsi et al., 1964; Lips et al., 2000) and the Early Cretaceous (e.g. Dixon and Dimitriadis, 1984; Wawrzenitz and Mposkos, 1997).

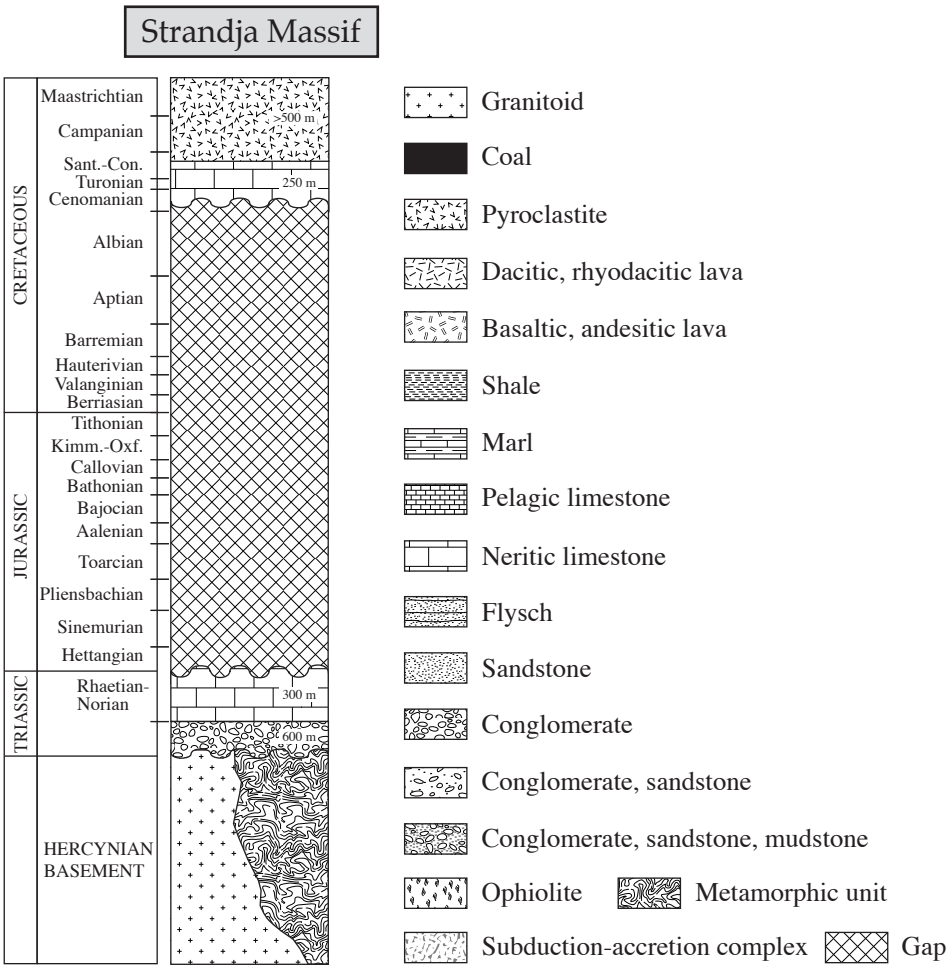

Figure 1.5. Synthetic stratigraphic section of the Strandja Zone based on Aydın (1984). Redrawn from Okay and Tüysüz (1999).

The Rhodope Massif of northern Greece and southern Bulgaria is in tectonic contact with the Serbo-Macedonian Massif along the Miocene Strymon valley detachment fault. In Greece, the massif comprises the lower metasedimentary unit of Pangeon and the upper metamorphic unit of Sidironero (Papanikolaou, 1984). The Rhodope massif, which has a Laurasian affinity, is made of Variscan continental crust, Mesozoic metasediments and remnants of oceanic crust (Burg et al., 1996), which suffered several phases of crustal thickening and exhumation during the Cretaceous and Tertiary (Dinter, 1998; Kilias et al., 1999; Krohe and Mposkos, 2002). Some series with mélange features, Early Cretaceous in age, also occur around the Greek-Bulgarian border (Boyanov and Russeva, 1989, c.f. chapter 2).

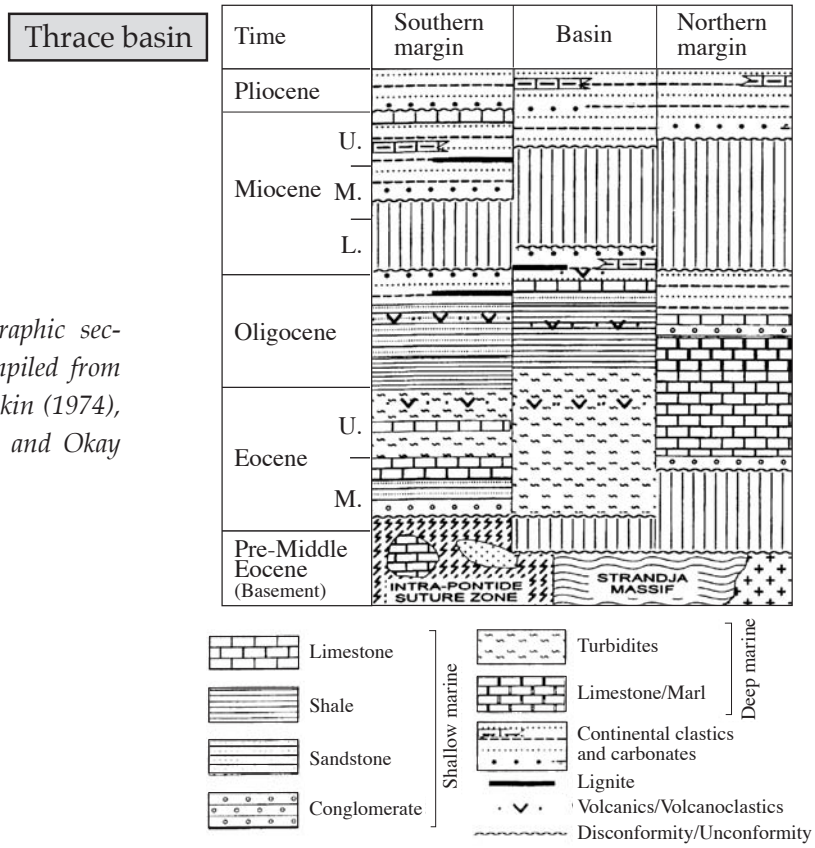

Figure 1.6. Synthetic stratigraphic section of the Thrace basin. Compiled from Doust and Arıkan (1974), Keskin (1974), and Turgut (1991), in Görür and Okay (1996).

The Rhodope Massif is directly correlated with the Strandja Zone of Turkey and southeastern Bulgaria, which represents its eastern continuation (Figure 1.3). As it is close to the Biga Peninsula, the focus of the thesis, the Strandja Zone is described into more details. From a stratigraphic point of view, it is made of a basement of highly deformed metamorphosed rocks in amphibolite facies intruded by late Variscan extensional Permian granites (Okay, 2001, and Figure 1.5). This basement is unconformably overlain by a Triassic transgressive sequence made of continental to shallow-marine metasediments. This sequence extends up to the Mid-Jurassic in the Bulgarian part of the Strandja Zone (Chatalov, 1988). The Late Jurassic-Early Cretaceous is a period of important deformational regime involving the previous units (Austrian phase or Balkan orogeny s.l., Georgiev et al., 2001). This major compressional event, characterized by greenschist-facies metamorphism and northward thrusting, may be related to the final closure of the southward subducting Meliata Ocean and the collision of the Vardar arc with the Rhodope (Stampfli, 2000). The deformation is sealed by Cenomanian conglomerates and shallow marine limestones,

followed by Senonian arc-related magmatic rocks. All the previous units have been finally involved in the Alpide orogeny s.l., creating a new generation of northward directed thrusts in the latest Cretaceous-Oligocene.

In Turkish southern Thrace, the Strandja Zone is covered by the sediments of the Tertiary Thrace basin, which obliterates the structural relation between the Strandja Zone and the southerly Sakarya Zone. The Thrace basin is a Tertiary depression filled by more than 9'000 m of sediments. The infill, mostly Middle Eocene to Early Oligocene in age, is made of a dominantly clastic shallowing-upward sequence (turbidites). Post-Early Oligocene sedimentation was mainly marginal marine to terrestrial (fig 1.6). It has been interpreted as a fore-arc basin above the northward subducting Intra-Pontide Ocean during the Middle Eocene-Oligocene period (Görür and Okay, 1996).

The Istanbul Zone (Turkey)

Located at the south-western margin of the Black Sea, the Istanbul Zone is a small continental fragment about 400 km long and 70 km wide (Figure 1.3).

It consists of a Precambrian crystalline basement unconformably overlain by an almost continuous sedimentary sequence extending from Ordovician to Carboniferous, which has been deformed during the Variscan orogeny (Görür et al., 1997, and Figure 1.4). This deformed Paleozoic sequence is unconformably overlain by a transgressive sequence of Scythian to Norian age in the Istanbul region, and by a coarse detritic sequence in the eastern part of the Istanbul Zone (Zonguldak area). In the western part of the Istanbul Zone, the Triassic rocks are unconformably overlain by upper Paleocene clastics, carbonates and andesitic volcanic rocks; the eastern part shows a thick Middle Jurassic to Eocene sequence marked by small unconformities (Okay et al., 1996; Okay and Tüysüz, 1999).

The Istanbul block shows a clear Laurasian affinity for the Paleozoic and at least the lower Mesozoic, both from the fauna and paleomagnetic point of view (e.g., Kerey et al., 1986; Saribudak et al., 1989). It is generally accepted that this continental fragment has been translated southward from the Odessa Shelf following the back-arc opening of the West Black Sea oceanic basin (Okay et al., 1994).

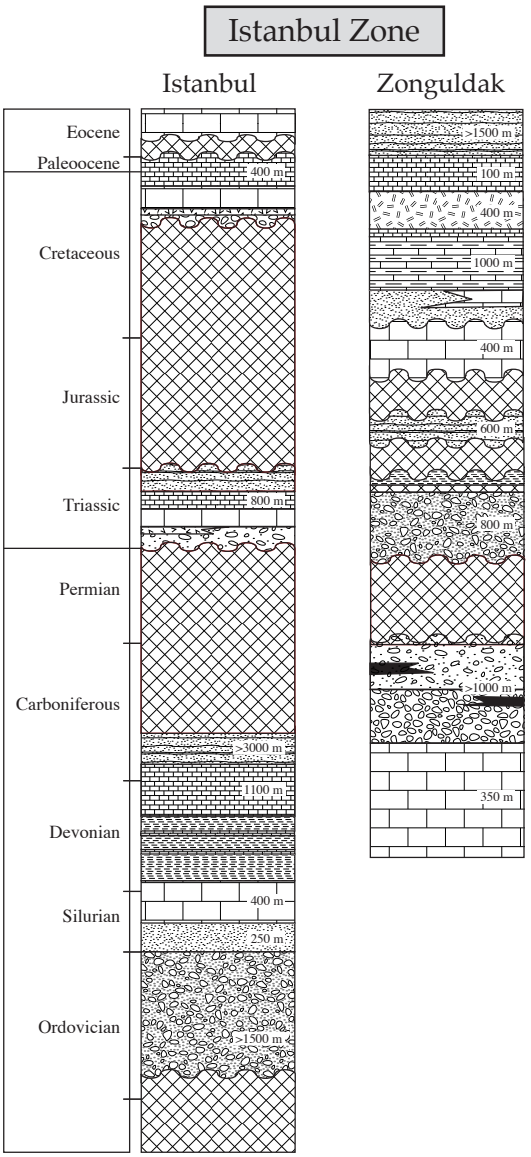

Figure 1.7. Synthetic stratigraphic section of the Istanbul Zone based on Yurttaş-Özdemir (1973), Dean et al. (1996) and Görür et al. (1997). Redrawn from Okay and Tüysüz (1999). Key on Figure 1.5.

The Sakarya Zone (Turkey)

The Sakarya Zone (or Sakarya composite terrane of Göncüoğlu et al., 1996-1997), about 1500 km long and 120 km wide, is bounded in its north-western border by the Strandja and Istanbul zones through the Intra-Pontide suture, and in its north-eastern part by the Black Sea (Figure 1.3). As the Istanbul and Strandja zones, the Sakarya Zone was close to the Laurasian margin, at least during the Liassic and the Late Cretaceous time (Channell et al., 1996). From a geographical point of view it includes the Sakarya continent of Şengör and Yılmaz (1981) and the Central and Eastern Pontides (Okay, 1989). The Biga Peninsula, where are found the two case studies of the thesis (the Çetmi mélange and the Ezine area), is geographically located at the western end of the Sakarya Zone.

From a stratigraphic point of view, the "basement" of the Sakarya Zone may be represented both by metamorphic rocks observed in few tectonic windows (Kazdağ, Uludağ and Kozak ranges), and by Devonian granitoids (e.g. the Çamlık granodiorite, Okay et al., 1996). Zircons from gneisses from the Kazdağ Massif have yielded Carboniferous ages (308 Ma, Okay et al., 1996), but a latest Oligocene age is proposed for the age of the whole metamorphic assemblage, based on new Rb/Sr ages (Okay and Satır, 2000). All these metamorphic rocks are cropping out in the westernmost part of the Sakarya Zone, in or close to the Biga Peninsula.

A more relevant basement for the Mesozoic succession would be represented by a widespread Triassic subduction-accretion complex, called the Karakaya Complex in the western part of the Sakarya Zone (Bingöl et al., 1975; Tekeli, 1981; Okay et al., 1991; Pickett et al., 1992). The Karakaya Complex is generally subdivided into four units; the lower unit, named as the Nilüfer unit, is a metabasite-marble-phyllite sequence with Triassic eclogite (Okay and Monié, 1997; Okay et al., 2001a) and blueschist lenses (Monod et al., 1996). It rests in tectonic contact over the Kazdağ and Uludağ ranges. The other units are grouped together here and tectonically overlie the Nilüfer unit; these Çal, Hodul and Orhanlar greywacke units (Diskaya Formation of Kaya, 1991) are made of unmetamorphosed but chaotically deformed clastic and basic volcanic rocks of Triassic age with exotic blocks of Carboniferous and Permian neritic limestone, basalt, Carboniferous and Permian radiolarian chert (previous ref., plus Kozur, 1994, Leven and Okay, 1996). From a tectonic point of view, the Nilüfer unit is either considered as an oceanic plateau (Okay, 2000) or a seamount (Pickett and Robertson, 1996). The Karakaya mélanges (mainly the Hodul unit) may be seen as a fore-arc/foreland basin related to the Paleotethys subduction along the southern margin of Eurasia (Stampfli et al., 2003).

The deformation and metamorphism of the Karakaya Complex, as well as its different units, are unconformably overlain by Liassic terrigenous to shallow marine clastic sedimentary rocks (Altıner et al., 1991, and Figure 1.8). These clastics are unconformably overlain by middle to upper Jurassic platform type neritic limestones, lower Cretaceous pelagic limestones and upper Cretaceous-Paleocene volcanic and sedimentary rocks (e.g. Rojay and Altıner, 1998). Senonian andesitic volcanism cropping out in the northern part of the Sakarya Zone is directly related to the northward subduction of the oceanic space south of the Sakarya continent occuring at that time.

Another important feature of the Sakarya Zone is the Küre Unit, located at its eastern boundary with the Istanbul Zone. The Küre Unit comprises thrust-imbricated siliciclastics sediments, interleaved with tectonic slices of a dismembered ophiolite (Ustaömer and Roberstson, 1994; Ustaömer and Robertson, 1997). The complex comprises the largest part

of the Paleotethys sensu Şengör (1979, 1985), but is now interpreted as a remnant of the Küre back-arc oceanic domain (see Kozur, 1997), opened in the Early Triassic north of the Sakarya margin as a result of the northward subduction of Paletoethys (e.g. Stampfli, 2000). It was closed by southward subduction during the Cimmerian collision (Şengör and Yılmaz, 1981; Şengör, 1984; Tüysüz, 1990; Pickett and Robertson, 1996), possibly leading to the back-arc opening of the Izmir-Ankara-Erzincan Ocean (see 1.2.2.2).

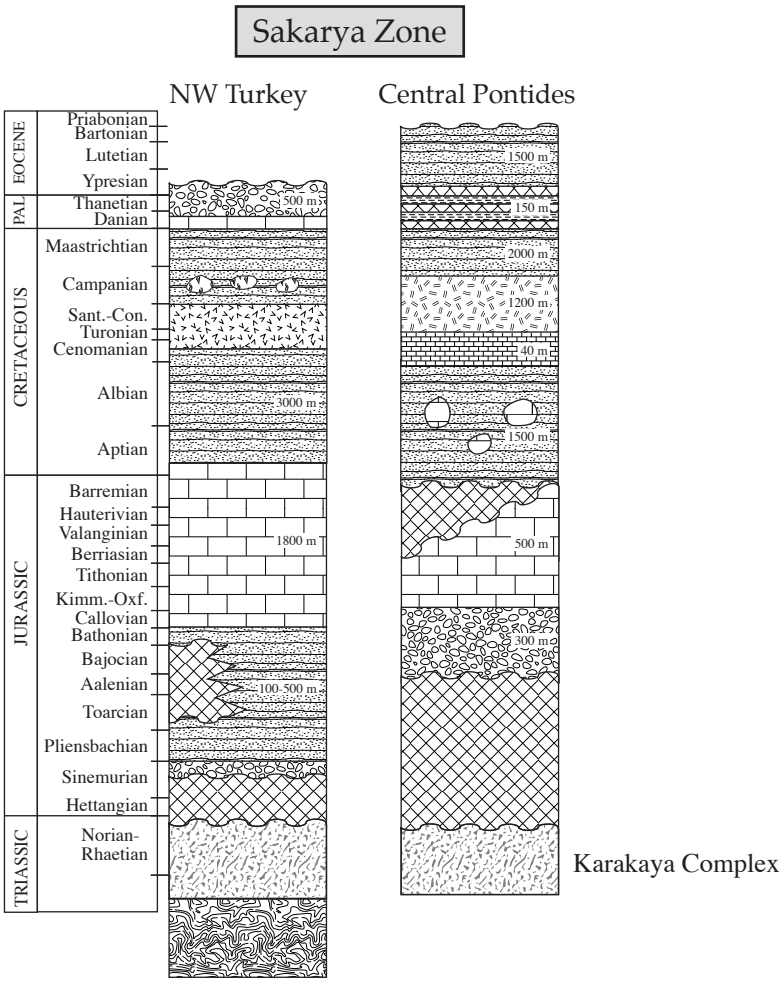

Figure 1.8. Synthetic stratigraphic section of the Sakarya Zone based on Saner (1978, 1980), Altıner et al. (1991) and Tüysüz (1993). Redrawn from Okay and Tüysüz (1999). Key on Figure 1.5.

The Pelagonia terrane (Greece)

The term Pelagonia terrane includes the Internal carbonate platform of the Hellenides (Papanikolaou, 1989) plus the Maliac-Othrys unit (Ferrière, 1982; De Bono, 1998). From west to east the Pelagonia terrane comprises the following paleogeographic units (Figures 1.4-1.9): (1) the Vardoussia sub-zone, which has a transitional character between the Pindos-Olonos Zone (see below) and the Parnossos Zone (Ardaens, 1978). (2) The Parnassos Zone, characterized by shallow-water carbonate sedimentation from Carnian to Maastrichtian with several emersive episodes and hiatus (Celet, 1962; 1979). The platform is broken up in horst and grabens at the Cretaceous/Tertiary boundary, followed by a flysch sedimentation

in the Middle Eocene (Richter et al., 1995). (3) The Beotian basin, westward extension of the Pelagonian platform and characterized by pelagic sedimentation since late Middle Jurassic (Robertson et al., 1991; Thiébault et al., 1994; Danelian and Robertson, 1998). The pelagic sequence is followed by an upper Jurassic-lower Cretaceous "Beotian Flysch", derived from the ophiolitic nappe emplacement onto the Pelagonian Zone (Richter et al., 1996). (4) The Pelagonian Zone, made of a Variscan basement followed by a syn-rift sequence of Late Permian-Early Triassic age (Vavassis et al., 2000; De Bono et al., 2001). Then come upper Triassic to middle-upper Jurassic carbonate platforms, locally followed by Bathonian to Tithonian radiolarites (Celet and Ferrière, 1978; Angiolini et al., 1992; Baumgartner et al., 1993). The continental margin succession is overthrusted by eastward derived ophiolites of Vardar origin (Eo-Hellenic orogenic phase, also observed on Lesvos Island, Hatzipanagiotou and Pe-Piper, 1995). The emplacement is recorded by the arrival of ophiolitic detritus and tectonic and sedimentary mélanges (Renz, 1955; Parrot and Guernet, 1972; Baumgartner and Bernouilli, 1976; Baumgartner, 1985; Robertson, 1990). Both the platform carbonates and the ophiolites are transgressed by Cenomanian-Campanian shallow-water limestones, that passed locally to Maastrichtian hemipelagic carbonates (Guernet, 1975; Richter et al., 1996). Te latter are overlain by a Paleocene-Eocene flysch (Bignot et al., 1971). (5) The Maliac-Othrys unit, located today at the western side of the Pelagonian Zone. It is made of a pelagic sequence of Carnian-Norian to Early-Middle Jurassic sediments, overlying middle-upper Triassic volcanic rocks. The type of sedimentation changes in the Late Jurassic following the onset of ophiolite obduction in the Middle to Late Bathonian. The Maliac-Othrys unit is considered as derived from the eastern flank of the Pelagonian platform (Ferrière, 1982; 1985; Thiébault et al., 1994) and seen as a distal part of the Pelagonian passive margin.

From a geodynamic point of view, the Pelagonia terrane is regarded as a detached Eurasian fragment drifted away in the Late Permian-Early Triassic. It was sited between the Meliata-Maliac oceanic basin in the north and the Paleotethys, then the Pindos domain, in the south (Vavassis et al., 2000; De Bono et al., 2001; see chapter 5).

1.2.2.2 Oceanic sutures of the Aegean domain

The Intra-Pontide suture (Turkey)

The Intra-Pontide suture (herein IPS) has been first formally defined by Şengör et al. in 1980: "between Gelibolu and the Ilgaz Massif, the ophiolitic suture, herein called the Intra-Pontide suture, separates the Rhodope-Pontide fragment from the Sakarya continent". From this first occurrence in the literature several authors have written on the subject, but without focussing specifically on the IPS (e.g. Okay et al., 1991; Okay et al., 1994; Görür and Okay, 1996; Okay et al., 1996; Göncüoğlu et al., 1996-1997; Robertson, 2002). Only few papers are directly related to it (Yılmaz et al., 1995; Okay and Tüysüz, 1999).

The IPS forms the limit between the Istanbul Zone and the Rhodope-Strandja Massif in the north and the Sakarya Zone in the south (Figure 1.3). Along its eastern segment, between the Istanbul and Sakarya zones, the IPS is clearly exposed in the field. However, a very important fact is that the major post-Miocene strike-slip North Anatolian Fault Zone (herein NAFZ, Barka, 1992; Armijo et al., 1999) directly coincides with the IPS along this segment. It means among other that all the pre-Miocene structural relations between the Istanbul and the Sakarya zones were disrupted. The suture is made of a tectonic mixture of several units coming from both the Istanbul and Sakarya zones, various metamorphic

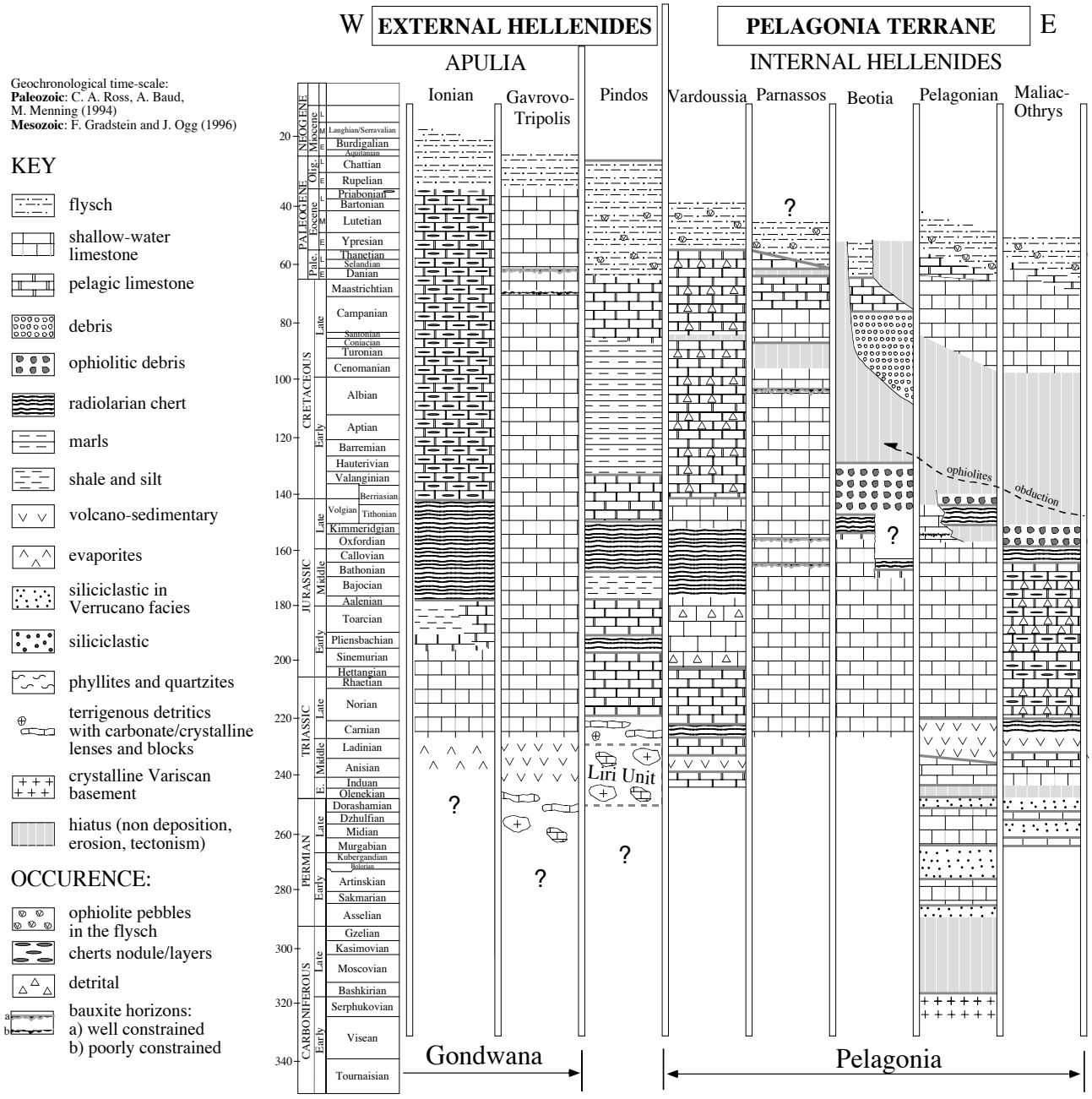

Ionian: Fleuri, 1980; Danelian, 1995; Neumann & Zacher, 1998
Gavrovo-Tripolis: Fleury, 1980; Thiébault, 1981; Seidel et al., 1983; Thiébault et al., 1985
Pindos: Fleury, 1980; De Wewer & Origlia-Devos, 1982a; De Wewer & Cordey, 1986; Richter & Müller, 1993a; Baumgartner et al., 1995; De Wever & Cordey, 1995

Vardoussia: Ardeans, 1978; Aerdens et al., 1979; Celet, 1979
Parnassos: Celet, 1962; Celet, 1979; Caminitti, 1985; Richter et al., 1995; Richter et al., 1996b
Beotia: Celet et al., 1976; Clément, 1983; Thiébault et al., 1994; Richter et al., 1996a; Danelian & Robertson, 1998
Pelagonian: Clément et al., 1971; Celet & Ferrière, 1978; Clément, 1983; Katsikatsos et al., 1986; Grant et al., 1991; Angiolini et al., 1992; Vachard et al., 1993; Richter et al., 1996; De Bobo et al., 1998
Maliac-Othrys: Ferrière, 1982; Baumgartner, 1985; Baumgartner et al., 1993; Danelian, 1994; Baumgartner et al., 1995; Richter et al., 1996b

Figure 1.9. Synthetic stratigraphic column from the External Hellenides and the Pelagonian terrane; from de Bono (1998).

rocks, plus dismembered meta-ophiolitic bodies (Geyve and Almacık ophiolites). Besides the NAFZ problem, the lack of reliable field data (particularly on the ages of metamorphic and ophiolitic rocks) prevents a clear understanding of the area. For instance there is still a debate on the age of the meta-ophiolite north of Mudurnu (Almacık ophiolite), considered either as Paleozoic (Abdüsselamoğlu, 1959; Gözübol, 1980; Yığıtbaş et al., 1999) or Late Cretaceous in age (Yılmaz et al., 1982; Yılmaz et al., 1995). The occurrence of Late Cretaceous pelagic limestone (Yılmaz et al., 1982) and possible Late Jurassic radiolarite (Brinkmann, 1966, both confirmed by this study, see chapter 2) as blocks/slices in tectonic mélanges associated with these ophiolites seems to be an argument in favour of the Late Cretaceous age of the ophiolites. We will see in chapter 5 that it is not a sufficient argument.

The suture is thought to continue westward under the Marmara Sea and to reappear onshore in the region of Şarkoÿ. Indeed, the region of Şarkoÿ displays a few small outcrops of the Çetmi mélange; these outcrops, but not the whole Çetmi mélange whose largest exposure is on the Biga Peninsula, have been interpreted as traces of the IPS (Şengör and Yılmaz, 1981; Okay and Tüysüz, 1999). This point will be discussed in chapter 2, together with the possible lateral correlations of the mélange.

As the field evidences from the IPS are scarce, the evolution of the corresponding Intra-Pontide Ocean (herein IPO) remains highly speculative. For instance, there are no clear data for the age of its opening, and for the age of its closure; generally, based on the age of the first unconformable cover sediments, it is placed in the Upper Cretaceous (Yılmaz et al., 1995), Paleocene-Eocene (Şengör and Yılmaz, 1981), Early Eocene (Okay et al., 1994; Wong et al., 1995), Early Eocene to Oligocene (Monod and Okay, 1999); these discrepancies are actually related to disagreements about the true location of the suture. Even the existence of the IPO has been recently challenged (Yığıtbaş et al., 1999). Finally, recent data from Tüysüz (1999) favour a juxtaposition of the Istanbul and Sakarya zones during the Cenomanian, much earlier than previously proposed (c.f. discussion in chapter 5).

The Izmir-Ankara-Erzincan suture (Turkey)

The c. 2000 km long east-west trending Izmir-Ankara-Erzincan suture (herein IAES) is extending from Izmir eastward through Eskişehir, Ankara, Tokat, Erzincan to the border with Armenia. It separates the Sakarya Zone in the north from the complex Anatolide-Tauride block in the south (Figure 1.3). As the geodynamic evolution of the oceans related to the IAES will be discussed in details in chapter 5, only the general geological features of the IAES are presented here.

First of all, as for the IPS, the suture in its present structural position and appearance is the result of post emplacement tectonic activity. Most of this tectonic activity is, however, distributed over a longer period of time, from Eocene to Miocene, and represents the final stages of continental collision between the Sakarya Zone and the Anatolide-Tauride Block (see below).

The suture zone is classically made of ophiolitic rocks associated with accretionary mélange units. The former are generally located to the north of the mélanges and represent the upper structural levels.

The ophiolites occur mainly as peridotite massif, lacking the complete ophiolitic sequence (gabbro, sheeted dykes, basalts and pelagic sediments). Radiochronologic data from sub-ophiolitic amphibolitic soles, interpreted as witnesses of the inception of the obduction, are rare and suggest Albian-Cenomanian ages (Önen and Hall, 1993; Harris et al., 1994).

The mélanges are commonly made of basalt, radiolarian chert, pelagic shale, pelagic or neritic limestone, greywacke/sandstone and serpentinite. All lithologies show dissimilar age, origin, facies and size, generally with strong tectonic imbrications. This clear tectonic fabric and the scarcity of a well-defined matrix tend to consider them as tectonic mélanges or imbricated thrust stacks rather than real ophiolitic mélanges. The age of the blocks ranges from Permian (reworked from the Karakaya Complex) to Late Cretaceous. The famous type locality for these mélanges is located near Ankara and is known under the name of Ankara mélange (Bailey and McCallien, 1953). One should note that the original Ankara mélange defined by Bailey and McCallien was in fact the close assemblage (or mixing) of the Karakaya complex (c.f. 1.2.2.1) and the real Late Cretaceous mélanges (e.g. Norman, 1993).

Ophiolite and accretionary mélanges related to the IAES are also cropping out farther south in Turkey (Lycian, Beyşehir, Mersin, Ali Hoca, Pozantı-Karşantı, Sarıkaraman and Çiçekdağ ophiolite, e.g. Yalınız et al., 1996; Collins and Robertson, 1998; Dilek et al., 1999; Floyd et al., 2000). More age data on the amphibolitic soles of these ophiolites are available than for those of the IAES s.s.; all of them are centered around 90 Ma (Dilek et al., 1999; Parlak and Delaloye, 1999; Robertson, 2002). These ophiolites and those belonging to the suture s.s. have structural positions and geochemical signatures typical for supra-subduction zone tectonic setting (Robertson, 1994; Lytwyn and Casey, 1995; Yalınız et al., 1996; Parlak et al., 2000).

From a structural point of view, the peridotites and the mélanges from the IAES s.s. occur mainly as south-vergent tectonic slices in tectonic contact with the underlying different units of the Anatolide-Tauride Block. However, as pointed out by Okay and Tüysüz (1999), some ophiolites and accretionary complexes usually related to the IAES are emplaced directly on the flexural margin of the Sakarya continent, along north-vergent thrust contacts when observed (Bergougnan, 1975; Okay and Şahintürk, 1997). This northward emplacement is never taken into account when reconstructing the geodynamic evolution of the area. This important point is treated in chapter 5 where a solution to this problem is proposed.

The oceanic domain related to the IAES is known as the Izmir-Ankara-(Erzincan) ocean (herein IAEO) or northern branch of Neotethys of some Turkish authors. Until recently, the age of its opening was considered as Liassic (Şengör and Yılmaz, 1981; Görür et al., 1983), but recent micropaleontological data may favour en earlier opening in the Late Triassic (Bragin and Tekin, 1996; Tekin et al., 2002). Because of its age, there is a general agreement to say that the Late Cretaceous ophiolites found today over the Anatolide-Taurides block are not derived from the IAEO. Many models are thus proposed to explain the emplacement of both the ophiolites and the acrretionary complexes (Görür et al., 1984; Norman, 1984; Tüysüz et al., 1995; Ustaömer and Robertson, 1997; Tankut et al., 1998; Okay et al., 2001b). However, they are only locally valid, but are not verified laterally. The evolution of the IAEO and related are discussed in chapter 5.

The Axios-Vardar Zone (Greece-former Yougoslavia)

The Axios Zone in Greece extends north-westward to the Vardar Zone of former Yugoslavia in the Dinarides (Kossmat, 1924). In Macedonia, the Axios-Vardar Zone was subdivided into three main branches, named Peonias, Païkon and Almopias (Mercier, 1968, and Figure 1.4 and 1.9). The main geological feature of the Peonias and Almopias zones is the widespread occurrence of ophiolitic rocks and associated mélanges, and Permo-Triassic

sequences similar to those of the Pelagonian Zone (e.g. Mercier and Vergely, 1972; Stais et al., 1990; Stais and Ferriere, 1991). The Paikon Zone is either regarded as a Jurassic volcanic-arc or as a Pelagonian tectonic window (Ricou et al., 1998; Vergely and Mercier, 2000, and ref. therein).

The Axios-Vardar Zone is the root zone for the Jurassic Vardar oceanic domain. As said before, remnants of its ophiolites are now found as allochthonous tectonic klippes overthrust on the Pelagonian and Pindos zones (Eohellenic phase). The Vardar is regarded as a back-arc basin (supra-subduction zone of Robertson et al., 1990) whose opening is related to the intra-oceanic subduction of the Meliata-Maliac ocean (see below, and Stampfli, 1996; Stampfli, 2000). The remnants of the Vardar ocean not obducted in the Late Jurassic-Early Cretaceous were involved in a northward subduction under the Rhodope in the Late Cretaceous. The evolution of the Vardar ocean is closely related to that of the IAEO (age of opening, life span), and thus will be discussed in chapter 5.

The Pindos-Olonos Zone (Greece)

The Pindos-Olonos Zone (herein POZ) comprises a well-known Middle Triassic to Paleocene sedimentary sequence of pelagic facies (Fleury, 1980; De Wever and Origlia-Devos, 1982; De Wever and Cordey, 1986). It ends progressively with a flysch of Paleocene-Oligocene age (e.g. Richter and Muller, 1993, and Figure 1.4 and 1.9). From a paleogeographic point of view, the POZ is regarded as a deep (oceanic ?) water basin since the Late Triassic.

A critical question is the provenance of the "Jurassic Pindos ophiolites" found as nappes in the POZ. The ophiolite are now thought to derive from the eastern Vardar domain (Bernoulli and Laubscher, 1972; Aubouin et al., 1977; Ferrière, 1985; Thiébault et al., 1994; Stampfli et al., 1998; De Bono et al., 2001; c.f. 1.2.2.5). However, some authors still consider them as coming from an oceanic area located in the Pindos realm and called the Pindos Ocean (Smith et al., 1975; Papanikolaou, 1989; Degnan and Robertson, 1990; Robertson, 1990; Robertson et al., 1990; Clift and Dixon, 1998).

The Maliac/Meliata Ocean (Greece and northwestward countries)

The remnants of this Triassic oceanic domain are known as ophiolitic obducted nappes and/or tectonic mélanges located in Austria, Slovak and Czech republics, Hungary and Romania (Kozur, 1991, and ref. therein, Kozur and Mock, 1996; Mello et al., 1998), and possibly as olistoliths in the obducted Late Jurassic-Early Cretaceous mélanges of the Vardar Ocean (Ferrière, 1982; Simantov and Bertrand, 1987; Pe-Piper, 1998; Vavassis, 2001; De Bono et al., 2002; Stampfli et al., 2003). The sea-floor spreading began in the Early Triassic, as shown by the occurrence of Early Triassic Mid-Ocean Ridge Basalt (MORB) in the Niculitel Formation of N-Dobrogea (Cioflica et al., 1980; Seghedi et al., 1990; Nicolae and Seghedi, 1996). The subduction began during the Jurassic and the closure was within the Oxfordian (Kozur, 1991). The Maliac/Meliata oceanic basin may be correlated (at least in time) with the Küre Ocean (Kozur and Mock, 1997).

1.2.2.3. Gondwana margin-Cimmerian continents

The Anatolide-Tauride Block (Turkey)

The Anatolide-Tauride Block (herein ATB) is bounded in the north by the Sakarya Zone through the IAES, in the southwest by the Mediterranean Sea, and in the southeast by the Arabian platform through the southeast Anatolian suture (or Assyrian suture, Figure 1.3). During the Late Cretaceous-Paleocene subduction, obduction and collision, the composite ATB was in lower structural position, so that it underwent much stronger deformation (mainly south-vergent nappes) and regional metamorphism than the northerly zones.

A convenient description of the ATB may be done by distinguishing the Taurides from the Anatolides; in this way the Anatolides represent the (metamorphic) northern margin of the ATB, whereas in the south the Taurides consist of a series of unmetamorphosed nappes (Figure 1.3).

The Anatolides are made of five tectonic zones: (1) the Bornova flysch Zone is a chaotically deformed Late Maastrichtian to Paleocene greywacke series, with middle Triassic-lower Cretaceous neritic limestones, Senonian red pelagic limestones, and rarer peridotite, radiolarian chert and basalt blocks (Şahıncı, 1976; Poisson and Şahıncı, 1988; Okay and Sıyako, 1993). (2) The Tavşanlı Zone is a belt of regionally metamorphosed and deformed blueschists tectonically overlain by the accretionary complexes and peridotite slabs of the IAES. The time of the blueschist metamorphism was Campanian (Okay, 1984; Okay and Kelley, 1994; Sherlock et al., 1999). (3) The Afyon Zone is a Paleozoic to Mesozoic sedimentary sequence that underwent greenschist metamorphism during the Paleocene. The lower part of the Afyon Zone consist of olistostromal meta-clastics alternating with meta-volcanics, black slates and lydites. The age of neritic limestone olistoliths ranges from Devonian to Early Carboniferous. The basement is unconformably overlain by clastics of Scythian age. The Middle Triassic-Campanian succession is made of platform carbonates overlain by lower Maastrichtian pelagic micrites, radiolarian chert and siliceous shales. They are followed by a thick olistostrome unit of Late Maastrichtian-Paleocene age, with ophiolite, blueschist, radiolarite and limestone blocks. Klippes of peridotites lie over the previous lithologies (Okay, 1984; Göncüoğlu et al., 1996-1997). The Afyon Zone plus the Tavşanlı Zone are the same as the Kütahya-Bolkardağ Belt from Göncüoğlu et al. (1996-1997). (4) The Menderes Massif consists in a thick succession made of a Precambrian gneiss basement , a Paleozoic "schist envelope" covering the gneissic core, and a Mesozoic-Cenozoic "marble envelope" overlying both. The Menderes Massif represents a core complex with a complicated tectonometamorphic history; the age of the greenschist to amphibolite metamorphism is Middle Eocene and the final exhumation phase took place in the Early Miocene (see Bozkurt and Oberhansli, 2001, and ref. therein). (5) The Central Anatolian Crystalline Complex (or Kirşehir Massif) consists of medium- to high-grade metasediments (mainly marbles) of Precambrian to Late Mesozoic age and meta-ophiolites. The regional metamorphism varies from greenschist to granulite facies and is thought to be Late Cretaceous (Göncuöglu, 1986). The metamorphic rocks are tectonically overlain by unmetamorphosed Late Cretaceous accretionary complexes of basalt, radiolarian chert, pelagic limestone, sandstone and serpentinite. The whole massif is intruded by voluminous Cretaceous calc-alkaline granitoids (e.g. Güleç, 1994; Akıman et al., 1993). Upper Maastrichtian sediments give an upper age limit for the regional metamorphism and the granitic magmatism.

The Taurides are made of a series of nappes (metamorphosed or not), both northerly (e.g. Lycian, Hadım, Hoyran, Beyşehir nappes), and southerly (e.g. Antalya nappe) derived. From a stratigraphic point of view, the Taurides are made of a pre-Cambrian basement, a discontinuous Cambrian to Devonian succession dominated by siliciclastic rocks, a Permo-Carboniferous sequence of intercalated limestone, shale and quartzite, and a thick upper Triassic to Upper Cretaceous carbonate sequence (Figure 1.10).

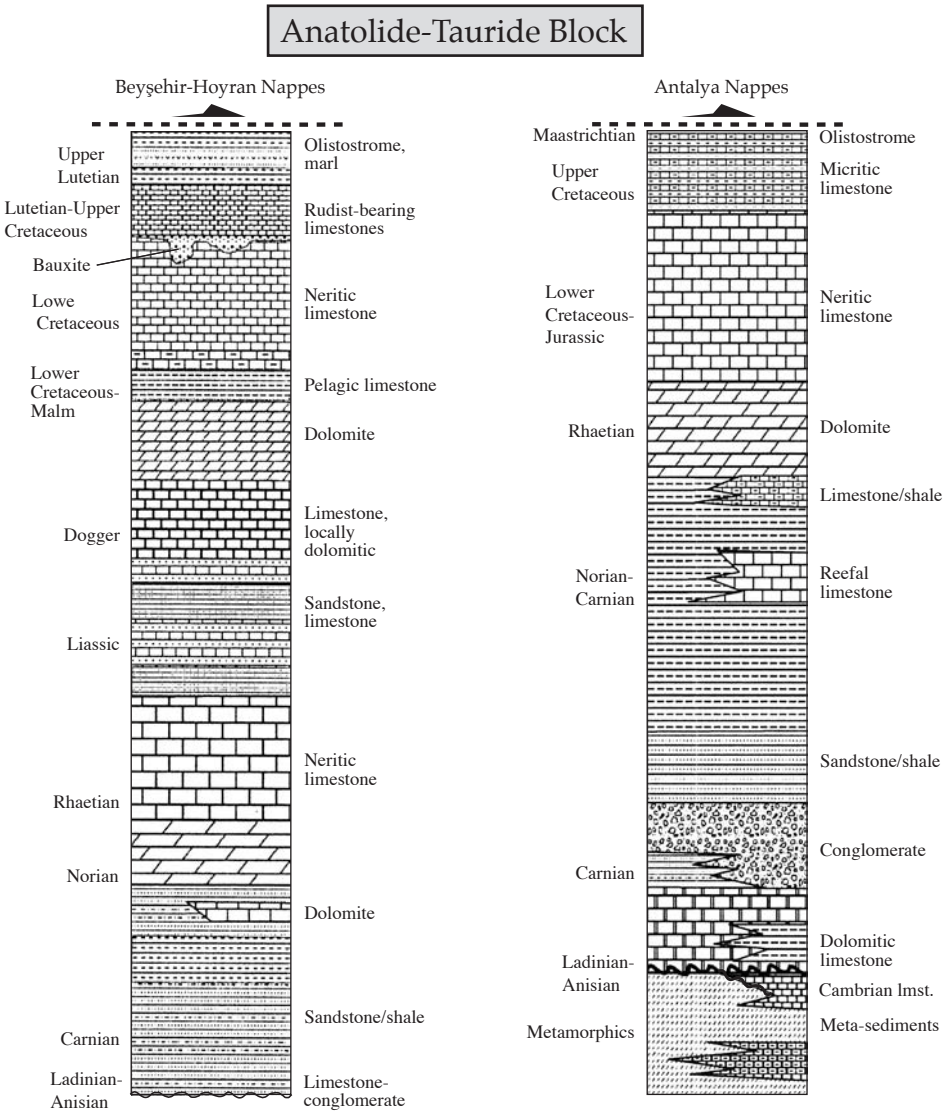

Figure 1.10. Two examples of stratigraphic sections from the Taurides, from Gutnic et al. (1979); left: Anamas-Akseki autochthon; right: Karacahısar autochthon.

In a paleogeographic perspective, most of the Taurides are a part of the Cimmerian ribbon-like continent, which has drifted away from Gondwana in the Permian, leading to the closing of the Paleotethys in the north and the opening of Neotethys in the south. The rest of the ATB has an Hercynian signature and was derived from Laurasia (Eo-Cimmerian event).

The External carbonate platform of the Hellenides (Greece)

The External carbonate platform of the Hellenides (herein EH) is located in the western part of continental Greece and in Crete (Figure 1.4-1.9). The EH comprises the non-metamorphic unit of Paxos, Kastellorizo, Ionian, Gavrovo and Tripolis and the metamorphic units (post-Upper Eocene age) of Mani, western Crete, Trypali, Amorgos, Olympos, Almyropotamos and Kerketas (Papanikolaou, 1989). Apart from the Ionian and Mani units which are made of pelagic sediments since the Liassic, all the units of the EH are characterized by Triassic to Eocene neritic sedimentation. All of them end by flysch sedimentation in the Late Eocene-Oligocene (Godfriaux, 1968; Fleury, 1980, and Figure 1.10). On the other hand, their pre-Late Triassic sequences are different due to changeable paleogeographic conditions. From a paleogeographic point of view, the EH are a part of Greater Apulia, one of the Cimmerian continents (Stampfli and Mosar, 1999).

1.3. Geology of the Biga Peninsula and main issues of the thesis

From a geographic point of view, the Biga Peninsula forms the northwest extremity of Turkey. It is bounded in the north by the Marmara Sea, in the east by the Aegean Sea and in the south by the Edremit Gulf, partially closed by Lesvos Island. The mythological city of Troy is the most famous place of the peninsula.

From a geological point of view, the peninsula represents the western end of the Sakarya Zone (Figure 1.3). At the first glance on a geological map (Figure 1.11), the geology of the Biga Peninsula is dominated by two main features: (1) the widespread occurrence of Tertiary plutonic and associated volcanic rocks (for the former always associated with metamorphic bodies), and (2) the general northeast-southwest trend of all the geological units, underlined by numerous, mainly strike-slip, dextral faults. Both features are characteristic of Middle-Late Tertiary events. The magmatism is the result of the arc emplacement related to the nortward subducting Mediterranean slab (references and discussion in Okay and Satır, 2000), whereas the tectonic activity is the expression of the combined activity of the southern branch of the NAFZ and the Aegean extension (e.g. Armijo et. al, 1999).

Another noteworthy feature is the large occurrence of the various units of the Karakaya Complex, as in the rest of the Sakarya Zone. Besides, it is to better describe and understand the Karakaya Complex that the whole mapping of the Biga Peninsula at the 1/25'000 scale has been led and completed by Okay and colleagues (1991). At the same time, they unexpectedly discovered and individualized the Çetmi mélange and the Denizgören ophiolite-Ezine Group (herein Ezine area), subjects of this thesis (Figure 1.11). The main interest of the thesis lies in the fact that no reasonable explanation for their genesis has been proposed since, and that most often they are not taken into account when dealing with the geological evolution of the region. Thus the first objective of the thesis was to refine our limited knowledge on these objects in order to propose a coherent scenario for their geodynamic evolution. The critical questions to answer will be:

-Where are coming the various lithologies found today in the Çetmi mélange from ?
-How were they brought together ?
-What are the primary relationships between the Denizgören ophiolite and the underlying Ezine Group ?

-Is there a direct or indirect link between the Çetmi mélange and the Ezine area ?

At a smaller scale, the Biga Peninsula is actually a key area for the understanding of the geological evolution of the Aegean domain; indeed, it is located at the crossroad of various paleogeographic domains, including the Rhodope-Strandja Zone (and Thrace basin) in the north, the Istanbul Zone, the Sakarya Zone, and the ATB in the Turkish side, and Greece in the west (Figure 1.3). It is the reason why the scenario for its evolution (and therefore that of the Çetmi mélange and Ezine area) must also take into account the geological constraints imposed by these bordering regions. This can only be done by comparison and tentative of correlation with the latter, trying to find good lateral equivalents to the Çetmi mélange and the Ezine area. In practical terms, the necessary regional approach will lead to reassess the interpretation of some of the neighbouring suture (IPS and IAES), and therefore to re-examine the evolution of their associated oceanic domains.

Nevertheless, whatever the envisaged scenario for the emplacement of the Çetmi mélange and the Ezine Group is, it could not explain the present-day situation. The Late Cretaceous-Tertiary period is marked in the region by several extensive (as well as compressive) phases which led to the exhumation of deeply buried rocks (e.g. in the Rhodope).

The Kazdağ Massif, located in southern Biga Peninsula, is an example of such extensive structure, exhumed in the Late Tertiary (Okay and Satır, 2000). An important point is that the Çetmi mélange is in the hanging-wall position during the exhumation history of the Kazdağ Core Complex (herein KCC). The second objective of the thesis is therefore to better constraint the exhumation processes of the KCC, in order to find a link between the pre-extensional (represented by the Çetmi mélange) and extensional regimes (represented by the KCC). Here again, The exhumation process must be compared with the cases already known in the region; this, in turn, will lead to propose a model for the Tertiary evolution of the Biga Peninsula.

Figure 1.11. (next page) Geological map of Biga Peninsula, Thrace basin and Lesvos Island. Compiled from Sıyako et al. (1989), Okay et al. (1991), Turgut and Eseller (2000), Sakınç et al. (1988), Hatzipanagiotou and Pe-Piper (1995), Kelepertsis and Velitzelos (1992).

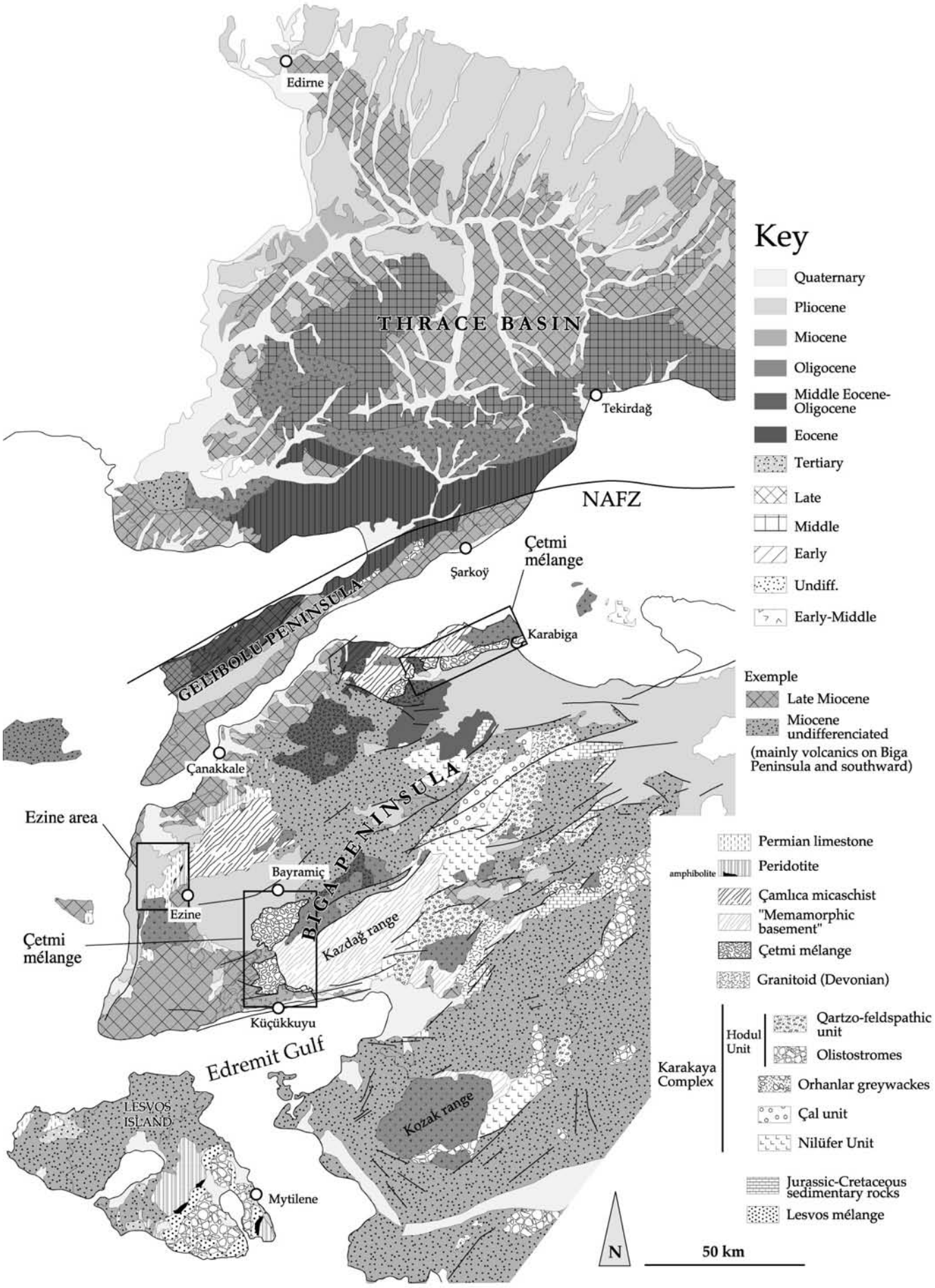
Edirne
THRACE BASIN
Tekirdağ
NAFZ
Şarkoÿ
Çetmi mélange
Karabiga
GELİBOLU-PENINSULA
Çanakkale
BIGA PENINSULA
Ezine area
Bayramiç
Ezine
Çetmi mélange
Kazdağ range
Küçükkuyu
Edremit Gulf
LESVOS ISLAND
Mytilene
Kozak range
Key
Quaternary
Pliocene
Miocene
Oligocene
Middle Eocene-Oligocene
Eocene
Tertiary
Late
Middle
Early
Undiff.
Early-Middle
Exemple
Late Miocene
Miocene undifferenciated
(mainly volcanics on Biga Peninsula and southward)
Permian limestone
amphibolite
Peridotite
Çamlıca micaschist
"Memamorphic basement"
Çetmi mélange
Granitoid (Devonian)
Karakaya Complex
Hodul Unit
Qartzo-feldspathic unit
Olistostromes
Orhanlar greywackes
Çal unit
Nilüfer Unit
Jurassic-Cretaceous sedimentary rocks
Lesvos mélange
N
50 km

- CHAPTER 2 -

THE ÇETMI MÉLANGE: GEOLOGY AND CORRELATIONS

This second chapter deals with the geological study of the Çetmi mélange, one of the three case-studies of the thesis (together with the geology of the Ezine area and the exhumation of the Kazdağ Massif). After an introduction to the concept of mélange, the geological characteristics of the Çetmi mélange, such as the nature of the blocks and the matrix, are described; the last part presents the possible correlations of the mélange with already known geological units of the north-Aegean region.

2.1. The concept of mélange in geology

Mélanges are now considered as classical geological objects, and their identification and understanding is essential, specifically in a paleotectonic and paleogeographic perspective. This first part gives an outline on the mélange concept and its signification.

2.1.1. Definition and classification of mélanges

Chaotic rock complexes were already recognized in the Late 19th and Early 20th century in the Himalaya Mountains; they were interpreted either as "volcano sedimentary formation" (rather with a sedimentary origin) or as the mixture due to the overthrusting of regional nappes (rather with a tectonic origin). These two interpretations are still influencing the understanding of such complexes today (Dimitrijevic et al., 2000).

The term mélange has been first used in a geological context by Greenly in 1919 to describe a chaotic unit in Anglesey, Wales (Gwna mélange). The term was resurrected (after more than 30 years of purgatory) by Bailey and McCallien in Turkey (Ankara mélanges, 1950, 1953), Gansser in Iran (coloured mélanges, 1955), Hsü in California (Franciscan mélanges, 1966, 1968), and the term mélange has been widely applied to rock bodies throughout the world. The advent of plate tectonics definitively confirmed the importance of the recognition of the ophiolitic mélanges in a geodynamic perspective.

This sudden success gave rise to a variety of definitions, following various descriptions and classifications throughout the world. The result was a confused situation in which everyone was giving its own definition according to his observations (table 2.1). A recurrent question encountered by authors was about the use of the term mélange: should it be reserved only for tectonic mixtures or used in a broader way (tectonic, sedimentary, diapiric or polygenetic mixture) ? In other words, should the definition be descriptive or genetic ? Other points were also discussed, such as the role of the composition of the matrix, the occurrence or not of exotic blocks, the fact that the definition must fit or not with Greenly's original criteria. The purpose of the Penrose Conference on mélanges (Santa Barbara, 1978) was to clarify this communication problem on their genesis and definition. But here again, no consensus was reached (Silver and Beutner, 1980).

Besides these semantic problems (which were actually hiding basic problems), new terms have been introduced in the geological vocabulary, such as olistostrome and ophiolitic mélange, still in use today. Olistostromes have been first defined by Flores (1955), as "a sedimentary slide deposit characterized by bodies of harder rocks mixed and dispersed in a matrix" (Flores, 1955, modified by Abbate et al., 1970); as for the term ophiolitic mélange, it

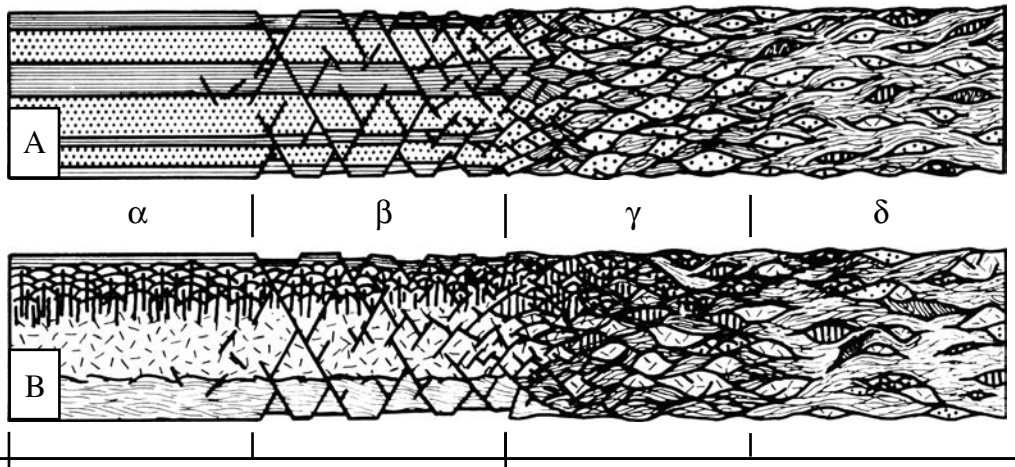

IA	Formation (or Complex)		Mélange (T) / Olistostrome (S)	
IB	Formation (or Complex)		Mélange (S or T)	
II	Formation (or Complex)		Mélange (*matrix ultramafic*) / Olistostrome (*matrix pelitic*)	
III	Formation (or Complex)		Mélange	*Tectonic mélange (T)* *Ophiolitic mélange (S & T)* *Olistostrome (S)*
IV	Formation (or Complex)	Broken Formation (T)		Mélange (T) / Olistostrome (S)
V	Formation *Fault block (T)* *Formation (S)*	Broken Formation (T)	*Tectonically broken fm.* *Endolistostromes*	Mélange *Tectonic mélange (T)* *Allolistostrome*
VI	Formation (or Complex)	Broken Formation (T)	Mélange	
VII	Formation (or Complex)		Broken Formation (T)	Mélange
VIII	Coherent Unit *Formation (S)* *Complex (I)*	Broken Unit *Broken formation (S & T)*	Dismembered Unit *Dismembered fm. or Complex (T)* *Endolistostrome (S)*	Mélange *Tectonic mélange* *Polygenetic mélange* *Allolistostrome*

Table 2.1. Character and classification of mélanges and related rock bodies (from Raymond, 1984). A-Schematic diagram depicting progressive fragmentation and mixing of interbedded sandstone / shale sequence. Continuum is divided into four types of unit (a, b, g, d). B-Schematic diagram depicting ophiolite progressively fragmented and mixed. IA-VIII: eight possible types of classification of the mélanges and related rock bodies from the literature. IA-Greenly (1919); IB-Cowan (1978), Hsu (1974); II- Knipper (1971), Kurenkov (1978), Zhang and Jin (1979); III- Gansser (1974); IV- Hsu (1968); V- Raymond (1978); VI and VII, no ref.; VIII- Raymond (1984).

has been introduced by Gansser (1974) to designate hybrid (both tectonic and sedimentary) mélanges, composed, at least in part, of ophiolitic material (including related pelagic sediments).

Finally, Raymond (1984) gave a new descriptive definition and classification of mélange (Type VIII in table 2.1), in the aim to gather in one definition all the different previous points of view: a mélange is then a *body of rock mappable at a scale of 1:24000 or smaller and characterized both by the lack of internal continuity of contacts or strata and by the inclusion of fragments and blocks of all sizes, both exotic and native, embedded in a fragmented matrix of finer-grained material*. Mélange are then subdivided into tectonic mélanges, sedimentary mélanges (allolistostromes), diapiric mélanges and polygenetic mélanges depending on the primary cause of fragmentation and mixing (tectonic, sedimentary, diapiric or a combination of these processes, respectively).

As it is often the case in geology, the pure descriptive approach seems to be the best, and Raymond's definition is still in use today. However, another trend in the literature is to use the term mélange as a synonym of fossil accretionary prism, with a tectonic connotation. The term olistostrome is then reserved for sedimentary mélanges, whereas the term broken formation is sometimes used to characterize formation broken by faults, but which retain substantial continuity of contacts.

Mélanges have been described in many tectonic environments, including subduction zones (Aalto, 1981; Kusky et al., 1997; Taira et al., 1997; Spötl et al., 1998; Halamic et al., 1999; Meschede et al., 1999; Wakabayashi, 1999), fore-arc and back-arc basins (Page and Suppe, 1981; Guangfu et al., 1994; Brown and Spadea, 1999), synorogenic thrust fault zone (Vollmer and Bosworth, 1984), oceanic transform faults (Saleeby, 1984), passive continental margins (Jacobi, 1984; Torelli et al., 1997). Therefore, active convergent margin represent only a possibility among all the possible tectonic settings for the mélange genesis; however, most of the recent studies deal with subduction- or accretion-related mélanges.

2.1.2. The study of mélanges: methods and techniques

It clearly appears from the literature that there are two radically different ways (but complementary) to approach the study of a mélange.

2.1.2.1. Mélange as structural objects

In this way, the mélange is considered "for and by itself", as a kind of big-scale laboratory. The aim is then to unravel its internal structure and complex organisation, by explaining the timing of the different deformation phases, and at a larger scale the mélange-forming processes. This local approach has been applied with success to the mélanges considered as pieces of former accretionary complexes. Authors propose different methods to obtain meaningful information; the most common is a classical structural approach based on a detailed field work (Mercier and Vergely, 1972; Barnes and Korsch, 1990; Needham, 1995; Chan, 1997; Channell and Kozur, 1997; Steen and Andresen, 1997; Cousineau, 1998; Kusky and Bradley, 1999; Vergely and Mercier, 2000; Harrington and Cloos, 2001; Vissers et al., 2001; Calon et al., 2002). Additional techniques may be used in complement of structural analysis, including seismic (Harris, 2000), mineralogy and petrography of metamorphic rocks (Tsujimori, 1998; Blake and Wentworht, 2000), fission track thermochronology (Hasebe et al., 1997; Ohmori et al., 1997), magnetic fabric analysis (Ujiie et al., 2000). A first attempt to use fractal properties of mélange in order to describe its internal organisation (based on geometrical self-similarity relationships) has been even done recently (Catani and Vannucchi, 1998).

2.1.2.2. Paleotectonic evolution inferred from the study of mélanges

Another way to study a mélange is rather to consider it as a witness of the history of the regional geology. For instance, instead of focussing only on the internal organisation of the blocks in the matrix, the geologist tries to know more on the block and the matrix themselves (e.g. nature, age, origin, etc…). By doing this, it is possible to obtain information not only about the formation of the mélange, but also on the evolution history of the adjacent areas. Here again, this regional approach showed its worth when applied to accretionary

mélanges, because they record what has happened both on the ocean and arc sides. Thus different methods, usually associated with a detailed field work, have been used by authors including stratigraphy (Koçyigit, 1991), tectonics (Tekeli, 1981; Collins and Robertson, 1997), (micro)paleontology (Wiedmann et al., 1992; Bragin and Tekin, 1996), geochemistry and petrography of magmatic rocks (Tankut, 1984; Floyd, 1993; Pickett and Robertson, 1996; Tankut et al., 1998; Robertson, 2000; Ucurum, 2000) (the examples are only taken from the literature on Turkish mélanges).

How did I proceed ?

The first approach provides information about the mechanics of deformation during the mélange emplacement (local and mechanical approach), whereas the second deals with the relationships in space and time between the mélange and neighbouring areas (regional and historical approach). In front of a mélange, a geologist would have to choose his way, depending on the question he wants to answer : how and why does a mélange work, or, how and why is there a mélange here ? The study of the Çetmi mélange mostly tries to answer the second one, so that I join up the second type of study.

This has of course implications on the methodology. The first one was to gather the maximum of data/information that may contain a potential for historical geology; this led to a special focus on the age of the various lithologies of the mélange. Another important implication was the systematic focus on the nature of the different lithologies (blocks and matrix) besides their age, such as their size, proportion, depositional paleotectonic environment, etc…, rather than on their deformational and structural aspect. The latter has of course been tackled, but not as a priority. However, the study of the Çetmi mélange is clearly a multidisciplinary approach (sedimentology, micropalaeontology, geochemistry, tectonics, etc…), and not the application of a single method. Because of the intrinsic nature of mélanges, such a multidisciplinary (integrated) approach has more chance to give a coherent result than the use of a single one. Then the fieldwork (mapping and sampling) had to be as exhaustive as possible, not to miss something important; much time has been spent in this way.

2.2. The Çetmi mélange: location and structural frame

The first map on which the area of the Çetmi mélange has appeared, is that of Van der Kaaden (1959) (Figure 2.1). In 1975, Bingöl et al. published the first complete map of the Biga Peninsula, including the regions covered by the Çetmi mélange (Figure 2.2). Both maps show that the mélange was not considered as a single entity, and that in a general way, the lithologies were believed to be older than their current age. However, the first occurrence in the literature of the mélange for itself is due to Okay et al. (1991), after the whole mapping of the peninsula at the 1/25'000 scale.

As demonstrated in the previous paper and confirmed by the first field-missions, the mélange is mainly cropping out in two different places through the peninsula (Figure 1.11): (1) in the northern part of the Biga Peninsula, north of Biga and westward of Karabiga to the Kemer Stream, and slightly farther west of it. (2) In the southern part of the peninsula, north of Küçükkuyu and south of Bayramiç. Because their similarities are more important than their differences, the two areas are treated together, with particular comments when necessary. The mélange west of Karabiga is equally called Karabiga mélange or northern

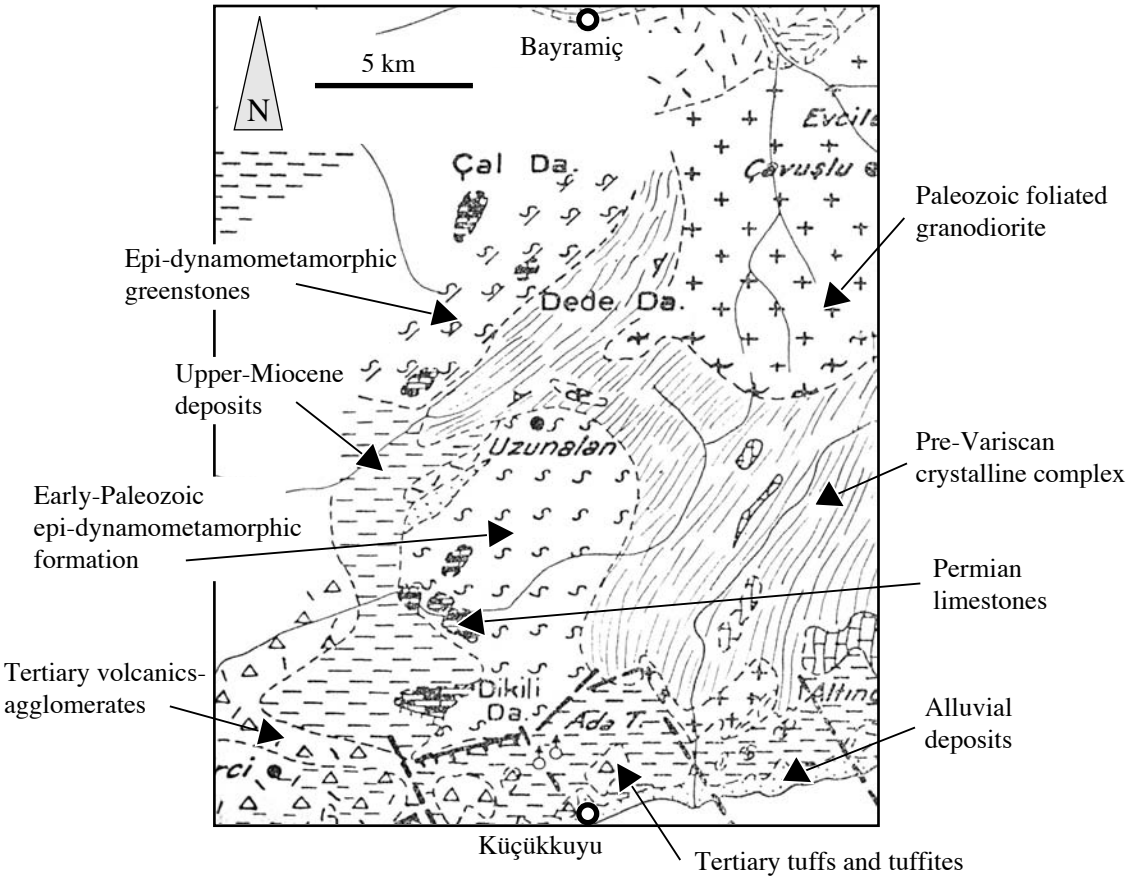

Figure 2.1. Detail of the geological map of the Kazdağ region and immediate surroundings, showing the area of the southern mélange, by Van der Kaaden (1959).

mélange, whereas the mélange north of Küçükkuyu is called southern mélange. Two small outcrops of the Çetmi mélange also occur in the Gelibolu Peninsula, north of Şarkoÿ (c.f. 2.4.2). The name of the Çetmi mélange derives from the Çetmibaşıyürükleri village north of Küçükkuyu.

Most of the northern mélange has been mapped at the 1/25'000 scale, and most of the southern mélange at the 1/15'000 scale, during several fieldworks in spring 1999, 2000, 2001 and 2002, and autumn 1999 and 2000. The corresponding maps at the 1/50'000 scale are found in plate 8, 9A and 9B respectively.

2.2.1. Outline on the geology of Çetmi mélange

The northern mélange

The Çetmi mélange in the northern area is an almost continuous elongated structure of c. 35 km long on c. 1 to 3 km wide, with a total surface of about 40 km^2.

In its northern side, the mélange, locally slightly metamorphosed, is in tectonic contact with the high-grade rocks of the Çamlıca micaschists. The contact consists of Late Tertiary E-W and NE-SW trending, steeply dipping faults, most of the time marked by serpentinite slivers (cross-sections Figure 2.3). The age of the Çamlıca micaschists is unknown, but similar micaschists in the eclogite facies west of Ezine have yield a Maastrichtian age (65-69 Ma on phengites with the Rb/Sr method, Okay and Satır, 2000). Due to the fact that

the micaschists must have been exhumed after the emplacement of the mélange, as seen from the present-day structural relationships, the serpentinites slivers may represent the base of the mélange. The mélange and the micaschists are both intruded by the Karabiga granodiorite. On its southern side, various Tertiary and Quaternary sedimentary and volcanic rocks unconformably overlie the mélange.

In order of decreasing abundance, the mélange is made of slices/blocks of altered basic and pyroclastic rocks in greenschist facies (spilites, 33.5%), sandstone/shale alternation (Doğandere Sandstone, 22%), blocks of upper Triassic neritic limestones (20%), serpentinite slices (11%), greywacke-shale alternation (matrix, 9%), blocks of upper Jurassic/lower Cretaceous red radiolarites and radiolarite/red micrite alternations (1.5%), and undetermined various lithologies (mainly small blocks of the previously cited, 3%) (Figure 2.4).

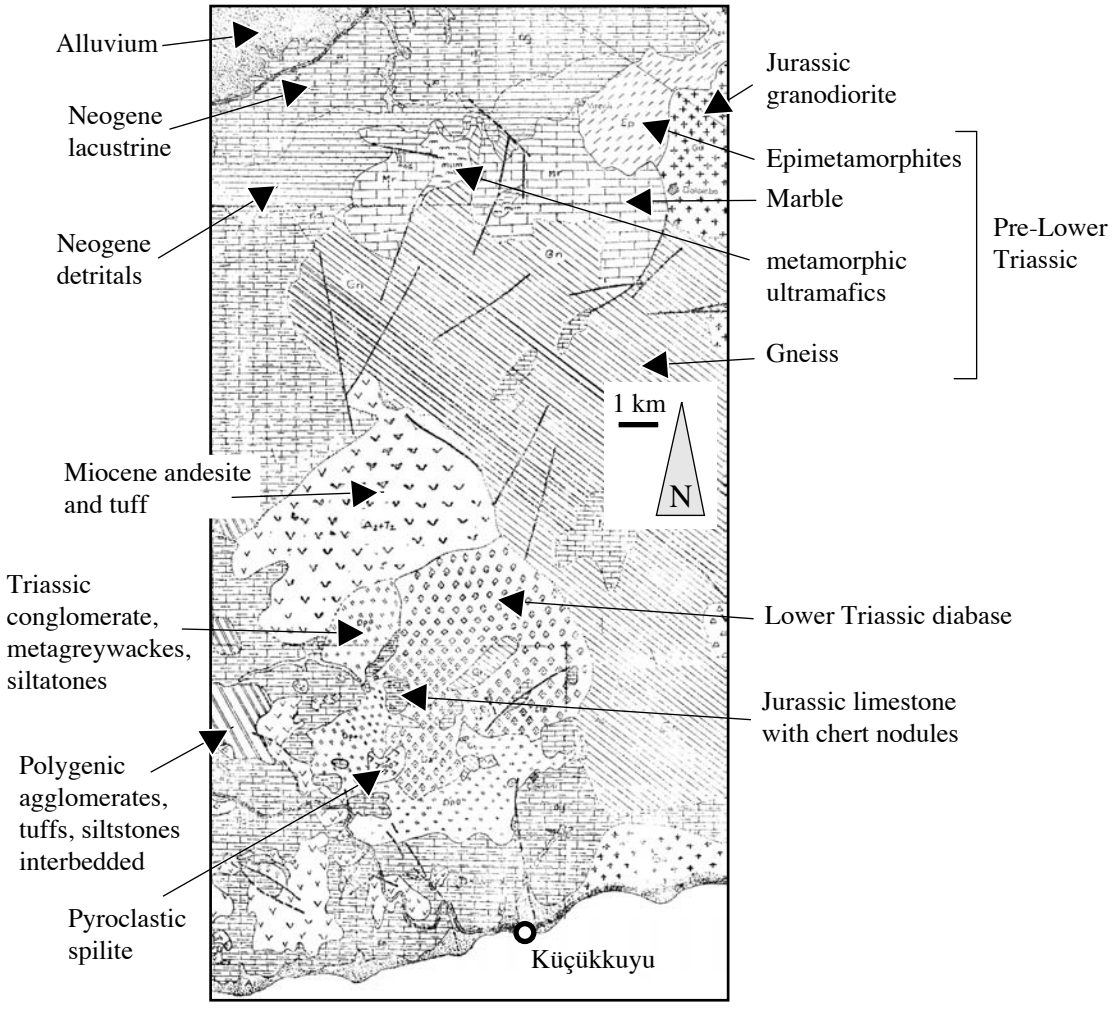

Figure 2.2. Detail of the geological map of the Biga Peninsula showing the area of the southern mélange, by Bingöl et al. (1975).

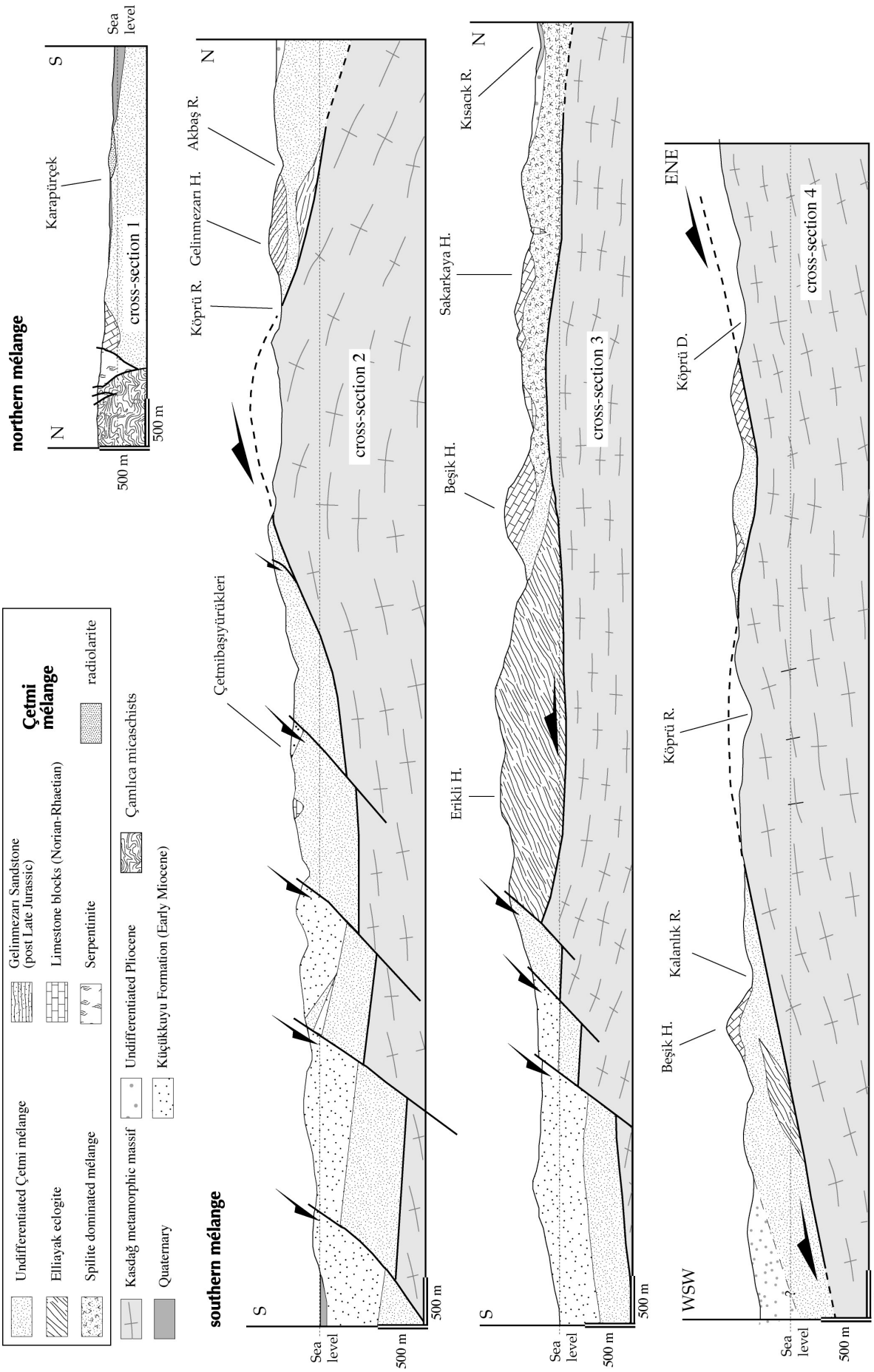

Figure 2.3. Cross-sections through the Çetmi mélange in the northern and southern area, both at 1/50'000 scale; see Figure 2.7 for location of cross-section 1, and Figure 2.6 for cross-sections 2, 3 and 4.

The southern mélange

The Çetmi mélange in the southern area is made of two subzones, the northern one south of Bayramiç, and the southern one north of Küçükkuyu. Its total surface is about 100 km^2.

The mélange is structurally underlain by the high-grade metamorphic rocks of the Kazdağ Massif (or Kazdağ Core Complex, thereafter KCC). South of Bayramiç, an intervening 2 km thick mylonitic zone (Alakeçi Mylonite Zone) makes the transition between the Çetmi mélange and the KCC. The transition between the unmetamorphosed mélange and the mylonites is partially marked by two tectonic lenses of serpentinite. Therefore, a common feature to the northern and southern mélange is the occurrence of serpentinite bodies at their base, marking in both places the transition to the underlying high-grade metamorphic rocks. North of Küçükkuyu, the mélange is directly in tectonic contact with the KCC through a low-angle normal dipping brittle fault (c.f. chapter 4). Moreover two exotic blocks of eclogite-micaschist occur in the southern subzone, at the lowest structural level (cross-sections 3 and 4, Figure 2.3). Between the two subzones the mélange is in tectonic contact with the KCC along a WNW trending sinistral transtensional strike-slip fault (Uzunalan fault). In the three places various types of Neogene sedimentary and volcano-sedimentary rocks unconformably overlie the mélange.

In order of decreasing abundance, the mélange is made of slices/blocks of altered basaltic-andesitic and pyroclastic rocks (spilites, 46%). blocks of upper Triassic neritic and pelagic limestones (31%), greywacke-shale alternation (matrix, 9%), undetermined various lithologies (mainly small blocks of the previously cited, 7%), slices of micaschist-eclogite (4%), sandstone-shale alternation (Gelinmezarı Sandstone, 2%), two slices of serpentinite/listvaenite (1%), and less than 0.5% of radiolarites (Figure 2.4).

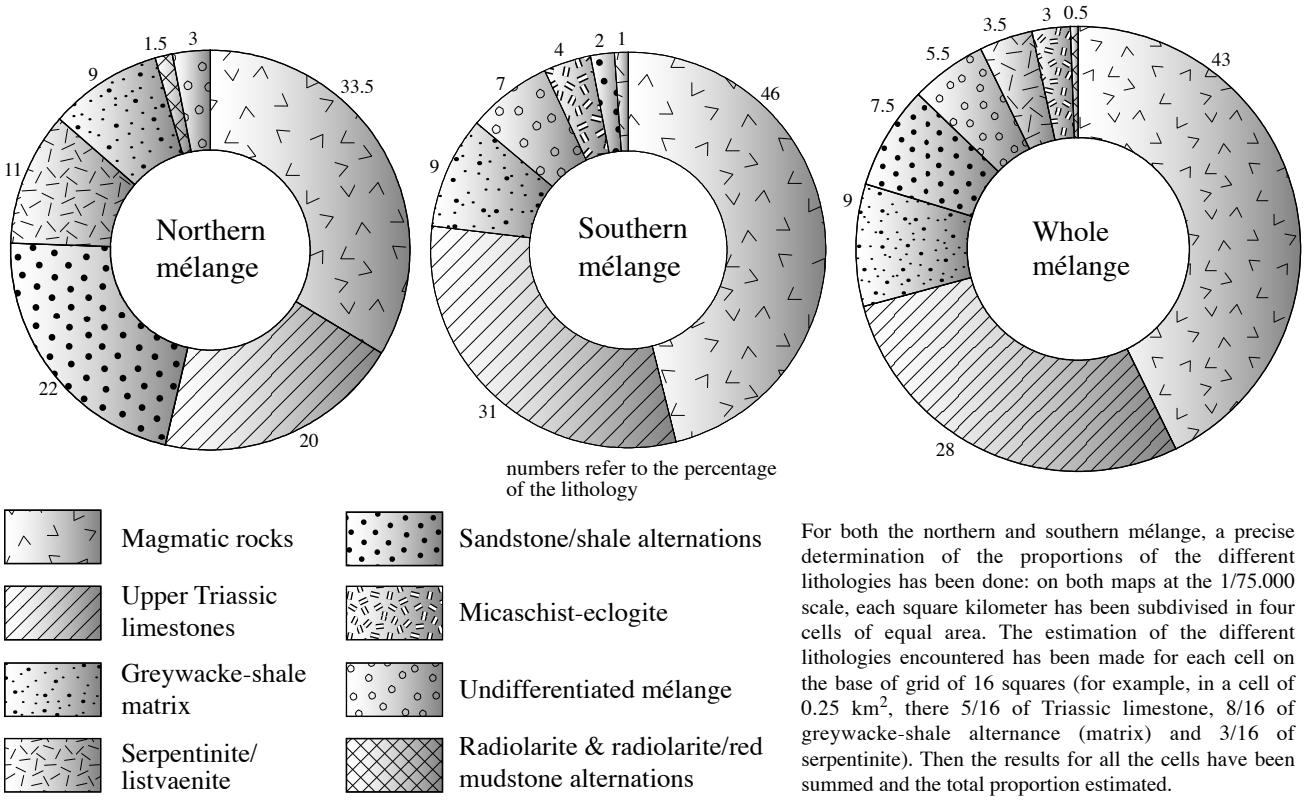

Figure 2.4. Estimation of the proportions of the different lithologies in the Çetmi mélange.

2.2.2. Structural observations, mode of emplacement

The Çetmi mélange shows a complex internal structure, which is at the origin of its name. Its present-day internal organisation is the result of several deformation stages which occurred during its evolution. However, the present-day structure is mostly the result of the Plio-Quaternary transtensional and extensional stages (propagation of the NAFZ in the north and final exhumation of the Kazdağ Massif in the south, chapter 4). The latter is for instance responsible for the pelicular aspect of the Çetmi mélange north of Küçükkuyu, which reaches the maximum thickness of several hundred metres (c.f. the cross-sections fig 2.3). This part deals with the structural aspect of some lithologies of the mélange, and the relationships between them.

The blocks

Late Triassic limestone

In the northern mélange, a several km long limestone block with a characteristic elongated shape occur south of the Karabiga granodiorite, and several smaller limestone blocks are aligned with it westward. In the northern subzone of the southern mélange, the two pluri-km limestone blocks show a clear east-west alignment. Finally, in the southern subzone, the limestone blocks are aligned on two roughly north-south trends. In both occurences, these alignments are parallel to the structural limits of the mélange with the underlying metamorphic rocks, and are probably related to their exhumation. However, this suggests that the limestone blocks were continuous before the pre-late Tertiary tectonics, without having the possibility to assure that this tectonic phase is responsible for the fragmentation.

The limestone blocks are usually in tectonic contact with the spilitic magmatic rocks. They are also in contact with the greywacke-shale matrix, but not very often; in this case, the contact is now tectonic but may have been conformable before. A common observation is that the blocks may show soft sedimentary folding, but the surrounding rocks do not show any similar or related deformation. The limestone blocks have either (1) been brought tectonically in contact with the spilitic magmatic rocks, after having suffered soft deformation, or (2) they may have been brought in contact with the greywacke-shale matrix tectonically or by sedimentary sliding.

In the southern mélange, the external contact of the limestone blocks with the other mélange lithologies (mostly spilite) is often made of red pink silicified rocks, commonly brecciated, whose protolith is the limestones themselves. This silicification and tectonic brecciation may be due to circulation of siliceous fluids at the contact of the limestones blocks during the late tectonic phase; the hydrothermal event, involving siliceous fluids, may be the same which gave birth to the listvenites (c.f. chapter 4).

Radiolarite

Most of the time, the radiolarite blocks display a complex deformation pattern, from very slight folding to strong random small-scale folding. As for the limestone blocks, it is interpreted as the result of post deposition folding, when the sediment was still soft

and unconsolidated. The radiolarites are in tectonic contact with the magmatic rocks and the greywacke-shale matrix. None of them are affected by a related folding. Thus the radiolarites may have been brought in contact with the greywacke-shale matrix either by tectonic or sedimentary sliding.

The question of the primary contact of the radiolarites and the magmatic rocks remains important. No preferential association has been found between the radiolarites and the magmatic rocks of the mélange (volcanic arc basalt or within-plate basalts, c.f. 2.3.1.4). However, inter-pillow sediments have been found (but unfortunately not dated) in the few places were pillow structures occur (only in the VAB); sedimentation was therefore existing at the time of pillow formation, and it is possible that at least a part of the radiolarites may have been deposited in close association with them. In this case, the deformation regime responsible for the characteristic folding of the radiolarites would have also affected the magmatic rocks; the absence of similar deformation may be explained by their more competent rheology.

The eclogite

The two exotic micaschist-eclogite tectonic lenses are cropping out in the southern subzone of the mélange north of Küçükkuyu in a north-south line. An interesting fact is that they represent the lower structural level of the mélange and mark the tectonic boundary with the underlying Kazdağ Massif (cross-sections Figure 2.3). They also disturb the surrounding magmatic rocks (occurrence of foliation plus greenschist metamorphism), that is not the case elsewhere in the mélange. These observations support the hypothesis of a late emplacement of the micaschist-eclogite bodies under the Çetmi mélange by unroofing, after the emplacement of the magmatic rocks (c.f. 2.4.2).

The matrix

The greywacke-shale matrix shows a complex internal deformation, like small-scale folding and pervasively anastomosing small-scale shear zones. The greywackes layers are mold by the shaly material. This matrix actually accommodates the general deformation and wraps the more competent blocks when present. In the southern subzone of the Çetmi mélange north of Küçükkuyu, the general trend of the bedding is rather north-south (Figure 2.5), subparallel to the limit between the mélange and the Kazdağ Massif.

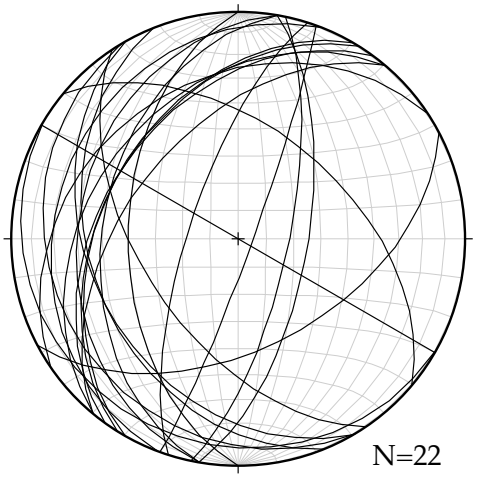

Figure 2.5. Bedding of the greywacke shale matrix in the southern subzone of the Çetmi mélange north of Küçükkuyu; equal area, lower hemisphere projection.

Conclusion

The primary cause of fragmentation and mixing of the various lithologies from the Çetmi mélange is tectonic, as seen from their contacts. However some sedimentary processes may have also occured, for instance gravity sliding of the limestone and radiolarite blocks in the matrix. Anyway, the Late Tertiary tectonic has certainly greatly modified the initial state of the mélange (pre-extensional state). In particular, the structural aspect of the mélange may have changed and the present day tectonic contacts may be due to the remobilization of former contacts, tectonic or not.

2.3. The blocks and the matrix of the Çetmi mélange

2.3.1. The blocks

2.3.1.1. Han Bulog limestone

These Han Bulog limestones (practically similar to the Hallstatt facies of the Northern Calcareous Alps) occur as rare tectonic blocks of red nodular limestones, only in the southern mélange. Their size ranges from several cm to several m for one block, with an average of a few dm. They are always located to the west of the upper Triassic limestone blocks.

The biggest one, about 7 m long and 3 m high, is cropping out along the Çaltıcak river, NW of the Kirca village (picture 2.1 plate 7A). It is the only block which gives an idea of the facies in its whole. It consists of slightly undulating beds of light pink to red micritic limestones, with some indeterminable ammonite prints; their thickness ranges from 5 to 40 cm. Its matrix is unfortunately not visible, the block being totally surrounded by the screes of the overhanging Sakarkaya limestone block.

Microfacies analysis and depositional environment.

The Han Bulog limestones have a light pink typical mudstone microfacies. The micritic matrix, which makes most of the thin sections, is slightly recrystallised and oxidized. Various allochems representing a maximum of 10% of the thin sections are present, including, from the most common to the less, thin characteristic bivalve shells (filaments, about 5%), microsparitic internal molds of radiolarians, some undetermined foraminiferas (rare), and very rare ostracods shells, sponge spicules and calcedonite recrystallisation in the pores. Pressure/dissolution surfaces marked by accumulation of insoluble oxidized and argillaceous residues are common (microstylolites), as well as calcite veins. The microstylolites tend laterally to a microbrechification of the micritic matrix. This microfacies association is typical of a pelagic environment, with possible influence of currents, due to the local imbrication and agglomeration of the filaments.

Age determination

10 samples from this type-block and from smaller blocks have been tested and processed for conodont preservation by repetitive leaching in 10 % formic acid (see appendix 1 for the preparation of the samples). Only three samples yielded an age-diagnostic conodont

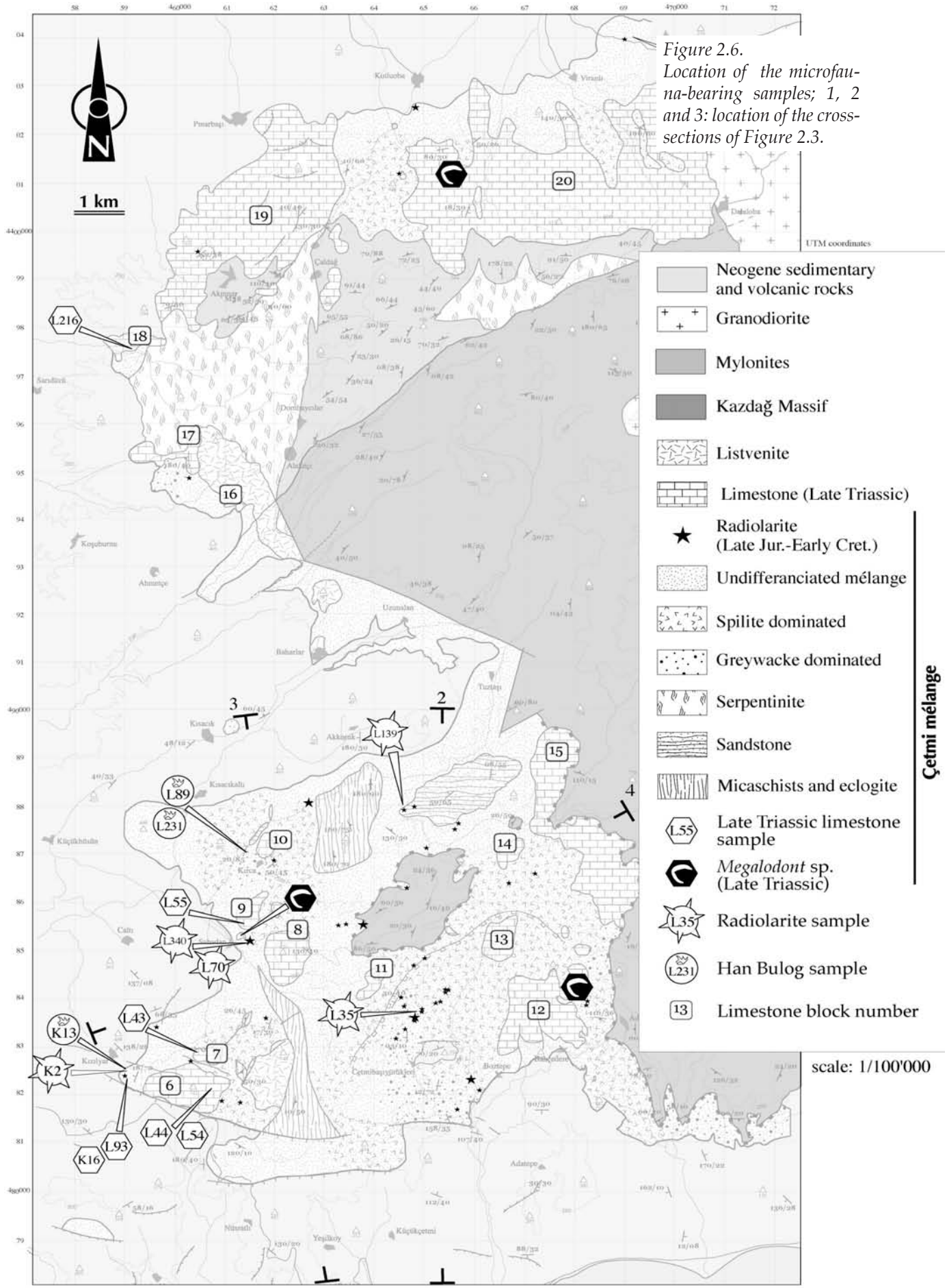

Figure 2.6.
Location of the microfauna-bearing samples; 1, 2 and 3: location of the cross-sections of Figure 2.3.

assemblages (determinations have been made by Dr. Kozur, Budapest); their CAI (Conodont Alteration Index) is 1, typical of a total absence of thermal alteration. The location of the samples is shown in Figure 2.6 and the pictures of the age-diagnostic taxa are found in plate 1. a) Sample L89 has yielded *Gladigondolella* sp., which is a pelagic conodont of latest Scythian to Middle Carnian age and *Nicoraella* cf. *kockeli* (Tatge). The latter is not identical with that species, but such forms are common in the open sea Tethys and have there a similar range as *Nicoraella* cf. *kockeli*. They occur mainly in the Pelsonian (Middle Anisian) but start already in the higher part of lower Anisian, where *Nicoraella* cf. *kockeli* is not yet present. The assemblage is therefore **Middle Anisian**, typical of fully pelagic, open sea environment (in agreement with the microfacies analysis). b) Sample L231 has yielded *Chiosella gondolelloides* (Bender), a conodont which occurs in the **uppermost Olenekian** (upper Spathian) and in the **lowermost Anisian** (Aegean). In absence of *Chiosella timorensis*, the index species of lowermost Anisian, this sample can be assigned to the late Spathian Chiosella gondolelloides Zone. c). Sample K13 has yieldedz *Paragondolella fueloepi* (Kovacs), a conodont typical of the **Ladinian**.

The Han Bulog limestones of the Çetmi mélange therefore records pelagic sedimentation in the **Late Scythian-Ladinian** interval.

2.3.1.2. Late Triassic limestone blocks

The light grey upper Triassic limestone blocks (picture 2.2 plate 7A) are a characteristic feature of the Çetmi mélange (Sakarkaya limestone from Okay et al., 1991). They occur in the southern mélange as well as in the northern one. Their size varies from a few metres (rare) to several kilometres; there is no pebble-size block.

In order (1) to make easier the understanding of the text by avoiding the multiplication of the Turkish names of the hills made by the blocks, and (2) to make easier the correspondence between the text and the map, a specific number has been attributed to each significant limestone block; the blocks from the Karabiga mélange thus range from 1 to 5 (*bn1* to *bn5*) and those from the southern area from 6 to 20 (*bn6* to *bn20*, see Figure 2.6 and 2.7); for instance the number 10 (*bn10*, for block number 10) is attributed to the block represented by Sakarkaya Hill, north of Kırca village.

The limestone blocks have been grouped in 2 sets based on their degree of recrystallization and are treated separately. Indeed some blocks show well-preserved original features, whereas others show recrystallized features, both in macro- and micro-observations.

Following the previous convention, *bn1, bn3, bn4, bn5, bn6, bn7, bn8, bn9, bn10, bn16, bn17* and *bn18* are belonging to the first category and *bn2, bn11, bn12, bn13, bn14, bn15, bn19* and *bn20* to the second. In the northern mélange as well as in the southern one, this spatial distribution is directly related to the occurrence of post mélange granodiorite, responsible for contact metamorphism and recrystallization.

Unrecrystallized limestone blocks

Lithology

Most of the limestones are medium to thickly bedded, except *bn8* and *bn10* which show 10-25 cm thick layers; some blocks display also chert nodules (*bn6*, *bn7* and *bn8*), sometimes abundant (*bn10*). Some intraformational breccias have been observed in *bn6*, *bn9* and *bn16*. Metre-scale red karstic fillings have been observed in *bn6*, but a karstic episode is also

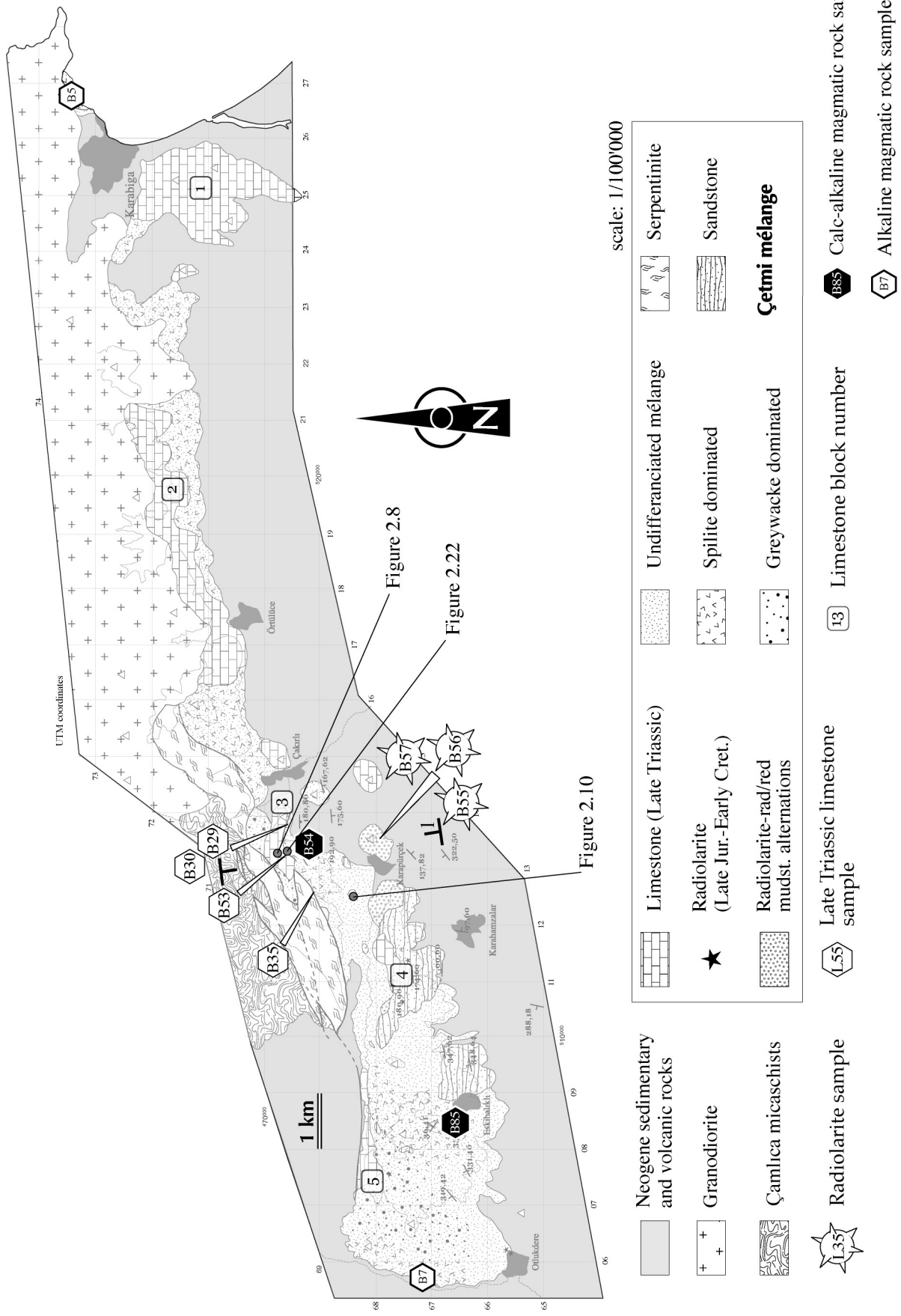

Figure 2.7. Location of the microfauna-bearing, magmatic samples and stratigraphic columns in the northern mélange area; 1: location of cross-section 1 of Figure 2.3.

suspected for some other blocks, based on indirect evidences (small filling-related red mudstones fragments in and around them).

Microfacies analysis and age determination

This paragraph describes the main characteristics of age-diagnostic samples. The location of the samples is shown in Figure 2.6 and 2.7, and pictures of age-diagnostic taxa are found in plate 2A, 2B, 2C and 2D (det. made by Dr. R. Martini and Pr. L. Zaninetti, Geneva).

Sample B29, B30, B53 from bn3

These sample are coming from *bn3* north of Karapürçek.
Microfacies analysis
The allochems (pellets, crinoid ossicles, foraminifera) are either edge-to-edge or arranged in a recrystallized sparitic cement. Authigenic quartz is common as well as calcite veins.
Classification (Dunham, 1962/Folk, 1962)
Packstone-grainstone/unsorted pelbiosparite
Age
B29 has yielded Duostominidae and *Pilamina* sp. of **Carnian-Rhaetian** age; B30 has yielded Duostominidae, *Aulotortus* gr. *sinuosus, Auloconus permodiscoides, Triasina hantkeni, Gandinella falsofriedli* of **Sevatian-Rhaetian** age; B53 has yielded Duostominidae, *Aulotortus* sp., *Glomospirella* sp. of **Middle-Late Triassic** age.

Sample B35

The sample is coming from a decametre-scale block west of *bn3* (not on the map) and is certainly a part of it detached by recent faulting. It has the same microfacies than B29 B30 and B53 from bn3.
Age
B35 has yielded *Ophtalmidiuim* sp., *Glomospirella* sp., *Gandinella falsofriedli* and *Aulotortus* sp. of **Sevatian-Rhaetian** age.

Sample L44 and L54 from bn6

These samples are coming from *bn6* which represent the biggest limestone block in the southern subzone of the mélange. Like *bn7*, the pale grey limestones are slightly recrystallized.
Microfacies analysis
The allochems, mainly made of crinoids ossicles (with syntaxial overgrowth), plus foraminifera, micritic pellets, rare gastropod and coral fragments, are often joined, but a micritic matrix and a sparitic cement are locally present. The whole is slightly dolomitized. Authigenic quartz is common and merges locally in quartz vein.
Classification
Packstone/poorly washed biopelsparite
Age
L44 has yielded *Ophtalmidium* sp. and "*Lenticulina*" sp. of **Carnian-Rhaetian** age and L54 has yielded *Ophtalmidium* sp., *Aulotortus* sp., *Frondicularia* sp. and Nodosariidae of **Carnian-Rhaetian** age as well.

Sample L43 from bn7

The sample is coming from *bn7* (east of Kızılyar village), which may represent a fragment of *bn6* separated from it by a recent fault. The limestones are slightly recrystallised.
Microfacies analysis
A secondary dolomitization has often modified the prevailing structure of the allochems (foraminifera, undetermined algae and micritic pellets), also obliterating the primary micritic nature of the matrix. Authigenic quartz and calcite veins are present.
Classification
Wackestone/sparse biopelmicrite
Age
This sample has yielded a poor foraminifera assemblage made of Duostominidae and Miliolidae characteristic

of the **Carnian-Rhaetian** interval (c.f. plate ?).

Sample L55 from bn9

It is coming from *bn9*, near Şabadan village. The light grey limestone block is made of medium size to massive layers. A abandoned quarry shows blocks with the Triassic Megalodontidae sp. bivalve (picture 2.3 plate 6A)
Microfacies analysis
The thin section shows a micritic matrix in which foraminifera, rare gastropods and ostracods occur. It also displays an isolated aggregate of preserved echinoderm ossicles embedded in the matrix. Authigenic quartz is common as well as calcite veins.
Classification
Mudstone/fossiliferous biomicrite
Age
This sample has yielded a rich foraminifera assemblage which comprises *Aulotortus* aff. *A. friedli*, *Aulotortus* aff. *A. communis*, *Aulotortus* aff. *communis*, *Glomospira* sp., *Auloconus permodiscoides* of **Norian-Rhaetian** age.

Sample L93

This sample is coming from a light grey decametre-scale block east of Kızılyar village (not on the map).
Microfacies analysis
The thin section displays various allochems such as crinoid ossicles, micritic pellets, undifferentiated bioclasts, foraminifera, and rare ostracods. A micritic matrix is rather rare, whereas sparitic calcite is common. There are many calcite veins.
Classification
Packstone/poorly washed biopelsparite
Age
The foraminifera assemblage is made of *Ophtalmidium* sp., Endotriada sp. and Duostominidae, typical for the **Middle-Late Triassic**.

Sample K16

The sample is coming from a small block east of Kızılyar village (not on the map), near from L93. It as the same microfacies than the latter (packstone).
Age
K16 has given a rich foraminifera assemblage comprising *Hoyenella inconstans*, *Endotriada tyrrhenica*, *"Trochammina"* aff. *almtalensis*, *Cyclogira* ? sp, Duostominidae and Miliolidae (**Carnian-Rhaetian**).

Sample L175

The sample is coming from a slightly recrystallized metre-scale block (not on the map) west of Kızıltepe village, in the northern part of the mélange. Despite its position in the eastern part of the southern mélange (i.e. near the Oligocene pluton) its primary features have been preserved.
Microfacies analysis
The thin section shows a common sparitic cement and a recrystallized micritic matrix in which it is difficult to recognize the original allochems (micritic pellets, crinoid ossicles, foraminifera). Many calcite veins occur, as well as an incipient secondary dolomitization.
Classification
Mudstone/fossiliferous pelbiomicrite
Age
The following poorly preserved foraminifera, *Endotebanella kocaeliensis*., *Endotriada thyrrhenica*, Miliolidae and Nodosariidae, gave a **Middle-Late Triassic age**.

Sample L216 from bn18

This sample is coming from a big limestone block (1 kilometre long, *bn18*) southwest of Akpınar village, in the northern part of the mélange.
Microfacies analysis
Allochems are widely represented by crinoid ossicles, foraminifera, micritic pellet, big ostracods, algae fragments (Thaumatoporella) and rare ooids. matrix and sparitic cement are both present, roughly in the same amount. Calcite veins are common.

Classification
Wackstone/poorly washed pelbiosparite
Age
A rich foraminifera assemblage made of *Glomospirella expansa*, *Triasina hantkeni*, *Aulotortus* gr. *sinuosis*, *Endotebanella kocaliensis*, *Auloconus permodiscoides* and Nodosariidae has given a **Norian (Sevatian)-Rhaetian** age.

The grey limestones of the Çetmi mélange in the northern and southern area have therefore been deposited during the **Norian-Rhaetian** interval.

Recrystallized limestone blocks

The recrystallized limestones, in close relation with Tertiary granodiorites, are characterized by "coarse grain" textures; the size of the calcite crystals is increasing with the decreasing distance to the pluton, where it commonly reaches 1 cm.

The recrystallized limestones show similar features than the fresh limestones, such as thin to medium-bedded layers, chert nodules (*bn11* and *bn15*), karstic filling (*bn11* and *bn12*); thin sections display sometimes remnants of echinoderm ossicles (*bn12*, *bn13* and *bn15*) and authigenic quartz (*bn15*). Moreover big bivalve traces, interpreted as Megalodontidae, occur in two places (*bn12* and *bn20*) (picture 2.4 plate 6A)

All the previous features indicates that the recrystallized limestones were similar in facies to the fresh ones prior to the Late Tertiary contact metamorphism. They are therefore considered as **Norian-Rhaetian** as well (i.e. all the limestones were unrecrystallized at the time the final emplacement of the mélange).

Depositional environment

The macroscopic observations, microfacies analyses and foraminifera assemblages allow to get an idea of the depositional environment of the Norian-Rhaetian limestones. The common occurrence of crinoid ossicles, pellets and authigenic quartz, the foraminifera assemblage (mostly Aulotortidae), the types of facies (mudstone-grainstone), occurrence or not of chert nodules, and the linked variation in the bed thickness favour a carbonate ramp environment, with some proximal (shallower, higher energy) to distal (deeper, lower energy) variations.

A Late Triassic volcano-sedimentary sequence in the Çetmi mélange

A small section north of Karapürçek has preserved a Late Triassic volcano-sedimentary sequence (Figure 2.8, location of the section on Figure 2.7). From base to top, the section is made of (det. by Dr. R Martini and Pr. L. Zaninetti, Geneva):

- 30 cm of a slightly recrystallized thinly bedded grey-pink radiolarian-bearing mudstone, with authigenic quartz; sample B97 yielded *Glomospirra sp*. from the Anisian-Rhaetian interval (facies A)
- 70 cm of slightly recrystallized dark grey limestone (facies B)
- about 1 m of facies A.
- 1.5 m of facies B; sample B98 yielded *Hoyenella* n. sp., characteristic for the Late Triassic. This sample constrains the age of the section to the Late Triassic.
- about 1 m of medium bedded slightly recrystallized dark grey limestone.
- 80 cm of a red microconglomerate reworking limestone clasts with authigenic quartz.
- 2 m of greenish-blue to red-pink (micro-) conglomerate reworking limestone and magmatic clasts in a volcanogenic matrix

- 5 m of thinly bedded fining-up calciturbidites with limestone and magmatic clasts in a volcanogenic matrix; planar bedding is observed in the thinnest layers.
- few dm of grey mudstone like facies A; sample B104 yielded possible *Aulotortus* sp. from the Middle-Late Triassic.

This section is underlain, through a possible tectonic contact by a undetermined volcanic rock a few metres thick. Its upper continuation is made by grey recrystallized limestones of possible Norian-Rhaetian age. It is the only place in the Çetmi mélange where Late Triassic volcanic activity is found.

2.3.1.3. Radiolarite and radiolarite/red mudstone alternations

Radiolarites

Field occurrence

True radiolarites (mostly red in colour) occur both in the northern and southern mélange; although they represent less than 1% of the total lithology of the whole mélange, they are a characteristic feature of the Çetmi mélange. They crop out as blocks with an average surface of c. 250 m^2, and are randomly distributed throughout the mélange. An outcrop of 0.25 km^2 is found in the northern mélange east of the Karapürçek village; this observation suggests the original occurrence of rather bigger blocks than those observed now.

Throughout the mélange, the radiolarite blocks are mainly in tectonic contact with the spilitic rocks and the greywacke-shale association, with a predominance of the former. The type of contact with the magmatic rocks is decisive because an association between radiolarites and oceanic effusive rocks is an important clue

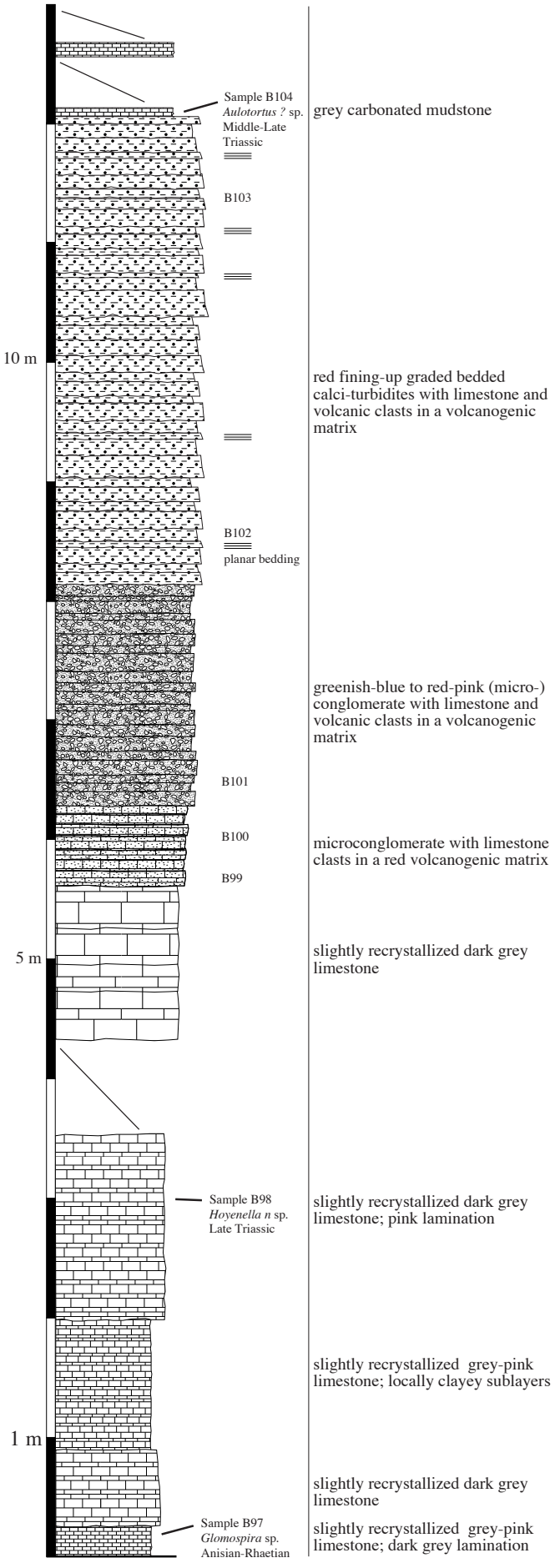

Figure 2.8. Stratigraphic column of an upper Triassic volcano-sedimentary sequence in the Çetmi mélange.

about sea-floor spreading. Due to the complex tectonic history underwent by the mélange, it is quite difficult to argue definitely that these contacts were stratigraphic at some moment, but the possibility has to be taken into account.

Age determination

42 samples have been processed and tested for radiolarians preservation by repetitive leaching in low-concentration hydrofluoric acid (see appendix 1 for sample processing). Recognizable radiolarians from all samples are scarce and poorly to moderately preserved. Only 9 samples yielded age-diagnostic taxa (det. by Dr. A-C Bartolini, Paris). The location of the sample is shown in Figure 2.6 and 2.7, and the pictures of the age-diagnostic taxa are found in plate 3A and 3B.

Sample L35

The sample is coming from a block of thinly bedded (cm scale thick) red radiolarites, located north of the Çetmibaşıyürükleri village (southern mélange). The radiolarites are folded and show boudinage (picture 2.5 plate 6A). They are in contact with spilitic magmatic rocks ; although the contact seems tectonic, it looks like still primary. In other words, the units may have moved one with regard to the other during the tectonic history of the mélange, but not enough to be definitely separated. The sample yielded

Tethysetta sp. *Tethysetta*	
Podobursa sp.	
Syringocapsa sp.	
Syringocapsa spinellifera BAUMGARTNER	UAZ 9-12
Pseudodicryomitra cfr. *P carpatica* (LOZYNIAK)	UAZ 11-21
Age: **Late Kimmeridgian-LateTithonian**	UAZ 11-12

Sample L70

The sample is coming from a tectonic block of thinly bedded (1-5 cm thick) red clayey mudstone about 30 m long and a few m high located north of the Yenioba village (southern mélange). Its relatively homogeneous bedding, although very slight folded, is dipping about 40 ° toward the NW. The block is bounded (tectonically ?) by spilitic magmatic rocks. The sample yielded:

Tethysetta usotanensis (TUMANDA)	UAZ 15-22
Archaeospongoprunum sp.	
Age: **Late Berriasian to Late Barremian-Early Aptian**	UAZ 15-22

Sample L340

The sample is located at the same place than L70. The sample yielded:

Transhsuum brevicostatum gr. (OZVOLDOVA)	UAZ 3-11
Tethysetta dhimenaensis ssp. A	UAZ 3-8
Tethysetta (?) *spinata* (VINASSA)	UAZ 3-10v
Tethysetta dhimenaensis s.l.	UAZ 5-11
Stichocapsa convexa YAO	UAZ 1-11
Palinandromeda podbielensis (OZVOLDVA)	UAZ 5-11
Tricolocapsa tetragona MATSUOKA	UAZ 5-5
Transhsuum maxwelli gr. (PESSAGNO)	UAZ 3-10
Tethysetta dhimenaensis dhimenaensis (BAUMGARTNER)	UAZ 3-11
Podobursa helvetica (RÜST)	UAZ 3-10
Parahsuum staleyens (PESSAGNO)	UAZ 3-8
Archaeodictyomitra (?) *amabilis* AITA	UAZ 4-7
Triactoma jonesi PESSAGNO	UAZ 2-13
Age: **Late Bajocian-Early Bathonian**	UAZ5-5

Sample K2

The sample is coming from a block of thinly bedded (5-10 cm thick) red radiolarites, located SE of the Kızılyar village (southern mélange). Its size is more than 250 m^2. Radiolarites exhibit strong random small-scale folding. They are in tectonic contact with grey radiolarian-bearing cherty micrites and siliceous brown shales. The sample yielded:

Acaeniotyle umbilicata (RÜST)	UAZ 10-22
Mirifusus dianae s.l. (KARRER)	UAZ 7-20
(?) *ZHamoidellum ovum* MATSUOKA	UAZ 9-11
Age: **Late Oxfordian-Hauterivian**	UAZ 10-20

Samples B55, B56, B57

The 3 samples are red radiolarites coming from a block of red clayey mudstone/radiolarites alternations, whose size is about 0.25 km^2, located east of the Karapürçek village (northern mélange). The block is isolated from the mélange and surrounded by Quaternary deposits. The alternations are mainly made of the red clayey mudstones and are affected by complex small-scale folding.

Sample B55 yielded:

Svinitzium depressum (BAUMGARTNER)	UAZ 13-18
Pseudodictyomitra carpatica (LOZYNIAK)	UAZ 11-21
Pseudodictyomitra nuda SCHAAF	UAZ 16-22
Age: **Valanginian**	UAZ 16-18

Sample B56 yielded:

Paradopocapsa furcata STEIGER	UAZ 13-16
Cinguloturris cylindrica KEMKIN AND RUDENKO	UAZ 12-17
Sethocapsa dorysphaeroides NEVIANI sensu SCHAAF	UAZ 7-22
Mirifusus dianae minor BAUMGARTNER	UAZ 9-20
Syringocapsa vicetina (SQUINABOL)	UAZ 13-17
Podocapsaamphitreptera FOREMAN	UAZ 9-18
Protunuma japonicus MATSUOKA AND YAO	UAZ 7-12
Tethysetta boesii gr. (PARONA)	UAZ 9-22
Age: **Tithonian-earliest Berriasian**	UAZ 12-13

Sample B57 yielded:

Tethysetta boesii gr. (PARONA)	UAZ 9-22
Pseudodictyomitra lancelotti SCHAAF	UAZ 20-22
Age: **Hauterivian-Aptian**	UAZ 20-22

In short, fully pelagic sedimentation, preserved as radiolarian cherts in the Çetmi mélange, prevailed during the **Middle Late Jurassic-Early Cretaceous** times (Bajocian to Aptian, Figure 2.9). The single radiolarite block north of the Karapürçek village (samples B55, B56 and B57) records a quasi-continuous pelagic sedimentation from the Tithonian to the Aptian.

Figure 2.9. Age of the radiolarites from the Çetmi mélange.

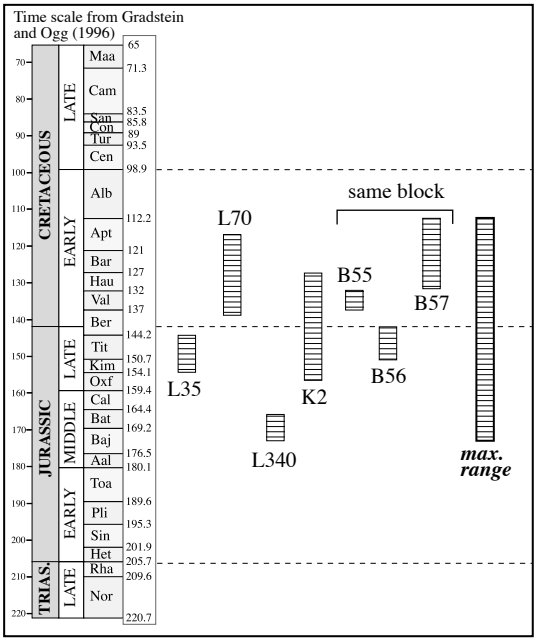

Radiolarite/red mudstone alternations

The radiolarite/red micrite alternations are cropping out both in the northern and southern mélange, as rare small metre-scale blocks, often close to radiolarite blocks. Figure

2.10 shows a detailed sedimentological column of these alternations drawn from an outcrop in a small quarry northwest of the Karapürçek village. They are characterized by the assemblage of three lithologies:

- The most common is made of red argillaceous mudstone whose layers do not exceed few cm thick. Each layer is actually the result of the superposition of mm. thick sublayers. The silica content sometimes increases so that beds look like radiolarites (but generally radiolarian are rare), sometimes they are almost exclusively made of clay and form darker red interlayers.

- True radiolarites form the second most occurring lithology in the section. Red in colour, they are 1 to 15 cm thick.

- The third lithology is made of red to pale pink radiolarian-bearing micritic mudstone, whose layers have an average thickness of a few cm. Layers show very thinly bedded alternations of micritic sublayers underlain by submillimetric argillaceous sublayers.

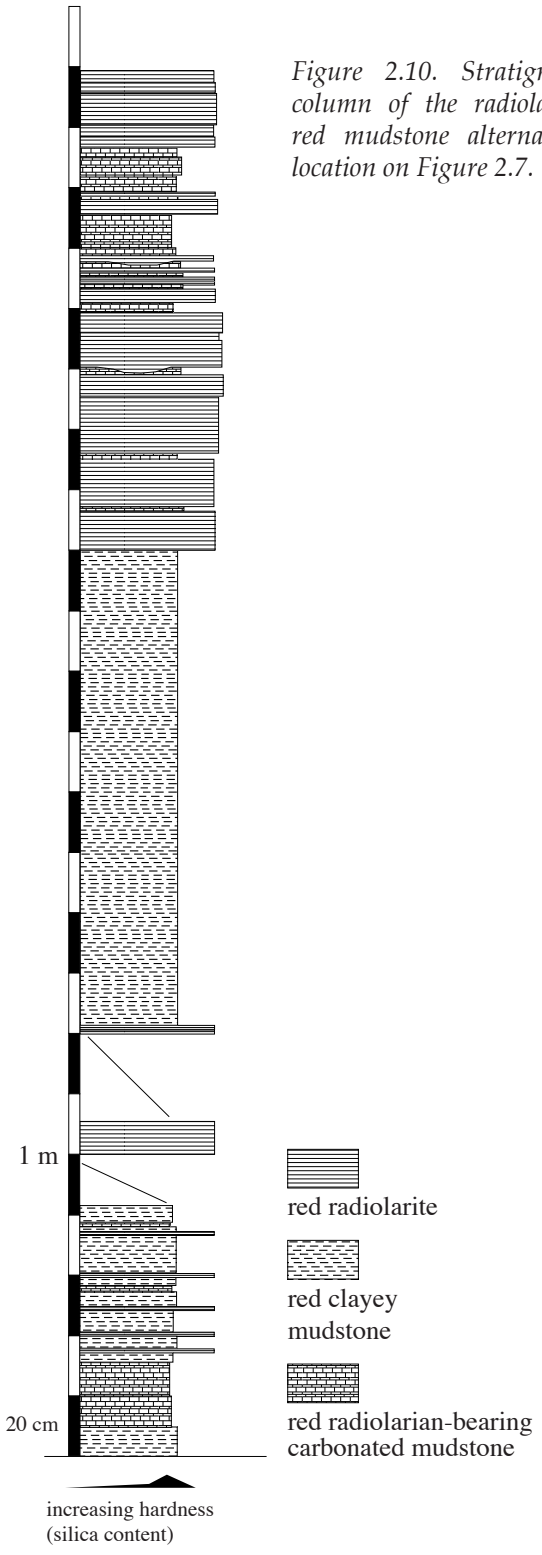

Figure 2.10. Stratigraphic column of the radiolarites/ red mudstone alternations; location on Figure 2.7.

The three lithologies generally show amalgamation or even discontinuity of their beds; however this does not reflect any particular feature of the depositional dynamics, but rather some post-depositional diagenetic evolution. Based on the previous characteristics, these alternations are interpreted as pelagic deposits, above but not far from the CCD.

Their age has not been directly determined as no radiolarian fauna has successfully been extracted from the radiolarites. As they are usually located close to the radiolarites and due to facies similarities, the association of the red radiolarites and the red mudstone alternations may either represent a lateral facies variation of the same depositional age, or a deepening or shallowing sequence (resp. if they are considered below or over the radiolarites). In the last case, and in the example of the previous stratigraphic column north of Karapürçek, the radiolarite/red mudstone alternance may either be considered as pre-Tithonian or post Aptian. The first hypothesis would be favoured because the Albian period is the time of the deposition of the greywacke-shale association (matrix of the mélange, c.f. 2.3.2).

2.3.1.4. Magmatic rocks

Introduction

The effusive magmatic rocks (spilites from Okay et al., 1991) represent by far the most abundant lithology of the Çetmi mélange, in the northern as well as in the southern area (resp. 33.5% and 46%). As the various limestone blocks and the radiolarites, the magmatic rocks are cropping out as tectonic slices or blocks. They occur mainly as massive and pyroclastic flows, but they sometimes display pillow structures (e.g. on the west of Kırca village). They show invariably brown to green patina, possibly due to (hydrothermal ?) alteration.

This part deals with the detailed characterization of the spilites, from a petrographic and geochemical point of view. The geochemical approach is used (1) to discriminate between possible different groups of magmatic rocks, and (2) to get an idea of the geotectonic setting in which they were emplaced.

Petrography

Twenty samples as fresh as possible have been selected for detailed petrographic and geochemical analyses (first in the field and then by examining thin sections): they consist of basalt to andesite, through basic andesite (12 samples), basic magmatic rocks with more or less clear greenschist facies overprint (7 samples) and andesitic-dacitic tuff (1 sample) (c.f. Figure 2.7 for the location of the samples from the northern mélange, and 2.11 for those of the southern mélange). A synthesis of the petrographic observation is presented in table 2.2.

It is really difficult to differentiate petrographically the basaltic from the andesitic rocks. All of them show primary phenocrysts of plagioclase feldspar, with or without pyroxene and olivine. The primary paragenesis is systematically overprinted by subsequent secondary alteration, with occurence of chlorite, calcite, epidote, sericite, oxides, serpentine, etc…

The metabasalts display low greenschist to greenschist facies, with the development of the common paragenesis made of epidote, chlorite, albite and possible amphibole. The two samples with the strongest greenschist overprint have totally lost their primary paragenesis and texture (samples B5 and B7).

The tuff sample (L36) is made of altered plagioclase with rare quartz and glassy fragments, with a possible andesitic-dacitic composition for the origin of the components.

An important point is the altered nature (and/or greenschist metamorphic overprint) of all the samples.

Whole-rock geochemistry

Whole-rock geochemistry (major, trace and rare earth elements) has been performed on the 20 previous samples (appendix 2). The major and trace elements have been determined in the Centre d'Analyses Minérales (CAM) of Lausanne University using X-ray fluorescence spectrometry (XRF), with Philips PW 1400 spectrometer and a combined Mo-Sc tube. FeO was measured with a photometer, and CO_2 with a coulometer. H_2O was recalculated from the loss on ignition (LOI) and FeO analyses. Standard error (2σ) for the major elements was 2-6 % relative, with a detection limit of 0.01 %; for the trace elements, it was 5-10 ppm, with a detection limit varying between 2 and 5 ppm. REE analyses have been performed at

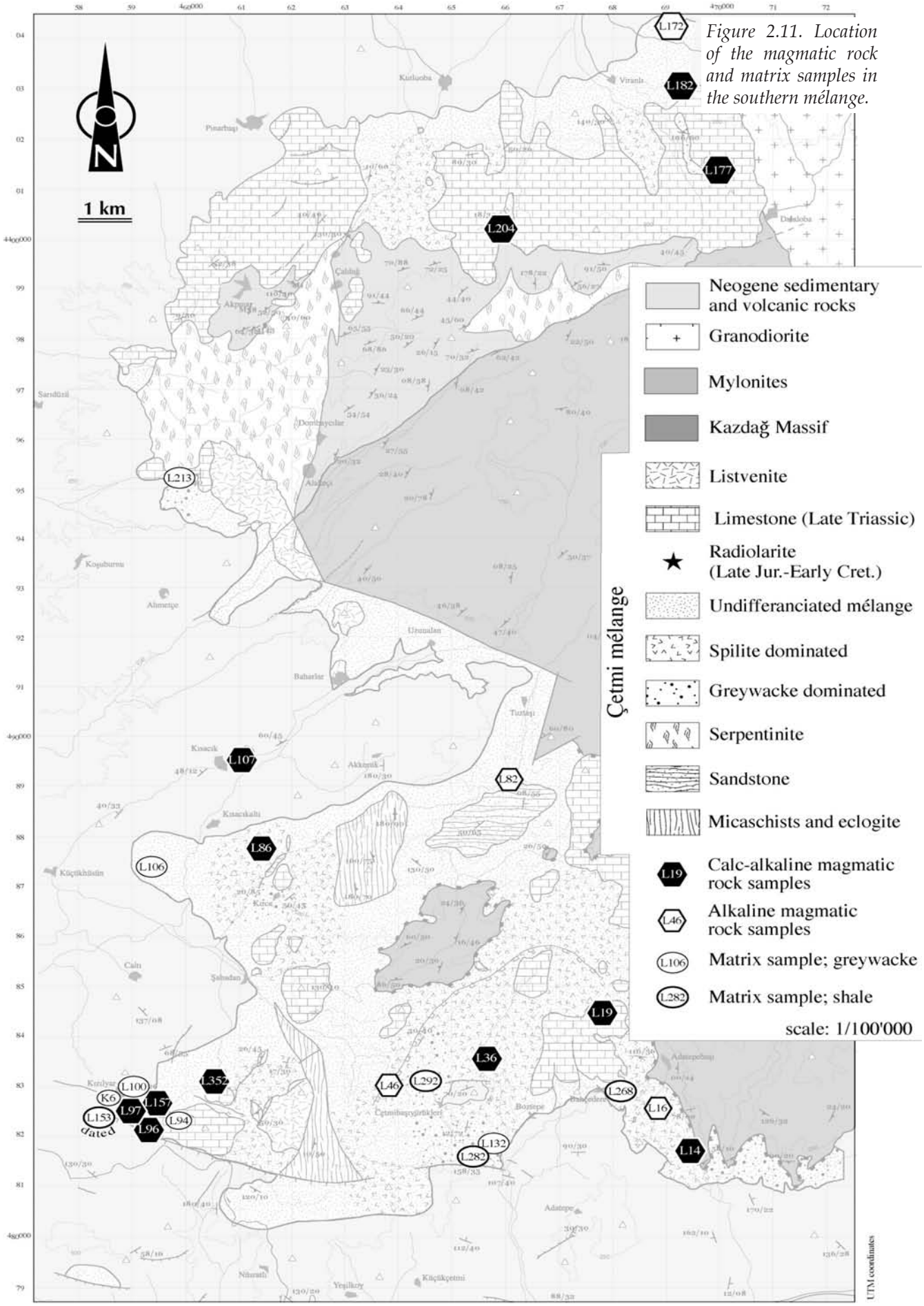

Figure 2.11. Location of the magmatic rock and matrix samples in the southern mélange.

the XRAL laboratory in Don Mills, Ontario, Canada, using Induced Coupled Plasma Mass Spectrometry (ICP-MS). The detection limit was varying between 0.05 and 2 ppm.

Sple	Rock-type	Primary minerals			Secondary minerals										Crystal-linity	Granula-rity	Texture
		PL	PY	OL	CHL	SER	AMP	EPI	QT	CA	OX	AP	AB	DO	SRP			
L16	Basalt	■			■	■		■	■	■					■	Holocr.	Aph. μcrist.	Subhedral-granular
L172	Basalte	■		?	■				■	■						Holocr.	Aph. μlitic.	Porphyric
L46	Aphyric basalt	■	?	?	■			■								Holocr.	Aph. μcrist.	Euhedral-granular
L352	Basalt	■			■	■				?				■		Holocr.	Aph.	Porphyric
L82	Basalt / andesite	■			■			■		■	■		■			Holocr.	Aph.	Porphyric
L86	Basic andesite	■	■	?	■			■								Holocr.	Aph. μcrist.	Porphyric
L19	Basic andesite	■	?	?	■	■	■									Holocr.	Aph.	Seriate
L96	Andesite	■	?		■	■			■		■				■	Holocr.	Aph. μcrist.	Seriate
L97	Andesite	■	■		■						■					Holocr.	Aph. μcrist.	Seriate
L157	Andesite	■	■		■				■	■	■					Hypocr.	Aph.	Seriate
L14	Andesite	■	■		■					■	■				■	Holocr.	Phanerocr.	Porphyric
L107	Andesitic-basalt	■	?		■				■	■	■					Holocr.	Aph. μlitic.	Porphyric
L204	Basalt LGS	■			■		■	■			■		?			Holocr.	Aph. μlitic.	Seriate
L177	Basalt LGS	■			■			?			■					Holocr.	Aph.	Porphyric
L182	Basalt LGS	■			■		■	■			■					Holocr.	Aph. μlitic.	Seriate
B5	Basalt GS				■			■					■			Ortho-prasinite, foliated		
B7	Basalt GS				■		■	■					■			Ortho-prasinite, unfoliated		
B54	Basalt LGS	■	■	?	■			?			■		■		■	Holocr.	Aph. μlitic	Porphyric
B85	Basalt LGS	■	■		■			■					■		■	Hypocr.	Aph.	Seriate
L36	Tuff	■			■				■		■	■				Andesitic to dacitic material		

Table 2.2. Petrographic features of the magmatic rocks from the Çetmi mélange. Samples beginning with L were collected in the southern mélange,those with B were collected in the northern mélange.
GS: greenschist facies, LGS: lower greenschist facies, PL: plagioclase, PY: pyroxene, OL: olivine, CHL: chlorite, SER: sericite, AMP: amphibole, EPI: epidote, QT: quartz, CA: calcite, OX: oxides, AP: apatite, AB: albite, DO: dolomite, SRP: serpentine - Crystallinity, Holocr.: holocrystalline, Hypocr.: Hypocrystalline - Granularity, Aph.: aphanitique, Aph μcrist.: aphanitique microcrystalline, Phanero: phanerocrystalline, Aph. μlitic: aphanitic microlitic.

Mobility of the major and trace elements

The petrographic study has shown that all the samples have suffered secondary alteration, or even greenschist overprint. This changes in the mineralogy may have modified the original geochemical signature of the more mobile elements.

Major elements

The SiO_2 content of the analysed samples shows either basaltic or andesitic values, in accordance with the petrographic observations. On the other hand, Na_2O and K_2O have generally higher values than those expected for basaltic or andesitic rocks. As the classifications of magmatic rocks using major element are based on K_2O and Na_2O content, no attempt to classify them in this way has been done.

Fe_2O_3/FeO ratio

As the ion Fe^{3+} is in a higher oxidation state than the ion Fe^{2+}, the ratio Fe_2O_3/FeO is a good indicator of the oxidation state of a given sample. Usual values for basalt and andesite are ranging from 0.2 to 0.35 (Middlemost, 1989), whereas the values from the selected samples are ranging between 0.56 and 3.39.

Measured CaO vs original CaO

Making some approximations (all the CO_2 is coming from carbonates and carbonates are only made of calcite) it is possible to recalculate for each sample the original content of CaO and to compare it with the measured value. In a general rule, the original CaO is lower than the measured content, suggesting that a part of the current CaO (or calcite) is due to late CO_2-rich fluids circulations.

Mobility diagrams

These diagrams displays for all the samples the relationships between the major elements and Zr, which is considered as immobile. As the samples are coming from the same mélange, it is assumed that they are coming from the same magmatic area; in this case, they are expected to show good correlation between all the elements and Zr. All major elements but TiO2 show scattered plots (Figure 2.12). Many reasons could explain the occurrence of the scattered plots (see Rollinson, 1993); the solution adopted here, following the petrographic results, is that secondary processes (mostly hydrothermal) have modified the abundance of the more mobile major elements.

Conclusion

The previous results suggest that the major elements, excepted Ti, behaved as mobile elements, and that the current contents are not representative of the original composition of the samples. This behaviour is in total accordance with the results of the petrographic study.

Trace elements

Mobility diagrams for trace elements have also been done. Only Nb and the REE show good to rather good correlations (e.g. Y, Nd, La, Figure 2.13); on the other hand, some mobile trace elements such as Na, Ca, Ba, Rb or Sr show scattered plots. Therefore, only the less mobile elements (particularly Y) will be considered as reliable indicators of the original composition of the samples.

The determination of the magmas affinities, as well as their geotectonic environments, is based on specific diagrams using equally the major and trace elements. Following the previous results on the mobility of major and trace elements, only Ti, Nb and the REE may be used in this way.

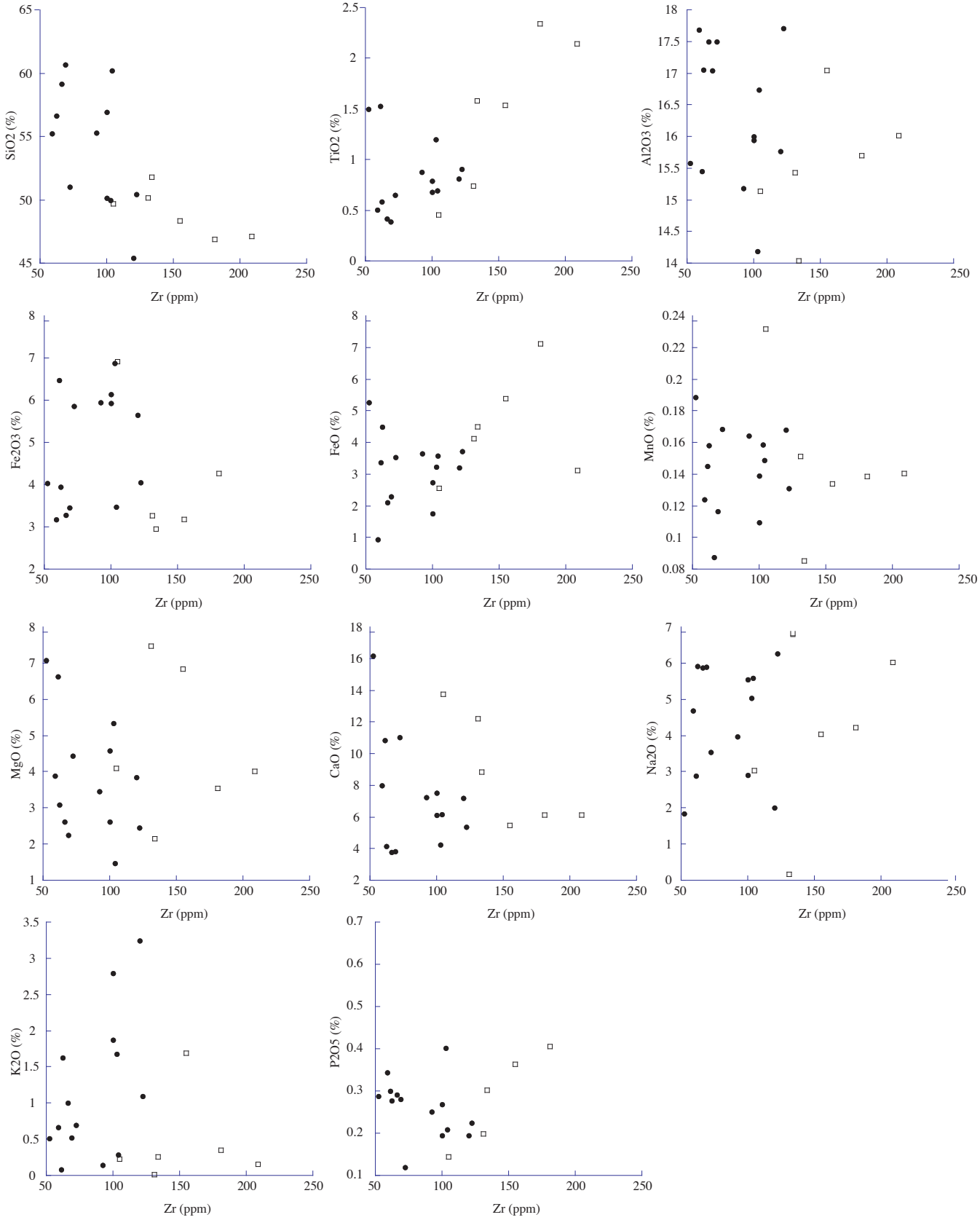

Figure 2.12. Mobility diagrams for the major elements of the magmatic rocks from the Çetmi mélange; black circles: set A; open squares: set B (explanations in the text).

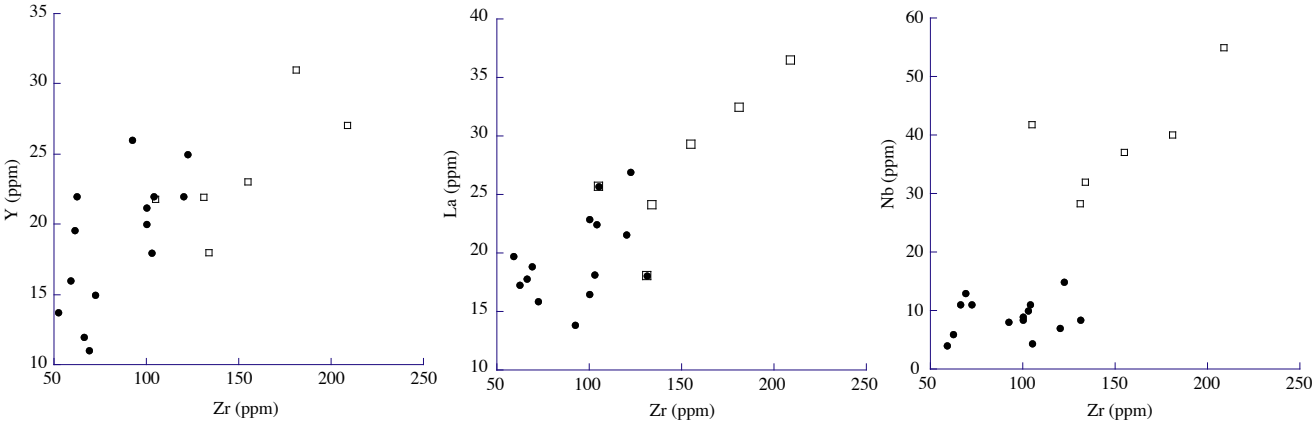

Figure 2.13. Mobility diagrams for selected trace elements (Y, La and Nb) of the magmatic rocks from the Çetmi mélange; black circles: set A; open squares: set B.

Using normalized multi-element diagrams

The existence of normalized multi-element diagrams is based on the variations of the behaviour of chosen incompatible or compatible elements during petrological processes; the element concentrations are normalized to a reference composition which depends mainly on the sample type. The basaltic to andesitic rocks from the Çetmi mélange have been plotted in three diagrams in order to determine their magmatic suite affinity.

MORB-normalized spider diagram

MORB-normalized spider diagrams are most appropriate for evolved basalts and andesites, that is the case for the Çetmi mélange. Figure 2.14-A & B shows the plot of element concentration normalized to MORB reference values from (Pearce et al., 1984). The samples are grouped in two different sets according to their geochemical signatures (thereafter sets A and B).

-Set A is characterized by strong negative anomalies in Nb, Zr and Ti, relatively high values of the mobile elements (Sr, K, Rb and Ba) and relatively low values of the immobile elements.

-Set B is characterized by a small negative anomaly in Zr, relatively low values of the mobile elements (Sr, K, Rb and Ba) and relatively high values of the immobile elements.

Set A elements pattern is typical of a calc-alkaline signature, while set B is typical of a more alkaline one. The few pillow lavas belong to set A.

Primitive mantle-normalized spider diagram

Figure 2.14-C & D show the plot of trace element concentrations normalized to the primitive mantle reference values of (McDonough and Sun, 1995) for set A and B.

-Set A displays negative anomalies in Nb and Ti (except B54 and B85 for the latter). The Nb negative anomaly is more or less masked by the variations in the contents of the mobile element K. A strong positive anomaly in Pb is also observed.

-Set B does not show significative anomalies, except for Ti and Sr, the latter being a mobile element, moreover fractionated by the plagioclase.

These observations confirm the distinction between a calc-alkaline (set A) and an alkaline (set B) signature. The two sets may therefore have a distinct mantle source. An interesting feature is the lower position of set B patterns with respect to the mean OIB values of Fitton

et al. (1991) and Sun & MsDonough (1989). It suggests that the source of set B has different (depleted) signature than the classical OIB source.

REE diagram from Boynton (1984)

The REE pattern of an igneous rock is controlled by the REE chemistry of its source and the crystal-melt equilibria which has taken place during its evolution. Figure 2.14–E & F

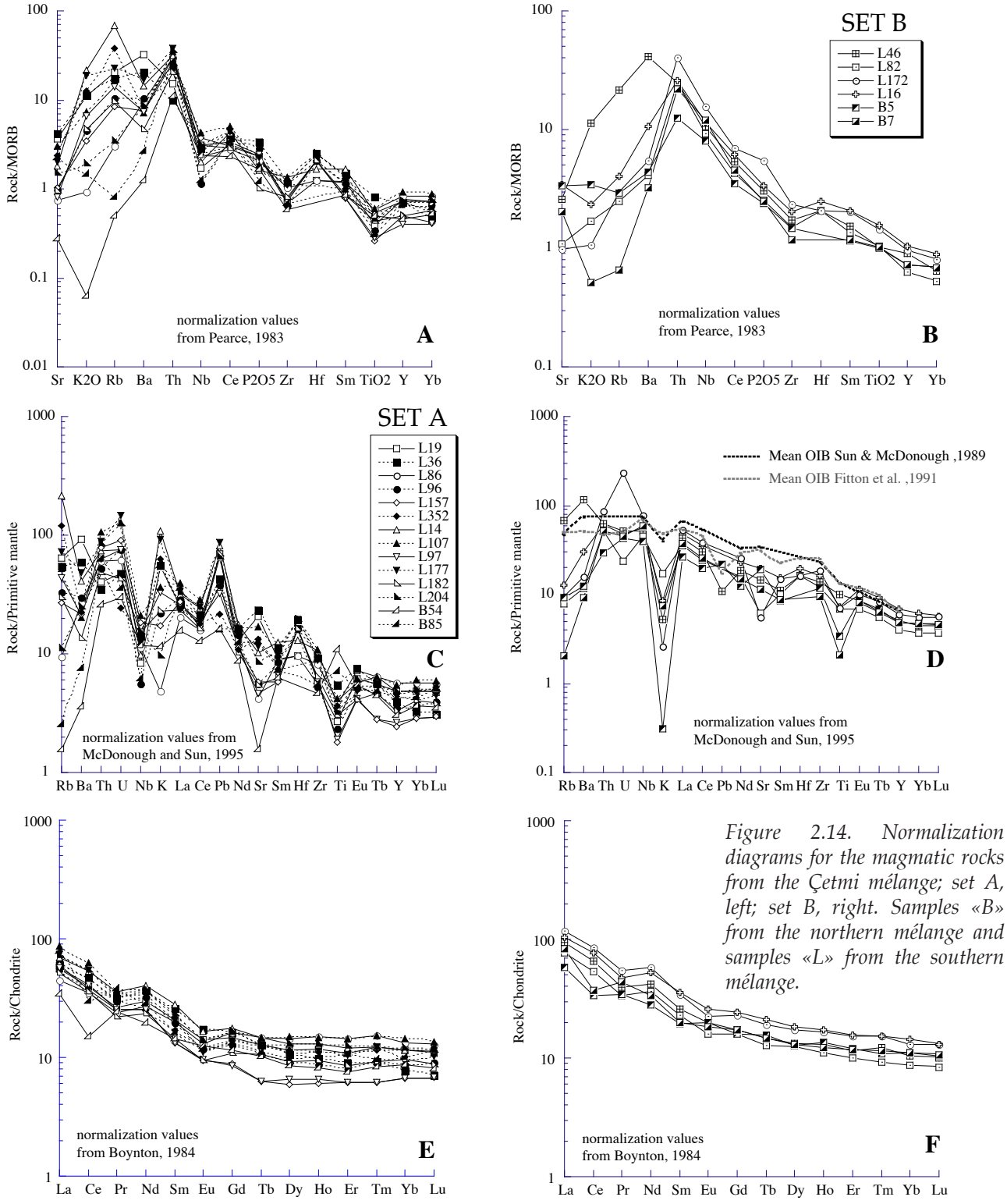

Figure 2.14. Normalization diagrams for the magmatic rocks from the Çetmi mélange; set A, left; set B, right. Samples «B» from the northern mélange and samples «L» from the southern mélange.

shows the plot of the REE concentrations normalized to the chondritic reference values from (Boynton, 1984).

Set B is characterized by a higher enrichment in light REE than set A (La/Sm average (A) = 4.98 - La/Sm average (B) = 5.45) ; on the other hand set A has an almost flat pattern for the heavy REE (Sm/Yb average (A) = 1.75) whereas a negative slope is present for set B (Sm/Yb average (B) = 2.15). These observations confirm the hypothesis of two different sources at the origin of the two sets; samples from set B have a deepest source (with possible presence of garnet) than samples from set A. Therefore it reinforces the hypothesis of two different sets of samples, one with an alkaline signature (deepest source, set B), one with a calc-alkaline signature (set A). As the magmatic rocks occur in a mélange (possibly active margin-related), it is tempting to attribute to set A a volcanic arc basalt (VAB) affinity and to set B an oceanic island basalt affinity (OIB, from seamounts).

Discrimination diagrams

The discrimination diagrams are used here to confirm the hypothesis made above (VAB and OIB samples), by approaching their geotectonic affinity. Only 3 diagrams, based on certain immobile element have been used (Figure 2.15).

In the Ti-Zr-Y diagram (Pearce and Cann, 1973), all the samples from the alkaline suite (set B) plot in the within plate basalt (WPB) field, whereas those from the calc-alkaline suite (set A) belong to the calc-alkali basalt field; it is the same in the Ti-Zr diagram (Pearce and Cann, 1973). The results confirm the hypothesis of a volcanic arc tectonic environment for set A. On the other hand, the diagrams cannot distinguish between the different types of within plate basalts, such as OIB and rift-related. Actually, no diagram can do this, and there is no way to distinguish between rift-related and OIB basalts on the base of the geochemistry of major and trace elements, as they could have the similar signatures (e.g. Wedepohl and Baumann, 1999). On the other way, the Zr/Y-Zr diagram from (Pearce, 1983) allows to discriminate between VAB with an oceanic or a continental crust component (Figure 2.15). The samples plot in the continental arc field, suggesting either a volcanic arc constructed on a continental crust, or the contribution from a source with a strong continental mantle signature.

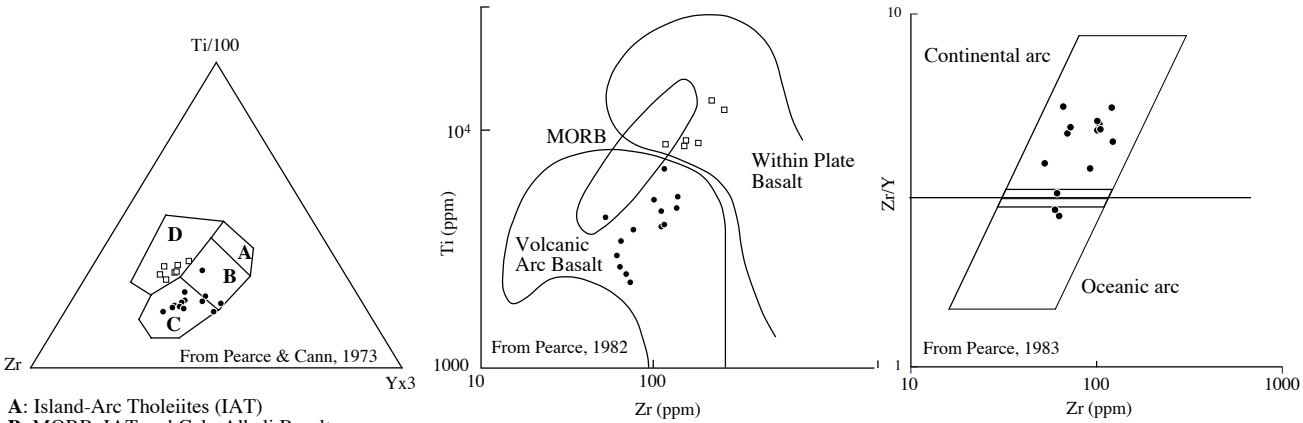

A: Island-Arc Tholeiites (IAT)
B: MORB, IAT and Calc-Alkali Basalts
C: Calc-Alkali Basalts
D: Within Plate Basalts

Figure 2.15. Discrimination diagrams for the magmatic rocks from the Çetmi mélange; black circles: set A; open squares: set B.

Conclusion

From a petrographical point of view, the magmatic rocks from the Çetmi mélange are made of basalt to andesite. Their whole-rock geochemical analyses allow to distinguish two different geodynamic environments for their emplacement: one is typical of a volcanic arc, with a continental contribution, and the other is either OIB- or rift-related.

2.3.1.5. Elliayak eclogite

Two north-south elongated exotic tectonic slices of eclogite and associated garnet-micaschist occur in the Çetmi mélange, at the lowest structural level in contact with the underlying Kazdağ Massif (deduced from the cross-sections Figure 2.3); following this, they may be seen as tectonic windows in the mélange. Such rocks are only present in the southern mélange.

The garnet-micaschists form well foliated, coarse-grained, silvery grey homogeneous rocks with horizons of eclogite, sometimes altered to blueschist. The foliation in the eclogite-micaschist is parallel to the elongation axis of the eclogite slices. Their surrounding rocks are made of metabasites with greenschist mineralogical assemblages and pronounced foliation, that is not usually the case for those rocks in the rest of the southern mélange.

The mineral assemblage in the garnet-micaschists is garnet + quartz + phengite + paragonite. The eclogites are greenish, massive, banded rocks with the mineral assemblage of garnet + omphacite + sodic amphibole + epidote + phengite + rutile ± quartz. The eclogite shows a greenschist facies overprint with the development of interstitial albite, partial replacement of garnet by chlorite, sphene rim around rutile; the occurrence of chlorite in the micaschist is also in favour of the retrogradation to greenschist facies.

The mineralogy of the eclogite and micaschist of the Çetmi mélange has been studied using an electron microprobe by Okay and Satır (2000). They obtained temperatures of 480 ± 50 °C and a pressure of 10 kbar for omphacite-garnet pairs. They have also dated two eclogite samples using the Rb/Sr method on phengite, and obtained Mid-Cretaceous ages of about 100 Ma. The same age has been found by Lips (1998) which has also dated the eclogite block (white mica with Ar/Ar method). He interpreted this age as a cooling age and concluded that the latter must postdate the eclogite facies metamorphism.

It is tempting to propose that the protolith of the eclogite was a ocean-related magmatic rock, while that of the garnet-micaschist was the associated sediments. To test this hypothesis, the whole-rock geochemistry of four garnet-micaschist samples and one eclogite sample has been done (appendix 3). As the rocks have undergone strong metamorphism and deformation, only the REE data have been used. The chondrite- and primitive mantle-normalized diagrams for the eclogite samples (values resp. from Boynton, 1984 and McDonough and Sun, 1995) show flat patterns characteristic for enriched MORB or OPB (Ocean Plateau Basalt, Figure 2.16). The LILE (Large Ion Lithophile Element) may have been remobilized during the metamorphism. The chondrite-normalized diagram for the micaschists show the typical pattern of the Upper Continental Crust (UCC) with a strong enrichment in the LREE and a marked negative anomaly in Eu (Figure 2.16). It is confirmed by the UCC normalized diagram (values from Taylor and McLennan, 1981) which shows fluctuating values around 1. The protolith of the micaschists was probably made of terrigenous sediments resulting from the erosion of an old crustal or sediment component (i.e. margin sediments). The micaschist-eclogite association represents therefore a piece of a former oceanic crust (MORB or OPB ?) with its associated sediments.

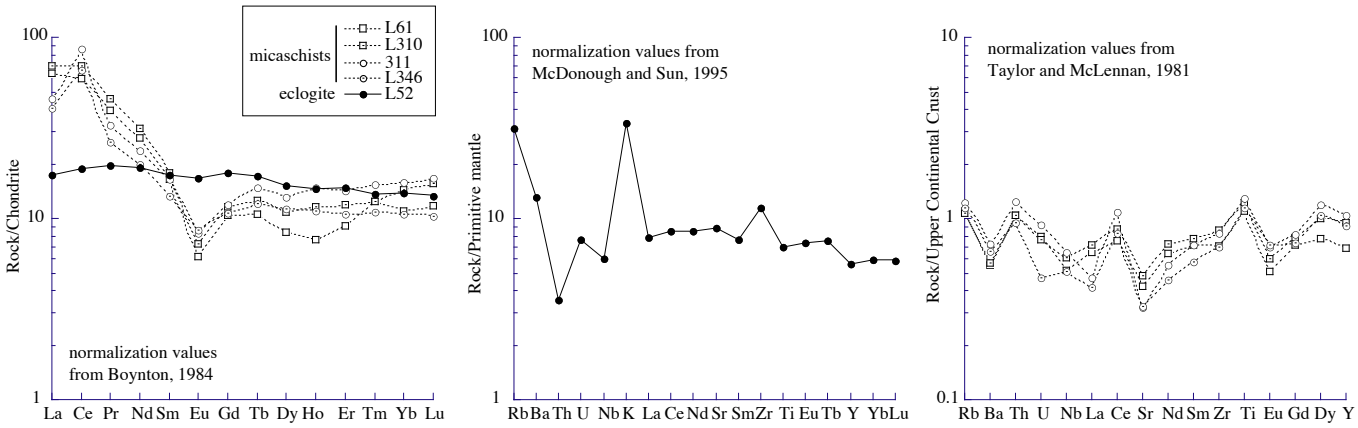

Figure 2.16. Normalization diagrams for the micaschists and eclogite from the Çetmi mélange.

1.3.1.6. Blocks made of detritic material

Tectonic slices of detrital turbiditic sequences are locally cropping out in both northern and southern mélange.

Doğandere Sandstone (northern mélange)

The Doğandere Sandstone represents the western end of the northern mélange, west of the Doğandere village (not shown on Figure 2.7 and plate 8). It consists of alternations of brown-grey sandstone and shales, with the latter dominating the sequence. Sandstone layers rarely reach the size of 30 cm. Petrographically the sandstones are poorly sorted quartz arkosic psammites, consisting of subangular quartz, plagioclase feldspar, authigenic muscovite and opaque, in a silty shale matrix.

Small-scale blocks of radiolarian chert, filament- and radiolarian-rich mudstone, and spilite also occur as olistoliths in the Doğandere Sandstone. One radiolarite sample (B80, plate 3A) yielded *Sethocapsa* (?) *sphaerica* (OZVOLDOVA), *Spongocapsula palmerae* PESSAGNO, *Spongocapsula perampla* (RÜST), *Emiluvia chica* s.l. FOREMAN, attributable to the **Middle Oxfordian-Tithonian** (UAZ 9-11) (determination made by Dr. A-C Bartolini, Paris). Okay et al. (1991) also found an **Aptian-Albian** foraminifera assemblage in a metre-scale limestone olistolith. The Doğandere Sandstone is therefore Albian to post-Albian in age.

The Doğandere Sandstone is in tectonic contact with the Çamlıca micaschists, through highly sheared, altered and sometimes silicified serpentinite slivers. The amount of neoformed micas in the shales increases toward the contact, as well as quartz veins and pebbles.

Sandstone and shale alternations are also cropping out west of the Eskibalıklı village and north of the Karahamzalar village. As they are petrographically similar to the Doğandere Sandstone they are treated together. A one m-scale large block of neritic limestone from the alternations north of Eskibalıklı has yielded the following microfaunal assemblage: Duostominidae, *"Trochammina"* aff. *almtalensis*, *Glomospira* ? sp, *Ophtalmidium* sp., *Cucurbita* sp., *Duotaxis* gr. *birmanica*, Triassic "Pachyphloia", *Aulotortus* sp., characteristic for the **Carnian-Rhaetian** interval. This age is similar to the ages coming from the Late Triassic limestone blocks found in the mélange.

Gelinmezarı Sandstone (southern mélange)

The Gelinmezarı Sandstone is a 2.5 km long and 1 km wide poorly outcropping tectonic lens made of laminated shale intercalated with medium bedded beige-grey sandstone, located south of the Tuztaşı village. The contact with the surrounding spilites and shale-greywacke association seems to be tectonic.

Petrographically the sandstones are poorly sorted quartz arkosic psammites; they consist of subangular quartz (with or without ondulose extinction), altered plagioclase feldspath, and mm sublayers of dark argilite, sometimes transformed into muscovite, in a silty-shale matrix. Lithoclasts of dark shales/siltites are common, as well as detrital zircons. The Gelinmezarı Sandstone is homogeneous in lithology and facies.

A few blocks of red radiolarite and white recrystallized limestone seem to be locally embedded in the sandstone/shale alternance on its western side. One sample (L139-2, plate 3B), coming from a block of thinly bedded (cm scale thick) red radiolarites, about 20 m long and a few m high, has yielded very poorly preserved *Mirifusus guadalupensis* PESSAGNO (UAZ 5-11), characteristic for the **latest Bajocian-Early Bathonian to Late Kimmeridgian-Early Tithonian** (determination made by Dr. A-C Bartolini, Paris). The Gelinmezarı Sandstone is therefore post Late Jurassic in age.

Moreover, an elongated 500 m long folded carbonated sandstone sequence north of the Kırca village also occurs in the southern mélange. It is made of detritic layers rich in quartz and feldspar alternating with radiolarian-rich micritic limestones.

Interpretation

The Gelinmezarı and Doğandere Sandstone tectonic slices may represent remnant of local small-scale turbiditic basins preserved in the Çetmi mélange (e.g. trench slope- or ponded-type basin). Due to petrographic observations they must have been close to their source rocks, which was rich in quartz and feldspar. These turbiditic sequences have reworked pelagic as well as neritic deposits.

2.3.1.7. Serpentinite/listvenite

Serpentinite lenses or slivers are a characteristic feature of the Çetmi mélange, both in the northern and southern areas.

In the northern mélange, highly sheared, possibly silicified, serpentinite slivers underline the tectonic contact between the Çamlıca micaschists and the various lithologies of the mélange (upper Triassic limestone, greywacke-shale association, spilite, Doğandere Sandstone). In the southern mélange, serpentinite lenses are partially marking the transition between the unmetamorphosed mélange and the underlying Alakeçi Mylonitic Zone. As already pointed out, serpentinite bodies seem to characterize the lowermost parts of the Çetmi mélange.

Another interesting feature is the occurrence of listvenites in the southern mélange. Listvenites are strongly altered rocks formed by hydrothermal alteration of serpentinized ultrabasic rocks (Koç and Kadioğlu, 1996, and ref. therein). Their occurrence, as a proof of low-to-medium temperature silica-carbonate-rich fluid circulation, may be an indicator of brittle fault activity (c.f. chapter 4). They occur east of Kızılyar and south of Alakeçi villages, close to brittle fault zones, and represent former serpentinite. Such rocks are common in mélanges with ultrabasic rocks (Çapan and Buket, 1975; Koç and Kadioğlu, 1996).

2.3.2. The matrix

By definition, the matrix of a mélange is the material in which the blocks are embedded, without any genetic, compositional, age or fabric connotation. At first glance, there is no clear evidence of a matrix in the Çetmi mélange; however, based on field observations, it is possible to find a lithology, the greywacke-shale association, which is in tectonic contact with all the other lithologies of the mélange (picture 2.6 plate 7A). Its representative outcrops are along Boztepe-Çetmibaşıyürükleri track, or along the track to Kırca for the southern mélange, and northwest of Eskibalıklı in the northern mélange. The following tectonic contacts, involving the greywacke-shale association have been observed: red radiolarite/greywacke-shale (e.g. Çetmibaşıyürükleri village-Çetmibaşı Hill track, picture 2.7 plate 7A), upper Triassic limestone/greywacke-shale (e.g. NW of Adatepebaşı village), magmatic spilitic rock/shale-greywacke (e.g. SW of Çetmibaşıyürükleri village), Han Bulog limestone/greywacke-shale (NE of Kızılyar), red radiolarian-bearing micritic limestones/greywacke-shale (NE of Kızılyar), tuff/greywacke-shale (Boztepe-Çetmibaşıyürükleri track, along Sarmısak river). The contacts are generally represented by narrow and crude shear zones, developed to the detriment of the less competent material, i.e. the greywacke-shale association. Therefore, the greywacke-shale association plays the role of a local matrix, although it represents less than 10 % of the total lithology of the mélange.

The greywacke-shale association is made of brown to black shales, sometimes silty or siliceous, broadly intercalated with dark grey greywackes; the latter occur generally as thin discontinuous minor layers or boudins, a few cm thick in maximum, and show rarely several dm thick layers (picture 2.8 plate 7A). Lateral variations are also observed at the scale of the mélange, so that in some places fine-grained material is dominant, whereas greywackes are dominant elsewhere. The whole sequence shows a characteristic shiny patina, due to white micas and clayey minerals.

The greywacke-shale association is present both in the northern and southern mélange, but its study has been mostly done in the mélange north of Küçükkuyu due to more favourable outcrop conditions.

2.3.2.1. Petrography of the greywackes

18 greywacke samples from the southern mélange have been selected for sedimentary petrography analysis; here is a summary of these observations:

In details, their composition are quite varied, including lithic arkosic wacke (7 samples), lithic arkosic psammite (3), arkosic wacke (2), quartz psammite (2), quartz wacke (2) and arkose (2). All of them fall in the arenite class, with an average in the fine grain-coarse grain interval. The grains, angular to subrounded, are generally floating in a clayey-silty matrix, which has the same mineralogical composition than the representative elements. The sediments are moderately to poorly sorted, and have poor textural and mineralogical maturity. Some samples show crude small-scale shear zones, underlined by insoluble minerals.

Quartz is the most occuring mineral; undulose extinction and two phases fluid inclusions are common, and polycrystalline structures are also present. It rarely shows calcite alteration.

Feldspar is also a very common mineral and is always present, even in small amount; plagioclase is by far the most abundant, whereas potassic feldspar is rare. Plagioclase shows

the characteristic albite and Carlsbad twinnings. They generally display patchy alteration due to sericitization and rarely kaolinization; calcite alteration is also common.

Accessory minerals include muscovite (both detritic and authigenic), secondary chlorite (sometimes abundant), secondary iron oxide, epidote, calcite and dolomite (rare), zircons and sphene.

Two main types of lithoclast are present: (1) metamorphic rock fragments are the more abundant; they are made of quartz, micas, K-feldspar, and show commonly schistose texture; (2) basic to intermediate volcanic rock fragments, made of altered plagioclase laths in an undetermined groundmass. There are also rare shale and sandstone s.l. fragments.

Thin sections show no evidence for metamorphism; however a metamorphic paragenesis (quartz, plagioclase (albite), green hornblende, epidote, cordierite, titanite, rutile, sphene) is present in one sample collected 1.5 km away from the Evciler granodiorite. Late low-temperature fluid alteration is sometimes responsible for the crystallization of chlorite, calcite and epidote, and the development of calcite and quartz veins.

These observations indicate that (1) depositional environment is not too far from the source rocks, and (2) source rocks may be of two types, a continental source responsible for the quartz and metamorphic fragments, and a possible volcanic arc source responsible for the great amount of plagioclase and volcanic fragments; quartz may also come from coeval granitoid intrusive rocks, although its characteristics are closer to those of metamorphic origin.

2.3.2.2. Age of the matrix

Seven samples from the siliceous/silty shale intercalation have been processed and tested for palynomorphs preservation; the palynologic preparations have been made at the National History Museum of London, England. Only one sample (L153) yielded an age-diagnostic palynomorph assemblage (Determinations by Dr. P. Hochuli, ETHZ). The sample is coming from the type outcrop of the Çetmi mélange, SE of the Kızılyar village and is made of brownish silty shale (location on Figure 2.11; pictures of age-diagnostic palynomorphs in plate 4).

The sample contains a quite diverse poorly preserved assemblage, dominated by terrestrial palynomorphs, mostly bisaccate pollen and spores-and phytoclasts, corresponding to marine environment with considerable terrestrial influx. Based on the co-occurrence of several dinoflagellate cysts such as *Protoellipsodinium spinocristatum*, *Protoellipsodinium spinosum*, *Pterodinium cingulatum*, *Protoellipsodinium* cf. *spinocristatum*, *Ischyosporites* sp., *Hamulatisporis* sp., *Cribroperidinium orthoceras*, *Plicatella* sp., *Gleicheniidites* sp., *Classopollis* sp., *Cicatricosisporites* div. spp., *Leberidocysta* cf. *chlamydata*, *Odontochitina operculata*, *Ellipsodinium rugulatum*, *Wrevittia helicoidea*, *Callaiosphaeridium asymmetricum*; an **Early to Middle Albian** age can be attributed to this sample. Jurassic and Triassic reworking has been found, as shown by the occurence of *Nannoceratopsis spiculata*, reworked from late Early - early Middle Jurassic, *Triadispora* sp., reworked from Middle – Late Triassic, *Ovalipollis* sp., reworked from Middle – Late Triassic, and Striate bisaccate pollen, reworked from Triassic.

2.3.2.3. Whole-rock geochemistry of the greywacke-shale matrix

Unlike magmatic rocks, major and trace element geochemistry of detritic sediments is rarely used to approach their tectonic setting. In the literature, geochemical data from sedimentary rocks are interpreted in two different ways:
(1) To get information on the tectonic setting of the sedimentary basin in which they have deposited. These "paleotectonic depositional environments" are quite the same as for magmatic rocks (Bhatia and Crook, 1986):

-Oceanic island arc: fore-arc or back-arc basins, adjacent to a volcanic arc developed on oceanic or thin continental crust or thin continental margins.

-Continental island arc: intra-arc, fore-arc or back-arc basins, adjacent to a volcanic arc developed on thick continental crust

-Active continental margin: Andean-type basins developed on or adjacent to thick continental margins.

-Passive continental margin: rifted continental margins developed on thick continental crust on the edge of continents; sedimentary basins on a trailing edge of a continent.

A few discrimination diagrams based both on major and trace elements are available from the literature.
(2) To characterize more precisely the source(s) of the sediment. Their whole-rock geochemical analyses may greatly contribute to the study of their provenance.

In the previous part, we have seen that the greywacke-shale association is suspected to have deposited in an active margin context. First, this hypothesis is tested by trying to specify the margin context (oceanic island arc, continental island or active continental margin). Then the provenance/source of the matrix will be determined by testing if there is a genetic link between the greywacke-shale association and the volcanic arc-type magmatic rocks from the Çetmi mélange. Nine samples from the southern mélange (6 greywackes and 3 silty black shales) were selected because of their relative unaltered aspect (Figure 2.10 for the localisation of the samples). The samples are one quartzwacke (L100), one quartz psammite (K6), two lithic arkosic wackes (L132 and L213), two lithic arkosic psammite (L94 and L106) and three black silty shales (L268, L282 and L292).

The major and trace elements have been determined in the Centre d'Analyses Minérales (CAM) of Lausanne University (c.f. 2.3.1.4 and appendix 4). REE analyses have also been performed in Lausanne at the Institute of Mineralogy and Geochemistry, using Induced Coupled Plasma Mass Spectrometry (ICP-MS). The detection limit was varying between 0.05 and 2 ppm.

Tectonic setting

Variation diagrams

-Harker diagram

We have seen previously that the magmatic rocks from the Çetmi mélange were altered enough not to use major elements in their interpretation. Even if the sample have been chosen because of their low degree of alteration, a qualitative checking is necessary.

This can be done by plotting the samples in Harker's diagrams, in which the oxides (in %) are plotted against the percentage of SiO_2. For detritic sediments, trends showing a decrease of the other oxides with respect to SiO_2 are expected; this is directly related to an increase in mineralogical maturity of the samples (increase in quartz and decrease in unstable detrital grains, Bhatia, 1983).

Harker's diagrams for the greywacke/shale alternations from the Çetmi mélange (Figure 2.17) show approximatively this kind of pattern for Al_2O_3, Fe_2O_3, K_2O, MgO, P_2O_5 and TiO_2. On the other hand, the plots for CaO, Na_2O and MnO show scattered trends. Therefore secondary processes have only slightly remobilized the major elements, except for CaO, Na_2O and MnO. A strong alteration would have resulted in a general scattering of the plots. So we may use major element in discrimination diagrams if necessary, excepted CaO, Na_2O and MnO.

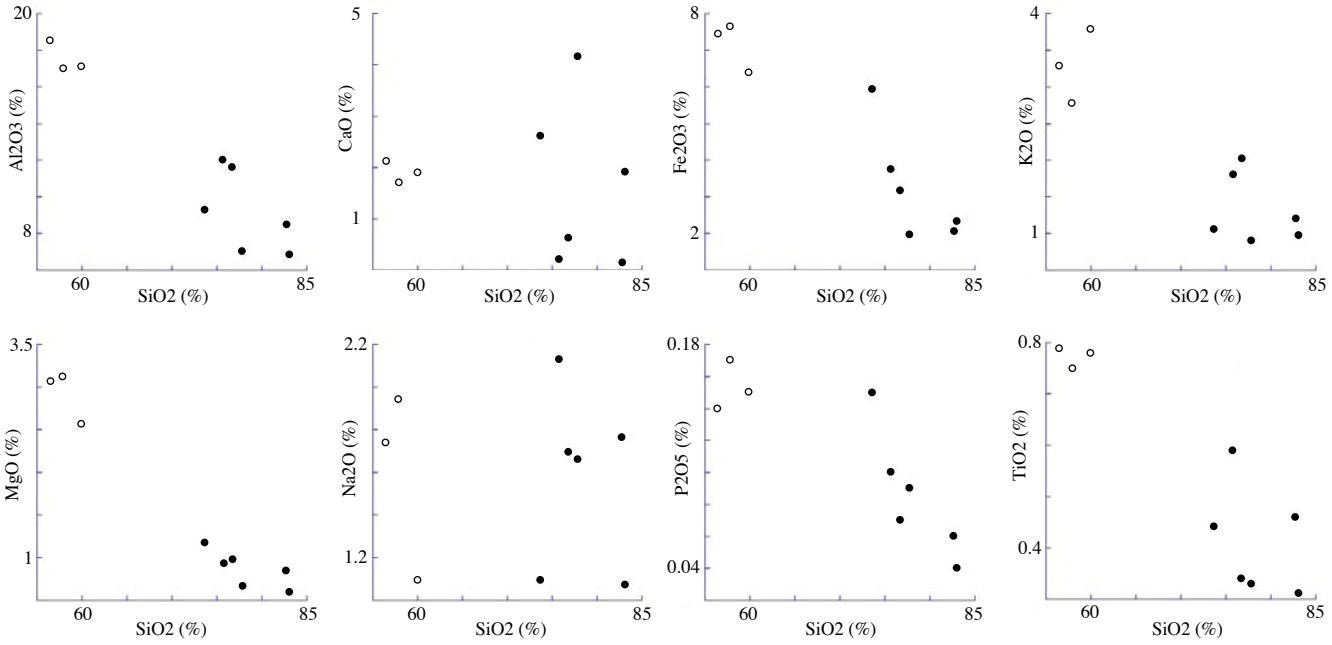

Figure 2.17. Harker's diagrams for the greywacke-shale association; open circles: silty shale; black circles: greywacke.

-Bivariate plot with Sc on the x-axis.

Major and trace element concentrations in sediments result from the competing influences of the provenance, weathering, diagenesis, sediment sorting and the aqueous geochemistry of the individual elements (in Rollinson, 1993). Because of their particular behaviour during sedimentary processes, selected trace elements may be used to identify the sedimentary provenance, such as the REE, Th or Sc.

A plot with Sc on the x-axis of the major and some selected trace elements useful in the discriminant diagrams may show trends (1) if weathering, diagenesis, sediment sorting and aqueous geochemistry of the given elements have broadly preserved their initial concentration and (2) if these elements have not been remobilized during post-deposit alteration.

The plots for the samples from the matrix display trends for all of the major elements, except CaO and Na_2O (Figure 2.18); only the test for the trace elements which are used in the discrimination diagrams has been done; the plots of Co, La and Th show trends, whereas

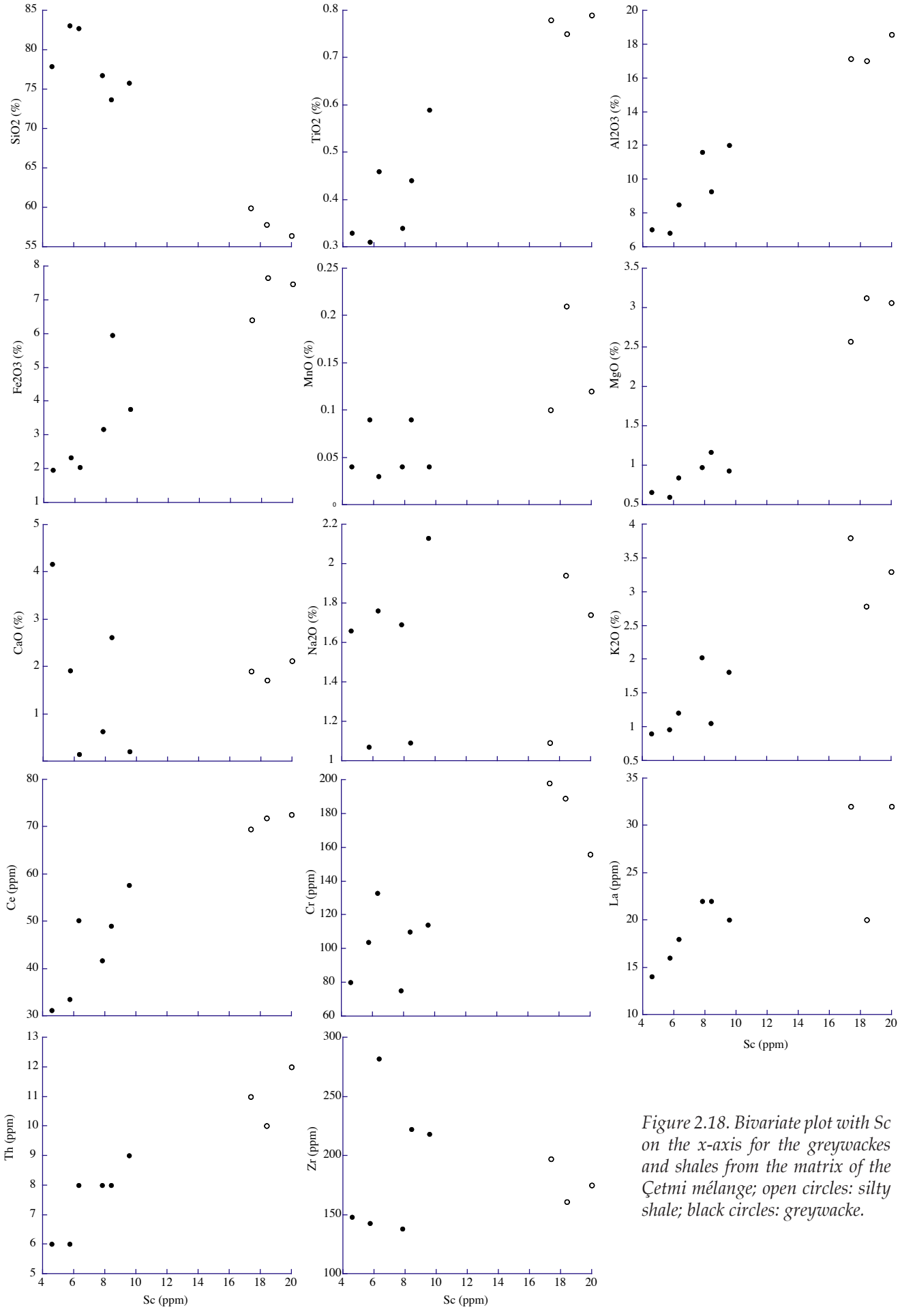

Figure 2.18. Bivariate plot with Sc on the x-axis for the greywackes and shales from the matrix of the Çetmi mélange; open circles: silty shale; black circles: greywacke.

it is not the case for Cr and Zr. However, Zr may be mechanically distributed according to grain size and also may be controlled by the concentration of heavy minerals ; moreover it is usually considered as relatively immobile during secondary alteration processes. Therefore the scattered trend observed in the Zr-Sc diagram suggests more a fractionation before the deposit than a secondary alteration. Regarding the REE, the charts display very good or good correlation when plotted against Sc.

Here again discriminant diagrams with major elements (except Ca and Na) may be used, as well as those with Sc, La, Th, Zr, trace elements and REE.

Discrimination diagrams (Figure 2.19)

These diagrams help characterizing the tectonic setting in which sedimentary rocks have been deposited. The hypothesis tested here is that the greywacke-shale association may have been deposited in an active margin environment.

-The TiO2 vs ($Fe2O3_{(tot)}$+MgO) and Al2O3/SiO2 vs ($Fe2O3_{(tot)}$+MgO) diagrams

These two diagrams are based on data from modern sandstones from the four different tectonic environments (Bhatia, 1983). Although the six samples are not very well clustered, they show a tendency to group themselves in or near the active continental margin field; at least they are far from the oceanic arc domain.

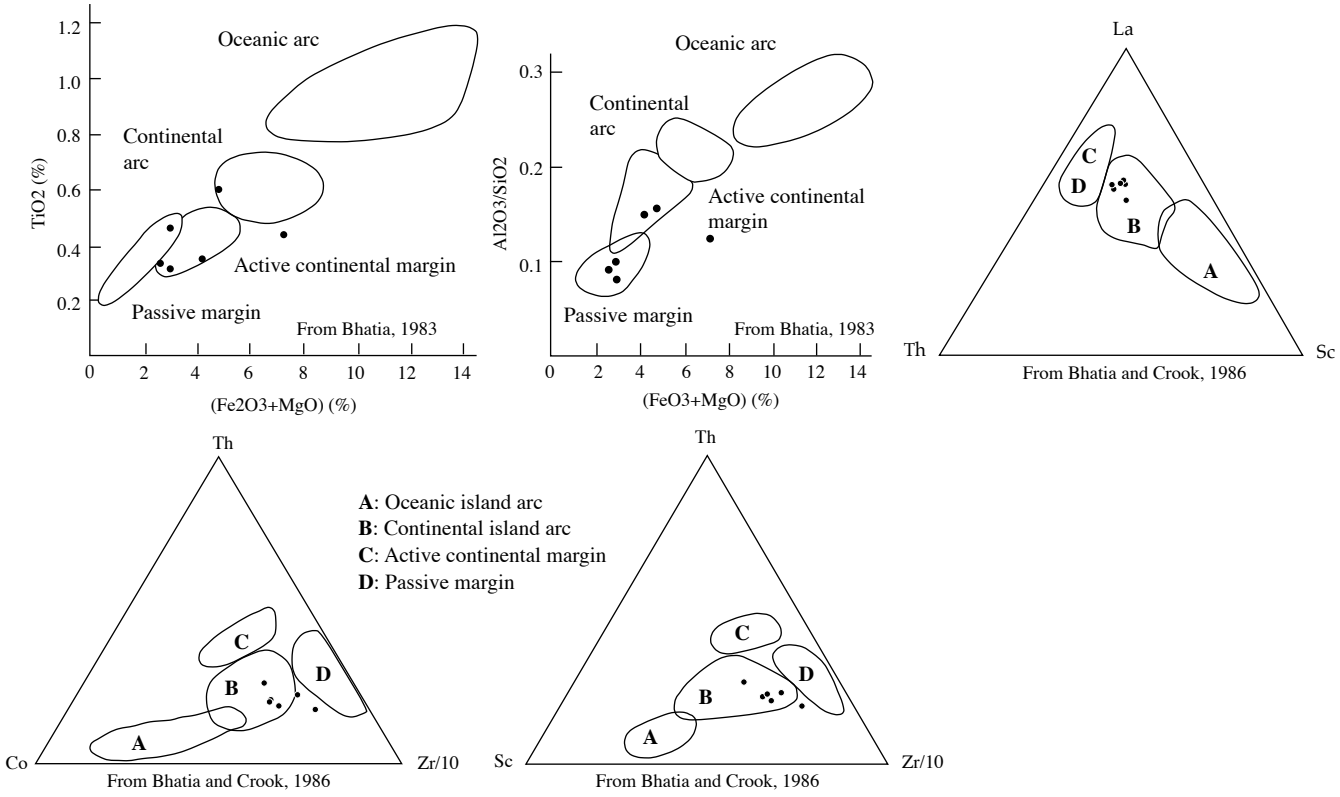

Figure 2.19. Discrimination diagrams for the greywacke from the matrix of the Çetmi mélange.

-The La-Th-Sc, Th-Sc-Zr/10 and Th-Co-Zr/10 diagrams

These three diagrams from Bhatia and Crook (1986) are only valid for the greywackes. In the La-Th-Sc, the greywackes are clearly grouped in the continental island arc. The two other diagrams also display the same pattern, although less marked.

Conclusion

The greywackes deposition is related to an active margin environment; the diagrams also clearly show a continental contribution to the tectonic setting in which the greywackes have been deposited (without distinguishing clearly between active continental margin and continental island-arc). This is in total adequation with the petrographic study, which was indicating a two-component source for the greywackes.

Provenance study

For a number of reason not listed in detail here, the single most factor contributing to the REE content of a clastic sediment is its provenance (McLennan, 1989). For instance, weathering and diagenesis have only minor effect on REE distribution.

From their petrographic study, the greywackes are suspected to have a double origin, one continental, bringing quartz and metamorphic fragment, and one of volcanic-arc type, responsible for the large amount of plagioclase feldspar and volcanic (andesitic) fragments.

Comparison with the volcanic arc basalts/andesites from the mélange

As the greywacke-shale association may have a volcanic-arc component, their REE patterns are compared with those of the volcanic arc basalts/andesites from the Çetmi mélange. Because the geochemical analyses of the sedimentary rocks concern only rocks from the southern mélange, they have been compared with the analyses of the magmatic samples from the southern mélange.

Moreover, the REE pattern of the source of a given sedimentary rock is most faithfully represented by the clay-sized fraction of the sediment (Cullers et al., 1987), as well as by the silt fraction of a sediment (Cullers et al., 1988). Therefore, even if the 9 samples are plotted, there will be a preferential focus on the 3 silty-shale ones.

The chondrite normalization of the sedimentary rocks, with the normalizing values from Boynton, (1984), shows a very similar pattern to that of the chondrite normalization of the VAB (Figure 2.20, to compare with Figure 2.14). Even the small Europium negative anomaly is reproduced.

The MORB normalization of the sedimentary rocks, with the normalizing values of Pearce, (1983), also shows a similar trend to that of the MORB normalization of the VAB (Figure 2.20, compared with Figure 2.14). Only the behaviour of the more mobile element is sometimes different (Sr, K2O, Rb and Ba); their normalized values are more homogeneous in the sedimentary rocks than in the magmatic rocks. If we focus on the behaviour of the silty-shales (c.f. above), they show a slight enrichment in the more mobile elements and lower concentration in P_2O_5, plus a higher concentration in Zr, which simulates an absence of the negative Zr anomaly observed in the magmatic rocks. On the other hand, the characteristic

negative anomalies in Nb and TiO_2 are reproduced.

Finally, the best way to compare the sedimentary and magmatic sets is to draw a diagram in which the REE values of the sedimentary rocks are normalized to the arithmetic mean of the REE concentration of the magmatic rocks (Figure 2.20). This diagram shows that the sediments, and specially the silty-shales, have almost the same REE values than the VAB (Figure 2.20, fluctuations around 1).

All the previous observations, plus the data from the petrographic study, suggest that the greywacke-shale association from the Çetmi mélange is made of the erosion products of the magmatic arc which gave birth to the VAB found in the mélange. As the source rocks (the VAB) and the erosion products (the greywacke-shale association) occur in the mélange, an important implication would be that the age of the sediments may be a rather good approximation of the minimum age of the source rocks. As the age of the greywacke-shale association is Early to Middle Albian, the volcanic arc responsible for the latter may not be younger than Middle Albian.

As said before, the petrographic study suggests a mixed origin for the greywacke-shale association, an hypothesis confirmed by the geochemical approach ; but it seems from the REE diagrams that only the volcanic arc component is recorded by the sediments. A possible explanation may be the following: the continental component of the greywackes is mainly due to the occurrence of quartz and metamorphic fragments (SiO_2% of about 75-80%). The quartz (i.e. SiO_2) is known to only have a diluting effect on the REE concentration, which does not affect the REE relative concentrations. This could be seen on the normalization diagrams in which the greywacke patterns show general depletion in REE compared to the silty-shale patterns (Figure 2.20). Therefore the observed REE patterns do not contradict a mixed origin, one continental and one of volcanic-arc type, and even confirms this hypothesis.

2.3.2.4. Conclusion

The greywacke-shale association plays the role of a local matrix of the Çetmi mélange, both in the northern and southern area. Its petrographic and whole-rock geochemical features demonstrate that it has been deposited in close connection with a volcanic arc, and that an important part of the sediments has a continental origin. The depositional environment of the greywacke-shale association may be either of fore-arc or trench basin type (respectively upper and lower plate), with periods of active detritic sedimentation (greywacke) alternating with periods of hemipelagic sedimentation (shale). The whole-rock analysis of the greywacke-shale association show similar geochemical signatures than those of the VAB of the mélange, hence there could be a genetic link between them. In this way, the Albian age of the matrix (one sample) could be a minimum age for the arc at the origin of the greywacke-shale association.

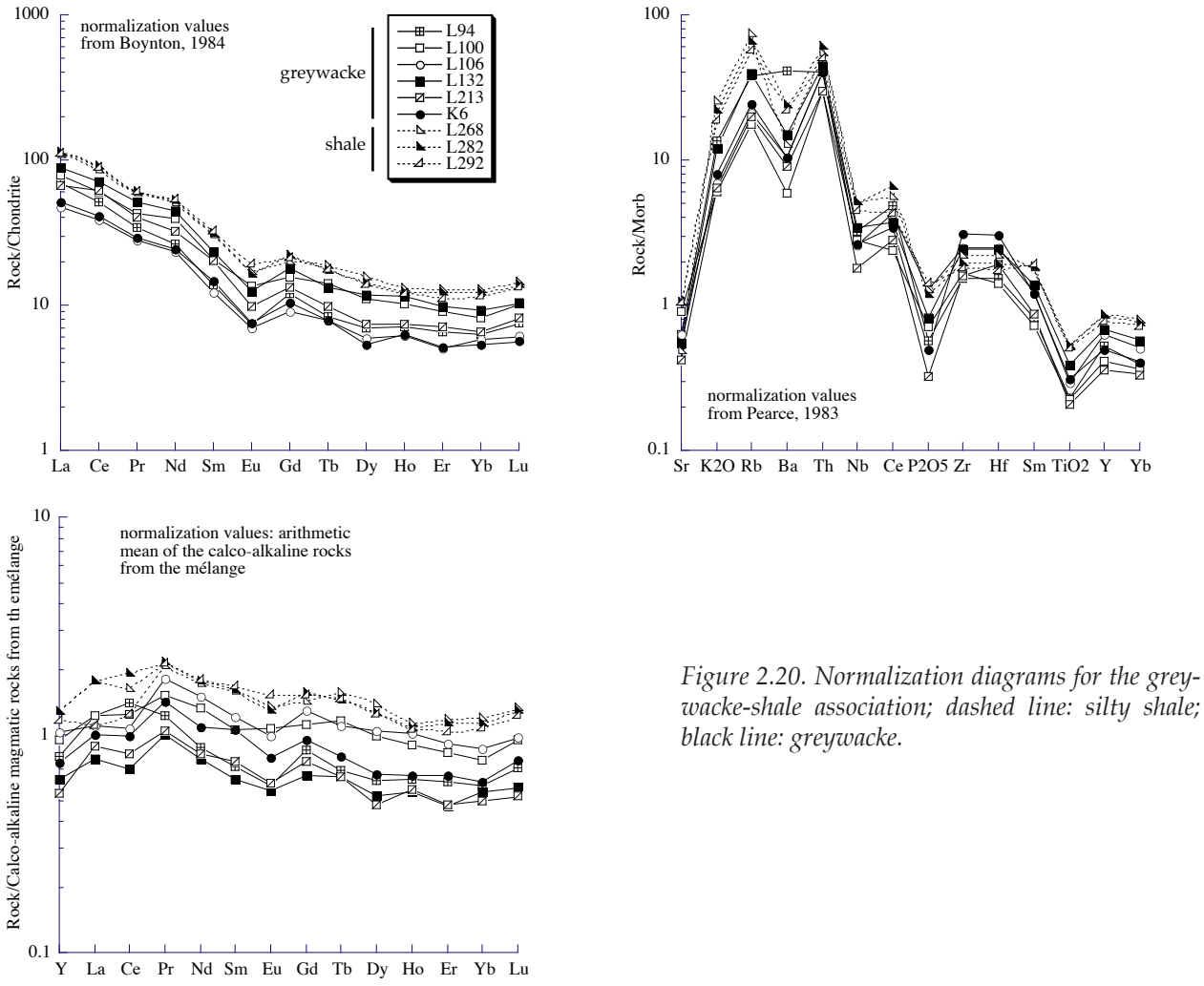

Figure 2.20. Normalization diagrams for the greywacke-shale association; dashed line: silty shale; black line: greywacke.

2.4. Interpretation and correlations of the Çetmi mélange

After the summary of the data obtained from the above study, this part discusses the moment at which the tectonic processes responsible of the Çetmi mélange emplacement were no more active, and examines its possible lateral correlations.

2.4.1. Summary of the data

This part is a reminder of the previous results from the study of the Çetmi mélange. Figure 2.21 shows a summary of the age data.

The Çetmi mélange is originally non-metamorphic.

The cause of initial fragmentation and mixing is mainly tectonic; possible sedimentological processes have occurred. The present-day structure is the result of Late Tertiary deformation.

Serpentinite lenses are always found at the base of the mélange, marking the contact with the underlying high-grade metamorphic rocks.

The oldest lithology of the Çetmi mélange is the rare Han Bulog limestone, whose age ranges between uppermost Scythian and Ladinian. It records pelagic sedimentation during this time interval.

Then come the Norian-Rhaetian limestones, which represent in proportion the second lithology of the mélange. They are typical of a carbonate ramp depositional environment. A small upper Triassic volcano-sedimentary sequence is also preserved.

No lithology from the Paleozoic or Liassic has been found.

Red radiolarite record pelagic sedimentation and their ages range between Bajocian and Aptian. A single block is recording quasi-continuous pelagic sedimentation from Tithonian to Aptian.

The greywacke-shale alternations are seen as the matrix of the Çetmi mélange. They record fore-arc type sedimentation, with a volcanic arc and a continental source; their age is Early to Middle Albian, making them the youngest lithology of the mélange.

Two local turbiditic basins are preserved in the mélange; their age is Late Albian to post-Albian (Doğandere Sandstone) and post Late Jurassic (Gelinmezarı Sandstone), as they rework respectively limestones and radiolarites of these ages.

Spilitic magmatic rocks (basalt to andesite) are the most common lithologies of the mélange. They have volcanic arc and within-plate basalts geochemical signatures. The VAB seem to be the arc component of the greywacke-shale matrix.

At this point of the study, it is not possible to attribute a precise and definitive tectonic affinity to the mélange; however we know that: (1) it must have been located at an active tectonic boundary between one or several oceanic domains and a continental margin, in order to gather in the same unit and in so close association lithologies with oceanic (radiolarite, serpentinite, possible OIB), continental margin (carbonate ramp, possible rift-related basalts), and volcanic arc (with a continental component) affinities; (2) it is partly made of a fore-arc or trench basin types sequences. Such mélanges are generally not isolated units and are expected to correlate laterally with formations with similar characteristics; (3) it is not metamorphic, so that its lithologies have not been buried from their time of deposition to the time of mélange emplacement.

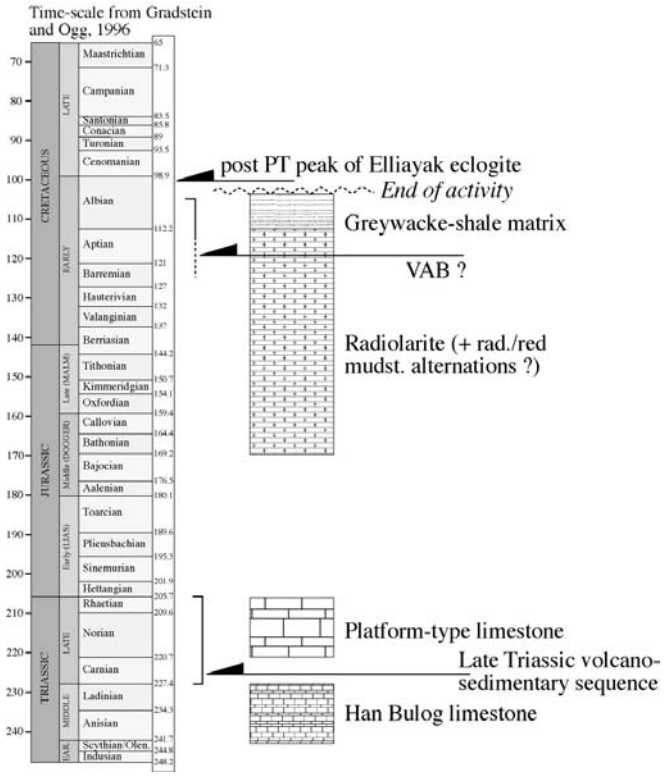

Figure 2.21. Summary of the age data from the Çetmi mélange (maximum ranges).

2.4.2. End of the activity of the Çetmi mélange

The mélange activity stopped when no more mélange-related lithologies were incorporated. There are two ways to date it: (1) to find the youngest lithology which gives a lower limit for the mélange activity, and (2) to find a unconformable contact recording the sealing or transgression of the mélange, which gives an upper limit for its activity.

The youngest lithology of the Çetmi mélange is the lower Albian greywacke-shale matrix, dated north of Küçükkuyu. Moreover, a very informative stratigraphic section from the northern mélange has yielded an upper limit for the mélange activity. It is located north of the Karapürçek village, in the southern side of block *bn3* (Figure 2.7 and 2.22). From bottom to top, it consists of:

- Partly recrystallized grey thickly bedded neritic limestones; they contain Duostominidae, *Aulotortus* sp., *Glomospirella* sp., typical from the **Middle-Late Triassic** (sample B53, det. by Dr. R. Martini and Pr. L. Zaninetti, Geneva). Their age can be more precisely estimated as **Norian-Rhaetian** because (1) of more precise data on the same block farther east (B29 and B30) and (2) facies similarities.
- About 6 metres of breccia made of the underlying grey limestones. The pebbles have a reddish carbonated matrix; beds thickness is ranging from 10 to 30 cm.
- About 4 metres of poorly outcropping thinly bedded partly recrystallized grey limestones; one sample (B44) has yielded Duostominidae, which is also typical for **Middle-Late Triassic**, and considered as Norian-Rhaetian for the same previous reasons.
- About 2 metres of greenish-grey tuffite. This is the first lithology not belonging to the mélange. The contact is poorly visible due to outcrop conditions, but is considered as unconformable.
- 2-3 metres of brownish-yellowish microconglomerate. It reworks some of the lithologies of the mélange, such as radiolarite, limestone, dolomite and magmatic clasts in a beige shaly matrix.
- 2 meters of grey carbonated litharenite with lamellibranch and crinoid fragments, metamorphic lithoclasts, quartz showing dynamic recrystallization, subangular quartz, muscovite. A few poorly preserved Orbitolina (or Mesorbitolina) have yielded a **latest Albian-Early-Middle Cenomanian** age (plate 5A, det. A. Arnaud-Vanneau, Grenoble).
- About 2 metres of bluish-grey tuff, in upper tectonic contact with the greywackes and the spilites of the mélange.

Because of the occurrence of a microconglomerate reworking typical lithologies of the mélange overlain by a latest Albian-Cenomanian litharenite, the upper part of the Karapürçek section gives a latest Albian-Cenomanian age as upper limit for the end of the activity of the mélange. The latter must therefore be located between the Early Albian and the latest Albian-Cenomanian, somewhere in the Middle-Late Albian. This age is confirmed by another close similar section found by Okay et al. (1991), who describe a disconformity between upper Triassic limestones and Cenomanian-Turonian silty micrites.

Another possibility would be that the Triassic limestones with their unconformity have been together incorporated as blocks into the mélange. In this case, (1) the end of the mélange activity would be post-Cenomanian-Turonian; but no younger rock than the Albian matrix has been found in the mélange, which would have been the case if the mélange was still incorporating rocks at that time; (2) whatever happened after latest Albian-Cenomanian times (e.g. reworking of the mélange due to strong tectonic activity, chapter 4), the previous unconformity has to be taken into account.

In the southern mélange a 2-3 m long single outcrop of transgressive (unconformable) upper Cretaceous (Turonian-Coniacian) red silty biomicrites in Couches-Rouges facies has also been found (Brinkmann et al., 1977). However, from the same place, Okay et al. (1991) interpreted it as a small block embedded in the greywacke-shale matrix. Here again, the

problem is to know wether the mélange was still active in the Turonian-Santonian times or not. Several observations support the first hypothesis of a transgressive contact: (1) the previous section from the northern mélange, (2) if it is a block in the mélange so it would be the youngest, and therefore we should expect to find much more similar blocks, (3) the scarcity of these transgressive upper Cretaceous pelagic limestones over the southern mélange and their absence in the northern one could be explained by their erosion following the important uplift of the underlying metamorphic rocks during the Late Tertiary (exhumation of the Çamlıca micaschists in the northern area and of the Kazdağ Massif in the southern area, Okay and Satır (2000a), and chapter 4). This last reason could also explain the scarcity of the Cenomanian unconformable contacts between detritic rocks (litharenite ans siltite) and the Triassic limestones (or other lithologies) in the northern mélange.

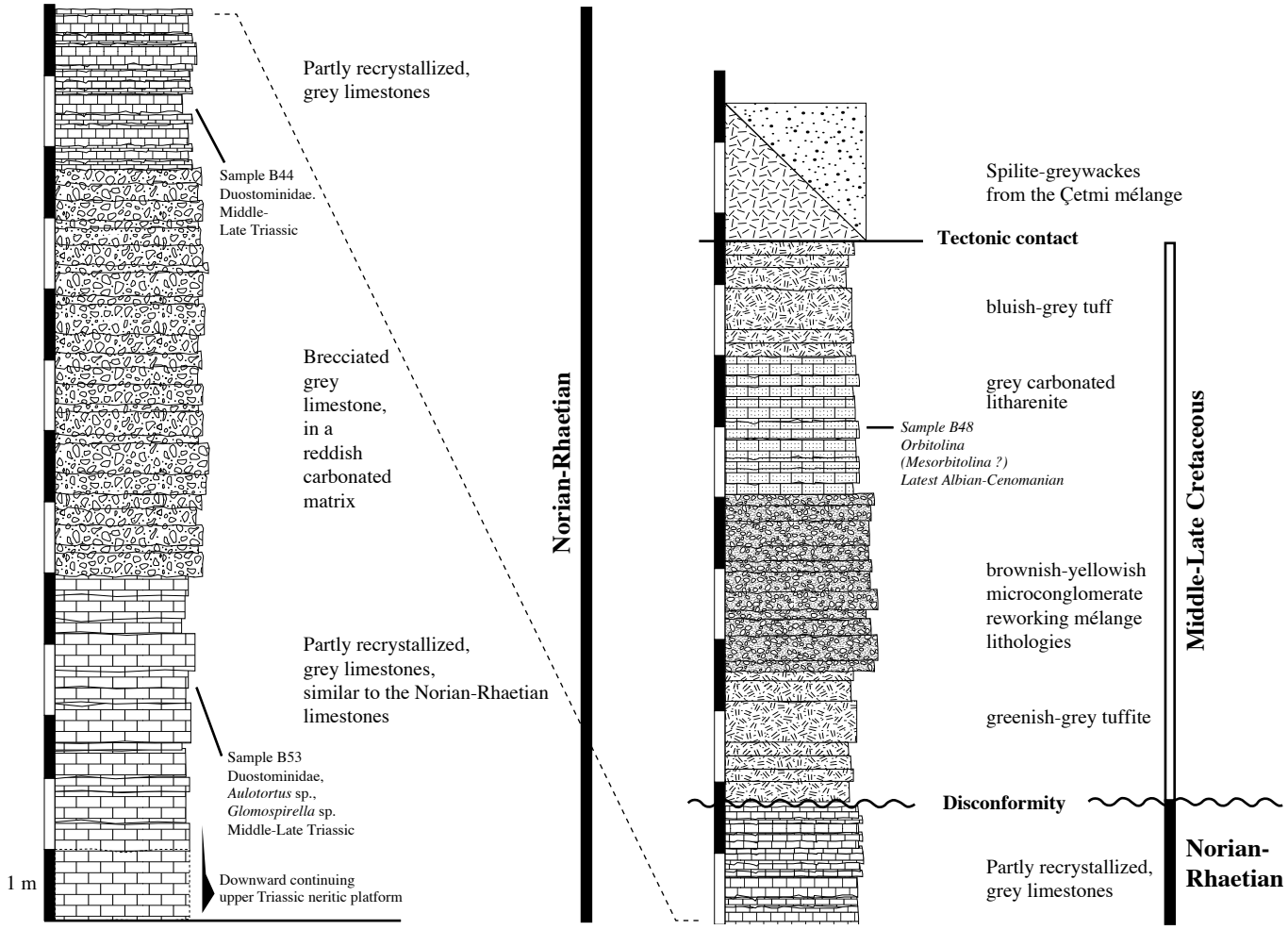

Figure 2.22. Stratigraphic column of the Karapürçek section showing the disconformity between the Late Triassic and the Middle-Late Cretaceous; location on Figure 2.7.

Rare pelagic upper Cretaceous (Maastrichtian) and middle Paleocene pelagic limestone blocks were also found in an Eocene olistostromal unit in the Gelibolu Peninsula, 5 km east of the small outcrops of the Çetmi mélange; as they are associated in the olistostrome with typical lithologies of the mélange (serpentinite, radiolarites, etc…), they have been considered as blocks derived from the Çetmi mélange as well (Okay and Tansel, 1992) so that they would be the youngest blocks of the mélange. However, such Paleocene

limestones are reported from a small place elsewhere in the Gelibolu peninsula, without being associated with the lithologies of the mélange (Lört Limestone, Siyako et al., 1989), indicating a possible extra-mélange origin. This idea is supported by the occurrence in the olistostrome of Eocene reefal limestone, which 5 km westward overlies unconformably the Çetmi mélange (see below and Figure 2.23), showing the possibility to incorporate in the olistostrome rocks younger than those belonging to the mélange.

The middle Paleocene deposits and the various upper Cretaceous pelagic limestones (including the Cenomanian transgression) postdate the mélange emplacement, which is considered as pre-Cenomanian. They may be related to further subsidence of the whole area in the Late Cretaceous, and therefore have unconformably covered the Çetmi mélange. However, there are only very few traces of this transgressive episode today, following the regional uplift of the whole area in the Tertiary (c.f. chapter 4) and the subsequent erosion of the uppermost lithologies.

But the main argument for a pre-Cenomanian end of mélange activity remains the total absence of blocks younger than this age; it is indeed difficult to imagine the total absence of the youngest blocks incorporated in a mélange which predate the end of its activity. For instance, the mélanges belonging to the IAES in Turkey contain Maastrichtian blocks, when they stopped to behave as accretionary mélange in the earliest Paleocene (Okay and Tüysüz, 1999). This critical point has a great importance for the geodynamic evolution of the Çetmi mélange and its place in the regional geology, as discussed below and in chapter 5.

Another implication is that the end of the activity of the Çetmi mélange is syn- or pre-exhumation and emplacement of the eclogite-micaschist bodies (whose peak-metamorphism occurred before 100 Ma); the precise timing depends on the uplift rate of the eclogite lenses.

The Çetmi mélange northwest of Şarkoÿ

The Çetmi mélange north of Şarkoÿ (Thrace) is poorly cropping out in the core of small post-Miocene anticlines (Okay and Tansel, 1992, and Figure 1.11). It is made of serpentinite, metabasite with blueschist to greenschist facies (Şentürk and Okay, 1984), gabbro, spilitic magmatic rocks, radiolarian chert (unfortunately not dated here) and the radiolarite/red mudstone alternations. The area has a complex tectonic history, still active today and related to the Ganos fault, a segment of the North Anatolian Fault Zone (Okay et al., 1999). It is therefore not the best place to study the Çetmi mélange and less time has been spent there.

However, a quarry north of Şarkoÿ displays a nice angular discordance between the Çetmi mélange (here made of the radiolarite/red mudstone alternations) and the overlying Eocene reefal limestone (Figure 2.23). The top of the pelagic sequence is made of a c. 10 m thick conglomerate reworking rounded to subrounded centimetric clasts of the radiolarite/red mudstone alternations and spilitic magmatic rocks. The unconformity is marked by the occurrence of a white Eocene reefal limestone, conglomeratic at its base, reworking the underlying conglomerate with an upward decrease of the clasts proportion within a few metres.

The discordance may be interpreted as an upper limit for the activity of the Çetmi mélange. However a first conglomeratic episode reworking the lithologies of the mélange below the angular discordance is a proof of a pre-Eocene erosional event. In this way the

limestones represent a late transgression episode with respect to the pre-Cenomanian end of the activity of the Çetmi mélange.

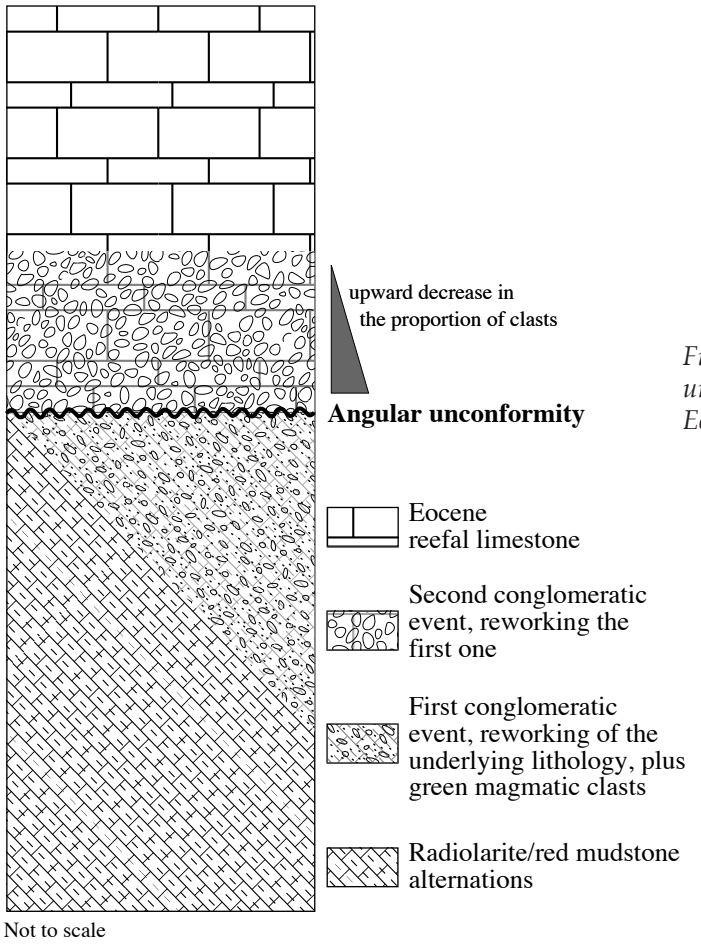

Figure 2.23. Schematic stratigraphic column of the unconformity between the Çetmi mélange and the Eocene reefal limestones, north of Şarkoÿ.

2.4.3. Correlation of the Çetmi mélange

This part deals with the possible lateral correlations of the Çetmi mélange. As said in chapter 1, the Biga Peninsula, and hence the Çetmi mélange, is located at a crossroad between different paleogeographic domains; it appears from the general geological frame of the region that there are two possibilities to link the mélange to the regional geology: (1) toward the east and southeast with a connection with the mélanges of the IAES and the IPS, and (2) toward the northwest with a connection with the Rhodope-Strandja Zone of Greece and eastern Bulgaria. The discussion is based on field-related geological facts, which give several criteria for the comparison: age of the radiolarites, age of the oldest and youngest blocks, nature and age of the matrix, nature of the magmatism, structural position; the geodynamic evolution of the Çetmi mélange will be treated separately in chapter 5, together with that of the Ezine area.

2.4.3.1. Stratigraphic comparison with the IEAS and IPS mélanges

Radiolarites

Radiolarian fauna from the IAES have been reported by several authors (the data are summarized in Figure 2.24). Servais (1982) reports Late Jurassic-Early Cretaceous radiolarian from cherts from an accretionary complex north of Kütahya. Eastward near Nallıhan, chert samples associated with MORB-like pillow basalts yielded Late Bathonian-Early Tithonian and Latest Hauterivian-Early Aptian radiolarian assemblages in an IAE mélange (Göncuöğlu et al., 2000). It is the only place all along the IAE suture where a certain association of MORB-type magmatic rocks and radiolarites is observed. In the Ankara region, Late Norian, Early Jurassic, Kimmeridgian-Tithonian, Early Cretaceous and Albian-Turonian radiolarian ages from mudstone-chert blocks have also been determined (Bragin and Tekin, 1996) in the most complete radiolarian study done along the suture. In the same region Boccaletti et al. (1966) described Late Jurassic-Early Cretaceous radiolarites in close stratigraphic association with "diabase". West of Ankara, a Valanginian age has been obtained from a radiolarite block in

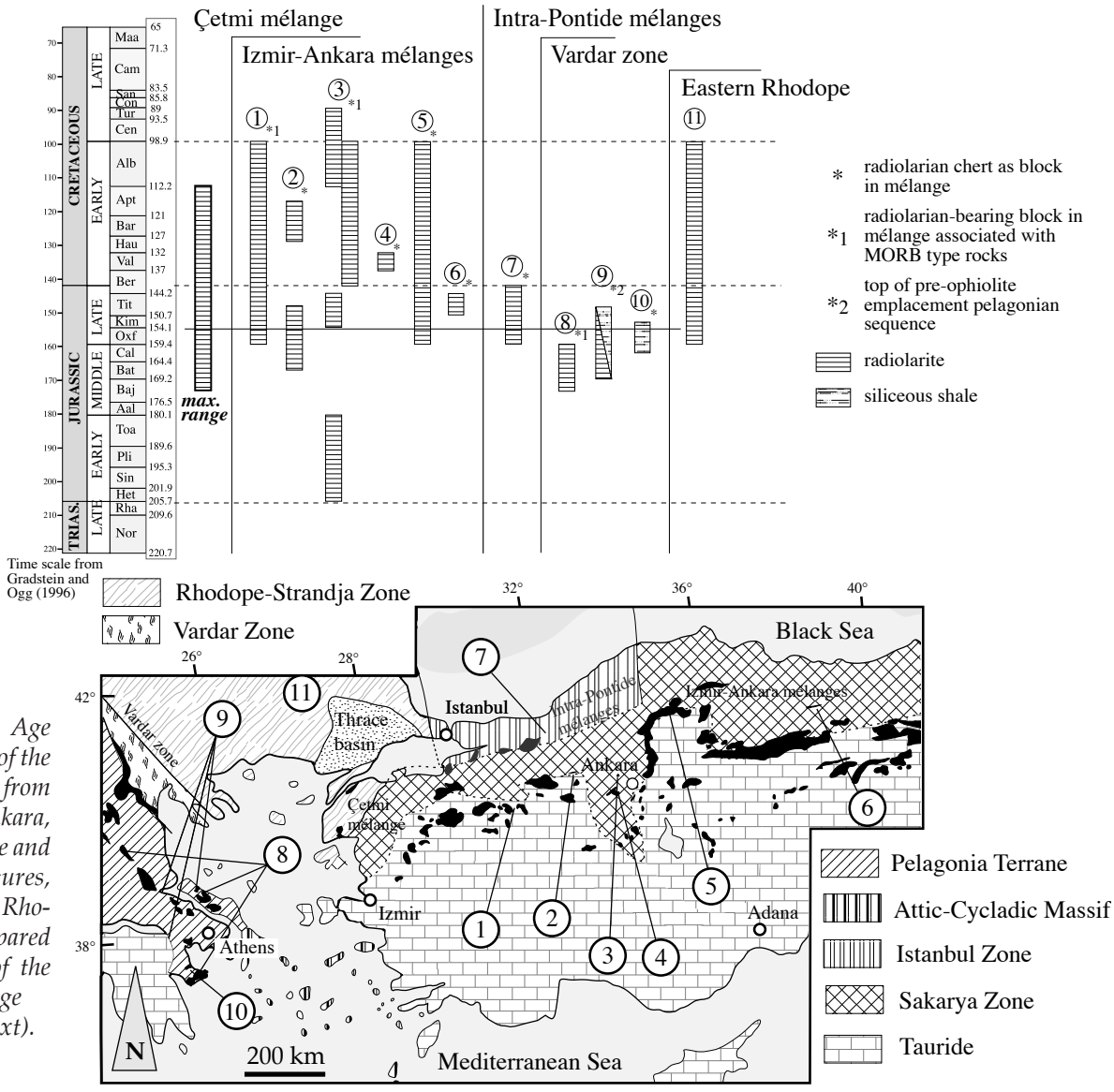

Figure 2.24. Age and location of the radiolarian from the Izmir-Ankara, Intra-Pontide and Vardar sutures, and eastern Rhodope, compared with those of the Çetmi mélange (ref. in the text).

a sedimentary mélange interpreted as a slope deposit on the southern flank of the Sakarya continent (Mekik, 2000). And finally, Tithonian radiolarites from a tectonic slice of Izmir-Ankara-Erzincan accretionary complexes imbricated in the Sakarya basement NW of the Tokat massif have also been described (Bozkurt et al., 1997). Therefore, the age range of the radiolarian cherts from the Çetmi mélange is in agreement with ages found in the IAES. One can just note that, unlike the Çetmi mélange, Late Cretaceous (Cenomanian-Turonian) radiolarian ages have been found in an IAES mélange.

As for the radiolarite ages from the IPS mélange, only Brinkmann (1966) gave a Late Jurassic radiolarian age from a mélange north of Mudurnu. A sample of red radiolarite from an IPS-related mélange (Abant Complex, near Bolu) has yielded upper Bajocian-middle Bathonian radiolarians (sample AB2, Plate 3A). But the small amount of data makes comparisons difficult.

The radiolarian ages from the Çetmi mélange are also compatible with those of the Vardar suture of Greece (Figure 2.24). The latter is considered as a good candidate for the westward continuation of the IAES (e.g. Stampfli, 2000). When dealing with the Vardar mélanges it is really essential to distinguish those associated with the Late Jurassic-Early Cretaceous obduction of the Vardar oceanic crust over the Pelagonian platform, from those related with the final closure of the remnant Vardar Ocean during the Late Cretaceous-Early Tertiary (Pamic, 2002). Only the former have yielded radiolarian ages at the moment. Radiolarites associated with oceanic pillows gave ages ranging from Middle Bajocian to Late Callovian (Baumgartner, 1984; Baumgartner, 1987; 1995; Danelian and Roberston, 2001), whereas radiolarites and radiolarian-bearing siliceous shale located in the flexural basin at the top of the Pelagonian platform gave ages ranging from Early Bathonian to Kimmeridgian-Early Tithonian (Baumgartner and Bernouilli, 1976; Danelian and Roberstson, 1995; Danelian and Robertson, 1998; De Bono, 1998). Late Callovian-Middle Kimmeridgian radiolarians from siliceous shale from a mélange in Argolis Peninsula have been also described (Baumgartner, 1995). Therefore, the age of the radiolarites from the Çetmi mélange is not a decisive argument to relate it to the IAES (or IPS), as they are also contemporaneous with those of the Vardar suture.

Oldest blocks

It is really difficult to give a significance to the oldest lithologies found in a mélange. Indeed, it is strongly possible that during its geological evolution, older rocks, which are not directly related to a mélange, may be incorporated into it. This is for instance the case in the Ankara mélange where the upper Triassic Karakaya Complex is remobilized and mixed in many places with the upper Cretaceous mélanges from the IAES (e.g. blocks of Permian age, Özkaya, 1982; Norman, 1993). In the hypothesis of a Çetmi mélange belonging to the IAES, the Han Bulog limestone may have the same origin, as such facies are also occurring in the Karakaya Complex (Kozur and Mock, 1997), but no other rock from the latter has been found.

However, this could not be the case for the Norian-Rhaetian limestone. The only Late Triassic rocks belonging to the Karakaya Complex of that age are those of the Hodul unit (and possibly the Orhanlar greywackes); in the Hodul unit the Norian-Rhaetian is characterized by fossiliferous grey silstone horizons with lamellibranch, brachiopod and gastropod, overlain by a black shale sequence with lamellibranches, such as *Halobia*, *Daonella* and *Posidonomya* (Okay et al., 1991; Okay et al., 1996). Except in the Karakaya Complex, no

Triassic rocks are found in the Sakarya Zone, whose main characteristics is the major Liassic transgression over the Karakaya units. This Liassic transgression is marked in the Biga Peninsula by a basal detritic sequence of Liassic age (Bayırkoÿ Fm) followed by the passive continental margin type deposits of the Bilecik Limestone (Late Jurassic-Early Cretaceous ?) and the Albian-Cenomanian Vezirhan Fm (Okay et al., 1991). None of these lithologies has been reworked in the Çetmi mélange.

Youngest blocks

The mélange of the IAES contains pelagic limestone blocks as young as Maastrichtian (e.g. Çapan and Buket, 1975; Tüysüz et al., 1995), and their matrix may be of Campanian age (matrix of Kırıkkale mélange in the Ankara region, made of red mudstone and turbiditic sandstones of Campanian age, Özkaya, 1982).

Mélanges from the IPS have also yielded pelagic limestone blocks from the Late Cretaceous (Late Santonian Couches Rouges in the Dağdibi clastics, Greber, 1997); however, it is not clear if these blocks are really belonging to the IPS or to a reworked overlying unit (Greber, 1997). A sample of pelagic limestone in Couches Rouges facies from the Abant Complex has yielded *Dicarinella asymetrica*, *Globotruncanita elevata*, *Dicarinella concavata*, *Dicarinella* aff. *concavata*, *Marginotruncana pseudolinneiana*, *Globotruncanita* sp., *Marginotruncana coronata*, *Hedbergella*, also characteristic for the Late Santonian (plate 5B, det. Pr. M. Caron, Fribourg).

Magmatic rocks

They are an important component of the IAES mélanges (Floyd, 1993; Tüysüz et al., 1995; Tankut et al., 1998), but are not considered here as a decisive factor for their comparison; indeed many types of magmatic rocks are expected to occur in an accretionary mélange (OIB, VAB, MORB, etc…), and it is difficult to compare them on the base of their geochemical signatures, especially if the rocks are not dated.

Conclusion

The Çetmi mélange has some common characteristics with the mélanges from the IAES and IPS, but cannot be strictly correlated with them on the basis of their stratigraphy:

- The age of the radiolarites is not a sufficient criteria to attribute the Çetmi mélange to the IAES or IPS.
- There is no possibility to correlate the Late Triassic platform-type limestone found in the mélange with the Triassic rocks known in the Sakarya Zone.
- The IAES mélanges contain blocks of Senonian age (and are still in activity at that time), whereas the Çetmi mélange has stopped its activity before the Cenomanian.
- The poorly known IPS mélanges possibly contain blocks of Santonian age; in this case they cannot be related to the Çetmi mélange.
- Only the Han Bulog limestone may have been reworked from the Karakaya Complex; but if true, other lithologies from the Karakaya Complex should be present in the mélange, what is not the case.

One should add that no eclogitic lenses, above all of pre-Cenomanian age, have been found in the IAES and IPS mélanges. One should therefore look elsewhere to find a lateral equivalent to the Çetmi mélange.

2.4.3.2. Evidences from eastern Rhodope

A possible lateral equivalent for the Çetmi mélange may be found in the allochthonous nappes of the Rhodope-Strandja Zone of northern Greece and eastern Bulgaria, where rare unmetamorphosed Mesozoic series occur in scattered areas as klippen over the crystalline basement (Figure 2.25).

In eastern Bulgaria near the Greek and Turkish boundaries, the magmatic-terrigeneous-pelitic (with magmatic rocks) Dolno Lukovo Fm of the Mâglenica Group is made of three members: the clasto-lava member, the olistostrome member and the concretion member (Boyanov and Russeva, 1989), whose total thickness is about 400 m:

-The clasto-lavas member is made of basalt to andesitic basalts with pillow structures and island arc signatures (Bonev and Stampfli, 2003). The magmatic rocks are intercalated in deep-water sediments, such as silstones, shales, marls, pelagic limestones and lower Jurassic radiolarites (Trifonova, 1988). The whole lithology is strongly tectonized and resembles an olistostrome. There is a doubt about the origin of this clasto-lavas member, which may actually belong to the Evros ophiolite (see chapter 3).

-The olistostrome member comprises sandstones, conglomerates, breccias in a clay-silty matrix. Marine siliceous rocks have yielded a Late Permian age (Trifanova and Boyanov, 1986), whereas upper Anisian and uppermost Ladinian conodonts have been found in grey limestones pebbles (Boyanov and Budurov, 1979); platform-type limestone pebbles have also yielded a Norian age (Boyanov and Trifonova, 1978); Late Triassic platform-type limestones are moreover a characteristic feature of the Rhodope-Strandja area (c.f. Figure 1.5).

-The concretion member is made of interbedded marls, silty-shales with siderite concretions bearing upper Jurassic-lower Cretaceous radiolarians (Trifonova, 1988).

The Dolno Lukovo Fm is thought to have a Late Jurassic-Early Cretaceous age following the previous considerations (Boyanov and Russeva, 1989). It contains lithologies similar to the Çetmi mélange, with compatible ages. There are, however, three important differences: (1) the Dolno Lukovo Fm has a more conglomeratic aspect with no large (hm) blocks as in the Çetmi mélange; (2) the red radiolarites are absent (the radiolarians are coming from siderite concretions); (3) the structural pattern retains stratigraphic succession and shows post emplacement compressional deformation in eastern Bulgaria (Alpine orogeny s.l., Maastrichtian-Middle Eocene).

The Dolno Lukovo Fm, as well as the underlying Mandrica Group and high-grade rocks, are overlain through a transgressive contact by the Meden Buk Formation (upper part of the Mâglenica Group). The base of the Meden Buck Fm is made of conglomerates and sandstones reworking the underlying lithologies, whereas its upper part is made of sandy and tuff-rich limestones which yielded Campanian foraminifera (Boyanov et al., 1982) with magmatic rocks of andesitic and dioritic type. The transgressive event between the Meden Buk Fm and the underlying units may be correlated with that of the Çetmi mélange, where it is Cenomanian in age. Moreover, the Cenomanian transgression is a very general feature of the region which marks the end of the Balkan orogeny in the middle Cretaceous (Georgiev et al., 2001). The upper part of the Meden Buk Fm is most probably related to the northward Late Cretaceous arc/back arc magmatic activity of the Srednogorie Zone in Bulgaria.

In northwest Greece, close to the Bulgarian and Turkish boundaries, the same features are observed, and the Mâglenica Group (mainly Dolno Lukovo) is correlated with the Drimos-

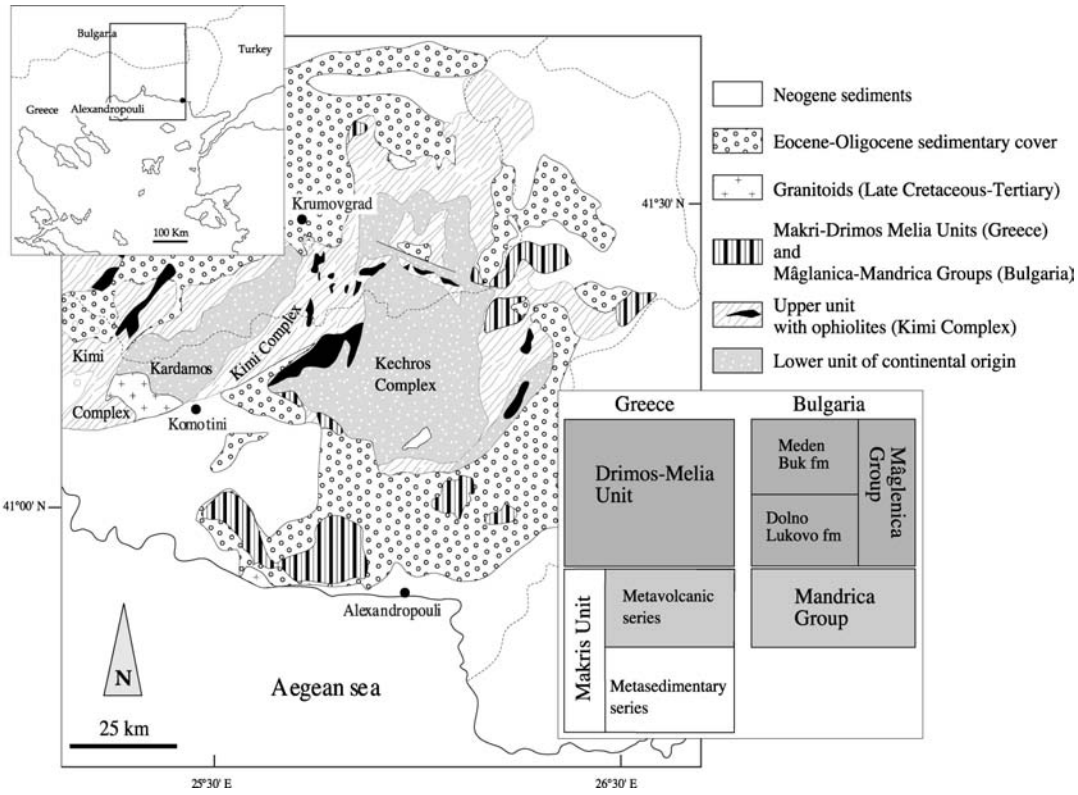

Figure 2.25. Simplified geological map of Eastern Rhodope, with the correlations between Greece and Bulgaria, modified from Bonev and Stampfli (2003).

Melia unit (Late Jurassic-Early Cretaceous), whereas the Mandrica Group is correlated with the Makri Unit (Triassic-upper Jurassic ?, Boyanov and Russeva, 1989; Papadopoulos et al., 1989; Braun, 1993, and ref. therein for micropaleontological data in Makri and Melia units).

Conclusion

Despite the poor knowledge on the geology of the Rhodope units of Greece and southeastern Bulgaria described above, it appears that the Çetmi mélange has some common characteristics with the Mâglenica and Drimos-Melia units (e.g. age of radiolarians, Norian pebbles, possible Cenomanian unconformity). There are however some differences, particularly in the aspect (conglomeratic in Rhodope area, radiolarian in concretions), but less significant than the similarities.

2.4.3.3. Structural position of the Çetmi mélange

The Biga Peninsula, and hence the Çetmi mélange, is located north of the IAES (Figure 1.3). It is widely demonstrated and accepted that the IAE mélanges have been emplaced southward over the Anatolide-Tauride Block in the Late Cretaceous. Nevertheless, a northward obduction of mélanges (accretionary complexes) over the Sakarya Zone also occurred in the Mid Cretaceous (Bergougnan, 1975; Koçyigit, 1991; Okay and Şahintürk, 1997; Okay and Tüysüz, 1999). In this way, the structural position of the Çetmi mélange north of the IAES, like the latter, could be related to this northward obduction event. A difference is that the IAE northerly mélanges were emplaced onto typical passive margin-types Sakarya sequences; the nature of the lower contacts of the Çetmi mélange is presently quite different (serpentinite, eclogite and the high-grade rocks of the Kazdağ Core Complex

	Çetmi mélange	**Izmir-Ankara mélanges**	**eastern-Rhodope mélanges**
End of activity	Pre-Cenomanian	Post Maastrichtian	Pre-Cenomanian ?
Structural aspect	Blocks of various size mostly in tectonic contact, few matrix Position north of IAE-Vardar suture	blocks of various size mostly in tectonic contact, few matrix Position south and locally north of IAE-Vardar suture	Conglomeratic aspect Position north of IAE-Vardar suture
Oldest block	Han Bulog limestones Late Scythian-Ladinian	Permian blocks, from Karakaya Complex	Late Permian siliceous pebbles
Radiolarians	Middle Jurassic-Early Cretaceous (red radiolarite)	Middle Jurassic-Early Cretaceous (red radiolarite)	Middle Jurassic-Early Cretaceous (in concretions)
Magmatic rocks	VAB-WPB	VAB, OIB	VAB
Matrix	Early-Middle Albian	Few data, locally Campanian	?
Comments	Norian-Rhaetian platform limestone	No (doesn't exist on Sakarya margins)	Yes, as pebbles Late Anisian-Late Ladinian grey limestones (conodont age)

Table 2.3. Comparative table of the Çetmi, Izmir-Ankara, and eastern-Rhodope mélanges.

and Çamlıca micaschists). On the other hand, the structural position of the Çetmi mélange is also compatible with the hypothesis of its westward correlation with the units of the eastern Rhodope area (the latter are also located north of the suture); moreover, both are tectonically underlain by high-grade metamorphic rocks, which have some similarities (c.f. chapter 4).

2.4.3.4. Conclusion

The comparative data are summarized in table 2.3.

The Çetmi mélange has some common characteristics with the Turkish mélanges, but they are less important than their differences. On the other hand, a correlation with the mélange-like units found in eastern Rhodope seems more straightforward. The decisive arguments are the major Cenomanian transgression (which marks the end of the Balkan orogenic phase), the reworking of Triassic limestones, which cannot come from the Sakarya margin (in particular the Norian ones), and the absence of Jurassic-Cretaceous passive margin type lithologies. It is interesting to note that the position of the Çetmi mélange north of the IAE-Vardar suture is a common feature to the mélanges of eastern Rhodope and Turkey (at least for some of them).

Finally, it appears that (1) the Çetmi mélange has no true lateral equivalent (uniqueness), (2) it shares some characteristics with mélanges both from Turkey (less) and Rhodope area (more), and (3) it was emplaced in a Balkanic logic (ante-Cenomanian northward thrusting). Therefore, the geodynamic evolution of the Çetmi mélange must take into account all these aspects. The latter will find its justification only if the geodynamic scenario is coherent with the regional geological frame; in particular, it must also integrate the data from the Ezine area, the subject of the next chapter.

- CHAPTER 3 -

GEOLOGY AND CORRELATIONS OF THE EZINE GROUP AND DENIZGÖREN OPHIOLITE

The north-south trending association of the sedimentary Ezine Group and the Denizgören ophiolite (plus its metamorphic sole) is located north of Ezine in the western part of the Biga Peninsula (Figure 1.11). The ophiolite and the sedimentary sequence are in tectonic contact with the underlying high-grade metamorphic rocks of the Çamlıca micaschists. The broad Permian age of the Ezine Group (Okay et al., 1991), the Early Cretaceous age of the basal amphibolite below the peridotite (Okay et al., 1996), plus their closeness to the Çetmi accretionary mélange (from which it is only separated by the conglomeratic infill of the 15 km wide Plio-Quaternary Bayramiç graben), were the reasons which decided to study the Ezine area into details.

Before its renewal of interest due to Okay et al. (1991), the region has been mapped by several authors (e.g. Kalafatçıoğlu, 1963, and ref. therein, Figure 3.1, Bingöl et al., 1975). The Ezine area has been mapped at the 1/20'000 scale during several fieldworks in spring 2000, 2001 and 2002. The corresponding map at the 1/50'000 scale is found in plate 10. The data from the Ezine Group and the overlying Denizgören ophiolite (and its metamorphic

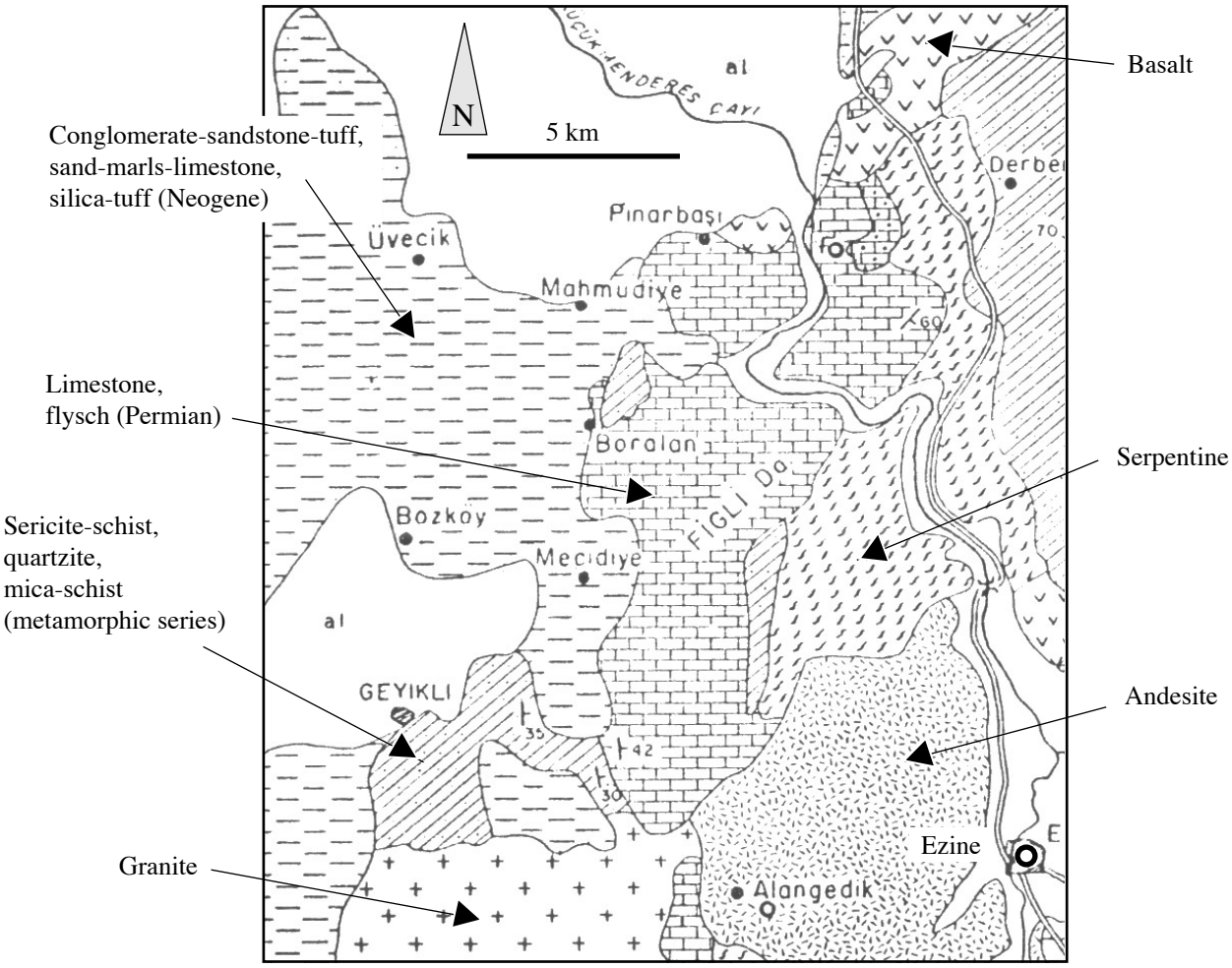

Figure 3.1. Extract of the geological map of the area around Ezine, by Kalafatçioğlu (1963).

sole) are first presented, together with their structural relationships; then their possible correlations are discussed.

3.1. The Ezine Group

The whole sedimentary sequence in the greenschist facies cropping out west and north-west of Ezine city (Karadağ Unit, Okay et al., 1991) is renamed as the Ezine Group; it has been subdivided into three new lithostratigraphic units based on common stratigraphic features: from the base to the top, the Geyikli Formation with a slight terrigeneous detritic nature, the Karadağ Formation with platform type sedimentation with detrital local input, and the Çamkoÿ Formation with a pronounced carbonated detritic nature (Figure 3.2).

3.1.1. The Geyikli Formation

The Geyikli Fm is poorly cropping out between the village of Geyikli to the west and the village of Gökçebayır to the east. Its thickness may be estimated at about 1500 m maximum. It has been subdivided into four members, which show a roughly north-south alignment; they are successively described below, from the base to the top.

The lower member

It mainly crops out directly south of the village of Geyikli. It is made of silty to sandy recrystallized limestones, whose thickness varies from a few cm up to 2 m. Subparallel to crossed mm-scale foresets are common. Argillaceous layers, a few mm to a few cm in thickness, are locally interlayered in the detritic limestones. However, as a general rule, the sequence does not show such fine-grain material. From the tectonic point of view, the whole sequence shows m to dm-scale open folding. The base contact of the member is unknown as it is covered by Quaternary deposits.

Its upper contact marks the transition to the intermediate member n°1; based on facies similarities it is thought to be stratigraphic, even though the contact is not clearly visible in the field.

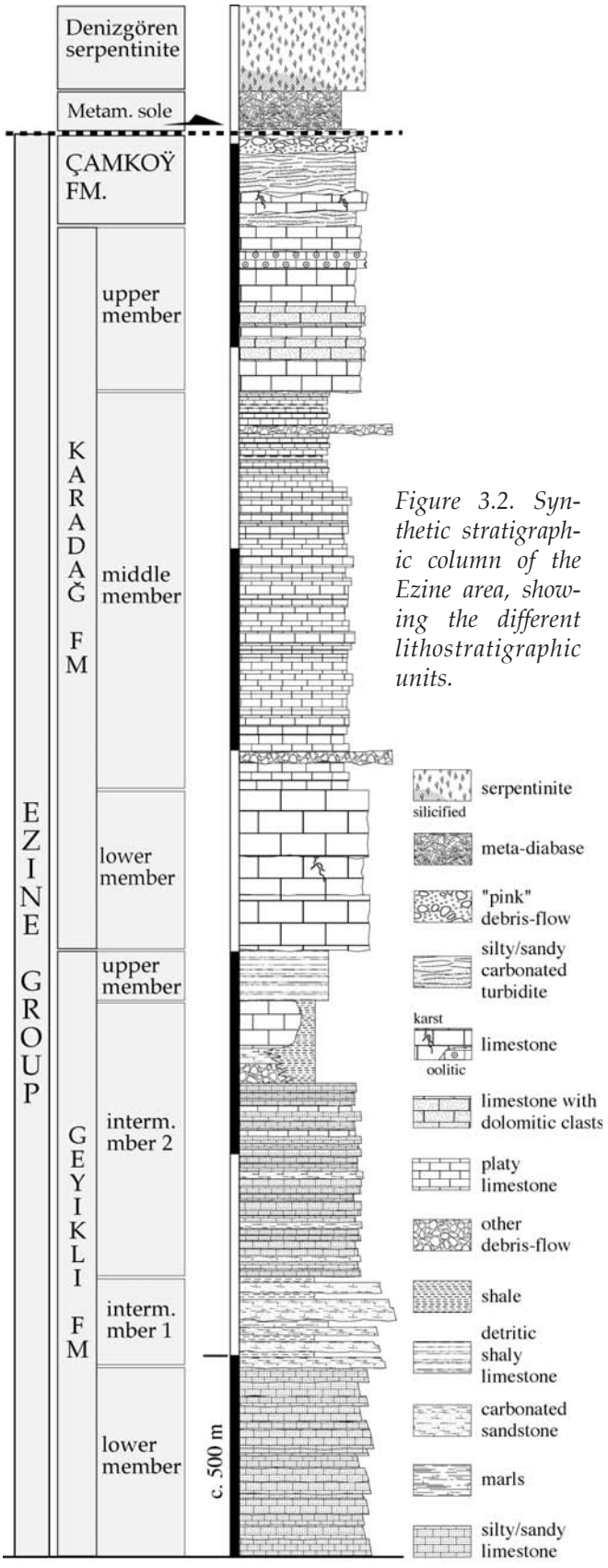

Figure 3.2. Synthetic stratigraphic column of the Ezine area, showing the different lithostratigraphic units.

The intermediate member n°1 (IM1)

This small member was cropping out relatively well along the road from Geyikli to Gökçebayır village, but recent roadworks have damaged the outcrop. It is made of alternations of detritic recrystallized limestones and silvery, green, metashales and metamarls. The thickness of the detritic limestones varies from 30 cm to about 10 m. Some quartz pebbles are reworked in the detritic limestones. The transition to the intermediate member n°2 seems to be progressive.

The intermediate member 2 (IM2)

This member crops out in the north of the road from Geyikli to Gökçebayır. It is made of recrystallized detritic limestones and rare recrystallized carbonated sandstones, few dm thick and showing a characteristic jellowish patina. These facies pass up to massive slightly detritic dark grey fetid limestones, occuring as olistoliths. The transition occurs in two different ways: either through a coarse to conglomeratic few meter thick detritic carbonated sequence (Bayırgölü Hill, fig 3.3), or through a metashale sequence, dark grey to black in colour (Zindan Hill). The transition to the upper member is not displayed around Bayırgölü Hill; it seems to be stratigraphic east of Zindan Hill, where the dark shale pass up to the detritic shaly limestones of the upper member.

The upper member

This small member crops out north-west and south-east of Gökçebayır. It is made of thin layers of recrystallized detritic shaly limestones (calcschists), yellowish to grey in colour. This member marks the end of the Geyikli Fm. The transition with the overlying Karadağ Fm is clearly stratigraphic and can be seen in the quarries north of Gökçebayır and east of Bozalan village (picture 3.1 plate 7B). Another lateral facies is made by the alternations of ancheritized carbonates sandy turbidites and greenish silstone (Figure 3.4); no direct contact with the Karadağ Fm has been observed.

Age of the Geyikli Fm

The whole sequence is dominated by detritic facies and only a *Permocalculus* has been found in a wackstone/packstone from

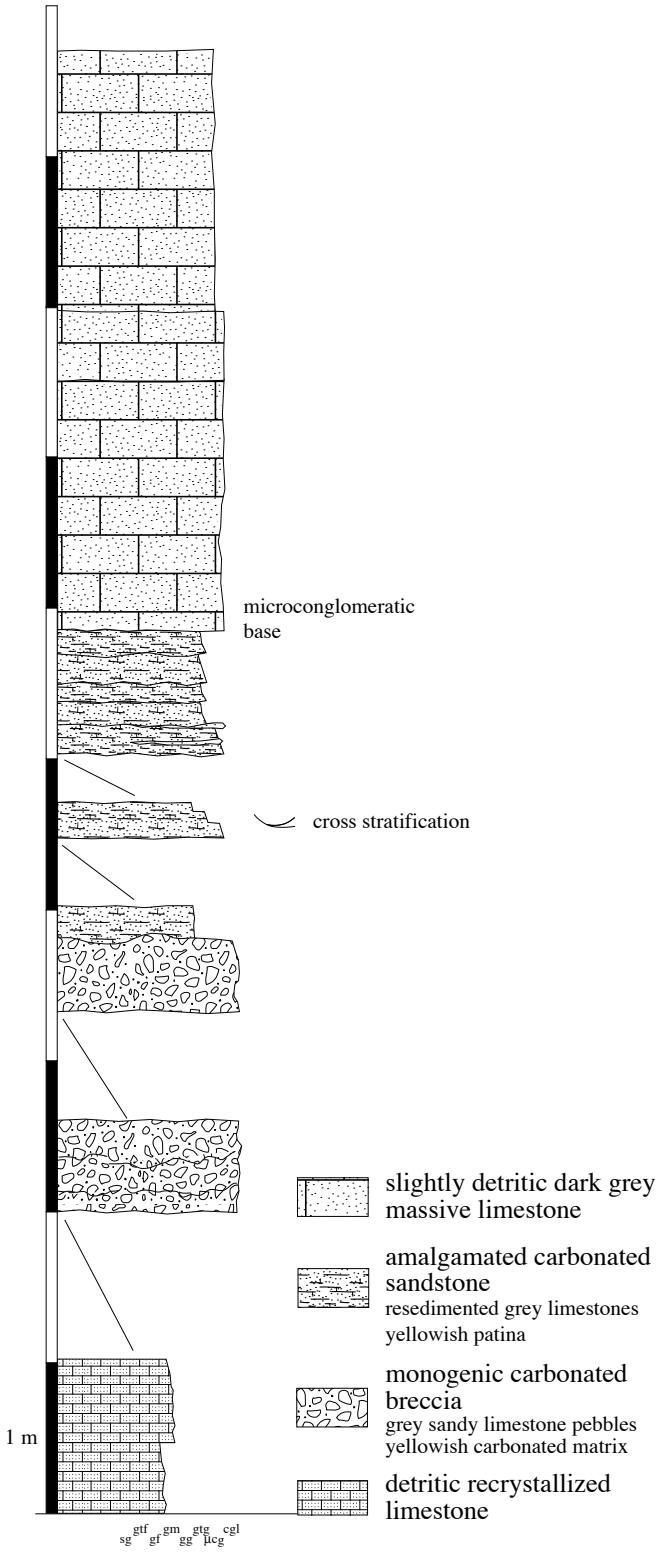

Figure 3.3. Upper part of the intermediate member 2 (Bayırgölü Hill); location on Figure 3.5.

the upper part of IM2 (sample E148, location in Figure 3.5); this algae (Gymnocodiacae) is characteristic for the Middle-Late Permian.

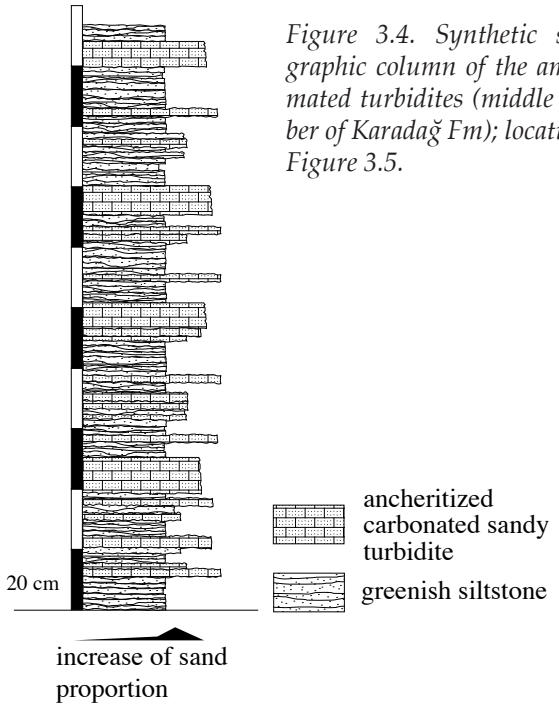

Figure 3.4. Synthetic stratigraphic column of the amalgamated turbidites (middle member of Karadağ Fm); location on Figure 3.5.

Depositional environment of the Geyikli Fm

The four members of the Geyikli Fm are considered in stratigraphic continuity and show a total estimated maximum thickness of about 1'500 m. The bulk of the rock is made of carbonated material, but the whole formation is characterized by a more or less important detritic component, represented by quartz grains and locally pebbles; The lower member and IM1 may represent open marine detritic sedimentation (coastal fan), with possible deepening in IM1 (typical turbiditic facies). IM2 is typical of a shallowing sequence marked by the occurrence of a Dacycladacea in slightly detritic limestones. The upper part of IM2 is marked by small-scale lateral facies variations; the dark massive limestone olistoliths at the top of IM2 prefigure the emplacement of the platform carbonate from the Karadağ Fm (e.g. olistoliths in front of the prograding platform). The upper member records quiet detritic sedimentation before the installation of the platform.

3.1.2. The Karadağ Formation

The Karadağ Fm represents the most important part in surface of the sedimentary sequence north-west of Ezine. It has been subdivided into three successive members, showing a clear north-south alignment. They are described below, from the base to the top.

The lower member

It is made of thickly-bedded to massive grey recrystallized limestones, cropping out around Gökçebayır and Bozalan villages. Its thickness may be estimated at about 400 m. As previously said, it is in conformable stratigraphic contact with the underlying calcschists of the upper member of the Geyikli Fm. Some rare dm-scale karstic features are present; coral structures may also occur, but they are difficult to recognize due to the generalized recrystallization. Because of their massive structure, these limestones would have been expected to crop out continuously from one place to another. However, they are only present in two places separated by more than 5 km. This observation can be compared to that of the possible reef structures, and the 2 outcrops might represent two isolated reefs.

Another facies, cropping out south-east of Bozalan, made of thinly to thickly bedded (10 cm to 6 m) light grey limestones, is also included in the lower member. The top of each bed is marked by a cm thick red oxidized horizons, interpreted either as emersion or condensed surface.

The transition to the middle member is stratigraphic and can be observed north of Gökçebayır.

The middle member

It is the most extensive unit in the Ezine Group. It crops out along a north-south alignment from Taştepe village in the north to Gökçebayır in the south. Its total thickness may be estimated at about 1'000 m. The

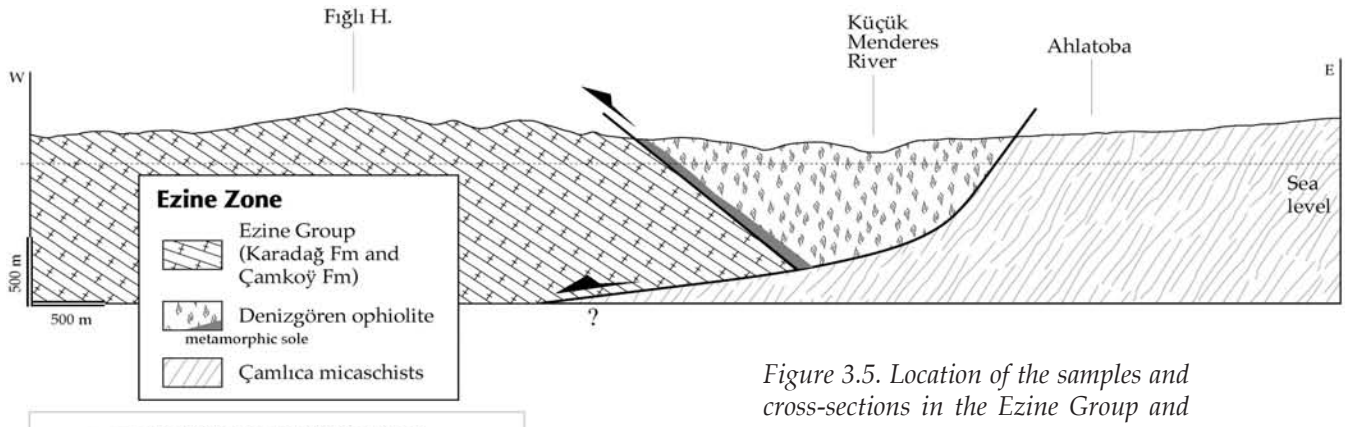

Figure 3.5. Location of the samples and cross-sections in the Ezine Group and in the metamorphic sole of the Denizgören ophiolite.

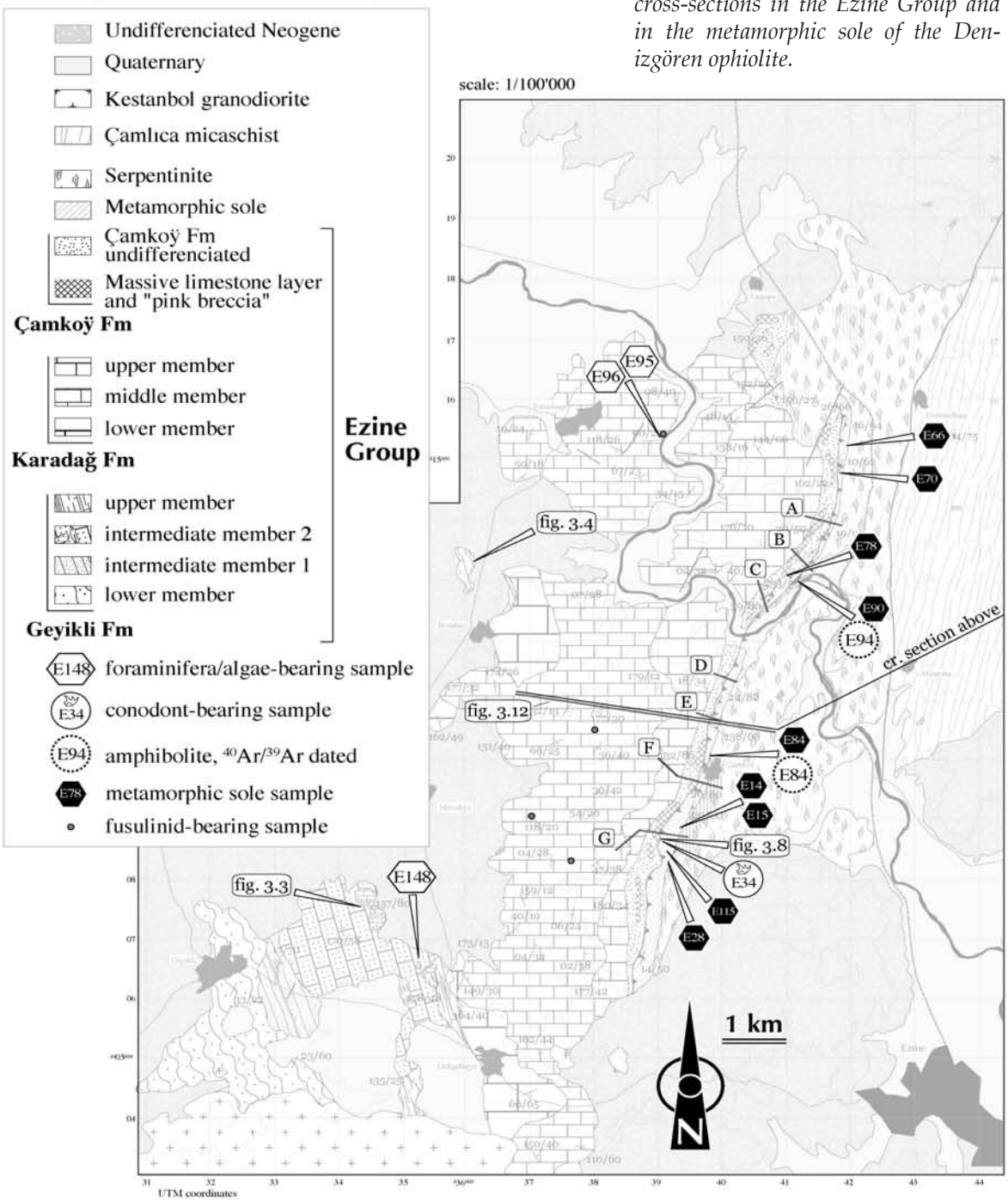

whole sequence is gently folded. The main facies is made of dark grey (sometimes light pink) recrystallized limestone, thinly to medium bedded (a few dm thick in general). Pyrite, birdeyes and traces of fossils locally occur. Toward the top of the unit, the grey limestones pass up progressively to thinly bedded platy limestones, displaying light pink, greenish and dark grey colours. These platy limestone are sometimes associated in space with dark meta-shale. In rare places, chert nodules intercalated in grey thinly bedded recrysallized limestones have been found.

Toward the base of the unit there is a first conglomeratic episode, intercalated in the dark grey limestones; its thickness varies between 1 and 10 m. The conglomerate is either monogenic (grey recrystallized limestone pebbles) or polymict (grey and red recrystallized limestone pebbles, green phyllite). The subrounded pebbles reach the size of 15 cm and the matrix is always carbonated (picture 3.2 plate 7B).

A second conglomeratic episode, looking like the first one, occurs toward the top of the sequence, generally over the platy limestones. Its thickness is about a few meters and in two places clear bedding and pebbles alignment (N-S) is observed; the conglomerate is either monogenic (grey recrystallized limestone pebbles) or polygenic (white, beige and dark grey recrystallized limestone pebbles). The subangular to subrounded pebbles reach the size of 10 cm; the matrix is always carbonated, pinkish to yellowish in colour (picture 3.3 plate 7B).

All the previous facies show important variability in their thickness but are always present where expected. The middle member passes up conformably and progressively to the upper member.

The upper member

The upper member crops out eastward of, and parallel to the middle member. At first glance it is totally made of thickly-bedded white recrystallized limestones (50 cm to 6 m thick). Its thickness may be estimated at about 500 m maximum. Two different facies, whose external aspects are almost the same, have been distinguished: one is made of carbonated resediments, with a very small terrigenous fraction, but reworking submm-scale fragments of dolomitic limestones; these clasts underline a parallel lamination. The other does not show any clear displacement features; on the contrary, it displays locally oolithic grainstone microfacies, and some traces of a Middle-Late Permian Gymnocodiacea have been observed in one place toward the top of the member, but below the oolitic limestones.

The transition between the upper member of the Karadağ Fm and the overlying detritic Çamkoÿ Fm is most often obliterated by recent fault activity. However, it is considered as primary (conformable), based on local observations and facies similarities and continuities.

Age of the Karadağ Formation

No fossil has been found in the lower and upper member of the Karadağ Fm. Only in one place of the middle member east of Pınarbaşı village, a sample from a dark grey-light pink recrystallized limestone layer has preserved the following assemblage (sample E96, location of the sample in Figure 3.5, and pictures of the age-diagnostic taxa plate 6): *Staffella* sp., *Nankinella* sp., *Gyroporella* sp., *Hemigordius* sp., *Globivalvulina* sp., *Geinitzina* sp., *Nodosaria* sp., *Agathaminna* sp., *Pseudovermiporella* sp, *Permocalculus plumosus*, ostracods, bryozoans, microgasteropods and echinoids, characteristic for the Middle-Late Permian. Moreover sample E95 (Figure 3.5 and plate 6), from the same place, has preserved *Rectostipulina quadrata* characteristic for the **Dzhulfian** (Late Permian). The middle member of the Karadağ Fm is therefore considered as Late Permian (Dzhulfian). These ages are in agreement with the ages already found around the same place by Kalafaçıoğlu (1963), Gözler et al. (1984) and Okay et al. (1991).

An important comment is that the upper Permian deposits in the Tethyan domain are rarely represented by white limestones such as those of the upper member. On the contrary, oolithic limestones are typical of the lower Triassic, so that the upper member of the Karadağ Fm may be Early Triassic in age, and may record the Permian-Triassic boundary.

Depositional environment of the Karadağ Formation

The three members of the Karadağ Fm are in stratigraphic continuity and represent a maximum thickness of about 1'700 m. The lower member marks the installation of the prograding platform over the more distal carbonate-detritic deposits. Few emersion events must have occured, as proved by the occurrence of rare karsts. The middle member, almost one km thick, records typical lagoonal-type sedimentation, as shown by the micro-faunal assemblage and the regular succession of dark facies with restricted features (pyrite, birdeyes). The upper part of the middle member shows a deepening of the depositional environment, with thinly bedded platy limestones intercalated with chert nodules and/or dark shale layers. This quiet environment is interrupted by two a few-m thick conglomeratic episodes (debris-flows), in the lower and upper part of the member. Both of them are reworking separately the underlying carbonated lithologies, as well as carbonates unrelated to the Ezine Group (e.g. the green phyllites); these two events may be considered as prefiguring the strongly disturbed sedimentation of the Çamkoÿ Fm. The upper member, possibly Early Triassic in age for its uppermost part, is characterized by an increase of the energy; the latter is marked either by transportation of very fine erosion products of landward dolomitic deposits, or by the emplacement of oolitic bars.

3.1.3. The Çamkoÿ Formation

The Çamkoÿ Fm crops out as a narrow band (about 300 m wide) east and over the Karadağ Fm. At first sight, the Çamkoÿ Fm shows a complex organisation without any logic. However, it is not quite the case, and several facies occuring roughly in the same order have been identified (Figure 3.6). They are described in their common succession of occurrence from the base to the top.

Light pink debris-flows

These thickly bedded conglomerates (up to 5 m thick with an average thickness of 0.5-1m) are mainly cropping out toward the top of the sequence in tectonic contact with the metabasites. They are made of various kinds of carbonated elements (fig 3.7): (1) elongated recristallized white limestone, sometimes with (dark) grey layers, up to 50 cm long and 10 cm wide; (2) subangular to rounded dark pink recrystallised limestone, with a diameter up to 20 cm; (3) light pink or grey recrystallised limestone, showing no preferential shape; (4) light pink/yellow dolomite; (5) dolomitic limestone. These elements have a typical hallstattoid facies. The matrix is made of the same lithologies as the element; it is always carbonated, and shows locally dolomitization; its colour varies from light pink to yellowish. The elements display broadly two morphologies: one is rounded to subangular, as classical conglomerate pebbles, the other is elongated, and the pebbles look like fragments of (banded)limestone layers. (pictures 3.4 and 3.5 plate 7B).

Silty to sandy carbonated turbidite

These thinly bedded recrystallized detritic (with quartz) limestones (average thickness of about 5 cm with a maximum of 30 cm) display a grey patina and a white, grey or light pink fracture. They occur mainly from the top of the sequence to the light pink debris-flows (picture 3.6 plate 7B).

Karstic massive grey limestone

These massive grey limestones (up to 3 m thick) are always found toward the top of the sequence, possibly as olistoliths. They are characterized by local but well preserved karstification features. They may also have a detritic component, and show local dolomitization (pictures 3.7 and 3.8 plate 7B).

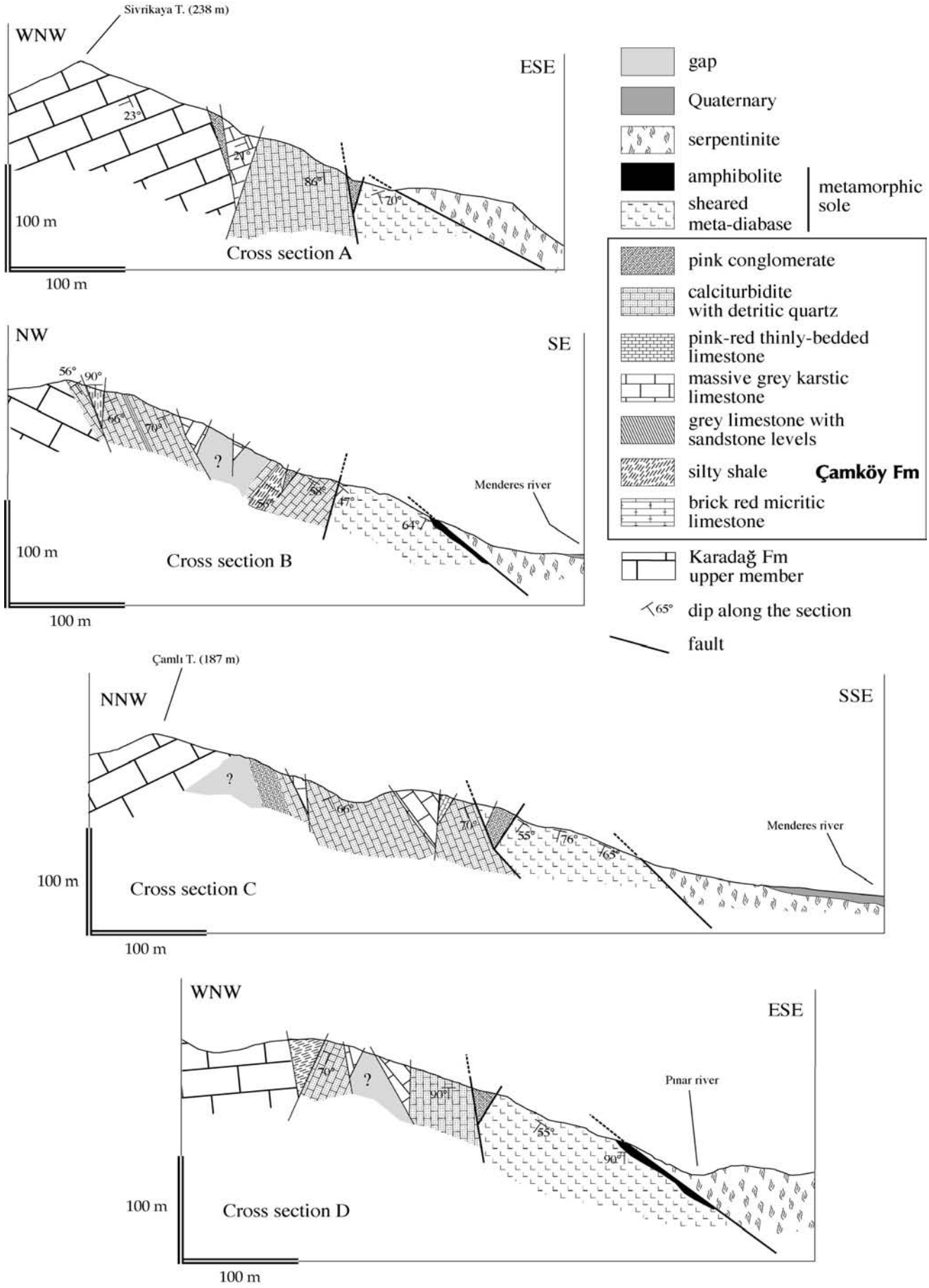

Figure 3.6. Cross-sections of the Çamkoÿ Fm at the 1/50'000; location in Figure 3.5.

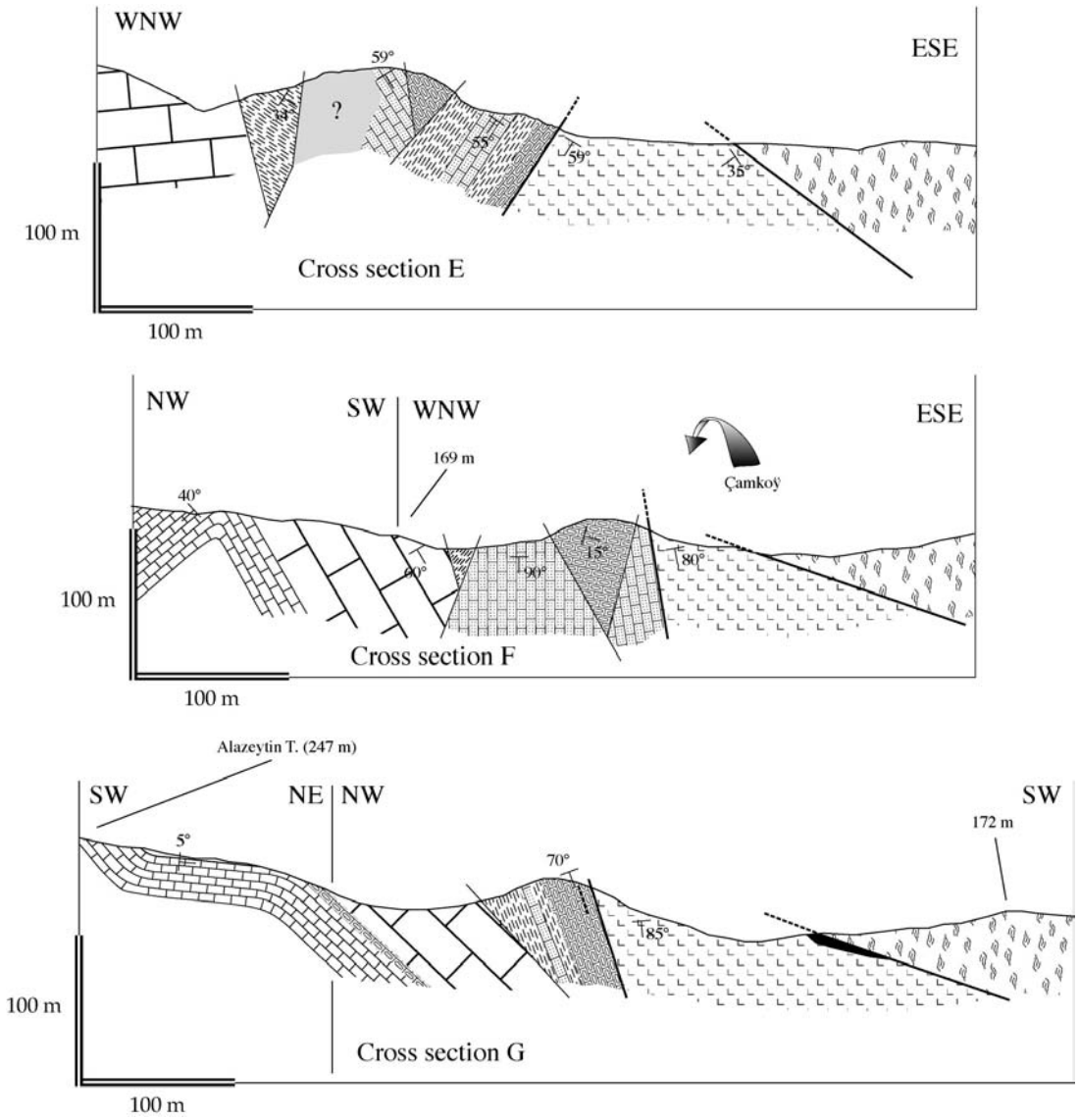

Figure 3.6. Continued.

Structure of the Çamkoÿ Fm

The contact between the more massive lithologies (light pink debris-flows and karstic massive grey limestone) and the other lithologies (mainly the silty to sandy carbonated turbidites) is most of time obliterated by recent (Tertiary, strike-slip ?) faulting. However, the original contact can be seen in some places, where it is clearly conformable. Therefore the whole Çamkoÿ Fm has recorded a continuum of sedimentation, and despite its chaotic aspect, it cannot be seen as a mélange-like formation, made of blocks in a matrix.

Age of the Çamkoÿ Fm.

Several other minor facies occur, either in several places or only locally: green shales, sometimes interfingering with thinly bedded carbonated turbidite, shaly silstones, green cherts, green tuffites and sandstones, red pelagic recrystallized limestones. The most important is the latter, because they are the only dated lithology of the formation. Only one

sample, E34 (location in Figure 3.5 and 3.8), has yielded the conodont *Gladigondollela* sp. (picture in plate 1) whose age ranges between Late Scythian (Spathian) to Middle Carnian (det. H. Kozur, Budapest). As suspected by the facies, this conodont is typical from open sea, deep pelagic environment.

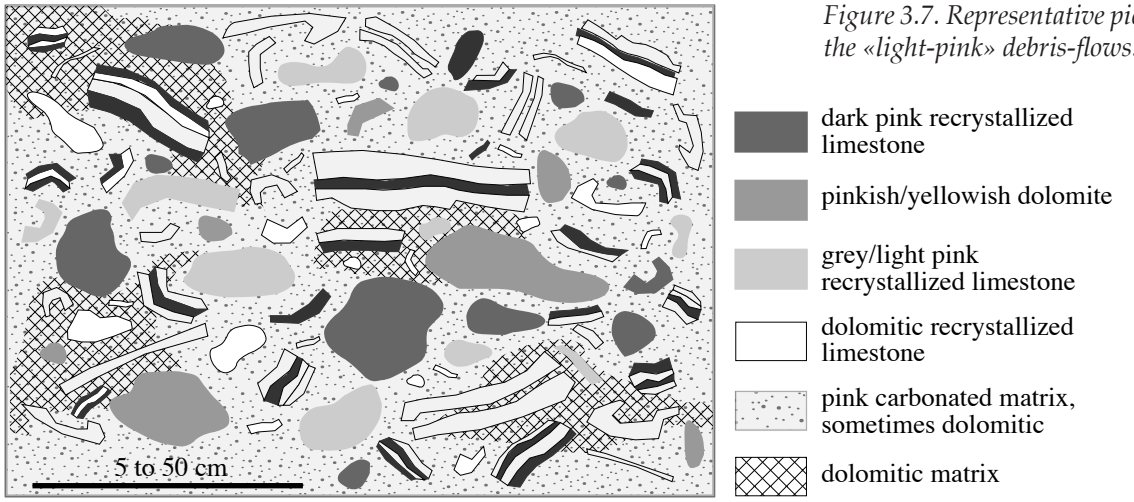

Figure 3.7. Representative picture of the «light-pink» debris-flows.

As shown in the cross-section (Figure 3.8), the red limestones are in stratigraphic contact with the underlying pink debris-flows and are overlain stratigraphically by carbonated turbidites. Actually, the whole section shows a stratigraphic continuity, that implies for the whole section an age which should not be too different than the age of the red pelagic limestones. By extension, the whole Çamkoÿ sequence is considered to have a Spathian-Carnian age, by facies similarities and continuities. However, it is a large time interval, and the real age of Çamkoÿ Fm is suspected to be closer to the Spathian than to the Carnian, because it is in stratigraphic continuation of the Late Permian-earliest Triassic (?) Karadağ Fm.
Moreover, calciturbidites from the Çamkoÿ Fm retain transported late Permian foraminifera (Okay et al., 1991), most probably derived from the underlying late permian Karadağ Fm.

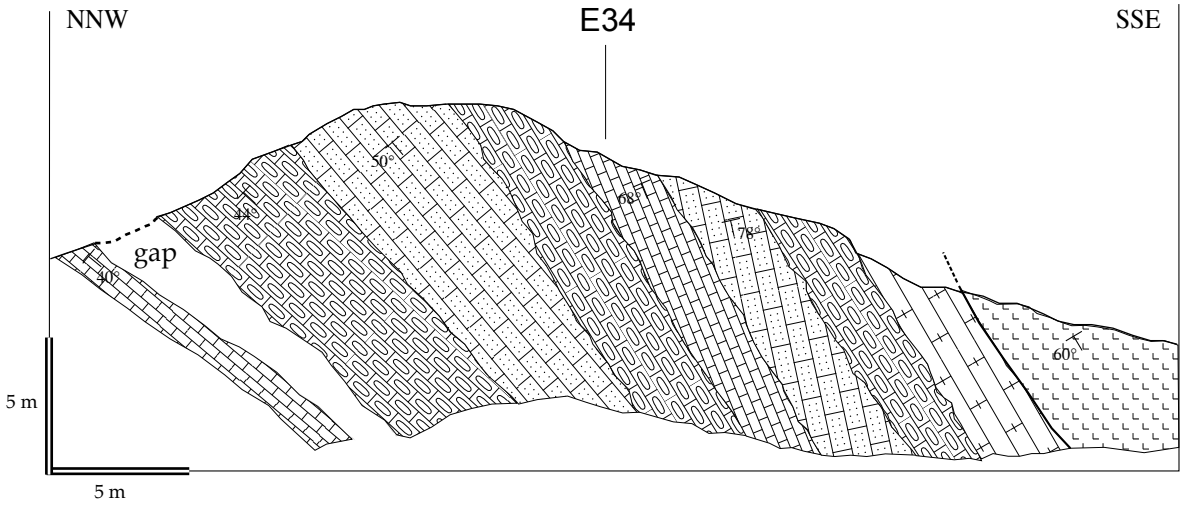

Figure 3.8. Cross-section in the Çamkoÿ Fm showing the location of sample E34, and the relationships between the debris-flows and the other facies; same caption as Figure 3.6.

Depositional Environment of the Çamkoÿ Fm.

The Çamkoÿ Fm records a dramatic increase of the energy, marked by the arrival of erosion products of carbonated platform-type deposits: possible olistoliths of karstified limestones, debris-flows with dolomitic and carbonated pebbles (or fragments of layers), carbonated turbidites. The debris flows are emplaced on pelagic red limestones, that implies a strong deepening of the depositional environment, confirmed by the occurrence of carbonated resediments. This deepening and strong coeval erosion may be due to landward fault activity, suggesting an extensive regime. Rare green tuffites, green sandstones and green shales suggest volcanic activity in the region.

3.1.4. The Ezine Group as a Permian –Triassic syn-rift sequence

In summary, very few age markers are available from the Ezine Group: the Geyikli Fm is considered as Middle-Late Permian, the Karadağ Fm as Late Permian and possibly Early Triassic for its uppermost part, and the Çamköy Fm as Spathian to Carnian. It is a major limit in the purpose of the precise understanding of the Ezine Group evolution; for instance, these very few ages cannot account for possible hiatus in the sequence. However, the Ezine Group is homogeneous from a structural point of view, as the various members and formations are in stratigraphic contact and the general bedding is uniform (Figure 3.9).

Another characteristic of the Ezine Group is its great thickness (c. 3'500 m max), most of it due to the Geyikli and Karadağ Fm. Independently of eustatic variations, this observation implies continuous and regular subsidence in the Middle Late Permian-earliest Triassic (?). The Geyikli Fm is the only one which shows erosion of continental-type material. The Çamkoÿ Fm marks a rapid change in the sedimentation conditions, with volcanogenic facies (green tuffites), and deepening and coeval erosion of landward rocks. The Ezine Group is also characterized by common lateral facies variations and thicknesses, which are the sign of local depositional condition changes. All these features are typical of a rift environment, and one can make two hypothesis:

(1) An ideal one would be that the Ezine Group represents a part of the infill of a single tilted block, whose sedimentation is controled by normal fault activity (Figure 3.10). In this case, the Geyikli and Karadağ

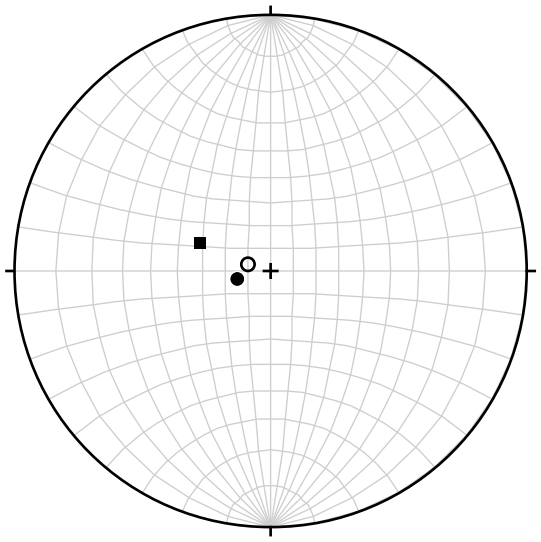

● Mean vector of the bedding of Geyikli Fm (N=25, trend 256.1-plunge 74.7)
○ Mean vector of the bedding of Karadağ Fm, middle member (N=84, 285.2-79.3)
■ Mean vector of the bedding of Çamkoÿ Fm (N=26, 290.7-57.4)

Figure 3.9. Bedding in the Ezine Group; equal area, lower hemisphere projection

Fm record regular subsidence at the beginning of the rifting, with limestone olistoliths (IM2 of Geyikli Fm) and two conglomeratic events (Middle member of Karadağ Fm) suggesting landward uplift and erosion of tilted blocks. Because the Karadağ Fm is characterized by more quiet carbonated sedimentation, it may represent a slowing down of the fault (rift ?) activity. The tectonic activity recorded in the Çamkoÿ Fm may accommodate a rise in the extensive regime following the previous subsidence, resulting in an increase of erosional processes in the landward domains. The scarcity of lithologies of continental origins ("basement"), may be explained by a distal position of the Ezine Group with respect to the rift shoulders. In this case, the pre-rift deposits, as well as the post-rift sedimentation, are unknown in Ezine area.

(2) A second hypothesis (Figure 3.10) would be that the Geyikli anf Karadağ Fm correspond to post-rift (transgressive) sedimentation following a previous phase of extensional tectonics in the Early-Middle Permian (not shown in Ezine area). The tectonic activity may have still continued, but remained limited. The Triassic Çamkoÿ Fm represents then the real, significative rifting phase. In this case, the Geyikli and Karadağ Fm are the pre-rift sequences with respect to the syn-rift Çamkoÿ Fm.

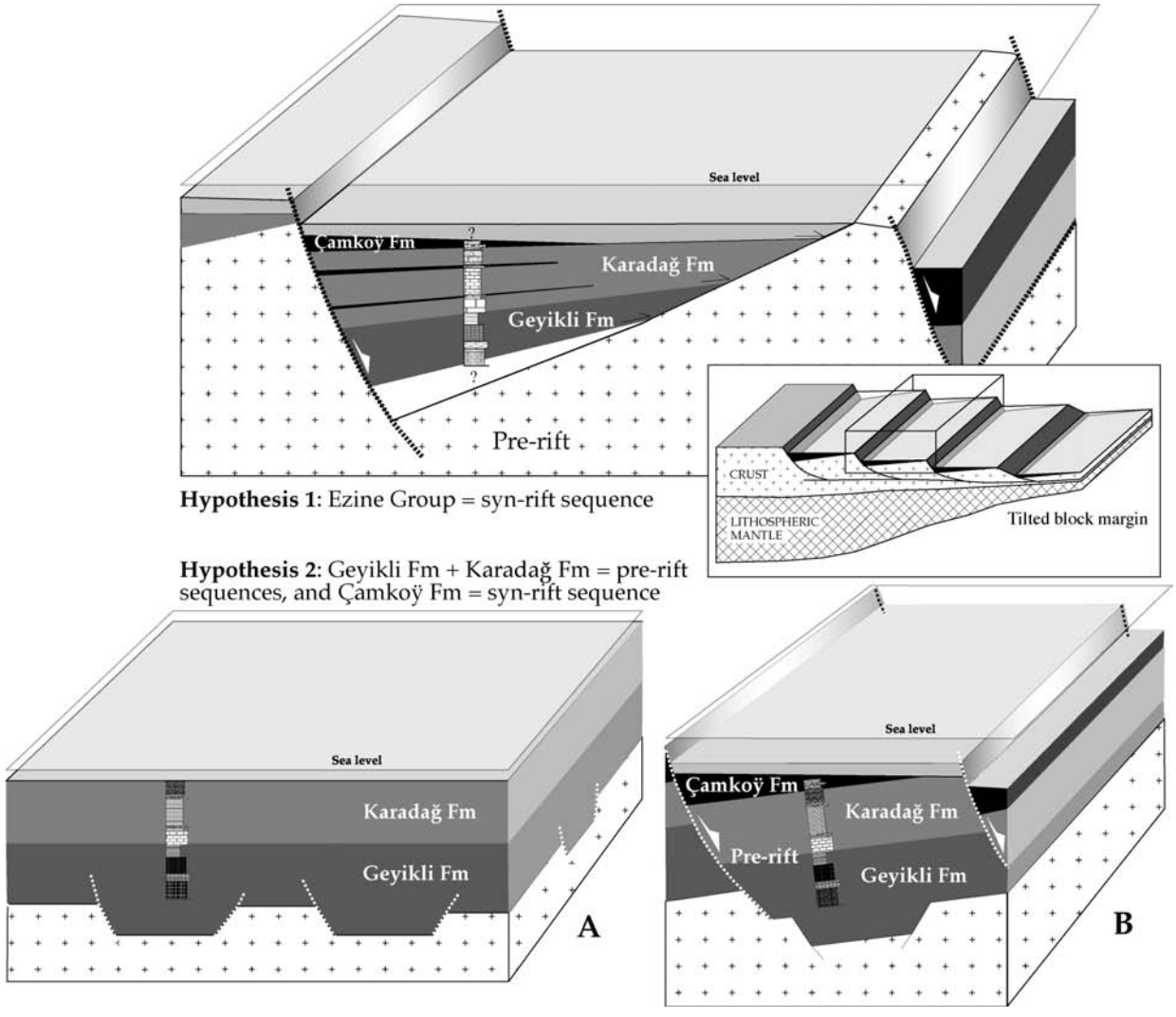

Figure 3.10. Schematic diagrams showing the two hypotheses for the Ezine Group genesis in the Middle Late Permian-Middle Triassic times.

3.1.5. The low-grade metamorphism of the Ezine Group

The whole Ezine Group shows recrystallized lithologies, well revealed in the microfacies observations. A first cause of metamorphism is the Late Oligocene-Early Miocene Kestanbol granodiorite, which intrudes the Geyikli Fm on its southern border (Fytikas et al., 1976; Birkle and Satır, 1995). The contact metamorphism of this intrusion has already been studied in detail (Birkle and Satır, 1992; Karacık and Yılmaz, 1998); in the Geyikli Formation, quartz veins crossing the bedding and quartz pebbles reworked in the olive tree fields, possibly related to silica-rich fluid circulations accompanying the pluton emplacement, are common. In the detritic limestones, the association of scarce neoformed quartz, albite, muscovite and graphite, indicates low greenschist conditions (200-300°C). However, the intrusion affects only its immediate surroundings, but cannot be responsible for the metamorphism farther north. Six samples of an east-west transect from the various limestones of the Karadağ Group have been processed for illite crystalinity measurement, in order to constrain the metamorphic grade.

Illite crystallinity

Methodology

Samples were crushed to millimetre size, in order to extract the clay fraction. Carbonates were removed from crushed samples by dissolution in 2M HCl for one day and were neutralized to pH 5.6 with distilled water. The size fraction < 2 μm was separated by centrifugation at pH 7.5 and saturated with $Ca2^{+}$ using 1M $CaCl_2$ for 36 hours. Clays were washed until defloculation. By pipetting, 3 ml of clay suspension were sedimented onto a glass slide. A Rigaku-Rotaflex diffractometer with a rotating Cu anode at 40 kV and 30 mA, a nickel filter, 0.5 ° divergence and scatter slits, 0.15 mm receiving slit and 5° Sollers slits were used. Finally, the Full Width at Half-Maximum (FWHM) of the first illite basal 10 Å reflection (001) on a X-ray diffractogram was obtained using a step scanning 0.01° 2θ steps counting time of 2 s per step. This measurement represents illite "crystallinity", previously the so-called "Sherrer width". Limits to estimate the low metamorphism are 0.39 Δ2θ° (CuKα) for the diagenesis-anchizone boundary, and 0.22 Δ2θ ° (CuKα) for the anchizone-epizone boundary (Figure 3.11) (Jaboyedoff and Thélin, 1996). Illite crystallinity values are given for air dried samples (size fraction < 2 μm). Glycoled and heated samples were also considered to test the validity of the illite crystallinity measurements.

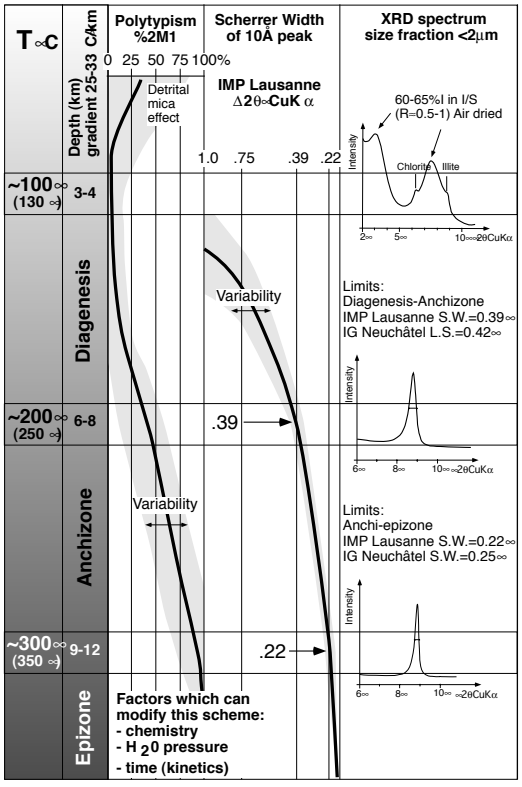

Figure 3.11. Scherrer width ideal evolution with respect to depth and temperature, Jaboyedoff and Thélin (1996).

Results

Because (1) the measurements have been done on the fraction < 2μm, (2) of the lithology (limestone), and (3) of the homogeneity of the Sherrer withs (SW), the illite is considered as a

neoformed mineral whose crystallization is due to the increasing temperature (burial). The Scherrer Width of the six samples ranges from 0.15 to 0.21 Δ2θ° (CuKα), with no significant metamorphic gradient along the transect (Figure 3.12, except perhaps in its western part). These values indicates that the illites have crystallized in epizonal conditions, at a temperature above 300°C, which corresponds to a burial of more than 10 km with a gradient of 30°C/km (Figure 3.11).

Moreover, secondary clay minerals, possibly as late phases, such as kaolinite and smectite, are present on the diffractogram of some samples (Figure 3.12).

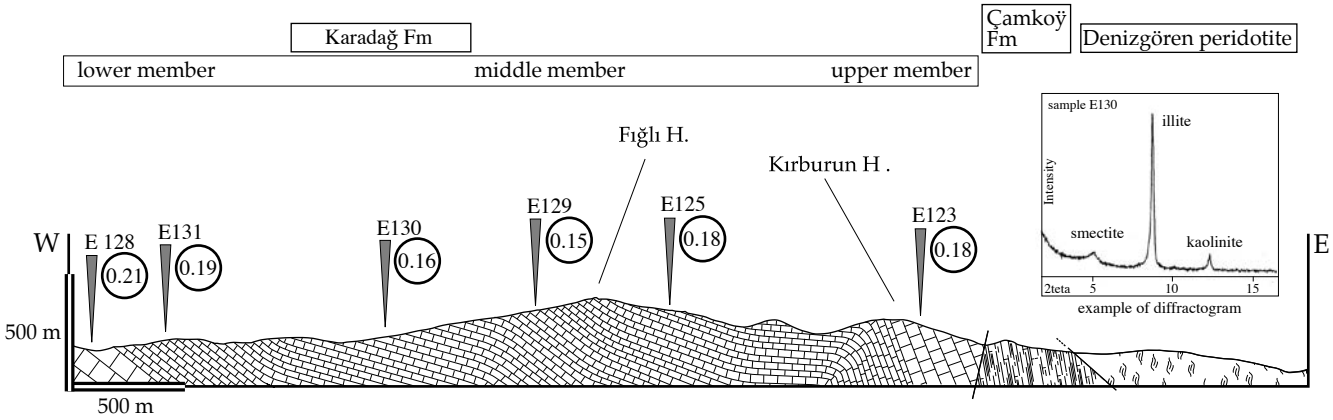

Figure 3.12. distribution of the samples and the corresponding Scherrer Width (in the circles) along an E-W transect in the Karadağ Fm; location of the cross-section in Figure 3.5.

Implications

As the Karadağ Fm is in stratigraphic contact with the underlying Geyikli Fm and the overlying Çamkoÿ Fm, the results from the six samples from the Karadağ Fm are extrapolated to the whole Ezine Group; hence the latter was buried to about 10 km depth before being eroded. This erosion may be related to various events such as the emplacement of the ophiolite or the exhumation of the underlying Çamlıca micaschists (c.f. chapter 4).

About the secondary phases, the temperature of crystallization of the smectite is less than 150°C and that of the kaolinite is less than 200°C.; they have therefore been neoformed after the crystallization of illite, which was formed at a minimum of 300°C. This implies a second lower-temperature event, postdating the illite formation. If the illite is assumed to have formed before the ophiolite emplacement or the updoming process (Early Tertiary), the secondary phases may be related to the Late Oligocene-Miocene magmatic activity that occurred in the Biga Peninsula, particularly around Ezine (Kestanbol pluton and associated volcanic products).

3.2. The Denizgören ophiolite and its metamorphic sole

3.2.1. The Denizgören ophiolite

The Denizgören ophiolite (from the village of the same name) is almost totally made of partially serpentinized harzburgite (Okay et al., 1991), whereas the crustal components

of a typical ophiolitic suite (various gabbros, sheeted dykes, basalts, etc…) are absent. Geochemical analyses from the peridotite suggest supra-subduction zone (SSZ) tectonic setting (Pickett and Robertson, 1996).

3.2.2. The metamorphic sole

Metamorphic basic rocks occur systematically between the Çamkoÿ Fm and the Denizgören ophiolite. The most common lithology is represented by mylonitized metabasalts in the greenschist facies (prasinite), whose thickness is about 100-300 m. Rare foliated amphibolite lenses occur also locally, between the ophiolite and the prasinites; their maximum thickness is about 50 m. The transition from the prasinites to the amphibolites is not continuous, but occurs along late tectonic strike-slip faults parallel to the general foliation.

Structure and petrography

Prasinite

The prasinites occur as green strongly foliated very fine-grain rocks with many small-scale brittle shear bands (mylonitic texture); they are in tectonic contact with the Çamkoÿ Fm and the ophiolite body or the amphibolites when present. Their foliation is homogeneous and parallel to the contact toward which they dip (Figure 3.13). In one place only, a little meta-basalt block has been found non-deformed. The mineral assemblage is commonly made of chlorite + epidote + albite + amphibole ± graphite ± calcite ± sphene ± serpentine (?), and suggests medium to high-grade greenschist conditions. The mylonitic texture is clearly visible in thin section where all the grains have a reduced size. It is important to know wether the greenchist metamorphism is syn-deformation or not; it seems to be the case as the minerals are oriented along mm shear bands parallel to the main foliation, and amphiboles are underlying the schistosity in some samples.

Amphibolite

The dark green foliated amphibolites occur only locally as coarse grain massive rocks at the base of the ophiolite body and over the prasinites. The foliation is parallel to that of the prasinite and the contact with the peridotite (Figure 3.13). Their typical mineral assemblage is made of hornblende + plagioclase ± quartz ± epidote ± sphene. The schistosity is particularly underlined by amphibole minerals. The occurrence or not of epidote characterizes some variations in the temperature of the amphibolite facies. Some later veins of calcite, quartz, albite and chlorite suggest a greenschist overprint.

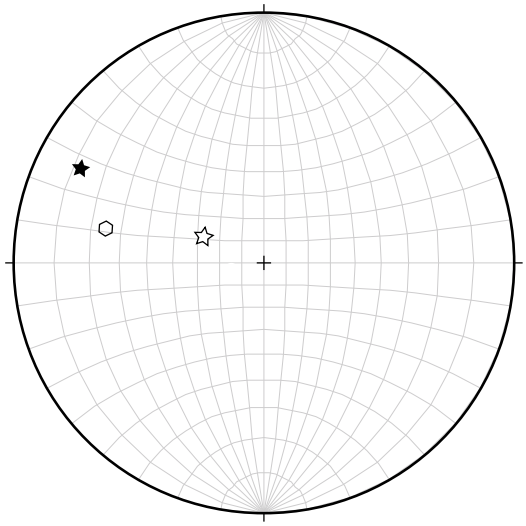

⬡ Mean vector of the foliation of the prasinites (N=39, azimut 281.9-dip 24.5)

★ Mean vector of the foliation of the amphibolites (N=3, 296.7-11)

☆ Pole of the thrust contact between the peridotite and the meta-basites, estimated from the map (azimut 293-dip 60) (= pole of the contact between the metabasites and the Çamkoÿ Fm.)

Figure 3.13. Foliation of the meta-basite from the metamorphic sole; equal area, lower hemisphere projection.

Whole-rock geochemistry

5 samples of prasinites and 4 samples of amphibolite have been processed for whole-rock geochemistry. The analytical conditions are the same than in chapter 2 (c.f. appendix 5 for the analytical results). The purpose of the geochemical analyses is to test the hypothesis of the oceanic origin of the samples. Only elements considered as immobile have been used.

The chondrite-normalized diagram (Figure 3.14, normalizing values from Boynton, 1984) shows typical MORB patterns for E84 and E90, and enriched-MORB pattern for the others samples. These observations are confirmed by the MORB-normalized diagram (Figure 3.14, normalizing values from Pearce, 1983).

The discrimination diagrams (Figure 3.14) are used here to confirm the MORB signature of the samples. It is the case for most of them; only E84, E90 and E14 are oustide of the MORB field; for the two amphibolite samples (E84 and E90) it may be due to remobilization of the elements during the metamorphic event; as for E14, it is the most enriched sample as observed from the chondrite-normalized diagram and hence points toward the WPB field.

The whole-rock geochemical analyse therefore confirms the oceanic origin (with a MORB signature) of the meta-basite samples, and is in accordance with the results of Pickett and Robertson (1996).

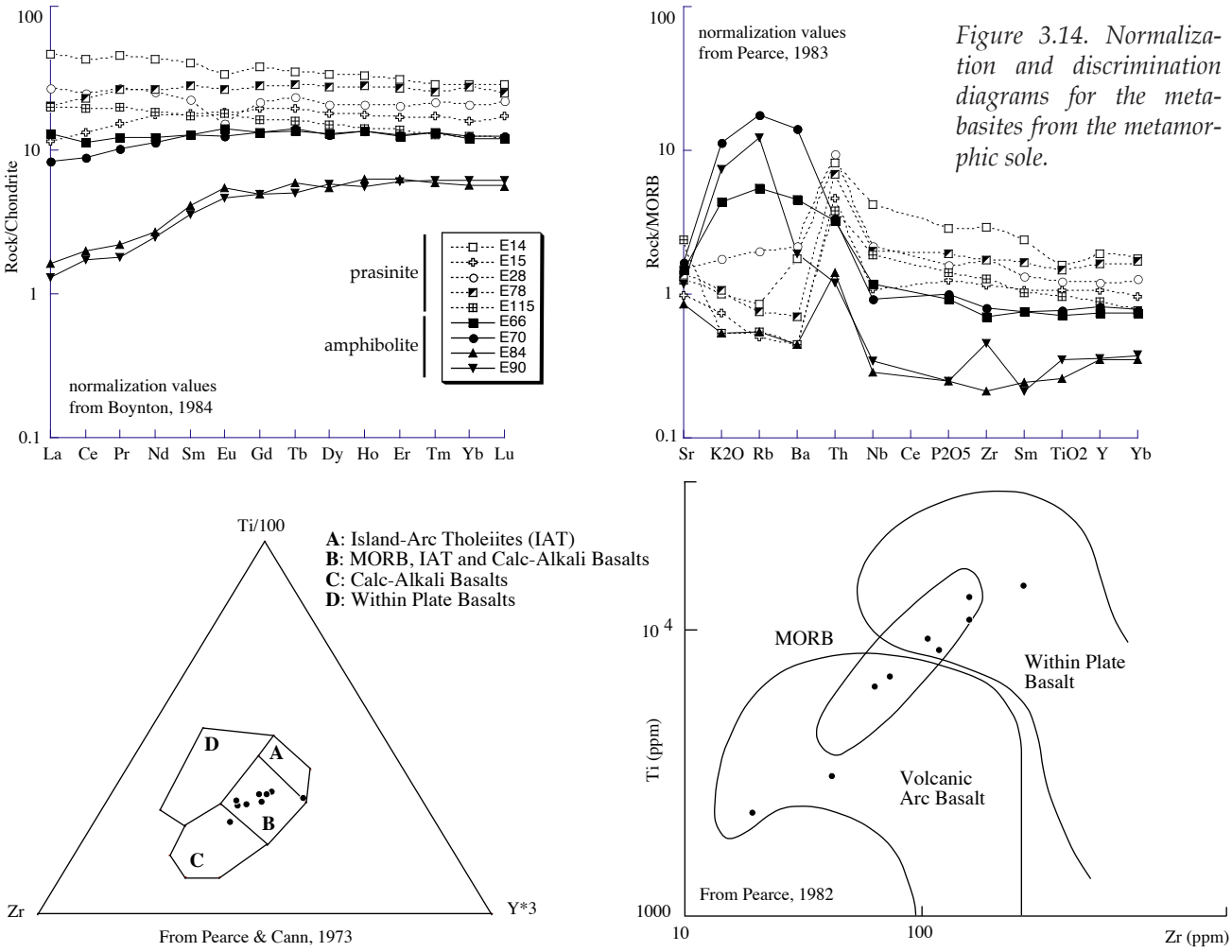

Figure 3.14. Normalization and discrimination diagrams for the metabasites from the metamorphic sole.

Interpretation

The metabasic rocks at the base of the Denizgören ophiolite represent a coherent sequence, which is characterized by a strong inverted metamorphic gradient, from the amphibolite facies close to the contact to the greenschist facies farther away. They have moreover MORB geochemical signatures. They are therefore interpreted as a metamorphic sole (or a part of it) recording the initial thrusting of the ophiolite at or near the oceanic ridge.

The existence of the metamorphic sole, which implies high-temperatures at the inception of obduction, rules out the hypothesis of a toe-of-the-margin peridotite (with no ophiolitic suite) for the Denizgören peridotite.

Age of the amphibolite facies

Two amphibolite samples have been processed for $^{40}Ar/^{39}Ar$ dating to get the age of the amphibolite facies. The datations have been performed by P. Monié (Montpellier); the analytical methods are the same than those described in Monié et al. (1997). The age spectra and isochron age for two hornblende minerals from samples E84 and E94 are shown in fig 3.15 (c.f. appendix 6 for the analytical results).

Results from sample E84 are prefered to those of sample E94, because they are more homogeneous. Moreover, the isochron age is chosen as reference because it is independent of the hypothesis on the original atmospheric Ar value used in the calculation of the plateau age. Therefore the age of the amphibolite facies is considered as 125 Ma ± 2. This age are interpreted as the age of the inception of the obduction process at or near the ridge. It is comparable but slightly older than the $^{40}Ar/^{39}Ar$ ages found by Okay et al (1996) for amphibolite samples from the same area (117±1.5 and 118.3±3.1 Ma).

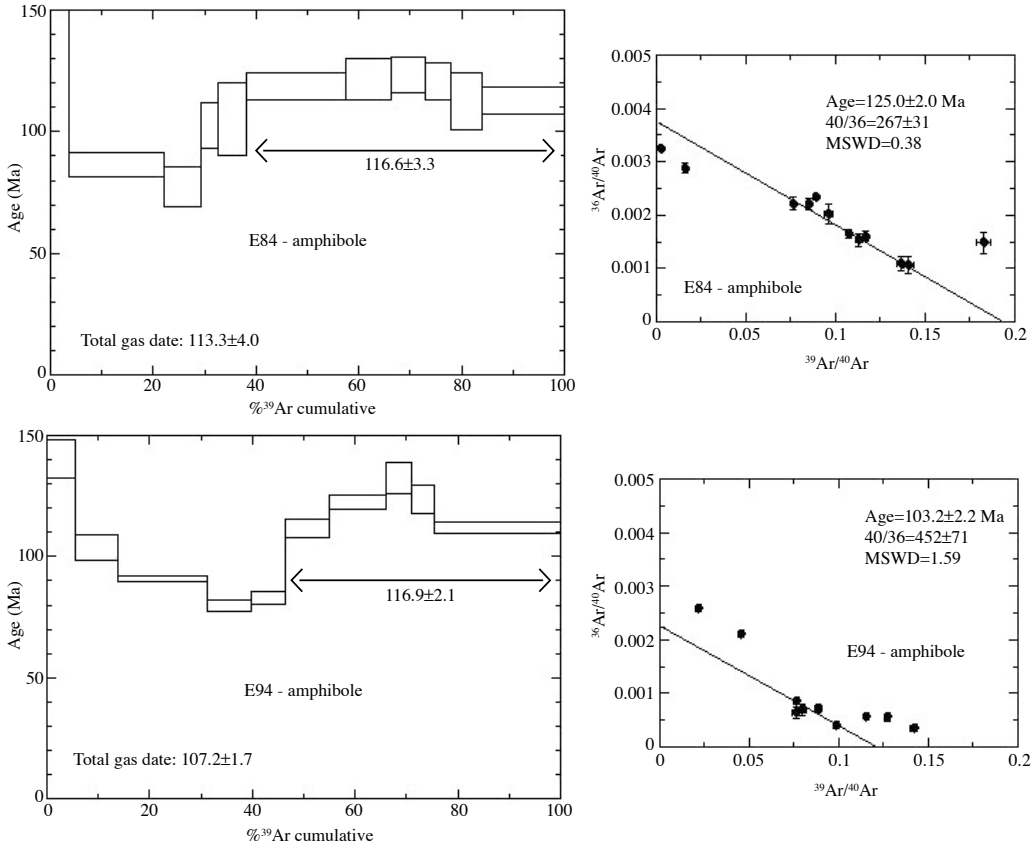

Figure 3.15. 39Ar/40Ar age spectra and isochron ages for samples E84 and E94 from the amphibolite sole of the Denizgören ophiolite.

Structural relations between the Ezine Group and the Denizgören ophiolite

The time gap of about 100 Ma between the Ezine Group (Carnian age of the Çamkoÿ Fm) and the Denizgören ophiolite (Barremian age of the metamorphic sole) raises the crucial question of the structural relationships between the two units. It is clear from field observations that the peridotite lies over the sedimentary sequence as expected. However some observations such as the disturbed aspect of the Çamkoÿ Fm and the silification of the hazburgite near the contact with the Ezine Group suggest a remobilization of the initial contact. But they are considered as evidences of late activity, and the thrust contact currently observed is regarded as a witness of the original emplacement of the peridotite slice over the margin. Moreover the time gap is not incompatible with this view, as there are at least three reasons for its explanation: (1) the ophiolite may have been emplaced directly on the Ezine Group as it is seen today (after erosion or non deposition of the younger lithologies), (2) the younger lithologies may have been transported farther away from the present day position during the ophiolite emplacement, (3) younger strata are represented by thin distal deposits, rare and difficult to sample.

3.3. Correlation of the Ezine Group and Denizgören ophiolite

As in chapter 2, the correlations are only based on geological features; the geodynamic interpretation will be discussed in chapter 5.

In northwest Turkey, the only sedimentary rocks of Permian age are found as olistoliths in the Hodul and Çal units of the Karakaya Complex (Bingöl et al., 1975; Okay et al., 1991; Leven and Okay, 1996). In the Hodul unit, the Permian blocks are represented by white, thickly bedded to massive limestones, which frequently contain fusulinids, algae, bivalves, gastropods and corals. More precisely, the most common olistoliths are of Late Permian age. In the Çal unit, the olistoliths consist also of white, thickly bedded to massive upper Permian limestones with corals, brachiopods, gastropods, ostracods and echinoids. These typical neritic blocks can reach the size of several km. The Karakaya Complex is still subject to discussion concerning its origin (fore-arc, back-arc, or rift, c.f. special session in the 1st Int. Symp. of ITU, Istanbul, 2002); nevertheless, a strong hypothesis for the origin of the shallow water Permian carbonates is that they were belonging to the cover of the Variscan Sakarya terrane (Kozur and Mock, 1997; Stampfli et al., 2003), before being later involved in the Karakaya Complex in the Late Permian-Triassic. Therefore, these olistoliths may be considered as lateral time equivalents of the Ezine Group, but have no relation with its geological evolution: even in the hypothesis of the rift basin for the Karakaya Complex (less and less accepted), the whole features of the latter are totally different than those of Ezine area, so that they cannot have a common geological evolution.

In the Eastern Rhodope, there are no similar sequences to those observed in Ezine; only the reworked upper Permian siliceous rocks in the Mâglenica Group are known (c.f. chapter 2, Trifanova and Boyanov, 1986).

On the other hand, well-constrained Permian-Early Triassic syn-rift deposits have been described in the Pelagonia terrane of Greece (Hydra and Evia Island, Figure 3.16). In Hydra Island, the Permian evolution is characterized by four main stratigraphic events, reflecting extensional tectonism with block faulting and tilting (Baud et al., 1990; Grant et al., 1991). In Evia Island, the presence of carbonate breccia, slight angular unconformity

and olistolith is interpreted as the result of syn-sedimentary extensional tectonics (De Bono, 1998; De Bono et al., 2001; Vavassis, 2001). Therefore, the Ezine Group, despite its poor age constraints, may be related to the Middle Late Permian-Early Triassic rifting phase also observed in Greece. In Greece, the Early Permian is transgressive on the Variscan granitic basement, that implies a large scale extensional event, recorded there by the cooling of the Late Carboniferous granites, and their erosion at the surface in Early Permian times (Vavassis et al., 2000). This observation may favour the second hypothesis, where the Geyikli and Karadağ Fm record syn-extensional transgressive sedimentation. The extensive event is related to the rifting of the future Maliac/Meliata oceanic domain, the Hydra and Evia sequences recording the syn-rift sedimentation of the southern margin (De Bono et al., 2002). The rifting was followed by the southward drifting of the Pelagonia terrane.

Based only on these stratigraphic data, it is not possible to discuss the position of the Ezine Group in the northern or southern margin of the Maliac/Meliata Ocean; and in any case, both margins were close one to the other during the rifting event. The comparison of the age from the overlying Denizgören ophiolite with that of the aegean ophiolites, as well as its structural position, can be helpful in this purpose.

Indeed, the age of the metamorphic sole of the Denizgören ophiolite (125 Ma, Barremian) is quite surprising if compared with the ages from the metamorphic soles from the ophiolites in the Aegean region (Figure 3.17); all the ophiolites from western Turkey have a Late Cretaceous age (Cenomanian-Turonian), whereas those from Greece have a Middle Jurassic age (Aalenian-Bajocian). In Greece, only the Lesvos ophiolite gives a younger age, its metamorphic sole being dated at 155

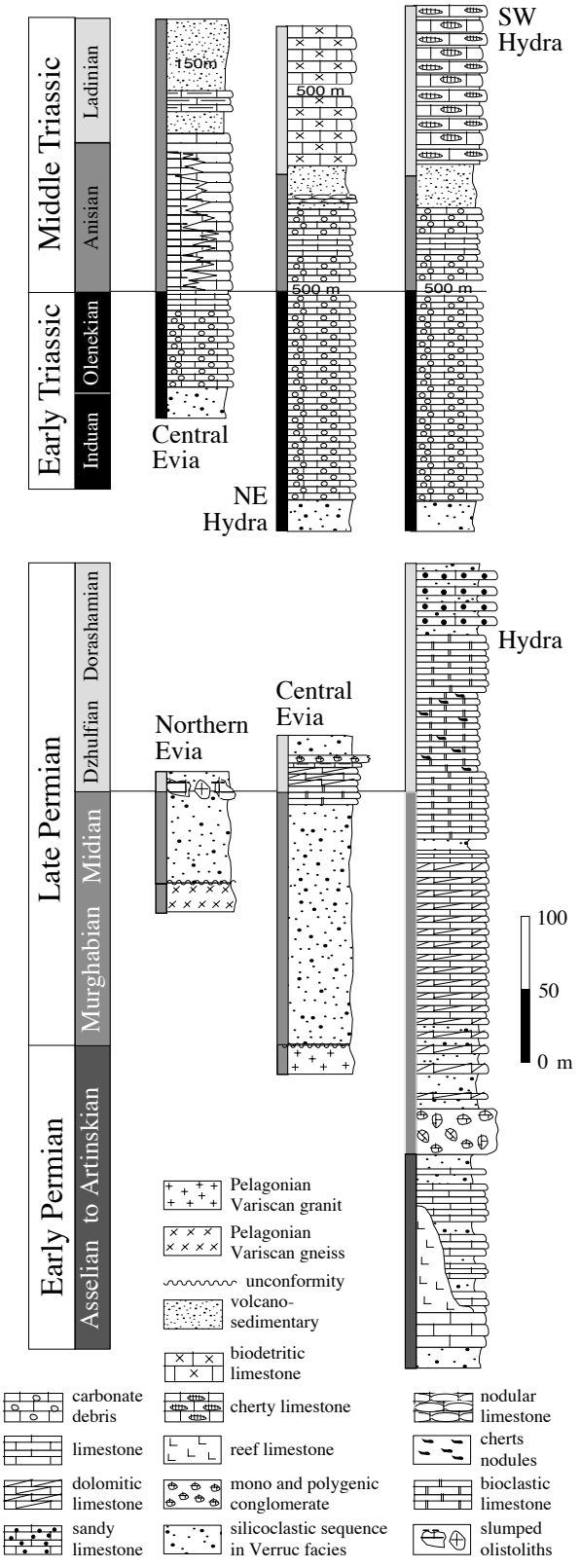

Figure 3.16. Stratigraphic columns for the syn-rift sequences of northern Pelagonia (de Bono, 1998), northern evia (Vavassis, 2001), central Evia (de Bono, 1998), Hydra (Baud et al., 1990; Grant et al., 1991).

Ma (Hatzipanagiotou and Pe-Piper, 1995). Moreover, dikes related to three ophiolitic complexes in Greece have also been dated; (1) the Guevgueli complex of central Macedonia, belonging to the Vardar Zone, yielded Late Jurassic radiometric ages (163-149 Ma, Spray et al., 1984); (2) diorite dikes from the Samothraki ophiolite yielded Oxfordian ages (155 Ma, Tsikouras et al., 1990); (3) In northern Greece, the basic and ultrabasic rocks of the Makri and Drimos-Melia Units (c.f. chapter 2, Figure 2.25) are closely associated in space and time and are considered as dispersed fragments of an incomplete supra-subduction zone ophiolite (Evros ophiolite, Magganas et al., 1991, 2002). Dikes associated with this ophiolite yielded Late Jurassic-Early Cretaceous ages (160-140 Ma, Bigazzi et al., 1989), and northward shear senses interpreted as recording the ophiolite emplacement have been described locally (Bonev and Stampfli, submitted). Therefore the Denizgören ophiolite (or metamorphic sole) has no time equivalent in Greece and Turkey.

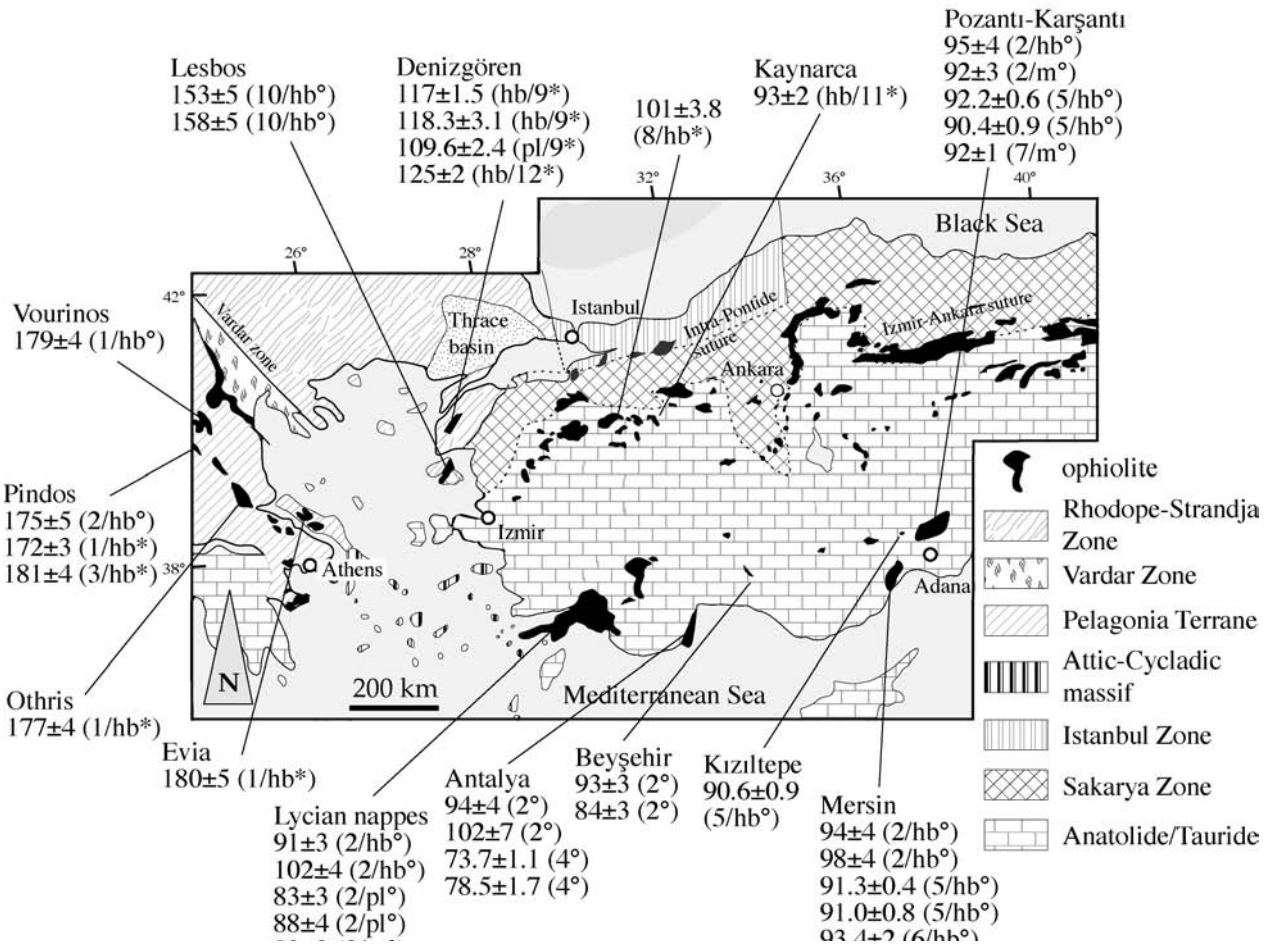

*Figure 3.17. Age of the metamorphic soles from the ophiolites from the Aegean region; hb: hornblende; pl: plagioclase; m: mica; *: Ar/Ar; °: K-Ar; 1: Spray and Roddick (1980); 2: Thuizat et al. (1981); 3: Roddick et al. (1979); 4: Yılmaz and Maxwell (1982); 5: Dilek et al. (1999); 6: Parlak et al. (1995); 7: Thuizat et al. (1978); 8: Harris et al. (1994); 9: Okay et al. (1996); 10: Hatzipanagiotou and Pe-Piper (1995); 11: Önen and Hall (2000);12: this work.*

Unlike its age, the structural position of the Denizgören ophiolite north of the (Vardar) Izmir-Ankara suture is not unusual. In Turkey the dated ophiolites are emplaced southward over the Anatolide-Tauride Block; nevertheless, there are also some local northward obduction events in eastern Turkey, where the peridotite bodies are emplaced over typical Sakarya units; there are very poor data concerning their ages, but the obduction seems to be younger (Late Cretaceous ?). In Greece, the main Jurassic obduction is related to the emplacement of Vardar ophiolites over the Pelagonia terrane (Eo-Hellenic phase, south of the Vardar suture), but at the same time, a northward obduction event is recorded in the Rhodope area (Guevgueli, Samothraki and Evros ophiolites).

It looks as if the Denizgören ophiolite was emplaced northward (with respect to the IAES) between the northward obduction found in Greece over the Rhodope margin and found in Turkey over the Sakarya Zone.

Conclusion

The Ezine Group records either syn-rift sedimentation of Middle Late Permian-Middle Triassic age, or pre-rift (transgressive) sedimentation in the Early-Middle Permian and syn-rift sedimentation in the Early-Middle Triassic (favoured here). This rifting event can be correlated with similar units in Greece, where they are interpreted to record the Maliac/ Meliata opening. The overlying Denizgören ophiolite has, moreover, no time equivalent in the Aegean region, neither in Greece, nor in Turkey, and a typical Eo-Hellenic origin for its obduction is excluded. This result is a major argument for the hypothesis of the northern margin origin (Rhodope) for the Ezine Group, as the whole Pelagonia terrane has undergone the Jurassic obduction. It is confirmed (1) by the southward occurrence of the Lesvos ophiolite, which has an Eo-Hellenic signature (Cadet, pers. comm.), and (2) by the Early Cretaceous age of the ophiolite which is in the time interval of the Balkanic orogen (ante-Cenomanian northward thrusting).

The Rhodope margin has also undergone local obduction in the Late Jurassic, so that the Ezine Group must represent a preserved segment of the margin until the Mid Cretaceous obduction of the Denizgören ophiolite. The uniqueness of an ophiolite of this age and the preservation of the sedimentary sequence (together with the ophiolite), suggest a strong strike-slip component for the general tectonic regime during and after the obduction process.

- CHAPTER 4 -

TERTIARY EXHUMATION IN THE BIGA PENINSULA: FOCUS ON THE KAZDAG MASSIF

North of Küçükkuyu, the Çetmi mélange is structurally underlain by the high-grade rocks of the Kazdağ Massif. In the continuation of the study of the Çetmi mélange, and following the first detailed description of the Kazdağ Massif as a core complex (Okay and Satır, 2000a), this chapter presents new preliminary data about the exhumation process of the Kazdağ Massif.

The Kazdağ Massif, bordering the northern side of the Edremit Gulf, is an NE-trending structural dome approximately 50 km long and 20 km wide. Meta-ultramafic rock and metagabbro occur in the core of the dome, and are enveloped by a marble-rich sequence, which passes up to felsic gneisses with marble and amphibolite intercalations. In its western part, the Kazdağ Massif consists of an intercalation of felsic gneiss, calc-silicate gneiss, amphibolite, marble and minor migmatite. The metamorphic assemblage, typical of the amphibolite facies, is thought to be of latest Oligocene age (24 Ma), with Carboniferous inherited zircon ages (Okay et al., 1996; Okay and Satır, 2000a).

The present study is limited to the western end of the Kazdağ Massif, where the massif is in tectonic contact with the overlying unmetamorphosed Çetmi mélange. In the southern area, the mélange, overlain by the sedimentary rocks of the Küçükkuyu Formation, rests on the Kazdağ Massif through a low-angle normal fault. In the northern area, the contact is defined by the Alakeçi Mylonitic Zone, which marks the transition between the mélange and the massif.

4.1. Southern flank of the Kazdağ Massif

4.1.1. The Küçükkuyu Formation

The Küçükkuyu Formation (herein KFm, Siyako et al., 1989) represents the filling of a small sedimentary basin (c. 20 km long and 5 km wide), closely surrounding the southern subzone of the Çetmi mélange north of Küçükkuyu. The stratigraphy of the basin is shown through 10 detailed sedimentary columns drawn from key areas; the location of the columns and the spatial distribution of the facies is shown on fig 4.1. The results of the investigations can be summarized as follow:

(1) The Küçükkuyu Formation is divided in three different members, based on facies associations and similarities.

-The lower member is cropping out in a narrow zone (less than 1 km wide) directly above the Çetmi mélange; its thickness may be estimated to a maximum of 150 m. Small synsedimentary normal faults with meter scale throw affects this sequence; large open folding is inferred from the dip and direction data of the bedding.

The Lower Member consists of a volcano-detritic sequence, with coarse reddish to greyish sandstone and conglomerate (picture 4.1 plate 7C), alternating with tuff, tuffite and acidic lava flow, also red-pink in colour (column 1, Figure 4.2). Toward the top, near the transition with the intermediate member, the sequence becomes carbonated (marl and limestone

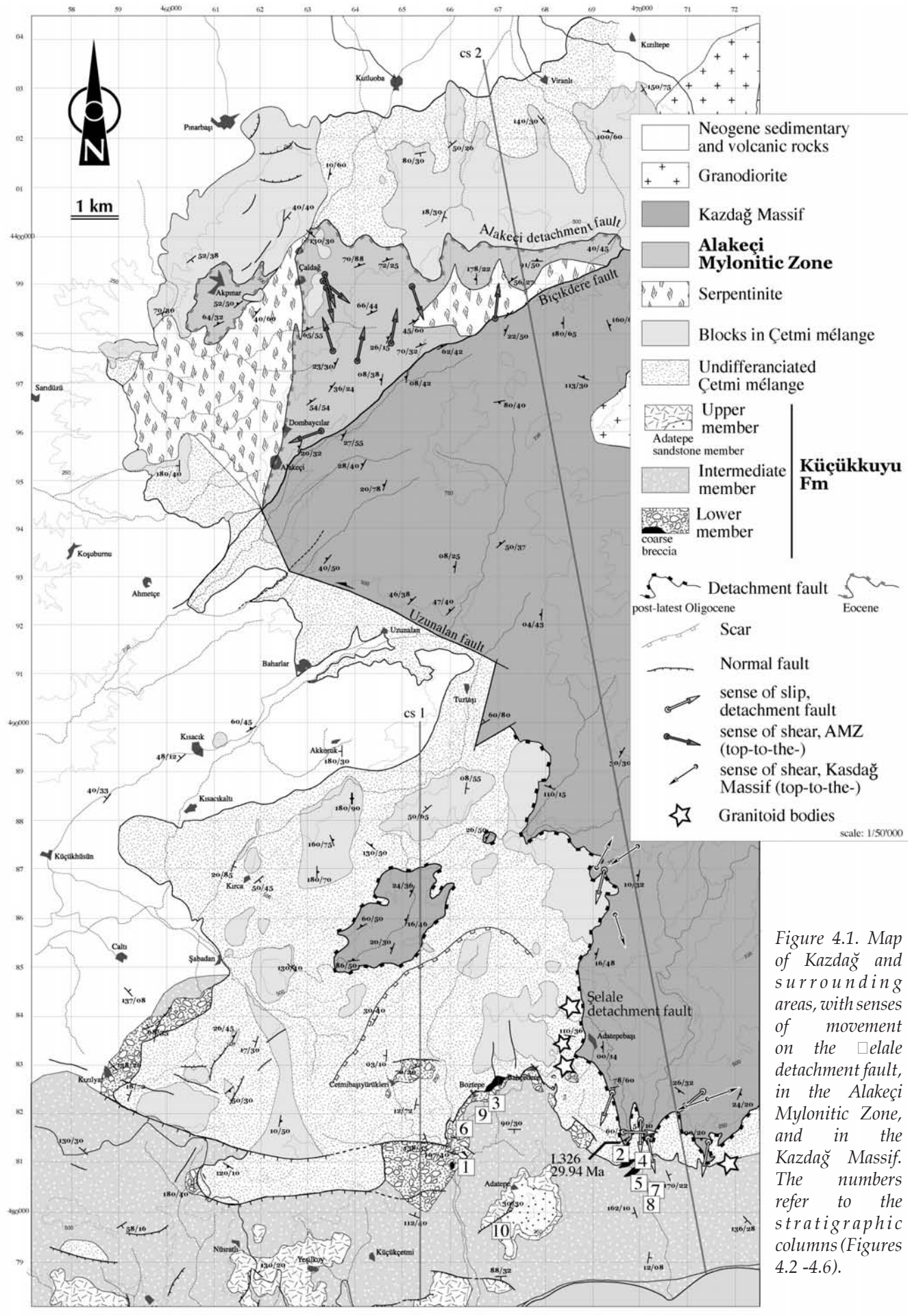

Figure 4.1. Map of Kazdağ and surrounding areas, with senses of movement on the Selale detachment fault, in the Alakeçi Mylonitic Zone, and in the Kazdağ Massif. The numbers refer to the stratigraphic columns (Figures 4.2 -4.6).

alternation, carbonaceous cement in microconglomerate, column 2, Figure 4.2, and 3, Figure 4.3). Columns 4 and 5 (Figure 4.4) show a lateral equivalent, which is made by green to red marls, alternating with grey, greenish limestone with charophytes and ostracods, interpreted as local lake sedimentation. The whole member is characteristic of continental fluviatile depositional environment (braided river type) with alluvial fan affinities, possibly grading laterally and toward the top to a proximal lake environment.

A striking feature of the lower member is the occurrence of breccias at its top, marking locally the transition to the intermediate member (columns 2, 3 and 6, Figure 4.4). Columns 7 and 8 (Figure 4.5) show a progressive transition from the lacustrine deposits to carbonated sandy layers, and then to the intermediate member; indeed, it is not clear from field relationships whether the breccias overly the lacustrine deposits, or whether they are lateral equivalent. In the latter case, a 2-3 meters thick conglomeratic episode may be a good lateral equivalent (column 7). The breccias are overwhelmingly monogenic, with cm to pluri-dm angular blocks, without any organization (chaotic aspect). The fabric is blocky-supported, and the matrix, when present, consists of the sandy fraction of the same material as the blocks. They are interpreted as subaerial footscarp deposits, following local fault activity.

The lower member is similar in facies and occurrence to the Kızılyar Formation, described farther west near the Kızılyar village (Siyako et al., 1989, cf. Figure 4.1). The presence of fan deposits, volcanic and tectonic activity, fault breccias, as well as the narrowness of the member, all suggest that a strong extensive tectonic activity controled the sedimentation of the lower member. A similar active tectonic setting has been proposed for the Kızılyar Formation (Yılmaz and Karacık, 2001); because of their same lithology, depositional environment, structural position and spatial proximity, the Kızılyar Formation is treated as an equivalent of our lower member and incorporated into it.

-The intermediate member of the Küçükkuyu Formation, c. 400 m in thickness, is made of rhythmic alternations of yellowish oxidized silty shale and silstone-sansdtone turbidites (column 9 and 10, Figure 4.5 and 4.6). The contact with the lower member is most of the time conformable.

The proportion of fine grain material is more important than the sandy material (in a ratio higher than 3 to 1). The layers are generally thin (less than 10 cm), with rare thicker beds (up to 3 m). They have generally carbonated cements. Erosional sole casts are rare, whereas loadcasts occur more frequently. The sandstone layers show typical A, B and C Bouma sequences, and the flow structures all indicate a southward direction of transport. Near the base of the sequence, sandstone beds rework cm to dm fibrous wood fragments. Some slump structures and syn-sedimentary normal faulting have been observed. Many open to gentle small-scale folds also occur. In the west of the area, the base of the sequence is made of yellowish dolomitic silty laminated limestones, alternating with locally bituminous shales.

Toward the top of the sequence, there is a renewed input of volcanogenic components (ash, feldspar) in the sediment; as a result, the rocks become more tuffitic, with sometimes a greenish colour. Near Adatepe village, the transition to the upper member is made through a 20 meters thick succession of massive coarse sandstone/miroconglomerate beds, with a clear tuffitic component (column 10).

Palynomorh assemblages from the base of the intermediate member, in the more dolomitic sequence, suggests (det. P. Hochuli, Zürich): (1) a fresh-brackish water environment indicating most probably a lacustrine environment (typical dinoflagellate, confirms the results of Inci, 1984), (2) the occurrence, near the basin, of conifer and deciduous forests

(pollens of pine, cypress, oak, etc…). The intermediate member is therefore interpreted as a turbiditic progressive filling of a lake basin, with increasing volcanic activity toward the top of the sequence.

-The upper member is made of 20-30 m of beige-yellowish amalgamated tuffite deposits. At the base, abundant oxidized wood fragments, green mud balls and detritic feldspar, still suggest moderately high energy hydrodynamic features. This thick tuffitic bed is a discontinuous marker bed, invariably found at the top of the Küçükkuyu Formation. Near Adatepe village, the tuffites progressively grade to coarse carbonated sandstones, with a strong volcanogenic component. All these features are characteristic of detritic shallow water environment, deposited in a more proximal setting than the Intermediate Member.

The whole Küçükkuyu Formation is interpreted as follow: the lower member recorded a strong volcanic and extensional tectonic activity, concomitant with the development of a small basin. The latter was progressively filled by shale-dominated lake turbidites (intermediate member). Such a rhythmic infill, together with slump and normal fault structures, suggest the continuation of the tectonic control on the sedimentation. The end of the filling and the starvation of the lake are marked by the upper member, which also confirms the return of a volcanic activity in the proximity of the basin.

(2) The age of the KFm is **Early Miocene**, based on a palynomorph association from the bituminous shales alternating with the dolomitic silty limestones in the western part of the intermediate member (Nüsratlı Fm of Inci, 1984).

A biotite from a tuffite from the upper member of the KFm has been dated with the $^{40}Ar/^{39}Ar$ method (performed in Montpellier by P. Monié); the age is 34.4±1.2 Ma (Figure 4.8). This latest Eocene age (Priabonian) is interpreted as the age of the volcanism, which was the source rock at the time of the deposition of the upper member. Similar ages have been found in autochthonous volcanic acidic rocks in the Biga Peninsula (Eocene Balıklıçesme and mostly Oligocene Çan volcanics, Ercan et al., 1995). The source was probably the andesitic to rhyolitic rocks of the Çan volcanics, as they are much closer to the present Küçükkuyu basin.

(3) The lithologies from the underlying Çetmi mélange are systematically reworked in the lower, middle, and upper members of the KFm (see the various stratigraphic columns). Because of their resistant nature, the red radiolarites are good markers of the continuous upstream presence of the Çetmi mélange during the basin evolution. Volcanic rocks, which must be close to the basin, represent another source for the detritals. No lithologies from the Kazdağ Massif has been found in the KFm. The occurence of erosional products coming from the Çetmi mélange in the Early Miocene implies that the latter was cropping out on a much more extended area than today.

Figure 4.2. (next page) Stratigraphic columns 1 and 2, Küçükkuyu Formation.

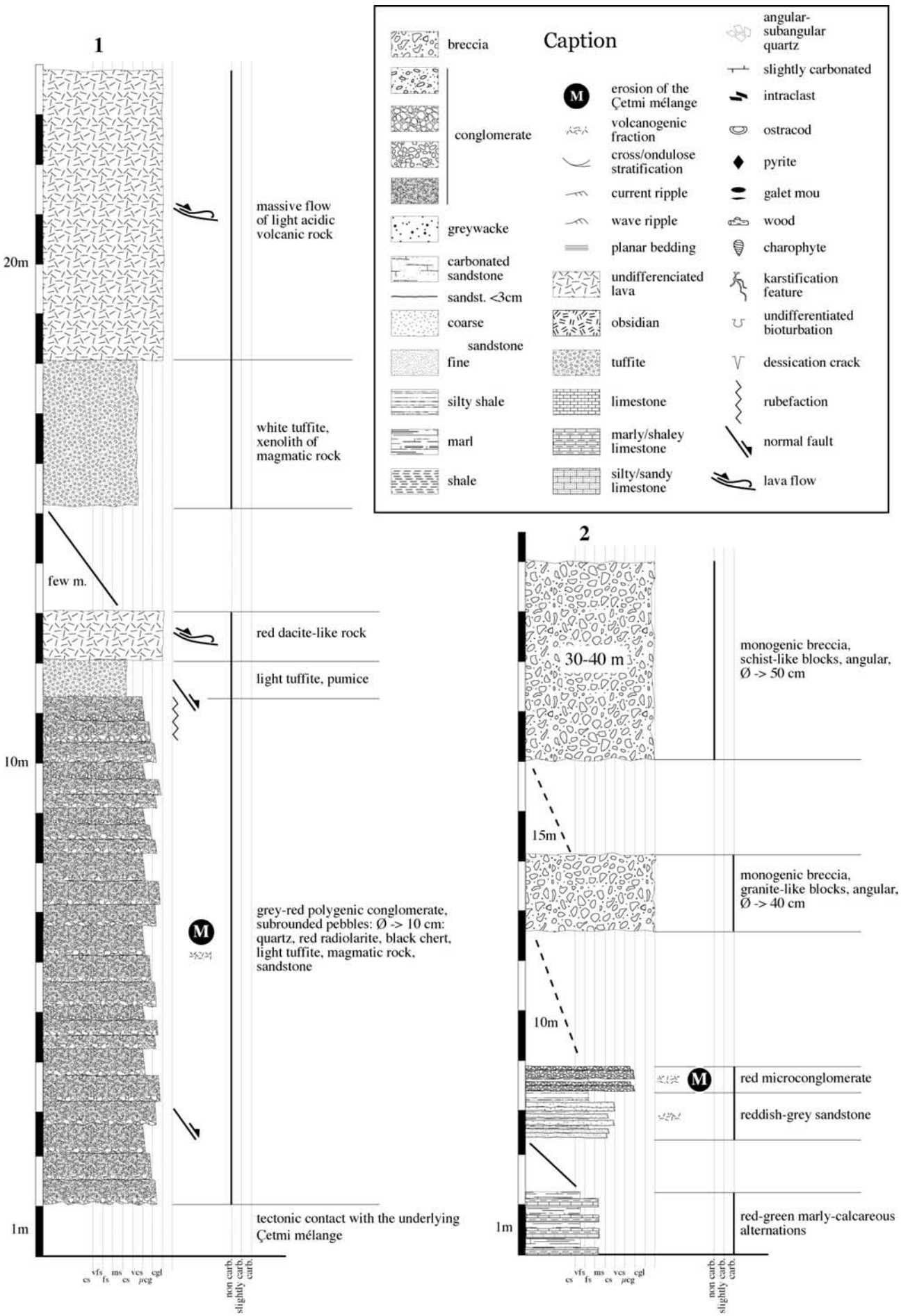
1
20m
10m
1m
few m.
massive flow of light acidic volcanic rock
white tuffite, xenolith of magmatic rock
red dacite-like rock
light tuffite, pumice
grey-red polygenic conglomerate, subrounded pebbles: Ø -> 10 cm: quartz, red radiolarite, black chert, light tuffite, magmatic rock, sandstone
tectonic contact with the underlying Çetmi mélange
vfs fs ms cs vcs cgl
cs pcg
non carb.
slightly carb.
carb.
Caption
breccia
conglomerate
greywacke
carbonated sandstone
sandst. <3cm
coarse sandstone
fine
silty shale
marl
shale
erosion of the Çetmi mélange
volcanogenic fraction
cross/ondulose stratification
current ripple
wave ripple
planar bedding
undifferenciated lava
obsidian
tuffite
limestone
marly/shaley limestone
silty/sandy limestone
angular-subangular quartz
slightly carbonated
intraclast
ostracod
pyrite
galet mou
wood
charophyte
karstification feature
undifferentiated bioturbation
dessication crack
rubefaction
normal fault
lava flow
2
30-40 m
15m
10m
1m
monogenic breccia, schist-like blocks, angular, Ø -> 50 cm
monogenic breccia, granite-like blocks, angular, Ø -> 40 cm
red microconglomerate
reddish-grey sandstone
red-green marly-calcareous alternations

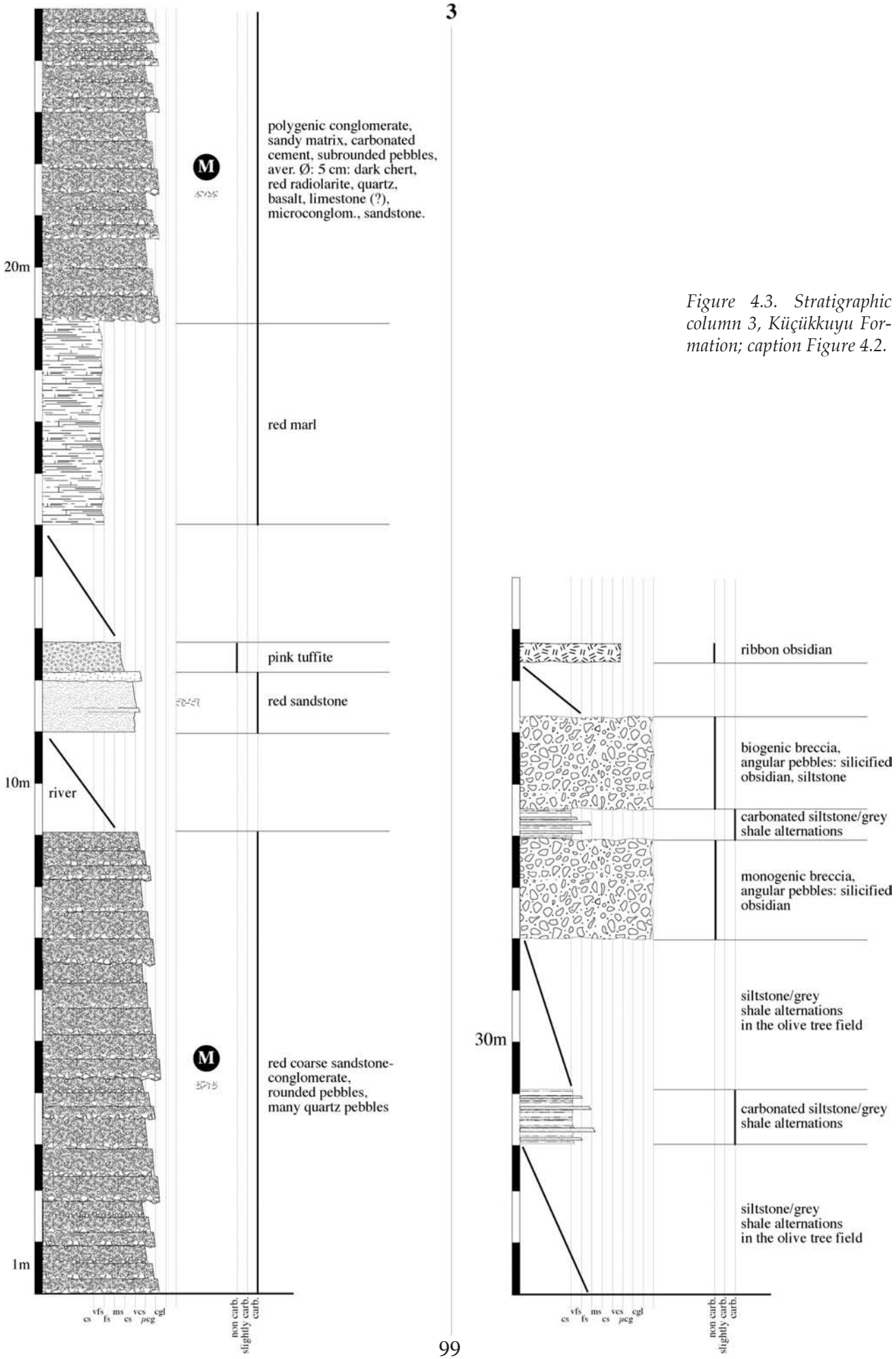

Figure 4.3. Stratigraphic column 3, Küçükkuyu Formation; caption Figure 4.2.

Figure 4.4. Stratigraphic columns 4, 5 and 6, Küçükkuyu Formation; caption Figure 4.2.

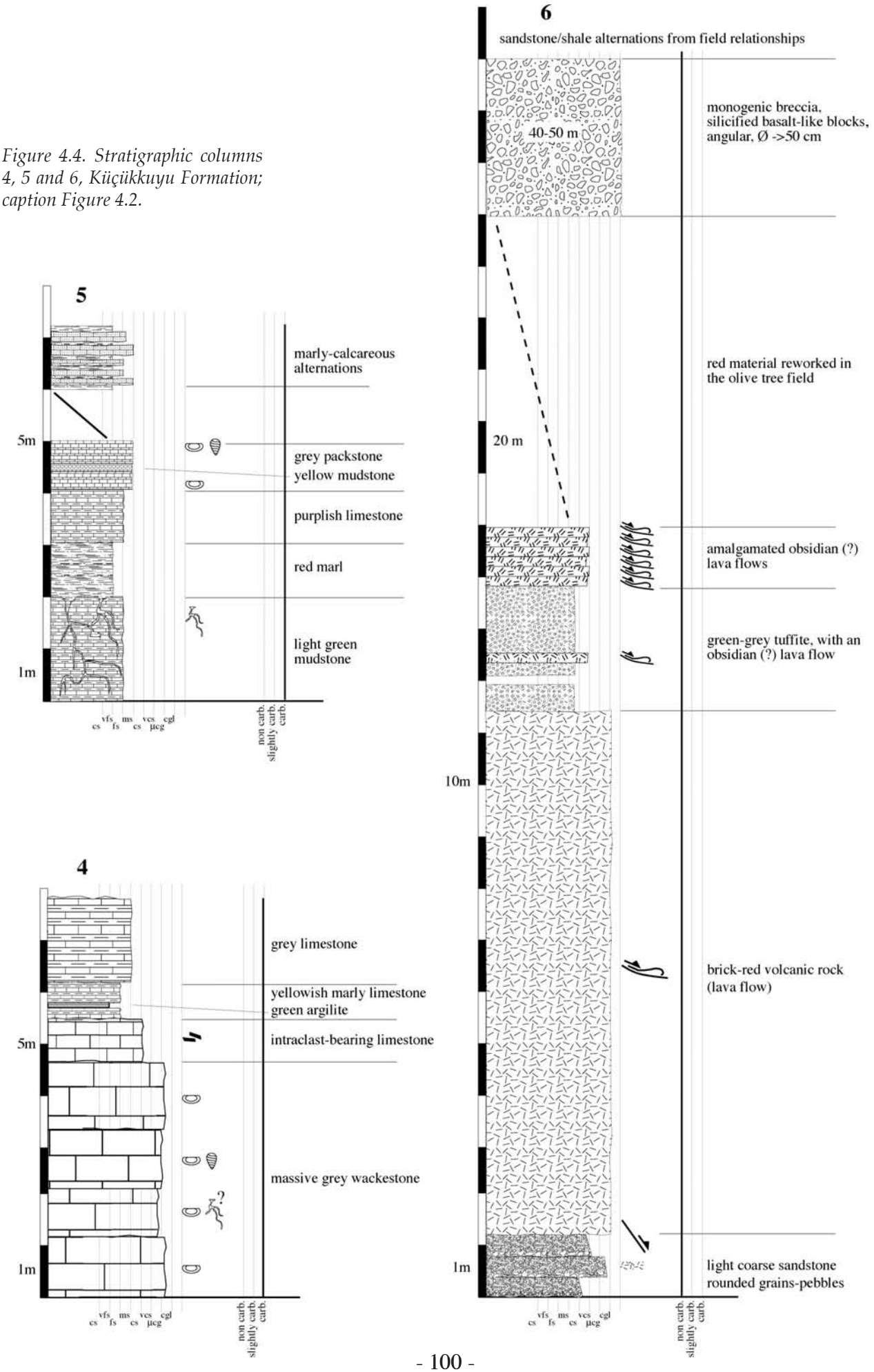

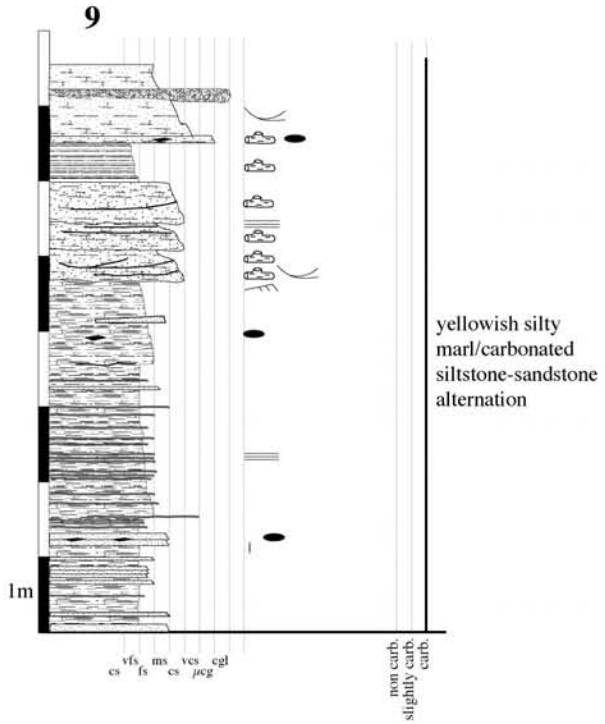

Figure 4.6. (next page) Stratigraphic column 10, Küçükkuyu Formation; caption Figure 4.2.

Figure 4.5. Stratigraphic columns 7, 8 and 9, Küçükkuyu Formation; caption Figure 4.2.

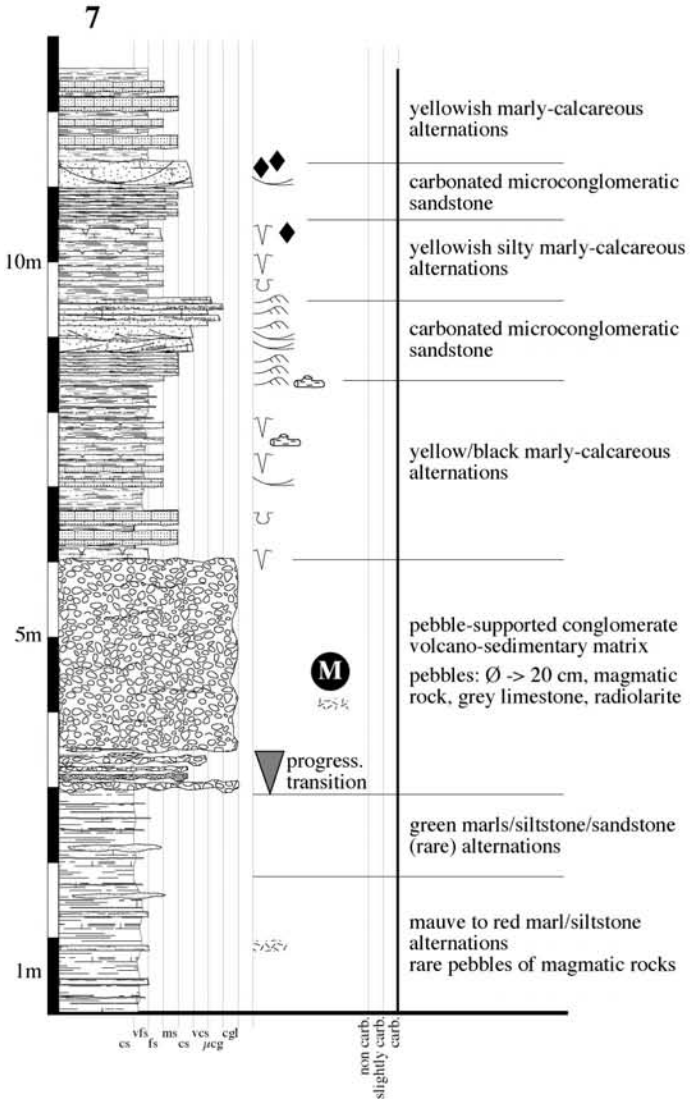

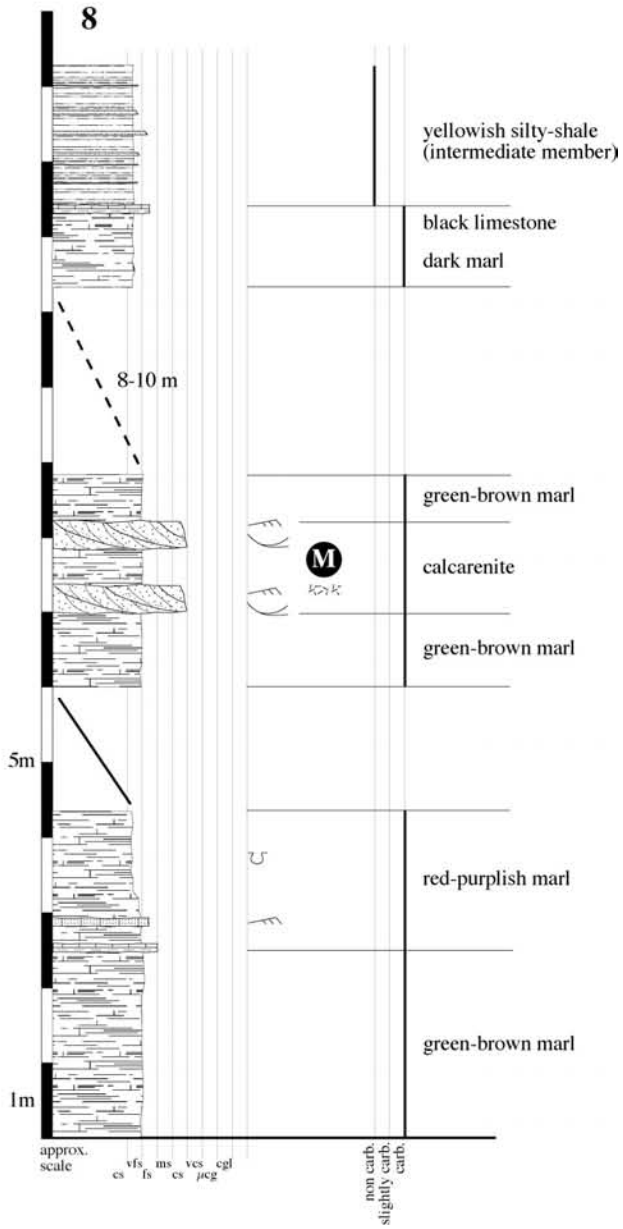

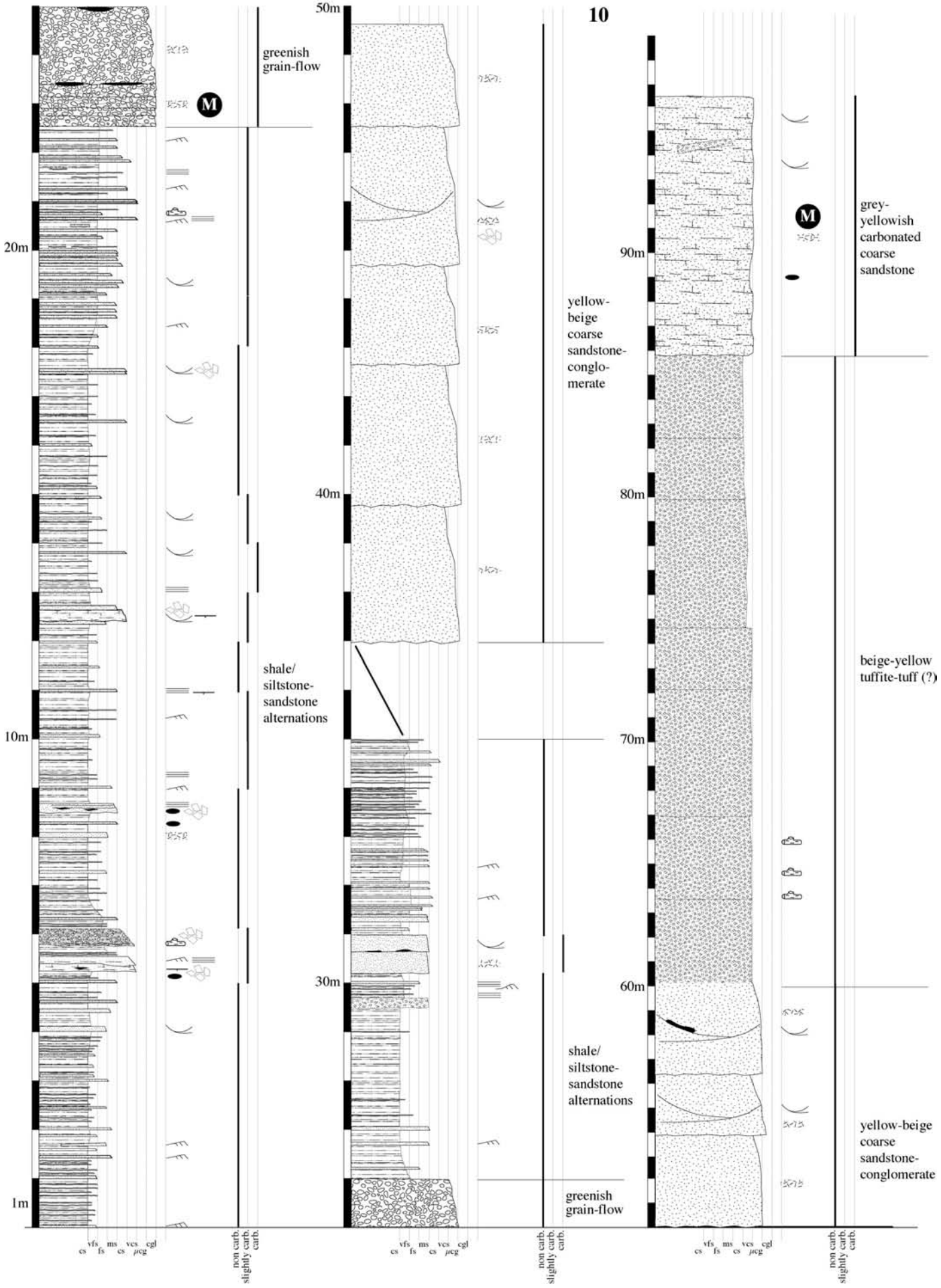
10
1m
10m
20m
30m
40m
50m
60m
70m
80m
90m
M
greenish grain-flow
shale/ siltstone-sandstone alternations
yellow-beige coarse sandstone-conglo-merate
shale/ siltstone-sandstone alternations
greenish grain-flow
grey-yellowish carbonated coarse sandstone
beige-yellow tuffite-tuff (?)
yellow-beige coarse sandstone-conglomerate
vfs fs ms cs vcs cs cgl µcg
non carb. slightly carb. carb.

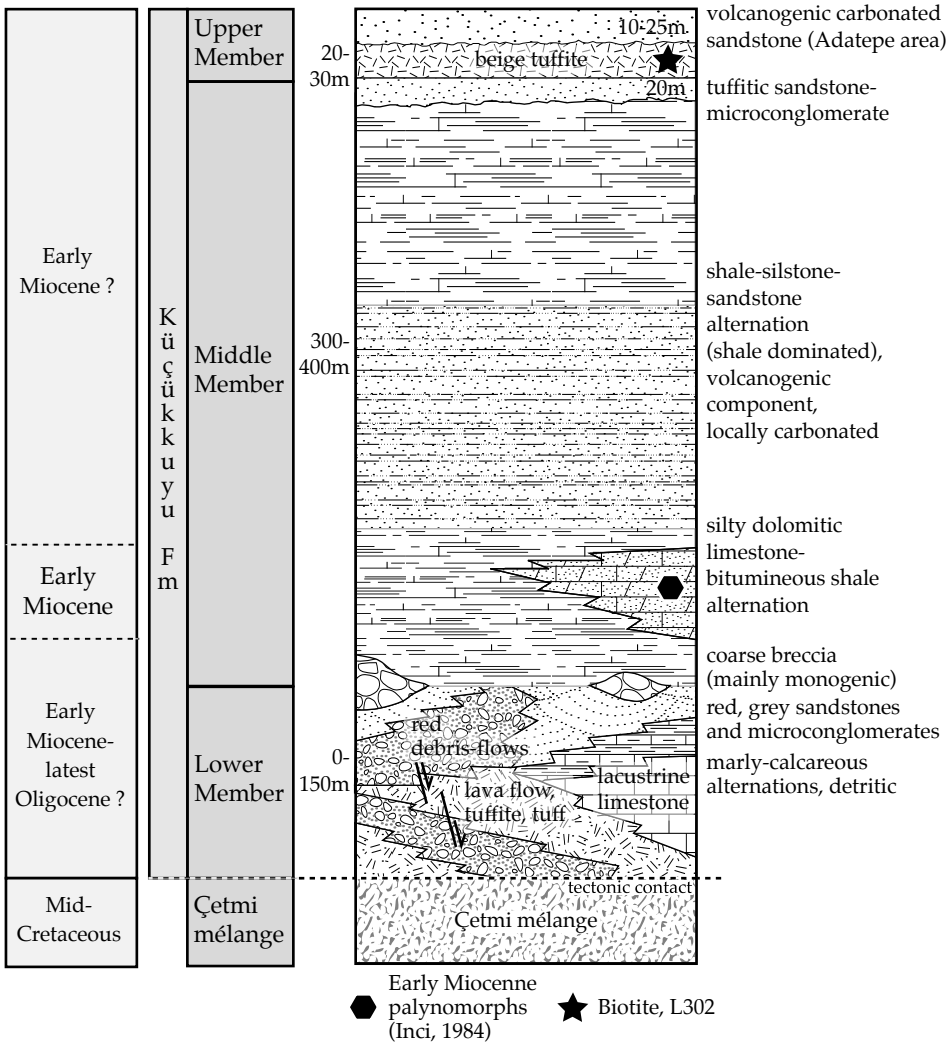

Figure 4.7. Synthetic stratigraphic column of the Küçükkuyu Formation.

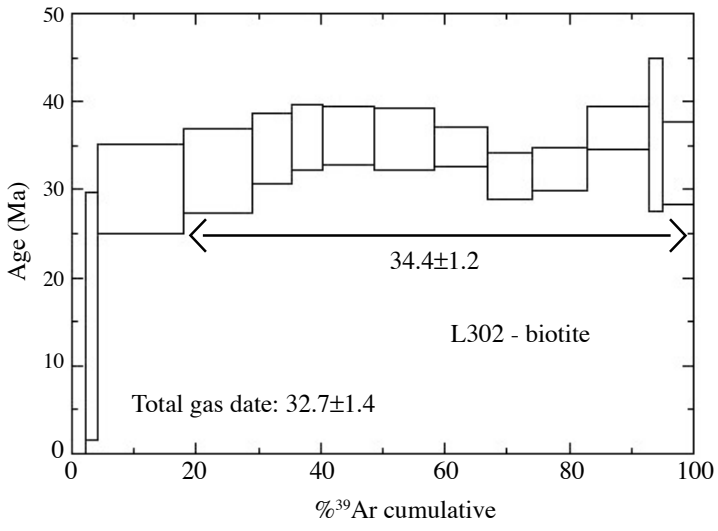

Figure 4.8. $^{39}Ar/^{40}Ar$ age spectra for sample L302 from the tuffitic upper member of the Küçükkuyu Formation.

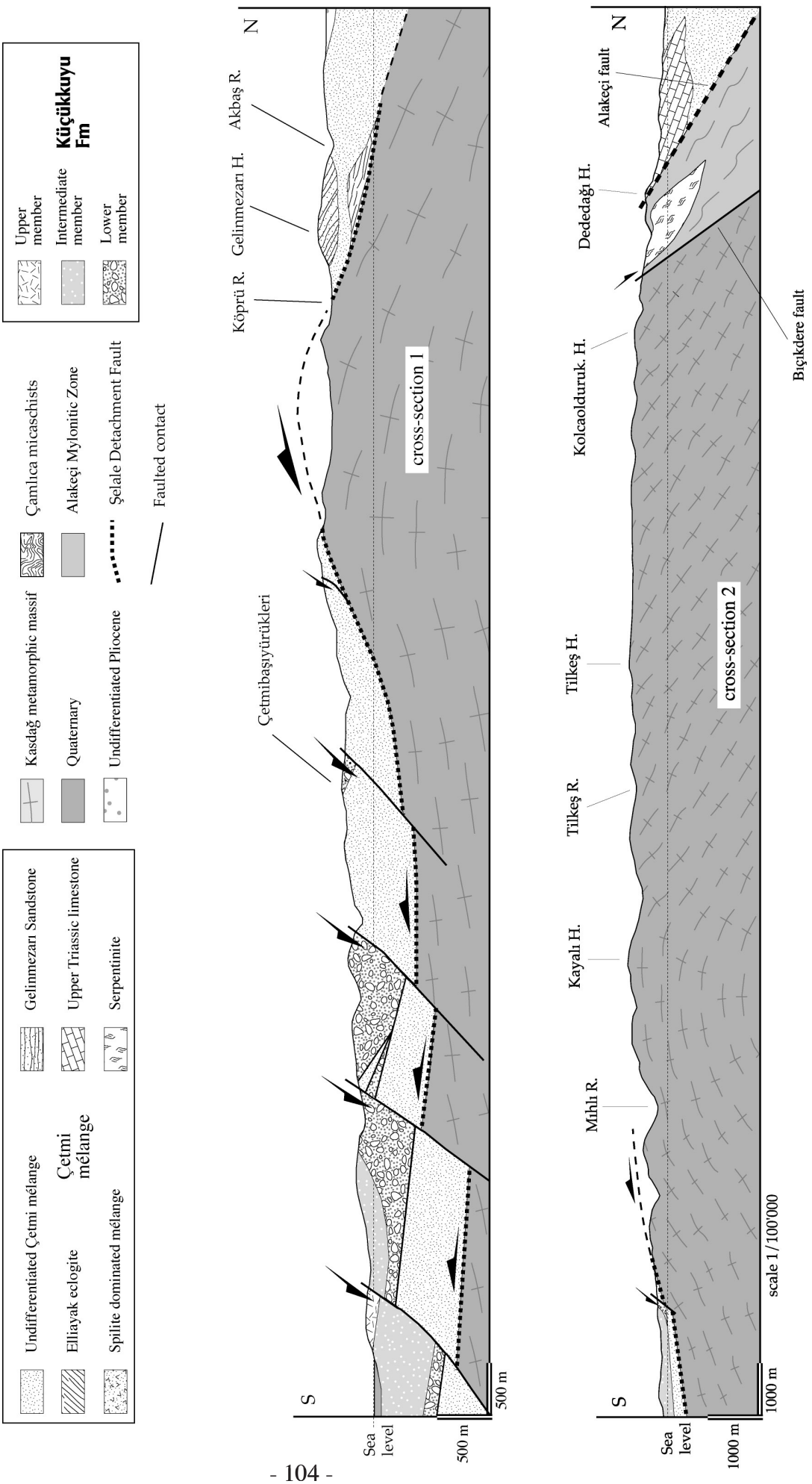

Figure 4.9. Cross-sections through the Kazdağ Massif, showing the structural relationships between the different units and the faults; location of the cross-sections on Figure 4.1.

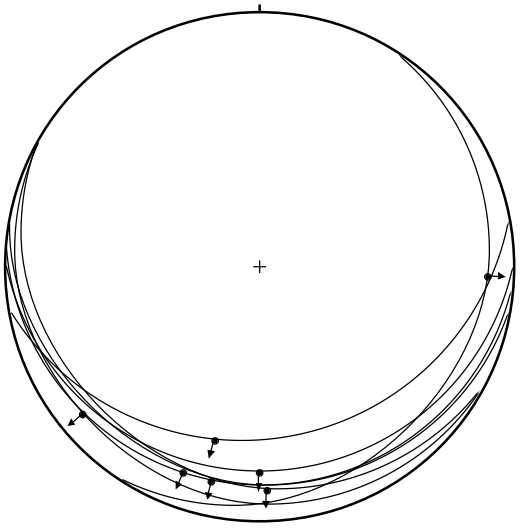

Figure 4.10. Slip-planes of the Şelale Detachment. Fault; equal area, lower hemisphere projection.

4.1.2. Şelale detachment fault

A major south dipping low-angle (15-20°) detachment fault (Şelale detachment fault, herein SDF, Figure 4.9 and 2.3), presently inactive, occurs between the Kazdağ Massif (foot-wall) and the Çetmi mélange/Küçükkuyu Fm (hanging-wall).

It displays well-developed fault planes (picture 4.4 plate 7C), with NNE trending slip lineations, indicating southward senses of movement (scarps and striations, see Figure 4.10 for the fault data). The fault planes show generally brecciation of the marbles or gneisses of the Kazdağ Massif (picture 4.5 plate 7C). In map view the SDF displays typical corrugations, which are a characteristic feature of many detachment faults. The present-day topography of the southern flank of the Kazdağ Massif in the area is still controlled by the low-angle geometry of the SDF; indeed, the general topography of the hills is smoothly going down to the sea with an angle of about 10°.

Several small elliptic granitoid bodies (150 m max. long for the longitudinal axis, Figure 4.1) crop out very close to the detachment fault in the mélange. They are internally undeformed but show evidences of mineral alteration. They are interpreted as predating the detachment activity, because (1) they occur only in the upper plate near the SDF, and are not randomly distributed; for instance they are not found in the Kazdağ Massif, and (2) one of these intrusions (a granodiorite) is clearly cut by the SDF.

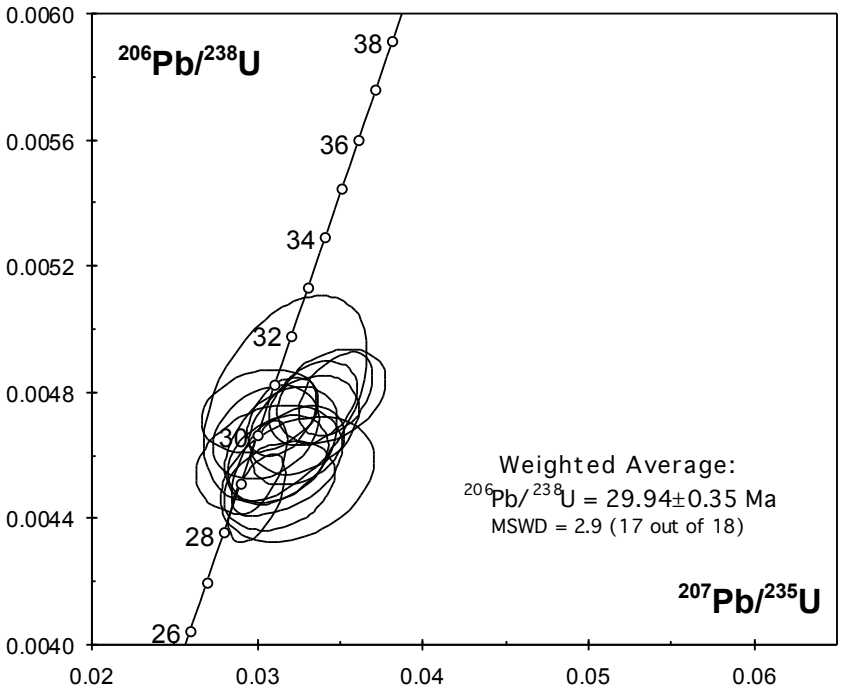

Figure 4.11. Concordia diagram for zircons from the granodiorite cut by the Şelale Detachment Fault.

Selected zircons from the latter (location on Figure 4.1) have been dated using U-Th-Pb in situ ion microprobe method (datation made at the CRPG Nancy, by D. Bosch, Montpellier). Because of the expected young age of the granodiorite (i.e. Tertiary), there was a doubt about the amount of radiogenic Pb. However, a very accurate concordia age of 29.94±0.37 Ma has been obtained from 18 spots on 16 grains (Figure 4.11 and appendix 7). This latest Early Oligocene age (Late Rupelian) is considered as a lower limit for the activity of the SDF.

The lower plate rocks are the metamorphic rocks of the Kazdağ Massif (picture 4.6 plate 6C); they have generally a mylonitic texture, and their foliation runs roughly parallel to the SDF, and dip toward it. Five oriented samples from gneisses, amphibolite and meta-sediment have been collected; two have a broad top-to-the southwest shear sense, one top-to-the north-east, one has two opposite shear senses, and one is inconclusive (Figure 4.1). The shear sense indicators are mainly mantled garnet and amphibole porphyroclasts and shear band cleavages. The shear deformation took place in the greenschist facies (retrogression of the amphibolite facies); evidences for this are the systematic crystallization of chlorite in the shear bands, chloritization of biotite, pre-deformation garnet partially replaced by chlorite and calcite. An unpublished latest Oligocene age from a mylonitic marble taken west of AdatepebaŞı village has been found by Lips (26.7±2.8 Ma, Ar-Ar method on white mica, 1998); this age is in agreement with the post–Rupelian age of the activity of the SDF.

The upper plate rocks are made by the various lithologies of the Çetmi mélange, mainly spilite and minor marble in the immediate vicinity of the detachment. Above the fault, on several tens of metres thick or more, the spilites (and other lithologies when they occur) are systematically brecciated or crushed, with strong siliceous, and more rarely carbonated hydrothermal alteration. Actually, the mélange appears to be totally disorganized, and to have lost its already complex primary features. Some secondary southward dipping low-angle faults between contrasted lithologies of the mélange also occur; they are interpreted as smaller-scale detachment faults, cogenetic with the main SDF. The mélange is then overlain through tectonic contacts (where observed) by the Küçükkuyu Fm of Early Miocene age.

The sediments of the KFm are considered to have been deposited above the Çetmi mélange in a typical supra-detachment basin (Friedmann and Burbank, 1995). Unlike many areas (e.g. Koçyigit et al., 1999), the detachment fault is not in direct contact with the overlying sedimentary basin, but with an intermediate unit (the mélange), which accommodates a part of the extension; this particular feature may be related to the weak rheological competence of the already disrupted Çetmi mélange. Sedimentation was synchronous with the ongoing deformation in the footwall (and also in the Çetmi mélange), as the KFm displays strong evidence of syn-tectonic sedimentation.

4.1.3. Step-like normal faults

The SDF and the KFm are cut by numerous roughly east-west trending southward dipping high-angle normal faults (Figure 4.1 and 4.9). A striking evidence for this is the southward down-shift and back-tilting of the discontinuous massive tuffitic upper member of the KFm. They also juxtapose these tuffitic beds to the lithologies of the Çetmi mélange.

They have also been described in the Kazdağ Massif north and west of the SDF (Gözler, 1986).

These normal faults, parallel to the Edremit graben, also occur in the Kazdağ Massif north and west of the SDF (Gözler, 1986), and west and east of the field area, where they are related to the Late Pliocene-Quaternary opening of the Edremit graben (Yılmaz and Karacik, 2001). The Plio-Quaternary graben fill, made of poorly consolidated coarse clastics, is observed on several hundreds metres in an exploration well drilled in the eastern part of the graben (Siyako et al., 1989; Yılmaz and Karacik, 2001). On the field area, east of Küçükkuyu, similar red coarse clastics reworking Kazdağ pebbles have been found, lying over the turbidites of the KFm through a northward tilted low-angle unconformity (c. 10°). The E-W trending Bayramiç graben, located north of the Kazdağ Massif, of the Alakeçi Mylonitic Zone and of the Çetmi mélange, is cogenetic with the Edremit graben (Yılmaz and Karacik, 2001); its Plio-Quaternary infill is also made of coarse red conglomerates reworking the metamorphic lithologies of the Kazdağ Massif, as well as upper Miocene-lower Pliocene limestones.

4.2. Northern flank of the Kazdağ Massif: the Alakeçi mylonite zone

The Alakeçi mylonitic Zone (herein AMZ, Figure 4.1 and 4.9) is a two km-thick zone of strong deformation, located between the Kazdağ Massif and the Çetmi mélange. Preliminary results from the study of the mylonites may be summarized as follow:

(1) The mylonites (picture 4.7 plate 7C) show a well-developed foliation and mineral lineation (fig 4.12); the foliation shows a general north-westward dip, whereas the lineation slightly plunges toward the north.

(2) The protoliths of the mylonites are the lithologies of the Çetmi mélange, at least in the northern half part of the AMZ; this is based (1) on the common occurrence of mylonitized dark greywacke/shale (matrix), and more rarely magmatic rocks (spilites) and radiolarite, (2) on the occurrence of ribbon marble lenses in the northern half part of the AMZ, which pass locally to the Late Triassic limestones of the Çetmi mélange, (3) on the occurrence of two big serpentinite lenses in the mylonites, attributed to the mélange (c.f. chapter 2).

The protolith of the mylonites, in a small-half southern part of the AMZ are the metamorphic rocks (gneisses) of the Kazdağ Massif.

(3) The deformation occurred in the greenschist conditions, and in the brittle to brittle-ductile transition zone, at least for the mélange-related mylonites; this is based (1) on the occurrence of broken quartz and feldspar, (2) mixed occurrence of fractures in feldspar and dynamic rescrystallization in quartz for the same sample, (3) foliation underlined by phyllosilicates wrapping almost undeformed quartz.

A decreasing gradient of temperature exists from the south to the north; it is not yet clear wether it is related (1) to a difference of temperature between the Kazdağ Massif and the mélange at the time of their formation (i.e. before the deformation), (2) to the deformation itself, (3) or to both of them.

(4) Shear criteria are not observable on the field, due to the very fine-grain nature of the rocks, except locally in the ribbon marble lenses. Thirteen oriented samples were collected, and two senses of shear were obtained from the marbles. Five up-dip top-to-

the-south shear senses, four down-dip top-to-the-north shear senses, and 6 inconclusive samples were obtained (Figure 4.1 and 4.12). The shear sense indicators are mainly mantled quartz and feldspar porphyroclasts, C'-type shear band cleavage (picture 4.8 plate 7C), and mica fish. Four top-to-the-north and two top-to-the-south samples (and one inconclusive) were collected by Okay and Satır (2000). Altogether, the fifteen critical samples display 7 top-to-the-south and 8 top-to-the-north shear senses. When the data are plotted together, it seems that the latter are mostly located in the southern part of the AMZ, and that the top-to-the-south samples were collected in the northern part.

(5) A poorly confined age of 55.05±6.2 Ma (Late Paleocene to Early Eocene) has been obtained by Lips (1998) from a carbonate mylonite north of the AMZ (Ar-Ar method on white mica). This age is either related to the mylonitic deformation (fabric age), or to the cooling of the sample below 350±30°C, after the formation of the mylonitic fabric (cooling age). In any case, the mylonite formation is pre- or syn- Late Paleocene to Early Eocene.

Moreover, an additional age data is provided by the Evciler granodiorite. It has intruded in the latest Oligocene-earliest Miocene times the Kazdağ Massif and the Çetmi mélange (but neither the AMZ, nor the Alakeçi detachment fault), and is considered as partially syn-extensional deformation of the Kazdağ Massif (Rb/Sr biotite cooling age of about 21 Ma, Okay and Satır, 2000a).

(6) The contact between the undeformed mélange (with respect to the mylonites) and the mylonite is marked by the Alakeçi fault. It is a northward low-angle fault, with dips ranging from 0° (near Akpınar) to 20-30° eastward. Neither fault plane, nor any sense criteria have been found along the fault; the spilites from the overlying mélange may display a crude foliation, and the limestones are brecciated. Both lithologies have been locally silicified by silica-rich hydrothermal fluids. The Alakeçi fault has all the characteristics of a presently low-angle northward dipping detachment fault, separating more or less strongly deformed rocks in the foot-wall (the AMZ) from undeformed rocks of the hanging-wall (Çetmi mélange, undeformed with respect to the AMZ).

The Kazdağ Massif, the AMZ and the Çetmi mélange are truncated in the southwest by the sinistral transtensional Uzunalan fault (because of the offset along it and it steep south-westward dip). The fault is characterized by a silicification of the underlying and overlying rocks, leading for instance to the listwaenitization of the serpentinites of the Çetmi mélange.

The contact between the AMZ and the Kazdağ Massif is made by the brittle NW-trending Bıçıkdere fault; the latter must have had at least a normal component, because it juxtaposes the less deformed gneisses (deeper) of the Kazdağ Massif in the footwall, with the mylonites (shallower) of the AMZ in the hanging-wall. The activity of the Bıçıkdere fault postdates that of the Uzunalan fault, as the former is parallel (and may control) to the present-day hydrographic pattern in the area, which cuts the Uzunalan fault. The Bıçıkdere fault may be either related to the opening of the parallel Bayramiç graben, or even to the dense network of NW-trending strike-slip faults occurring north-westward, crossing the Biga Peninsula, and related to the southern branch of the North-Anatolian Fault Zone.

4.3. Discussion on the role of the Şelale and Alakeçi detachment faults during the exhumation of the Kazdağ Massif

It appears from the previous results that (Figure 4.13):

(1) The low-angle southward dipping normal SDF must have played an important role in the exhumation processes of the Kazdağ Massif during the Late Oligocene-earliest Miocene; the Kazdağ Massif was in foot-wall position, whereas the Çetmi mélange and the KFm were in hanging-wall position. Main evidence for this are (1) the occurrence of an Early Miocene supra-detachment basin (the KFm) above the SDF, (2) the Late Oligocene age of a carbonated mylonite from the footwall and the Early-Oligocene age of the pre-detachment granodiorite, and (3) the greenschist retrogression of the amphibolitic rocks near the SDF. The sediments were deposited in the hanging-wall while the foot-wall was progressively mylonitized and exhumed. An important source of the sediments was the Çetmi mélange, which behaved as an intermediate unit also accommodating the extensional process; the mélange was passively elevated during the exhumation process, and its erosion products were feeding the KFm. This post latest Oligocene exhumation phase may be correlated with that of the Thasos Island (Wawrzenitz and Krohe, 1998).

(2) The Kazdağ Massif itself did not reach the surface before the Late Pliocene-Quaternary period, because no metamorphic detritus are found before in the surrounding sedimentary basins. This exhumation up to the surface is closely related to the opening of the Edremit and

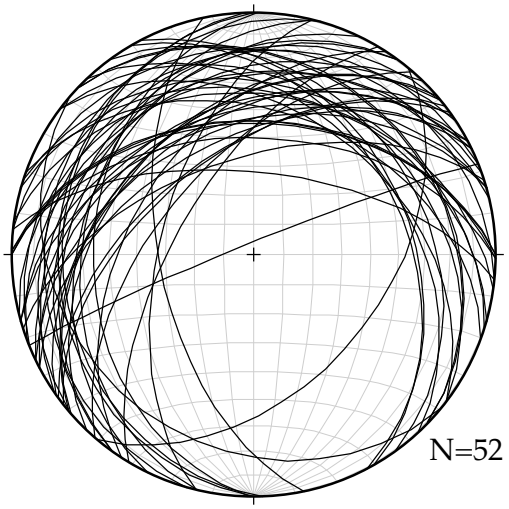

Foliations in the AMZ

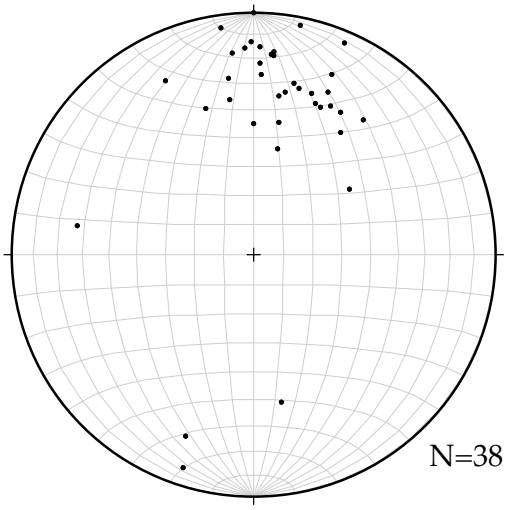

Lineations in the AMZ

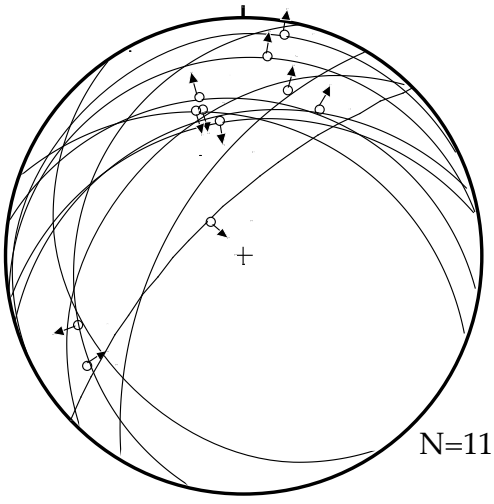

Senses of shear in the AMZ

Figure 4.12. Foliation, lineation and sense of shear in the Alakeçi Mylonitic Zone; equal area, lower hemisphere projection.

Bayramiç grabens. High-angle normal faults parallel to the Edremit graben, and related to its opening, are cutting and displacing the SDF and the KFm. The fault activity is still going on today, as shown for instance by strain data from GPS measurements (Straub et al., 1997), and the occurrence of hot-water springs (Pfister et al., 1997).

(3) It is not clear wether the exhumation process was continuous from the latest Oligocene to Present; however, Yılmaz and Karacık (2001) have found evidence for a short compressional phase at the end of the Middle Miocene in the region (final collision with Anatolia ?). Folding in the KFm may be related to this short compressional event.

(4) The deformation of a large part of the AMZ, whose protolith is made of the Çetmi mélange lithologies (northern part), was pre-50 Ma. Shear sense indicators in this part suggest top-to-the-south displacement. Then, this part of the AMZ must have stayed in upper plate position with respect to the latest Oligocene-Early Miocene exhumation of the Kazdağ Massif. The southward up-dip displacement observed in the northern part of the AMZ points to a compressional geometry; however, this is not the original pattern because of the post deformation tilting due to the post latest Oligocene- updoming of the Kazdağ Massif, so that the northern part of AMZ may have recorded a down-dip, southward extension. The Alakeçi detachment fault may have accomodated this extensional event (but may have been reactivated during the Late Oligocene –Early Miocene phase).

Another evidence for an Early Eocene exhumation phase in the Biga Peninsula comes from the Çamlıca micaschists, which are in tectonic contact with the Denizgören ophiolite north of Ezine, and with the Çetmi mélange west of Karabiga (c.f. chapter 2 and 3). They have preserved eclogite-facies metamorphic conditions, whose age is about 65-69 Ma (Maastrichtian, Rb/Sr method on white mica, Okay and Satır, 2000b). The Çamlıca micaschists must have been exhumed before the Eocene, because in their occurrence west of Karabiga, they are unconformably overlain by Eocene volcanics (Ercan et al., 1995), and lower Eocene sediments (Siyako et al., 1989). The micaschists north of Ezine have moreover similarities with units from the Rhodope Massif (Okay and Satır, 2000b); it is particularly the case for the Kimi Complex (Mposkos and Krohe, 2000, Figure 2.25), which suffered an eclogite metamorphism at 73 Ma, (Liati et al., 2002); moreover, a similar time interval than for the Çamlıca micaschists has been suggested for its exhumation (between 65 and 42 Ma, Krohe and Mposkos, 2002).

The shear sense indicators in the southern part of the AMZ suggest top-to-the-north displacement, which could be contemporaneous with the activity of the SDF. In this case, the exhumation of the Kazdağ Massif was a bivergent process. The sinistral Uzunalan fault could be seen as a lateral ramp accommodating the extensional process; The detachment faulting was accompanied by silica-rich hydrothermal circulations, leading locally to the listvenitization of the serpentinites from the mélange north and south of the Kazdağ Massif.

(5) It is not clear wether the future Kazdağ Massif was already at mid-crustal level in the Eocene; in other words, it may have or not suffered the first exhumation phase.

(6) In the Biga Peninsula, the Tertiary activity has a strong (crucial) influence on the morphology and geology of the studied objects (Çetmi mélange and Ezine area); for

instance, it is responsible for the pellicular aspect of the mélange, with possible reactivation of former sedimentary or tectonic contacts.

In summary, it appears that at least two phases of exhumation of deep- to mid- crustal level have occurred in the Biga Peninsula, and that the Çetmi mélange was in upper plate position in both cases. These two events may be linked to what is known from the eastern Rhodope area; one took place in the Eocene (Çamlıca micaschists, northern part of the AMZ, Kimi Complex), and one in the post latest Oligocene times (Kazdağ Massif, Thasos Island).

It is tempting to link the Eocene exhumation of the Çamlıca micaschists with the possible southward extensional event recorded in the AMZ; the reasons for that are the present-day position Çetmi mélange southeast of the Çamlıca micaschists (in both northern and southern occurrence), and the southward direction of extension in the mylonites. Then, the southern mélange underwent passively the updoming of the Kazdağ Massif in the Early Miocene.

Due to comparison with regional studies, the Eocene exhumation stage may be directly related to an Eocene collisional setting (subduction-collision related, or syn-orogenic extension), and the Late Oligocene-Early Miocene exhumation stage to the extensional tectonics following the slab roll-back of the Mediterranean slab (post-orogenic extension), as proposed by Okay and Satır (2000) (see Jolivet and Goffé (2000) for a comparison between syn- and post- orogenic extension, see Jolivet and Patriat (1999) for a discussion on the extension in the Aegean domain, see Dinter (1998), Kilias et al. (1999), Mposkos and Krohe (2000) for a discussion on the Rhodope area, see Acta Vulcanologica, vol. 10, (1998) for discussions on the Tertiary magmatism related to collisional and extensional processes in the Rhodope region).

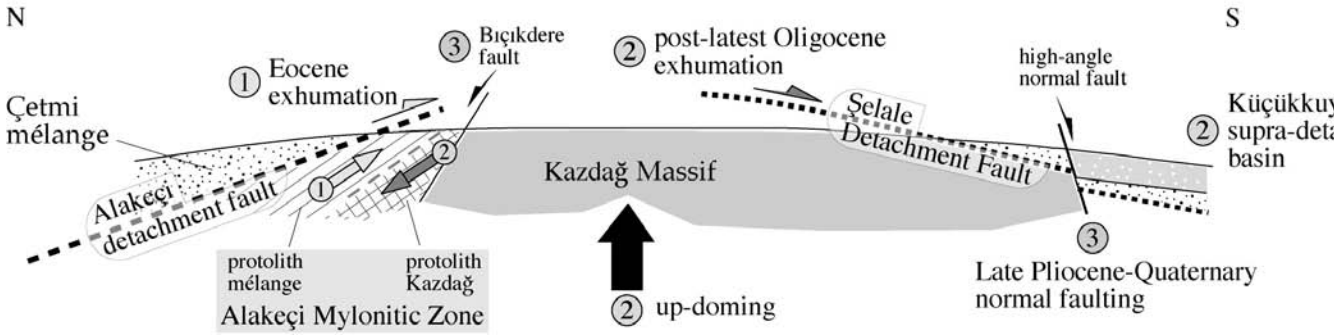

Figure 4.13. Schematic cross-section of the Kazdağ Massif and the overlying units, with the successive extensional phases.

- CHAPTER 5 -

CONCLUSION, GEODYNAMIC EVOLUTION OF THE BIGA PENINSULA AND ADJACENT AREAS

This chapter deals with the geodynamic evolution of the Biga Peninsula and adjacent areas, with a special focus on the Çetmi mélange and the Ezine area. Unlike the previous chapters, which were showing the difficulty to find good lateral equivalents based on geological data, this chapter proposes a paleotectonic scenario for their evolution through space and time, based on a plate tectonic model.

After a brief introduction to the latter and its basic geodynamic concepts, a geodynamic scenario replacing the Biga Peninsula in the frame of the regional geology is proposed, with some discussions on controversial questions.

5.1. The plate tectonic model

The data obtained from the previous field studies on the Çetmi mélange and the Ezine area, plus those from the regional geology, have been input in the plate tectonic model proposed by Stampfli and Borel (2002). This model, which gives a general frame for the Tethyan evolution during the Paleozoic and Mesozoic times, is based on several basic ideas, summarized below (the reader is referred to the previous paper for detailed explanations):

-The model is based on the concept of dynamic plate boundary (e.g. active spreading ridge, subduction zone, and transform fault); this allows (1) to use in the reconstructions lithospheric plates and not only continents (because a continent is generally attached to a larger plate), and (2) to define more precisely the location of the spreading ridges and to restore subducted oceanic basins.

-The input data of the model are (1) geological data from the field and the literature (stratigraphic, sedimentologic, paleontologic, tectonic, etc…), and (2) paleomagnetic and paleobiogeographic data.

-The model is governed by geodynamic forces (mainly slab-pull) and takes into account various geodynamic events, such as the onset of subduction, mid-ocean ridge subduction, presence-absence of slab roll-back and related plate motions, and plate buoyancy criteria.

-All the previous parameters are integrated together in the model in an iterative approach.

A major implication of the model is the great importance of lateral displacements of terranes through time (3 dimensions + time); that is (1) terranes which are now along the same transect may have been away one to the other before, and (2) a lithospheric cross-section may be only valid at one moment in a definite place. This 3D approach helps the geologist to have a more realistic view of the geodynamic evolution of a given area.

5.2. Geodynamic evolution

It appears from chapters 2 and 3 that (1) the geological evolution of the Ezine Group may

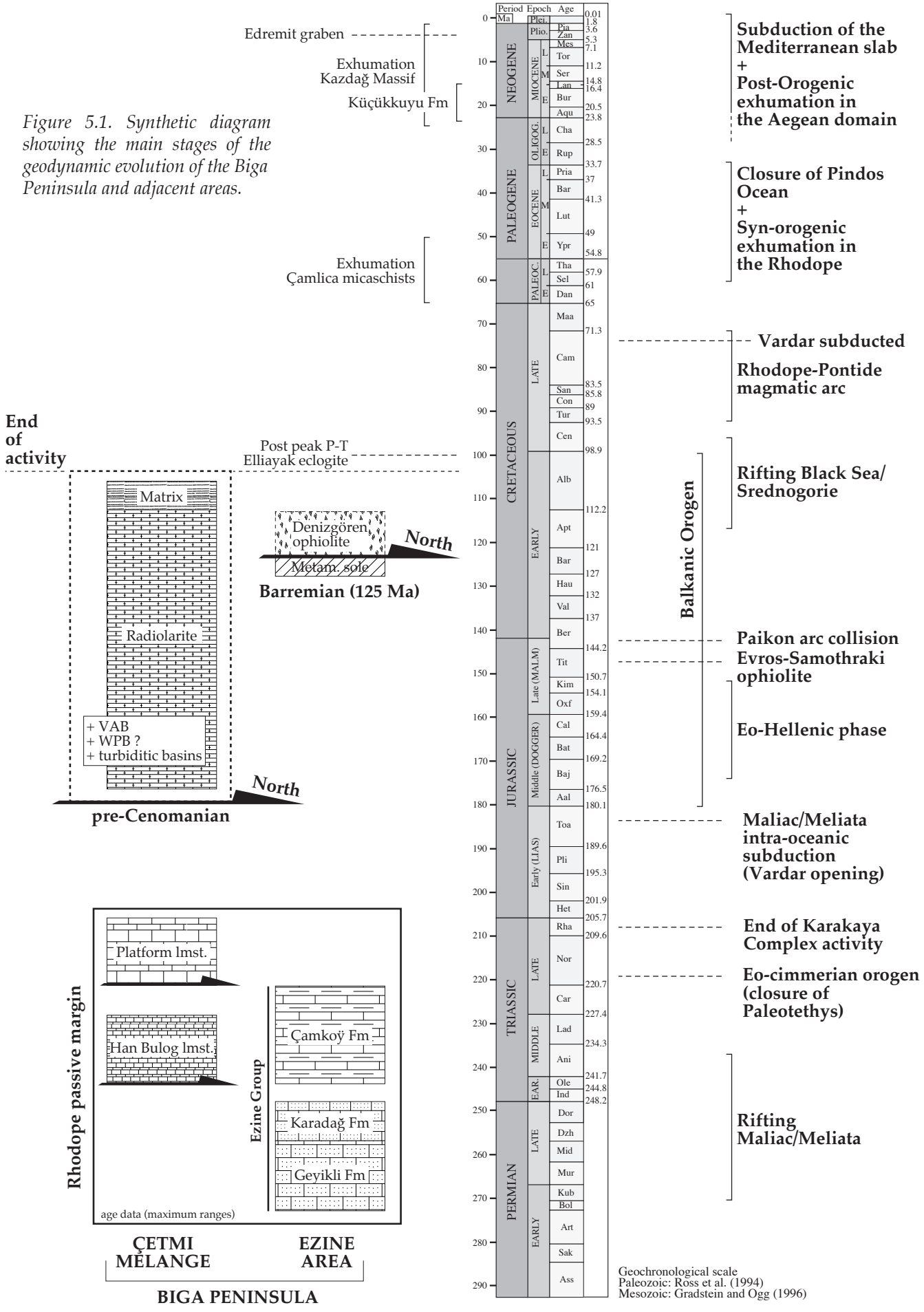

Figure 5.1. Synthetic diagram showing the main stages of the geodynamic evolution of the Biga Peninsula and adjacent areas.

record the rifting of the Maliac/Meliata oceanic domain (northern margin), and that (2) the Çetmi mélange and the Denizgören ophiolite have been emplaced in a Balkanic logic (i.e. ante-Cenomanian northward thrusting). Following this, a key for the understanding of the geodynamic evolution of the Biga Peninsula is to see the Çetmi mélange as a continuous stratigraphic sequence, and to place it in the continuation of the Ezine Group.

The proposed scenario, which jumps from the scale of the Biga Peninsula to that of the Aegean region, is illustrated by selected cross-sections and corresponding paleotectonic reconstructions; the latter have been modified from Stampfli (2000) to take all the results of the thesis into account. The chapters 1 and 4 contain the regional information and references used here, unless mentioned. Figure 5.1 shows a summary of the main data from this study and the main geodynamic events.

Late Permian

In the Late Permian (Figure 5.2), the Paleotethys was still subducting northward under Laurasia; a strong slab roll-back effect following the subduction of its ridge was responsible for back-arc rifting along this margin; the Maliac/Meliata rift system is one of these new rifts, and the Ezine Group represents the sedimentation during the rifting phase(s) in the Late Permian-Early Triassic on the future northern margin of the ocean (southern margin of the Rhodope). The scarce Han Bulog limestones from the Çetmi mélange may be lateral equivalent of the pebbles in Hallstatoid facies found in the "pink breccias" of the Çamkoÿ Fm in the Ezine Group. The Hydra and Evia sequences of Greece record the rifting phase(s) in the southern margin (northern margin of the westward Pelagonia terrane), whereas a possible opposite, closer equivalent of the Ezine Group may be found in Karaburun (Rosselet, Ph-D in prep.). In the north, the Rhodope was delimited by another rift (south Balkan or Kotel rift), which never reached sea-floor spreading, but stayed an active area until the Early Tertiary. Eastward, another rift had developed (future Küre Ocean), with the Karakaya Complex active south of it; the latter was reworking Permian neritic limestone, considered as possible lateral-equivalent to those of the Ezine Group.

Figure 5.2. (next page) Cross-section and paleotectonic reconstruction for the Permian (250 Ma).

Caption: 1-passive margin; 2-synthetic anomaly; 3-seamount; 4-intra-oceanic subduction; 5-active ridge; 6-subduction; 7-rift; 8-suture, inactive thrust; 9-thrust; 10-foreland basin.

Ad: Adria s.s.; Ag: Aladağ; An: Antalya; Ap: Apulia s.s.; Ar: Arna accr. cpl.; As: Apuseni-south ophiolites; At:Attika; Av: Arvi; Ba: Balkanides external; Bd: Beydağları; Bk: Bolkardağ; Bn: Bernina; Br: Briançonnais; BS: Black Sea; Bu: Bucovinain; Bü: Bükk; BS: Bator-Svarvasko ophiolites; Bv: Budva; Ca: Calabria autochthon; cB: central Bosnia; cD: central Dinarides ophiolites; CL: Campania-Lucania; Cn: Carnic-Julian; Co: Codru; cR: circum Rhodope; Da: Dacides; Db; Dent Blanche; Dg: Denizgören ophiolite; Do: Dobrogea; Ds: Drymos ophiolite (Evros); Du: Durmitor; eA: east Albanian ophiolites; El: Elazığ Güleman ophiolites-arc; eP: east Pontides; Fa: Fatric; gC: great Caucasus; Gd: Geydağ-Anamas-Akseki; Ge: Gemeric; GT: Gavrovo-Tripolitza; Gt: Getic; Gü: Gümüşhane-Kelkit; He: Helvetic rim basin; Hg: Huğlu-Boyalı Tepe; hK: high Karst; Hr: Hronicum; Hy: Hydra; iA: intra Alpine terrane; Ig: Igal trough; Is: Istanbul; Jv: Javavic; Ja: Jadar; Ka: Kalnic; Kb: Karaburun; Ke: Kotel flysch; Ki: Kirşehir; Kk: Karakaya fore-arc; Ko: Korab; Kr: Karpinski; KS: Kotel-Strandja rift; La: Lagonegro; Le: Lesvos ophiolite; Lo: Lombardian; Ma: Mani; Mc: Maliac rift/Ocean; Md: Mozdak; Me: Meliata rift/Ocean; Mi: Mirdita authochthon; Mm: Mamonia accr. cpl.; Mn: Menderes; Mr: Mrzlevodice fore-arc; MP: Mersin Pozantı ophiolites; MS: Margna-Sella; Mz: Munzurdağ-Keban; nC: north Caspian; Ni: Nilüfer seamount; Ns: Niesen Flsych; Nt: Nish-Troyan trough; Ot: Othrys-Evia-Argolis ophiolites; Oz: Otztal-Silvretta; Pi: Piemontais; Pk: Paikon intra-oceanic arc; Pl: Pelagonian; Pn: Pienniny rift; Rh: Rhodope; Sc: Scythian platform; Sd: Srednogorie rift-arc; Se: Sesia; Si: Sicanian; Sj: Strandja; sK: south Karawanken fore-arc; Sk: Sakarya; Sl: Slavonia; SM: Serbo-Macedonian; Sr: Severin ophiolites; SS: Sanandaj-Sirjan; St: Sitia; Sv: Svanetia rift; TB: Tirolic-Bavaric; tC: trans-Caucasus; TD: Trans-Danubian; To: Talea Ori; Tt: Tatric; Tu: Tuscan; Tz: Tizia; Tv: Tavas+Tavas seamount; UM: Umbria Marches; Va: Valais trough; Ve: Veporic; Vo: Vourinos (Pindos)-Mirdita ophiolites; wC: western-Crete (Phyl-Qrtz) accr. cpl.; Zi: Zlatibar ophiolites; Zo: Zongüldak.

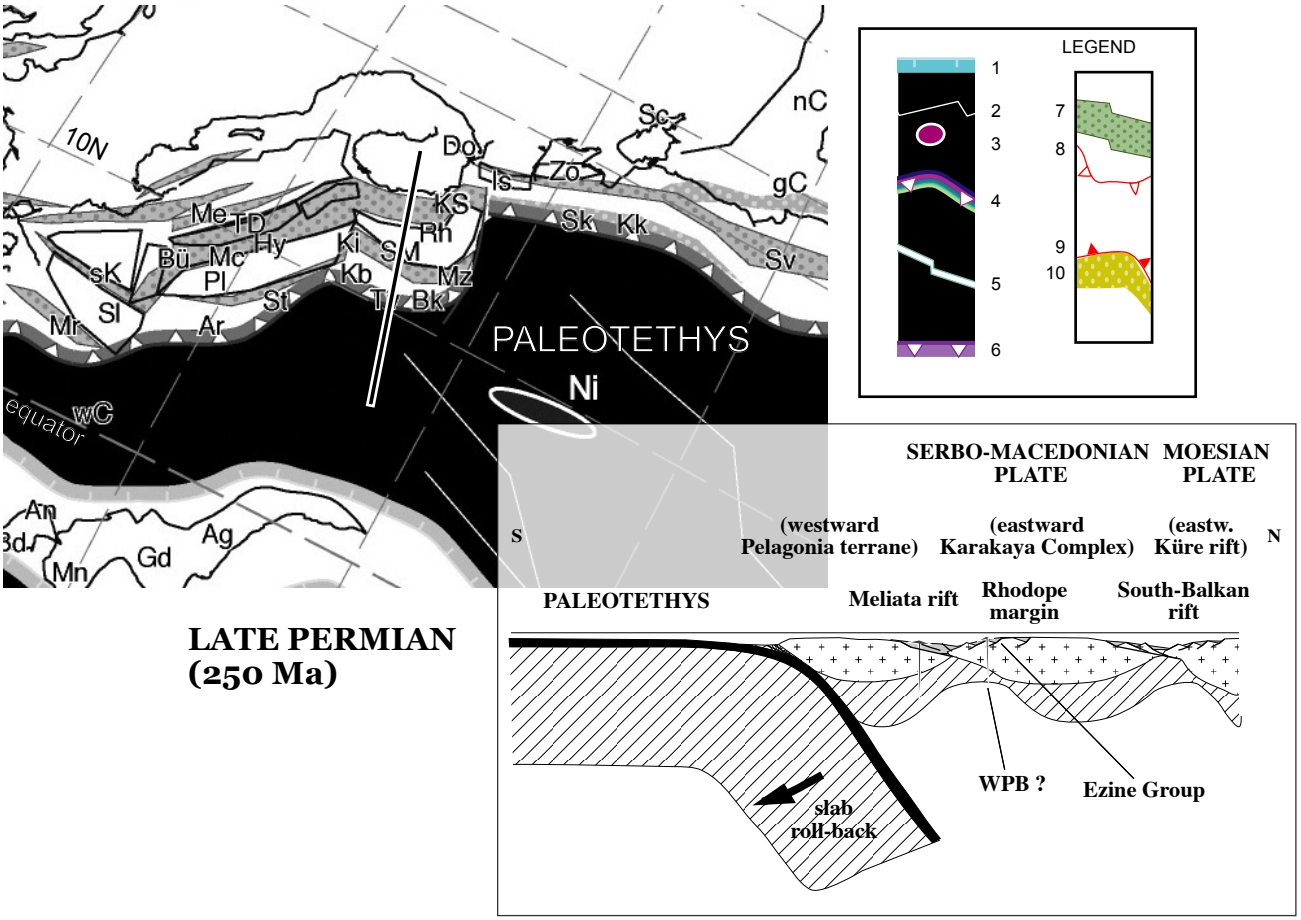

Norian

In the Norian times (Figure 5.3), the Paleotethys has totally subducted in the western Tethyan domain (Eocimmerian collision, well constrained in the Anatolide-Tauride Block (ATB) for instance). The passive margin stage on the Rhodope margin started in the Middle Triassic. It is testified by a high subsidence ratio balanced by carbonate sedimentation and propagation of carbonate platform in the whole area, locally until the Mid Jurassic (Strandja region in Bulgaria); the Norian-Rhaetian carbonated ramp limestones of the Çetmi mélange are considered as evidences of this post rift sedimentation. The northern margin of Pelagonia records the same post-rift features. Sea-floor spreading of Maliac/Meliata Ocean lasted from Early Triassic to Carnian time. Eastward, the Küre back-arc basin has already started to subduct southward under the Sakarya-Karakaya terrane.

Toarcian/Aalenian

In the Aalenian times (Figure 5.4), the southward subduction of the Küre Ocean, combined at a smaller scale with the westward rotation of Africa relative to Europe from the Late Triassic (opening of Atlantic and northward subduction of Neotethys), may had two effects:
(1) Late Triassic (?)-Early Jurassic intra-oceanic subduction and roll-back of the old and cold Maliac-Meliata lithosphere; the latter is responsible for the opening of a new back-arc basin, the Vardar oceanic domain. From that time onwards the Rhodope margin lost its passive

margin features, and suffered a transpressional regime (beginning of the Balkanic orogen); the latter led to the rejuvenation and northward inversion of the Kotel basin, which became a foreland basin.
(2) Liassic opening of the Izmir-Ankara-Erzincan back-arc oceanic domain, marked by the typical Liassic transgressive sequences over the Karakaya Complex. Some authors favour a Late Triassic (Carnian) opening of the IAE Ocean, based on the occurrence of Carnian pillow lavas and cherts on the northern edge of the Anatolide-Tauride Block; but they are rather seen here as possible Maliac or Pindos remnants (Stampfli et al., 2003), the Anatolide-Tauride block not being south of the Sakarya block at that time.

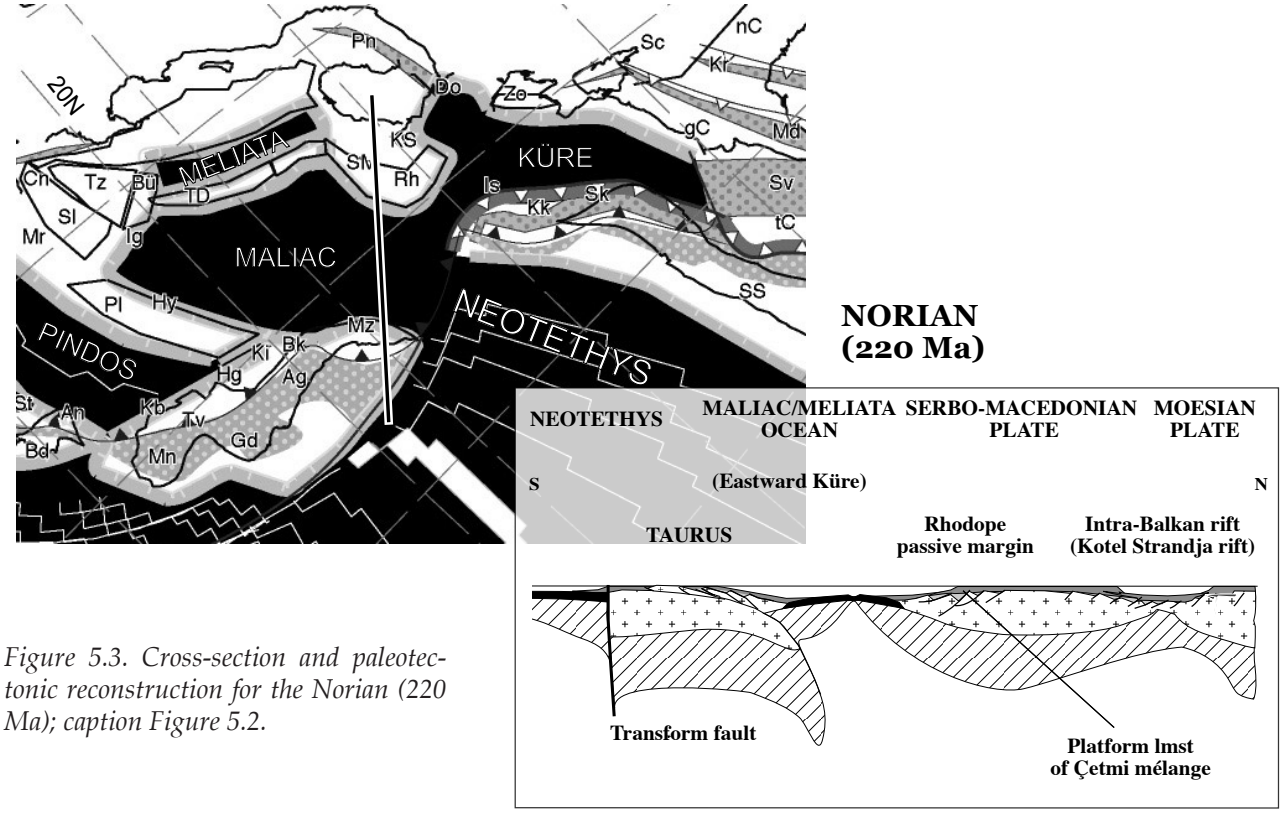

Figure 5.3. Cross-section and paleotectonic reconstruction for the Norian (220 Ma); caption Figure 5.2.

Late Oxfordian

In the Late Jurassic (Figure 5.5), the Vardar Ocean had totally replaced the Maliac/ Meliata domain. At that time, the Vardar ocean obducted southward onto the Pelagonian margin (Eo-Hellenic phase); in the north, there are also evidences of northward obduction of Vardar ophiolites onto the Rhodope margin (Evros-Samothraki ophiolites), and collision of the latter with the Païkon arc, consider as an intra-oceanic arc of the subducting Maliac/ Meliata Ocean (continuation of the Balkanic orogen). A solution for the absence of Liassic deposits in the Çetmi mélange is their possible erosion at that time (flexuration of the Rhodope passive margin). However, the northward obduction of the Vardar must have had a strong strike-slip component (dextral), due to the strong slab roll-back of the Maliac/ Meliata ocean and its replacement by the Vardar Ocean; the preservation of some parts of the Rhodope passive margin (e.g. Ezine Group) supports this interpretation.

The spreading may have stopped in the IAE Ocean, which is bordered by two passive margins, The Sakarya microcontinent in the north and the western end of the Sanandaj-Sirjan block in the south.

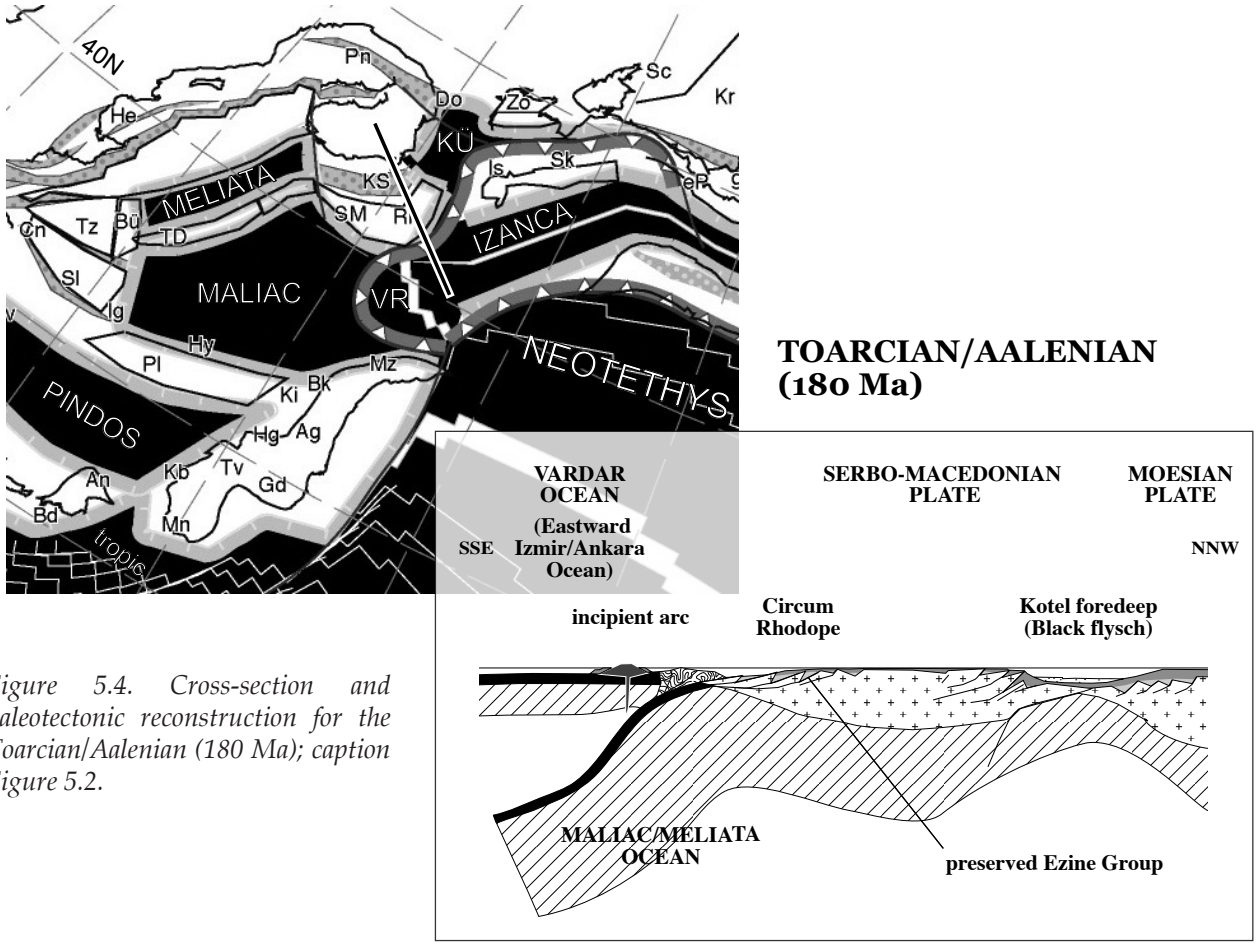

Figure 5.4. Cross-section and paleotectonic reconstruction for the Toarcian/Aalenian (180 Ma); caption Figure 5.2.

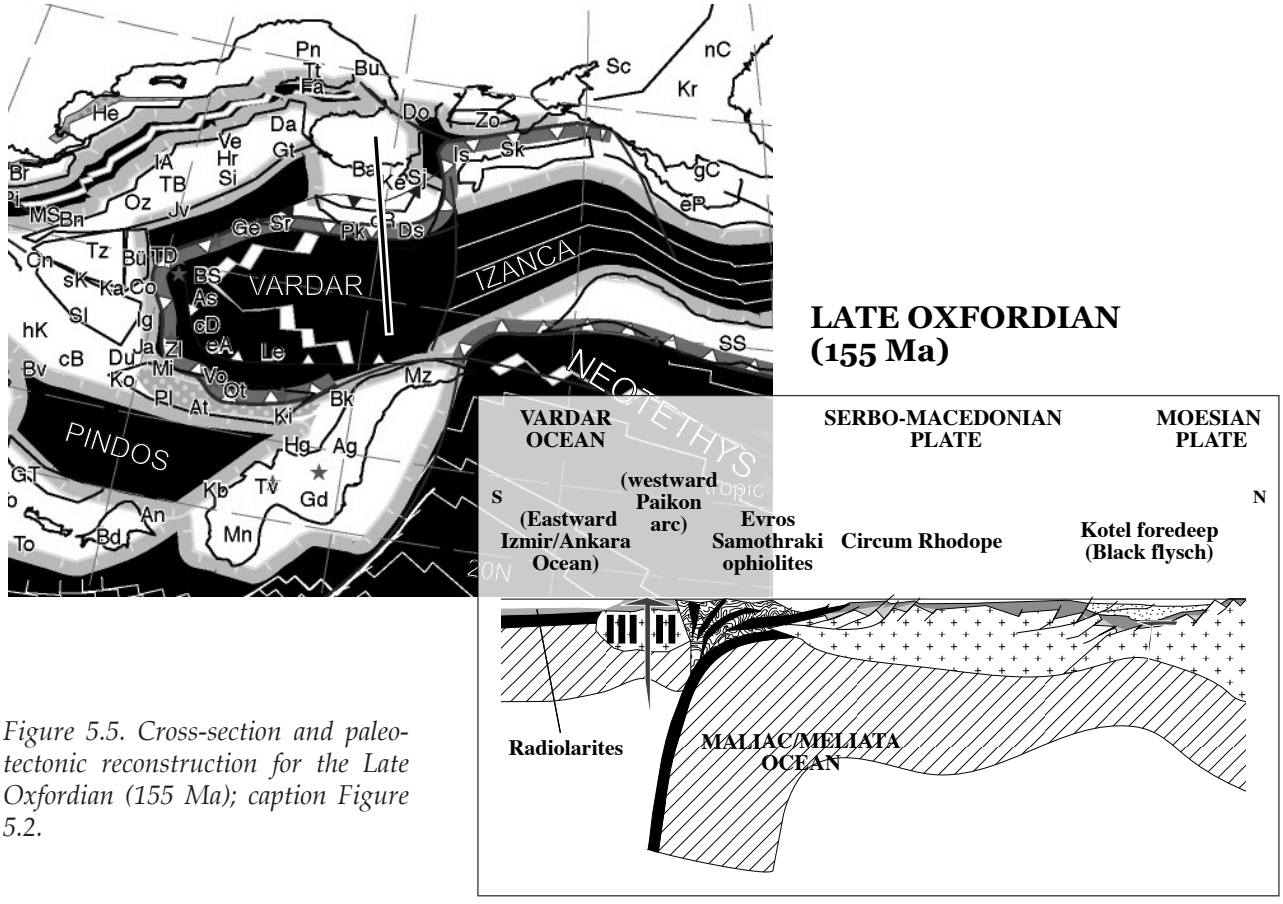

Figure 5.5. Cross-section and paleotectonic reconstruction for the Late Oxfordian (155 Ma); caption Figure 5.2.

Barremian-Aptian

Close to the Barremian/Aptian boundary (Figure 5.6), the Rhodope margin was still suffering the Balkanic orogenic phase, as evidenced by the filling of the Nish-Troyan foreland basin until the Late Barremian times (Georgiev et al., 2001). At the same time, the old and cold oceanic lithosphere of the IAE Ocean began to roll-back toward the east, opening a new back-arc basin, newly defined here as the Lycian Ocean (because it will obduct later on the ATB passive margin to give the Lycian ophiolites). As for the Vardar domain, this slab roll-back must have created a strong strike-slip regime (sinistral) along the southern Rhodope margin. A triggering cause for this slab roll-back would be the eastward escape of the ATB microplate with respect to Europe in the late Jurassic-Early Cretaceous (itself related to the opening of the Atlantic Ocean).

The Denizgören ophiolite may have been emplaced onto the preserved Rhodope passive margin according to the same balkanic logic. A hypothesis is that the inception of obduction took place near the newly created Lycian oceanic ridge in the Barremian; the emplacement of the ophiolite onto the Rhodope margin occurred shortly after, in a transpressive regime.

The Çetmi mélange, and possibly the Drimos-Dolno Lukovo units, must have been emplaced in the same way some times later, before the Albian/Cenomanian boundary.

The radiolarites found in the Çetmi mélange may represent pelagic sediments from the IAE Ocean (and not from the Vardar), as a single block records pelagic sedimentation from Tithonian to Aptian. They have been incorporated into the prism/fore-arc related to the IAE subduction.

The VAB found as tectonic slices in the mélange may come either from remnants of the (older) Vardar arc accreted to the Rhodope margin, or from a possible (younger) arc related to the IAE Ocean subduction. Both cases are compatible with a continental component for the magmatic source, as they have been developed very close to continental areas. However, the second hypothesis is preferred because the greywacke-shale matrix of Early –Middle Albian age seems to be closely associated with the VAB. The matrix marked the last sedimentation event before the mélange emplacement, possibly with the Doğandere Sandstone. The other turbiditic basin (Gelinmezarı Sandstone) has a more confused origin and may be older.

All the previous lithologies (radiolarites, VAB, matrix, turbiditic basins) have been emplaced onto a preserved segment of the flexural lower plate Rhodope passive margin, represented in the mélange by the Han Bulog and carbonate ramp-type limestones. Perhaps it would be better to speak about accretion rather than emplacement (i.e. obduction), because of the inferred strike-slip regime. The absence of metamorphism (i.e. no-burial) both in the passive margin and oceanic units supports this hypothesis.

In the same way, the eastward propagation of the IAE Ocean slab roll-back may be an explanation for the northward emplacement of mélanges onto the Sakarya passive margin. Indeed, in several places, the Sakarya margin shows a typical flexural lower plate pattern (c.f. Figure 1.8), which could be linked to the transpressive obduction of the Lycian ocean/prism. The age of mélange emplacement in the eastern Pontides is Turonian-Coniacian (Okay and Şahintürk, 1997), which supports the eastward propagation of the process.

The Çetmi mélange, as well as the whole Rhodope area, is sealed by Cenomanian deposits, which marks the end of the Balkan orogenic phase; from this time onwards, the Çetmi mélange, the Ezine Group and the Denizgören ophiolite passively suffered further deformations.

An interesting point is that the westward Istanbul and Sakarya zones could have been juxtaposed in the Cenomanian times (Tüysüz, 1999); thus the Intra-Pontide suture may be seen as a part and/or continuation of the Balkanic suture. In this way, the occurrence of younger pelagic limestones in the suture (c.f. chapter 2) cannot be related to an Intra-Pontide Ocean. Actually, the IP Ocean does not appear in the reconstruction, for mainly two reasons: (1) there are no constraints on its opening age, and disagreement on its closure age; (2) strong strike-slip motions occurred in the Late Cretaceous-Eocene and Pliocene (NAFZ) periods (Barka, 1992; Yığıtbaş et al., 1999; Göncuöğlu et al., 2000, and the paleotectonic reconstructions), which might have favoured some duplications of the IAES, or at least lateral transportation of lithologies from the latter.

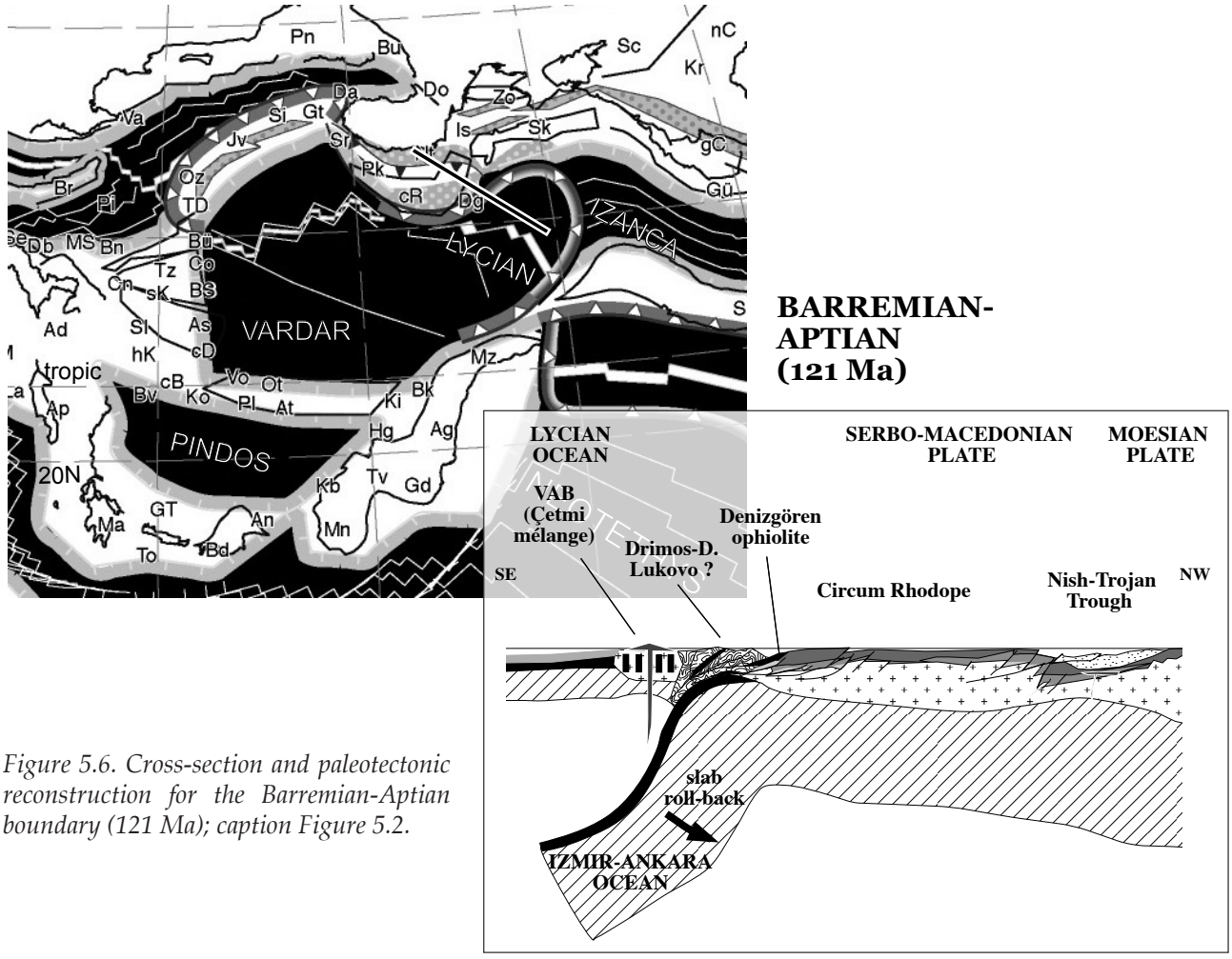

Figure 5.6. Cross-section and paleotectonic reconstruction for the Barremian-Aptian boundary (121 Ma); caption Figure 5.2.

Santonian-Maastrichtian

In the Santonian-Maastrichtian interval (Figure 5.7), the Lycian Ocean has totally replaced the IAE Ocean. The ATB has moved about 1000 km eastward from the Barremian-Aptian times, to reach approximately its present position south of the Sakarya Zone (beginning of opening of the north Atlantic Ocean, inferring the eastward motion of Africa and related continents, such as the ATB). This strong strike-slip motion triggered simultaneously the southward obduction of the Lycian Ocean onto the ATB, and the northward subduction of

the Lycian and Vardar oceans under the Rhodope-Sakarya zones (c.f. Robertson, 2002, for review).

The Late Cretaceous obduction is very well constrained by the numerous peridotite bodies and mélanges resting on its northern margin, as well as by the development of the Bornova Flysch Zone.

There are also many evidences of the second event, such as the development of the Turonian-Campanian Rhodope-Pontide magmatic arc, and the correlative opening of the Black Sea-Srednogorie rift (e.g. Robinson et al., 1995; Georgiev et al., 2001). The consecutive opening of the western Black Sea oceanic basin (whereas the Srednogorie rift aborted) induced the southward displacement of the Istanbul and Sakarya zones, which took approximately their present position east of the Rhodope margin. The juxtaposition of the Rhodopian Biga Peninsula and the western end of the Sakarya Zone dates from this time. Therefore, the boundary between these two units may be a trace of the western Black Sea fault, which accommodated the opening of the western Black Sea basin in the Late Cretaceous (Okay et al., 1994).

In the Santonian, the Elliayak eclogite has been exhumed or is on the point of doing so. As it is made of former oceanic sediments and magmatic rocks, it could represent a piece of the northward subducted Vardar oceanic floor. A hypothesis for its exhumation would be to consider it in the frame of the Srednogorie/Black Sea rift; in this case, the extensive syn-rift tectonics could lead to the exhumation of the eclogite by the unroofing of the overlying rocks.

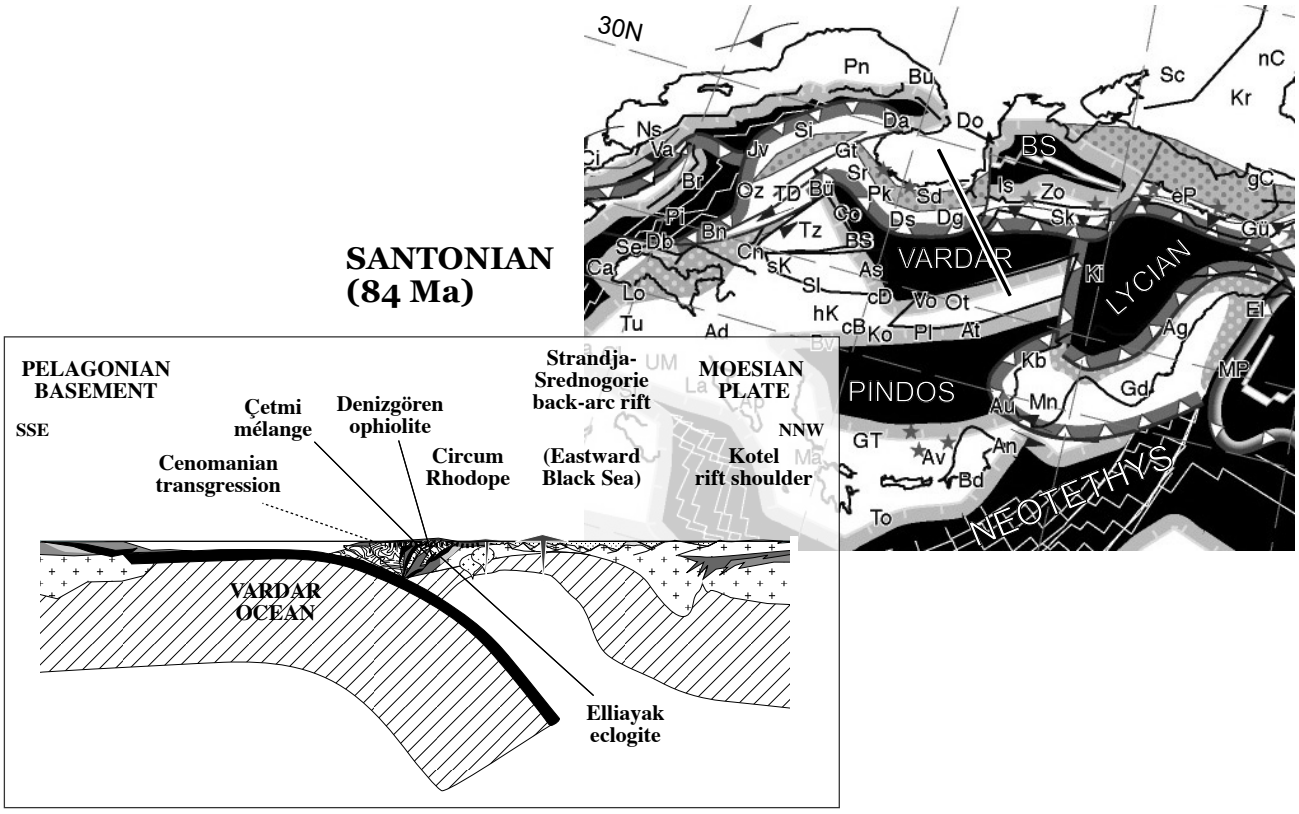

Figure 5.7. Cross-section and paleotectonic reconstruction for the Santonian (84 Ma); caption Figure 5.2.

The ongoing northward motion of the ATB leads to the final closure of the Vardar Ocean, probably in the Maastrichtian.

The Turonian-Coniacian limestones from the southern mélange may mark the flexuration and deepening of the Rhodope-Sakarya margin following the onset of Vardar subduction. As for the Maastrichtian-Paleocene limestones from Gelibolu Peninsula, they may represent post-rift sedimentation after the opening of the Black Sea basin (thermal subsidence).

Tertiary

The final closure of the remnant oceanic basins (Pindos, Lycian) and the consecutive continental collision (between Pelagonia and Rhodope domains) continued until the Eocene-Early Oligocene, accompanied by syn-orogenic exhumation processes in the Rhodope area (Çamlica micaschists, northern part of the Alakeçi Mylonitic Zone, Kimi Complex, Figure 5.8). Some sedimentary basins developed at the same time, such as the Thrace basin in NW Turkey (Burchfiel et al., 2000).

The transition from the Eocene-Early Oligocene closure of the Pindos ocean to the subduction of the Mediterranean slab at the Oligocene-Miocene boundary is complex, and not well understood. The exhumation of the Kazdağ Massif, and many other places in the Aegean region (Rhodope, Menderes, Cycladic blueschists) clearly comes within the context of the upper Oligocene-Miocene Aegean extension; the latter is still strongly

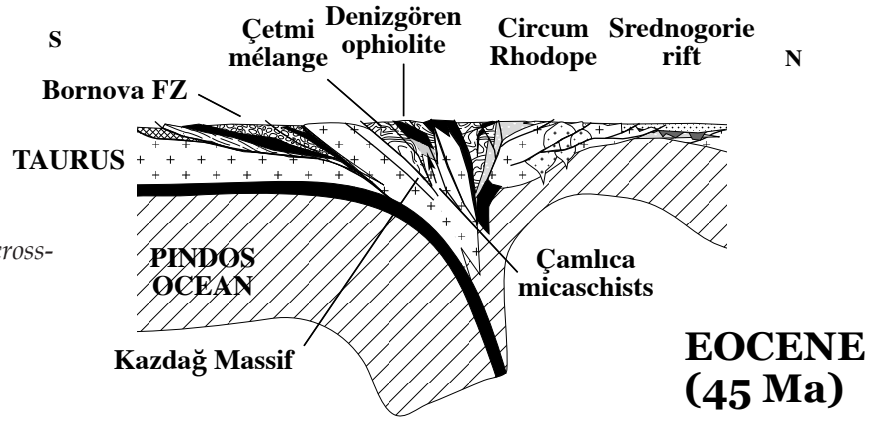

Figure 5.8. North-south cross-section for the Eocene.

going on farther south today, due to the Mediterranean slab retreat. In northwest Turkey, exhumation occurred not only in the Kazdağ area, but also in the Ezine and Kozak regions (uplift and erosion of upper Oligocene-lower Miocene granitoids and their sedimentary cover, Schindler, 1997), where it is also associated with a strong magmatic activity.

In Biga Peninsula, the combination of the southward extensional regime, plus the dextral activity of the southern branch of the North Anatolian Fault Zone, led to the opening of the Plio-Quaternary Edremit and Bayramiç grabens. The tectonic activity is still substantial nowadays, with the occurrence of several earthquackes in Biga Peninsula in the last dedades (Herece, 1990).

Concluding remarks

The Biga Peninsula, represented by the Ezine Zone and the Çetmi mélange, is paleogeographically related to the Rhodope margin. This is confirmed by its total absence of Sakarya-related outcrops, such as the Karakaya Complex, the Liassic transgression, and the Mesozoic passive margin sediments. Its juxtaposition with the western margin of the Sakarya microcontinent dates from the Late Cretaceous. This major tectonic limit may have been used later by the NAFZ to propagate southwestward across the Biga Peninsula.

The scenario also shows the importance of the strike-slip displacements through time (e.g. the eastward displacement of the Taurus plate), so that the 3D approach becomes crucial to tackle the geodynamic evolution of the area.

From a more general point of view, this work has shown the importance of a multidisciplinary approach in the study of complex geological objects, such as accretionary-type mélanges or obduction-related sequences.

For instance, because of the obliterating Tertiary tectonics, the methods of structural geology cannot be applied here to give satisfactory results on emplacement (timing, sense) of the Çetmi mélange and the Ezine area. Only the gathering of data obtained from various methods (detailed mapping, sedimentology, tectonics, micropaleontology, geochemistry, metamorphism), plus the necessary comparison with the regional geology, could constrain in this case the correlation and emplacement of these units.

Then, the integration of the various methods and associated results may be used as a base for further smaller-scale paleotectonic and paleogeographic considerations.

- REFERENCES -

Aalto, K.R. 1981. Multistage melange formation in the Franciscan Complex, northernmost California. *Geology* **9**: 602-607.

Abbate, E., Bortolotti, V. and Passerini, P. 1970. Olistostromes and olistoliths. *Sedimentary Geology* **4**: 521-557.

Abdüsselamoğlu, Ş. 1959. Geology of the Almacıkdağı and the region between Mudurnu and Göynük (in Turkish). *Istanbul Üniversitesi Fen Fakültesi Monografileri* **14**.

Akıman, O., Erler, A., Göncuöglu, M.C., Güleç, N., Geven, A., Türeli, K. and Kadioğlu, Y.K. 1993. Geochemical charactersitics of granitoids along thr western margin of the Central Anatolian Crystalline Complex and their tectonic implications. *Geological Journal* **28**: 371-382.

Altiner, D., Koçyiğit, A., Farinacci, A., Nicosia, U. and Conti, M.A. 1991. Jurassic-Lower Cretaceous stratigraphy and paleogeographic evolution of the southern part of northwestern Anatolia. *Geologica Romana* **18**.

Angiolini, L., Dragonetti, L., Muttoni, G. and Nicora, A. 1992. Triassic stratigraphy in the island of Idra (Greece). *Rivista Italiana di Paleontologia e Stratigrafia* **98**: 137-180.

Ardaens, R. 1978. Géologie de la chaîne du Vardoussia, comparaison avec le massif de Koziakas (Grèce continentale). *Thèse 3ème cycle, Université de Lille,* 234 p.

Armijo, R., Meyer, B. and Hubert, A. 1999. Westward propagation of the North Anatolian fault into the northern Aegean : Timing and kinematics. *Geology* **27**: 267-270.

Aubouin, J., Le Pichon, X., Winterer, E. and Bonneau, M. 1977. Les Hellénides dans l'optique de la tectonique de plaques. In: *Vi Colloquium on the Geology of the Aegean Region,* pp. 1333-1354, Athens.

Bailey, E.B. and McCallien, W.J. 1953. Serpentinites lavas, the Ankara melange and the Anatolian thrust. *Transaction of the Royal Society of Edinburgh* **62**: 403-442.

Bailey, E.B. and McCallien, W.J. 1950. The Ankara Melange and the Anatolian Thrust. *Nature* **166**: 938-940.

Barka, A.A. 1992. The North Anatolian fault zone. *Annales Tectonicae* **VI**: 164-195.

Barnes, P.M. and Korsch, R.J. 1990. Structural analysis of a Middle Cretaceous accretionary wedge, Wairarapa, New Zealand. *New Zealand Journal of Geology and Geophysics* **33**: 355-375.

Baud, A., Jenny, C., Papanikolaou, D., Sideris, C. and Stampfli, G.M. 1990. New observations on the Permian stratigraphy in Greece and geodynamic interpretation. *Bulletin of the Geological Society of Greece* **XXV**.

Baumgartner, P.O. 1984. A Middle Jurassic-Early Cretaceous low-latitude radiolarian zonation based on Unitary Associations and age of Tethyan radiolarites. *Eclogae Geologicae Helvetiae* **77**: 729-837.

Baumgartner, P.O. 1985. *Jurassic sedimentary evolution and nappe emplacement in the Argolis Peninsula (Peloponesus, Greece),* **99**. Mémoires de la Société Helvétique des Sciences Naturelles, Birkhäuser, Basel, 111 pp.

Baumgartner, P.O. 1987. Age and genesis of Tethyan Jurassic radiolarites. *Eclogae Geologicae Helvetiae* **80**: 831-879.

Baumgartner, P.O. 1995. Towards a Mesozoic radiolarian database - Updates of works 1984-1990. In: *Middle Jurassic to Lower Cretaceous Radiolaria of Tethys: Occurences, Systematics, Biochronology* (Ed P. De Wever), Mémoires de Géologie, Lausanne, **23**: 689-700.

Baumgartner, P.O. and Bernouilli, D. 1976. Stratigraphy and Radiolarian Fauna in the Late Jurassic-Early Cretaceous Section near Achladi (Evvoia, Eastern Greece). *Eclogae Geologicae*

Helvetiae. **69**: 601-626.
Baumgartner, P.O., Danelian, T., Dumitrica, P., Gorican, S., Jud, R., Dogherty, L.O., Carter, B., Conti, M., De Wever, P., Kito, N., Marcucci, M., Matsuoka, A., Murchey, B. and Urquart, E. 1993. Middle Jurassic-Early Cretaceous radiolarian biochronology of Tethys: implications for the age of radiolarites in the Hellenides. *Bulletin of the Geological Society of Greece* **XXVIII**: 13-23.
Bergougnan, H. 1975. Affrontement des blocs européen et arabique dans l'Est-Anatolien. *Annales Universitaires A.R.E.R.S* **13**: 47-60.
Bernoulli, D. and Laubscher, H. 1972. The palinspastic problem in the Hellenides. *Eclogae Geologicae Helvetiae* **65**: 107-118.
Bhatia, M.R. 1983. Plate tectonics and geochemical composition of sandstones. *Journal of Geology* **91**: 611-627.
Bhatia, M.R. and Crook, K.A.W. 1986. Trace element characteristics of greywackes and tectonic setting discrimination of sedimentary basins. *Contribution to Mineralogy and Petrology* **92**: 181-193.
Bigazzi, G., Delmoro, A., Innocenti, F., Kyriakopoulos, K., Manetti, P., Papadopoulos, P., Norelli, P. and Magganas, A. 1989. The magmatic intrusive complex of Petrota, West Trace. Age and geodynamic significance. *Geologica Rhodopica* **1**.
Bignot, G., Fleury, J.J. and Gurnet, C. 1971. Sur la stratigraphie du Crétacé supérieur et du flysch en Eubée moyenne (zone pélagonienne, Grèce). *Bulletin de la Société Géologique de France* **(7), XIII**: 484-489.
Bingöl, E., Akyürek, B. and Kormazer, B. 1975. Geology of the Biga Peninsula and some characteristics of the Karakaya blocky series. In: *Congress of Earth Sciences on the occasion of the 50th anniversary of the Turkish Republic* (Ed M.T.v.a. Enstitüsü), pp. 71-77, Ankara.
Birkle, P. and Satır, M. 1992. Petrology, geochemistry and geochronology of a quartz-monzonite intrusion ("Kestanbol-Granite") and their host rocks near Ezine, Biga-Peninsula, NW-Anatolia, Turkey. *Berichte der Deutschen Mineralogischen Gesellschaft* **1**: 29.
Birkle, P. and Satır, M. 1995. Dating, geochemistry and geodynamic significance of the Tertiary magmatism of the Biga-Peninsula (Ezine, NW Turkey). In: *Geology of the Black Sea region* (Ed S. Örçen), General Directorate of Mineral Research and Exploration, Ankara: 171-180.
Blake, M.C.J. and Wentworht, C.M. (Eds) **2000**. *Structure and metamorphism of the Franciscan Complex, Mt. Hamilton area, Northern Carolina*. (Ed R.G. Coleman), *Tectonic studies of Asia and the Pacific Rim,* **International Book Series, 3**. Bellwether Publishing for the Geological Society of America, Columbia, 295-302.
Bonneau, M. 1984. Correlation of the Hellenide nappes in South-east Aegean and their tectonic reconstruction. In: *The Geological Evolution of the Eastern Mediterranean* (Ed A.H.F. Robertson), Geological Society, London, Special Publication **17**: 517-527.
Bonev, N. and Stampfli, G. 2003. New structural and petrologic data on Mesozoic schists in the Rhodope (Bulgaria): geodynamic implications. *Comptes-Rendus Geoscience* 335: 691-699.
Borsi, S., Ferrara, G. and Mercier, J. 1964. Détermination de l'âge des séries métamorphiques du Massif Serbo-Macédonien au Nord-Est de Thessalonique (Grèce) par les méthodes Rb/Sr et K/Ar. *Annales de la Société Géologique du Nord* **LXXXIV**: 223-225.
Boyanov, I. and Budurov, K. 1979. Triassic conodonts in Carbonate Breccia within the Low-grade Metamorphic Rocks of the East Rhodopes. *Geologica Balcanica* **9**: 97-104.
Boyanov, I. and Russeva, M. 1989. Lithostratigraphy and tectonic position of the Mesozoic rocks in the East Rhodopes. *Geologica Rhodopica* **1**: 22-34.

Boyanov, I., Russeva, M. and Dimitrova, E. 1982. First find of Upper Cretaceous foraminifers in East Rhodopes. *Geologica Balcanica* **12**: 20.
Boyanov, I. and Trifonova, E. 1978. New Data on the Age of the Phyllitoid complex from the Eastern Rhodopes. *Geologica Balcanica* **8**: 3-21.
Boynton, W.V. 1984. Geochemistry of the rare earth elements : meteorite studies. In: *Rare earth element geochemistry* (Ed P. Henderson), Elsevier: 63-114.
Bozcu, A. and Yağmurlu, F. 2001. Correlation of sedimentary units in the Western Taurides from the point of petroleum geology. In: *4th International Symposium on Eastern Mediterranean Geology* (Eds Ö. Akıncı, M. Görmüş, M. Kuşcu, R. Karagüzel and M. Bozcu), Isparta, Turkey, pp. 139-148.
Bozkurt, E., Holdsworth, B.K. and Koçyigit, A. 1997. Implication of Jurassic chert identified in the Tokat Complex, northern Turkey. *Geological Magazine* **134**: 91-97.
Bozkurt, E. and Mittwede, S.K. 2001. Introduction to the Geology of Turkey - A Synthesis. *International Geology Review* **43**: 578-594.
Bozkurt, E. and Oberhansli, R. 2001. Menderes Massif (Western Turkey): Structural, metamorphic, and magmatic evolution-a synthesis. *International Journal of Earth Sciences* **89**: 679-708.
Bragin, N.Y. and Tekin, U.K. 1996. Age of radiolarian-chert blocks from the Senonian Ophiolitic Mélange (Ankara, Turkey). *The Island Arc* **5**: 114-122.
Braun, E.v. 1993. The Rhodope Question viewed from Eastern Greece. *Zeit Schrift der Deutschen Geologischen Gesellschaft* **144**: 406-418.
Brinkmann, R. 1966. Geotektonische Gliederung von Westanatolian. *Neues Jahrbuch: Geologisch, Paläontologish Monatshefte* **10**: 603-618.
Brinkmann, R. 1976. *Geology of Turkey*. Elsevier, 158 p.
Brinkmann, R., Gümüs, H., Plumhoff, F. and Salah, A.A. 1977. Höhere Oberfreide in Nordwest-Anatolia und Thrakien. *Neues Jahrbuch: Geologisch, Paläontologish Abhanlungen* **154**: 1-20.
Brown, D. and Spadea, P. 1999. Processes of forearc and accretionary complex formation during arc-continent collision in the southern Ural Mountains. *Geology* **27**: 649-652.
Bullard, E.C., Everett, J.E. and Smith, A.G. 1965. The fit of the continents around Atlantic. *Philosophical Transactions of the Royal Society of London* **A258**: 41-51.
Burchfiel, C.B., Nakov, R., Tzankov, T. and Royden, L.H. 2000. Cenozoic extension in Bulgaria and northern Greece : the northern part of the Aegean extensional regime. In: *Tectonic and magmatism in Turkey and the Surrounding area* (Ed J.D.A. Piper), Geological Society, London, Special Publications **173**: 325-352.
Burg, J.P., Ricou, L.E., Ivanov, Z., Godfriaux, I., Dimov, D. and Klain, L. 1996. Syn-metamorphic nappe complex in the Rhodope Massif. Structure and kinematics. *Terra Nova* **8**: 6 - 15.
Calon, T., Buchanan, C., Burden, E., Feltham, G. and Young, J. 2002. Stratigraphy and structure of sedimentary rocks in the Humber Arm Allochton, southwestern Bay of Islands, Newfoundland. *Current Research - Newfoundlland* **Geological Survey Branch**: 35-45.
Çapan, U. and Buket, E. 1975. Aktepe-Gökdere bölgesisin jeolojisi ve ofiyolitli melanj. *Bulletin of the Geological Society of Turkey* **18**: 11-16.
Catani, F. and Vannucchi, P. 1998. A fractal approach to the structural analysis of melanges. *Annales Geophysicae* **16**: 341.
Celet, P. 1962. Contribution a l'étude géologique du Parnasse-Kiona et d'une partie des regions meridionales de la Grèce continentale. *Annales Géologiques des Pays Helléniques* **7**:

1-358.
Celet, P. 1979. Les bordures de la zone du Parnasse (Grèce). Evolution Paléogéographique au Mésozoique et caractères structuraux. In: *6th Colloquium on the Geology of the Aegean Region (Athens, 1977)* (Ed G. Kallergis), **2**, Institute of Geological and Mining Research, Athens, pp. 725-40.
Celet, P. and Ferrière, J. 1978. Les Hellénides internes: Le Pélagonien. *Eclogae Geologicae Helvetiae.* **71**: 467-495.
Chan, W.-S. 1997. Mesoscopic structures developed in the Lichi Melange during the arc continent collision in the Taiwan region. *Journal of the Geological Society of China* **40**: 415-434.
Channell, J.E.T. and Kozur, H.W. 1997. How many oceans ? Meliata, Vardar and Pindos oceans in Mesozoic Alpine paleogeography. *Geology* **25**: 183-186.
Channell, J.E.T., Tüysüz, O., Bektaş, O. and Sengör, A.M.C. 1996. Jurassic-Cretaceous paleomagnetism and paleogeography of the Pontides (Turkey). *Tectonics* **15**: 201-212.
Chatalov, G.A. 1988. Recent development in the geology of the Strandzha Zone in Bulgaria. *Bulletin of the Technical University of Istanbul* **41**: 433-465.
Cioflica, G., Lupu, M., Nicolae, I. and Vlad, S. 1980. Alpine ophiolites of Romania: tectonic setting, magmatism and metallogenesis. *An. Inst. Geol. Geofiz.* **56**: 79-96.
Clift, P.D. and Dixon, J.E. 1998. Jurassic ridge collapse, subduction initiation and ophiolite obduction in the southern Greek Tethys. *Eclogae Geologicae Helvetiae.* **91**: 123-138.
Collins, A.S. and Roberston, A.H.F. 1998. Processes of Late Cretaceous to Late Miocene episodic thrust-sheet translation in the Lycian Taurides, SW Turkey. *Journal of the Geological Society, London* **155**: 759-72.
Collins, A.S. and Robertson, A.H.F. 1997. Lycian melange, southwestern : An emplaced Late Cretaceous accretionary complex. *Geology* **25**: 255-258.
Cousineau, P.A. 1998. Large-scale liquefaction and fluidization in the Cap Chat Melange, Quebec, Appalachians. *Canadian Journal of Earth Sciences* **35**: 1408-1422.
Cullers, R.L., Barrett, T., Carlson, R. and Robinson, B. 1987. Rare-earth elements and mineralogic changes in Holocene soils and stream sediments: a case study in the Wet Mountains, Colorado, U.S.A. *Chemical Geology* **63**.
Cullers, R.L., Basu, A. and Suttner, L.S. 1988. Geochemical signature of provenance in sand-size material in soils and stream sediments near the Tobacco Root batholith, Montana, U.S.A. *Chemical Geology* **70**: 335-348.
Danelian, T. and Roberston, A.H.F. 2001. Neotethyan evolution of eastern Greece (Pagondas Melange, Evia Island) infereed from radiolarian biostratigraphy and the geochemistry of associated extrusive rocks. *Geological Magazine* **138**: 345-363.
Danelian, T. and Roberstson, A.H.F. 1995. Radiolarian evidence of Middle Jurassic collapse of the pelagonian carbonate platform (Kallidromon Mountains, Central Greece). *Geological Society of Greece, Special Publication* **4**: 175-180.
Danelian, T. and Robertson, A.H.F. 1998. Palaeogeographic implications of the age of radiolarian-rich sediments in Beotia (Greece). *Bulletin of the Geological Society of Greece* **XXXII/2**: 21-29.
Danelian, T., Robertson, A.H.F. and Dimitriadis, S. 1996. Age significance of radiolarian sediments within basic extrusives of the marginal basin Guevgueli Ophiolite (northern Greece). *Geological Magazine* **133**: 127-136.
De Bono, A. 1998. *Pelagonian margins in Central Evia Island (Greece). Stratigraphy and geodynamic evolution*. http://www-sst.unil.ch/publications/pdf/phd_debono.pdf, Université de Lausanne, Unpublished Ph-D Thesis.

De Bono, A., Martini, R., Zaninetti, L., Hirsch, F., Stampfli, G.M. and Vavassis, I. 2001. Permo-Triassic stratigraphy of the pelagonian zone in central Evia island (Greece). *Eclogae Geologicae Helveticae* **94**: 289-311.
De Bono, A., Vavassis, I., Stampfli, G.M. and Bartolini, A.C. 2002. Late Paleozoic-Mesozoic evolution of the Pelagonian internal margin (Greece). *Eclogae Geologicae Helvetiae,* submitted.
De Wever, P. and Cordey, F. 1986. Datation par les Radiolaires de la Formation des Radiolarites s.s. de la Serie du Pinde-Olonos (Grèce): Bajocien (?)-Tithonique. *Marine Micropaleontology* **11**: 113-127.
De Wever, P. and Origlia-Devos, I. 1982. Datations nouvelles par les radiolaires de la serie des radiolarites S.P. du Pinde-Olonos (Grece) (New radiolarian agesof the S.P. radiolarite series of Pindus-Olonos, Greece). *Comptes Rendus des séances de l'Academie des Sciences, Série 2: Mécanique, Physique, Chimie, Sciences de la Terre, Sciences de l'Univers* **294**: 399-404.
Degnan, P.J. and Robertson, A.H.F. 1990. Tectonic and sedimentary evolution of the Western Pindos Ocean: N. W. Peloponnese, Greece. In: *5th Congr. Geol. Soc. Greece., Bulletin of the Geological Society of Greece.*, **XXV**, pp. 263-273, Thessaloniki.
Dercourt, J., Ricou, L.-E. and Vrielink, B. (Eds) **1993**. *Atlas Tethys-Palaeoenvironmental maps,* Paris.
Dilek, Y., Thy, P., Hacker, B. and Sidsel, G. 1999. Structure and petrology of Tauride ophiolites and mafic dike intrusions (Turkey): Implications for the Neotethyan ocean. *GSA Bulletin* **111**: 1192-1216.
Dimitrijevic, N.M., Dimitrijevic, M.D., Karamata, S., Sudar, M., Kocacs, S., Dosztaly, L., Gulasci, Z. and Pelikan, P. 2000. Olistostrome/melanges in Yugoslavia and Hungary ; an overview of the problems and preliminary comparison. *Geologica Carpathica* **50**: 147-149.
Dinter, D.A. 1998. Late Cenozoic extension of the Alpine collisional orogen, northeastern Greece: origin of the north Aegean basin. *GSA Bulletin* **110**: 1208-1230.
Dixon, J.E. and Dimitriadis, S. 1984. Metamorphosed ophiolitic rocks from the Serbo-Macedonian Massif, near Lake Volvi, North-east Greece. (Ed A.H.F. Robertson), Geological Society, London, Special Publication **17**: 603-618.
Egeran, N. 1947. *Tectonique de la Turquie,* Nancy, 197 pp.
Ercan, T., Satır, M., Steinitz, G., Dora, A., Sarifakioglu, E., Adis, C., Walter, H.-J. and Yildirim, T. 1995. Biga yarımadası ile Gökçeada, Bozcaada ve Tavsan adalarındaki (KB Anadolu) Tersiyer volkanizmasının özellikleri (in Turkish). *MTA Dergisi* **117**: 55-86.
Favre, P. and Stampfli, G. 1992. From rifting to passive margin: the Red Sea, the central Atlantic and the Alpine Tethys as examples. *Tectonophysics* **215**: 69-97.
Ferrière, J. 1982. Paléogéographie et tectoniques superposées dans les Hellenides internes: le massifs de l'Othrys et du Pelion (Grèce continentale). *Société Géologique du Nord, Publication* **8, 1**: 1-493.
Ferrière, J. 1985. Nature and developpement des ophiolites helleniques du secteur Othrys et du Pelion (Grece continentale). *Ofioliti* **10**: 225-278.
Fleury, J.-J. 1980. Les zones de Gavrovo-Tripolitza et du Pinde-Olonos (Grèce continentale et Péloponèse du nord). Evolution d'une plate-forme et d'un bassin dans leur cadre alpin. *Société Géologique du Nord, Publication* **4**: 1-473.
Flores, G. 1955. Discussion. *4th World Petroleum Conference* **Sec I/A/2**: 121-122.
Floyd, P.A. 1993. Geochemical discrimination and petrogenesis of alkalik basalt sequences in part of the Ankara melange, central Turkey. *Journal of the Geological Society, London* **150**: 541-550.

Floyd, P.A., Göncuöglu, M.C., Winchester, J.A. and Yalınız, M.K. 2000. Geochemical character and tectonic environment of Neotethyan ophiolite fragments and metabasites in the Central Anatolian Crystalline Complex. In: *Tectonics and magmatism in Turkey and surrounding area* (Ed J.D.A. Piper), Geological Society, London, Special Publication **173**: 183-202.

Frech, F. 1916. *Geologie Kleinasiens im Bereich der Bagdadbahn*, **68**. Zeitschr. Deutsch. Geol. Ges., Berlin.

Friedmann, S.J. and Burbank, D.W. 1995. Rift basins and supradetachment basins: intracontinental extensional end members. *Basin Research* **7**: 109-127.

Fytikas, M., Giuliani, O., Innocenti, F., Maarinelli, G. and Mazzuoli, R. 1976. Geochronological data on recent magmatism of the Aegean Sea. *Tectonophysics* **31**: 29-34.

Gansser, A. 1955. New aspects of the geology of Central Iran, **Sec. I/A/5**, pp. 279-298. Proceedings of the 4th World Petroleum Conference.

Gansser, A. 1974. The ophiolite melange, a world-wide problem on Tethyan examples. *Eclogae Geologicae Helveticae*. **67**: 469-507.

Georgiev, G., Dabovski, C. and Stanisheva-Vassileva, G. 2001. East Srednogorie-Balkan rift Zone. In: *Peri-Tethys Memoir 6 : Peri-Tethyan Rift/Wrench Basins and Passive Margins* (Ed S. Crasquin-Soleau), Mémoires du Muséum National d'Histoire Naturelle, Paris, **186**: 259-293.

Godfriaux, I. 1968. Etude géologique de la région de l'Olympe (Grèce). *Annales Géologique des Pays Helléniques* **19**: 1-281.

Göncuöglu, M.C. 1986. Geochronological data from the southern part (Niğde area) of the Central Anatolian Massif. *Bulletin of the Mineral Research and Exploration* **105/106**: 83-96.

Göncüoğlu, M.C., Dirik, K. and Kozlu, H. 1996-1997. Pre-Alpine and Alpine terranes in Turkey : explanatory notes to the terrane map of Turkey. *Annales Géologiques des Pays Helléniques* **37**.

Göncuöğlu, M.C., Turhan, N., Şentürk, K., Özcan, A., Uysal, Ş. and Yalınız, K. 2000. A geotraverse across northwestern Turkey : tectonic units of the Central Sakarya region and theur tectonic evolution. In: *Tectonics and magmatism in Turkey and the Surrounding Area* (Ed J.D.A. Piper), Geological Society Special Publications, London, **173**: 139-161.

Görür, N., Şengör, A.M.C., Akkok, R. and Yılmaz, Y. 1983. Sedimentological data regarding the opening of the northern branch of Neotethys in the Pontides (in Turkish). *Türkiye Jeoloji Kurumu Bülteni* **26**.

Görür, N., Monod, O., Okay, A.I., Şengör, A.M.C., Tüysüz, O., Yığıtbaş, E., Sakinç, M. and Akkok, R. 1997. Paleogeographic and tectonic position of the Carboniferous rocks of the western Pontides (Turkey) in the frame of the Variscan belt. *Bulletin de la Société géologique de France* **168**: 197-205.

Görür, N. and Okay, A.I. 1996. A fore-Arc origin for the Thrace Basin, NW Turkey. *Geologische Rundschau* **85**: 662-668.

Görür, N., Oktay, F.Y., Seymen, I. and Şengör, A.M.C. 1984. Paleotectonic evolution of the Tuzgölü basin complex, Central Turkey : sedimentary record of a Neo-Tethyan closure. In: *The geological evolution of the Eastern Mediterranean* (Ed A.H.F. Roberstson), Geological Society of London, Special Publication, London, **17**: 467-482.

Gözler, M.Z. 1986. Geologic and petrographic investigation of Mihli dere valley (Kazdağ, northwestern Turkey) (in Turkish). *Bulletin of the Geological Society of Turkey* **29**: 133-142.

Gözler, M.Z., Ergül, E., Akçaören, F., Genç, S.C., Akat, Ü. and Acar, Ş. 1984. Çanakkale Boğazı doğusu-Marmara Denizi güneyi-Bandırma-Balıkesir-Edremit ve Ege Denizi

arasındaki alanın jeolojisi ve kompilasyonu. *MTA Report*.
Gözübol, A.M. 1980. Geological investigation of the Mudurnu-Dokurcun-Abant area (Bolu Province) and the structural behaviour of the North Anatolian Transform Fault. *Istanbul Üniversitesi Fen Fakültesi Mecmuası* **45**: 9-34.
Grant, R.E., Nestell, M.K., Baud, A. and Jenny, C. 1991. Permian Stratigraphy of Hydra Island, Greece. *Palaios* **6**: 479-497.
Greber, E. 1997. Stratigraphic evolution and tectonics in an area of high seismicity : Akyazı/ Adapazarı (Pontides, Northwestern Turkey). In: *Active Tectonics of Northwestern Anatolia - The Marmara Poly-Project* (Ed M. Pfister), vdf, Zürich.
Greenly, E. 1919. The geology of Anglesey. *Great Britain Geological Survey Memoir* **1**, 980 pp.
Guangfu, Z., Liwei, H. and Xianke, Y. 1994. Charactersitics of the Garze-Litang ophiolite melange zone ant its tectonic implications. *Acta Geologica Sichuan* **14**: 17-24.
Guernet, C. 1975. Sur l' existence en Eubée moyenne d'une nappe constituée principalement de roches vertes et de leur couverture mésozoique. *Extrait des Annales de la Société Géologique du Nord* **XCV**: 59-66.
Güleç, N. 1994. Rb-Sr isotope data from the Ağaçören granitoid (east of Tuz Gölü): geochronological and genetic implications. *Turkish Journal of Earth Sciences* **3**: 39-43.
Gutnic, M., Monod, O., Poisson, A. and Dumont, J.F. 1979. Géologie des Taurides occidentales (Turquie). *Mémoire de la Société Géologique de France* **137 / LVIII**: 109.
Halamic, J., Gorican, S., Slovenec, D. and Kolar-Jurkovsek, T. 1999. A Middle Jurassic Radiolarite-Clastic Succession from the Medvednica Mt. (NW Croatia). *Geologica Croatica* **52**: 29-57.
Harrington, D.F. and Cloos, M. 2001. Deformation of blocks and matrix in Franciscan melange, San Simeon, California ; implication for melange genesis. *Abstract with programs - Geological Society of America* **33**: 25.
Harris, N.B., Kelley, S. and Okay, A.I. 1994. Post-collision magmatism and tectonics in northwest Anatolia. *Contribution to Mineralogy and Petrology* **117**: 241-252.
Harris, R. 2000. Melange genesis in the Banda Arc subduction-collision transition, Indonesia. *AAPG Bulletin* **84**: 1434.
Hasebe, N., Tagami, T. and Nishimura, S. 1997. Melange-forming processes in the development of an accretionary prism ; evidence from fission track geochronology. *Journal of Geophysical Research, B* **102**: 7659-7672.
Hatzipanagiotou, K. and Pe-Piper, G. 1995. Ophiolitic and sub-ophiolitic metamorphic rocks of the Vatera area, southern Lesbos (Greece): geochemistry and geochronology. *Ofioliti* **20**: 17-29.
Hsü, K.J. 1977. Tectonic evolution of the Mediterranean basins. The eastern Mediterranean. In: *The Eastern Mediterranean* (Ed F.G. Stehli), *The Ocean Basins and Margins*, Plenum Press, New-York, **4A**.
Inci, U. 1984. The stratigraphy and organic properties of Demirci and Burhaniye bituminous shales (in Turkish). *Bulletin of the Geological Congress of Turkey* **5**: 27-40.
Jaboyedoff, M. and Thélin, P. 1996. New data on low metamorphism in the Briançonnais domain of the Préalpes, Western Switzerland. *European Journal of Mineralogy* **8**: 577-592.
Jacobi, R.D. 1984. Modern, submarine sediment slides and their implications for melange and the Dunnage Formation in the north-central Newfoundland. In: *Melanges : Their Nature, Origin and Significance* (Ed L.A. Raymond), Geological Society of America, Boulder, Colorado, **198**: 81-102.

Jolivet, L. and Goffé, B. 2000. Les dômes métamorphiques extensifs dans les chaînes de montagne. Extension syn-orogenique et post-orogenique. *Comptes-Rendus de l'Académie des Sciences de Paris* **330**: 739-751.

Jolivet, L. and Patriat, M. 1999. Ductile extension and the formation of the Aegean Sea. In: Mediterranean Basins: *Tertiary extension within the Alpine Orogen* (Eds Durand, B, Jolivet, L., Horvath, F., Seranne, M.), Geological Society, London, Special Publication **156**: 427-456.

Kaaden, G.v.d. 1959. Age relations of magmatic activity and of metamorphic processes in the northwestern part of Anatolia - Turkey. *Bulletin of the Mineral Research Exploration Institute of Turkey* **52**: 15-33.

Kalafatçıoğlu, A. 1963. Geology around Ezine and Bozcaada, the age of the limestones and serpentinites. *Bulletin of the Mineral Research and Exploration Institute of Turkey* **60**: 61-70.

Karacık, Z. and Yılmaz, Y. 1998. Geology of the ignimbrites and the associated volcano-plutonic complex of the Ezine area, northwest Anatolia. *Journal of Volcanology and Geothermal Research* **85:** 251-264.

Kaya, O. 1991. Stratigraphy of the Pre-Jurassic sedimentary rocks of the western parts of Turkey; type area study and tectonic considerations. *Newsletters on stratigraphy* **23**: 123-140.

Kelepertsis, A. and Velitzelos, E. 1992. Oligocene Swamp Sediments of Lesvos Island, Greece (Geochemistry and Mineralogy). *Facies* **27**: 113-118.

Kerey, I.E., Kelling, G. and Wagner, R.H. 1986. An outline stratigraphy and paleobotanical records from the middle Carboniferous rocks of north-west Turkey. *Annales de la Société Géologique du Nord* **55**: 203-216.

Kilias, A., Falalakis, G. and Mountrakis, D. 1999. Cretaceous-Tertiary structures and kinematics of the Serbomacedonian metamorphic rocks and their relation to the exhumation of the Hellenic Hinterland (Macedonia, Greece). *International Journal of Earth Sciences* **88**: 513-531.

Kober, L. 1929. Beiträge zur Geologie von Attika. *Sitz. Akad. Wiss. Wien* **138**: 299-327.

Koç, Ş. and Kadioğlu, Y.K. 1996. Mineralogy, geochemistry and precious metal content of Karacakaya (Yunsemre-Eskişehir) listwaenites. *Ofioliti* **21**: 125-130.

Kockel, F. and Walther, H.W. 1965. Die Strimonlimie als Grenze zwischen Serbo-Mazedonischen und Rila Rhodope Massiv in Ost Mazedonien. *Geologische Jahrbuch.* **83**: 575-602.

Koçyigit, A. 1991. An example of an accretionary forearc basin from northern Central Anatolia and its implications for the history of subduction of Neo-Tethys in Turkey. *Geological Society of America Bulletin* **103**: 22-36.

Koçyigit, A., Yusufoğlu, H. and Bozkurt, E. 1999. Evidence from the Gediz graben for episodic two-stages extension in western Turkey. *Journal of the Geological Society of London* **156**: 605-616.

Kossmat, F. 1924. Geologie der Zentralen Baklanhalbinsel. *In WILSER et al., ed., Die Kriegsshausplatze 1914-1918 geologisch dargestellt, Berlin, Borntraeger.*

Kozur, H. 1991. The evolution of the Meliata-Hallstatt ocean and its significance for the early evolution of the Eastern Alps and Western Carpathians. *Palaeogeography, Palaeoclimatology, Palaeoecology* **87:** 109-135.

Kozur, H. and Mock, R. 1996. New paleogeographic and tectonic interpretations in the Slovakian Carpathians and their implications for correlations with the Eastern Alps. Part I : Central Western Carpathians. *Mineralia Slovaca* **26**: 151-174.

Kozur, H. and Mock, R. 1997. New paleogeographic and tectonic interpretations in the Slovakian Carpathians and their implications for correlations with the Eastern Alps. Part II

: Inner Western Carpathians. *Mineralia Slovaca* **29**: 164-209.
Krohe, A. and Mposkos, E. 2002. Multiple generations of extensional detachments in the Rhodope Mountains (northern Greece): evidence of episodic exhumation of high-pressure rocks. In: *The timing and location of Major Ore Deposits in a Evolving Orogen* (Ed A. Von Quadt), Geological Society, London, Special Publications **206**: 151-178.
Kusky, T.M. and Bradley, D.C. 1999. Kinematic analysis of melange fabrics : examples and applications from the McHugh Complex. Kenai Peninsula, Alaska. *Journal of Structural Geology* **21**: 1773-1796.
Kusky, T.M., Bradley, D.C., Haeussler, P.J. and Karl, S. 1997. Controls on accretion of flysh and mélange belts at convergent margins : Evidence from the Chugach Bay thrust and Iceworm mélange, Chugach accretionary wedge, Alaska. *Tectonics* **16**: 855-878.
Leven, E.J. and Okay, A.I. 1996. Foraminifera from the exotic Permo-Carboniferous limestone blocks in the Karakaya Complex, northwest Turkey. *Rivista italiana di Paleontologia e Stratigrafia* **102**: 139-174.
Liati, A., Gebauer, D. and Wysoczanski, R. 2002. U-Pb SHRIMP-dating of zircon domains from UHP garnet-rich mafic rocks and late pegmatoids in the Rhodope zone (N Greece); evidence for Early Cretaceous crystallization and Late Cretaceous metamorphism. *Chemical Geology* **184**: 281-299.
Lips, A.L.W. 1998. *Temporal Constraints on the Kinematics of the Destabilization of an Orogen - Syn- to Post-Orogenic Extensional Collapse of the Northern Aegean Region*, PhD Thesis, Vrije University, Amsterdam.
Lips, A.L.W., White, S.H. and Wijbrans, J.R. 2000. Middle-Late Alpine thermotectonic evolution of the southern Rhodope Massif, Greece. *Geodinamica Acta* **13**: 281-292.
Lytwyn, J.N. and Casey, J.F. 1995. The geochemistry of postkinematic mafic dike swarms and subophiolitic metabasites, Pozantı-Karşantı ophiolite, Turkey: evidence for ridge subduction. *Geological Society of America Bulletin* **107**: 830-850.
Magganas, A., Sideris, C. and Kokkinakis, A. 1991. Marginal Basin-Volcanic Arc Origin of Metabasic Rocks of the Circum-Rhodope Belt, Thrace, Greece. *Mineralogy and Petrology* **44**: 235-252.
Mart, Y. and Woodside, Y. 1994. Preface: Tectonics of the Eastern Mediterranean. *Tectonophysics* **234**: 1-3.
McDonough, W.F. and Sun, S. 1995. The composition of the Earth. *Chemical Geology* **120**: 223-253.
McLennan, S.M. 1989. Rare earth elements in sedimentary rocks: influence of provenance and sedimentary processes. In: *Geochemistry and mineralogy of rare earth elements* (Ed G.A. McKay), *Review in Mineralogy*, **21**: 169-200.
Mekik, F.A. 2000. Early Cretaceous Pantanelliidae (Radiolaria) from Northwest Turkey. *Micropaleontology* **46**: 1-30.
Mello, J., Reichwalder, P. and Vozarova, A. 1998. Bôrka Nappe : high-pressure relic from the subduction-accretion prism of the Meliata ocean (Inner Western Carpathians, Slovakia). *Slovak Geological Magazine* **4**: 261-273.
Mercier, J. 1966. Paléogéographie, orogénèse, métamorphisme et magmatisme des zones internes des Hellenides en Macédonie (Grèce): vue d'ensemble. *Bulletin de la Société Géologique de France* **8**: 1020-1049.
Mercier, J. 1968. Etude géologique des zones internes des Hellénides en Macédoine centrale (Grèce). *Annales Géologiques des Pays Helléniques* **20**: 1-792.
Mercier, J. and Vergely, P. 1972. Les mélanges colorés ("Coloured-Mélanges") de la zone

d'Almopias (Macédoine, Grèce). *Bulletin de la Société Géologique de France* **2**: 70-73.
Meschede, M., Zweigel, P., Frisch, W. and Völker, D. 1999. Mélange formation by subduction erosion : the case of the mélange in southern Costa Rica. *Terra Nova* **11**: 141-148.
Middlemost, A.E.K. 1989. Iron oxidation ratio, norms and the classification of volcanic rocks. *Chemical Geology* **77**: 19-26.
Monié, P., Caby, R. and Arthaud, R.H. 1997. The Neoproterozoic Brasiliano Orogeny in Northeast Brazil; (super 40) Ar/ (super 39) Ar and petrostructural data from Ceara. *Precambrian Research* **81**: 241-264.
Monod, O., Okay, A., Maluski, H., Monié, P. and Akkök, R. 1996. Schistes bleus du Trias supérieur en Turquie du NW : comment s'est fermée la paléeo-Tethys ? In: *16 ème Reunion des Sciences de la Terre* (Ed S.G. Fr), Orleans.
Monod, O. and Okay, A.I. 1999. Late Triassic Paleo-Tethyan subduction : evidence from Triassic blueschists in NW Turkey. In: *EUG 10*. Terra Nova abstract **11**, Strasbourg, France, pp. 880.
Mposkos, E. and Krohe, A. 2000. Petrological and structural evolution of continental high pressure (HP) metamorphic rocks in the Alpine Rhodope Domain (N. Greece). In: *Third International Conference on the Geology of the Eastern Mediterranean* (Ed J. Malpas), Nicosia, Cyprus, pp. 221-232.
Needham, D.T. 1995. Mechanism of mélange formation : examples from SW Japan and southern Scotland. *Journal of structural Geology* **17**: 971-985.
Nicolae, I. and Seghedi, A. 1996. Lower Triassic basic dyke swarm in North Dobrogea. *Romanian Journal of Petrology* **77**: 31-40.
Norman, T.N. 1984. The role of the Ankara Melange in the development of Anatolia (Turkey). In: *The geological evolution of the Eastern Mediterranean* (Ed A.H.F. Roberstson), Geological Society, London, Special Publication **17**: 119-146.
Norman, T.N. 1993. Remobilization of two mélanges in Central Anatolia. *Geological Journal* **28**: 267-275.
Ohmori, K., Taira, A., Tokuyama, H., Sakagushi, A., Okamura, M. and Aihara, A. 1997. Paleothermal structure of the Shimanto accretionary prism, Shikoku, Japan : Role of an out-of-sequence thrust. *Geology* **25**: 327-330.
Okay, A., Siyako, M. and Bürkan, K.A. 1991. Geology and tectonic evolution of the Biga Peninsula, northwest Turkey. *Bulletin Technique de l'Université d'Istanbul* **44**: 191-255.
Okay, A.I. 1984. Distribution and characteristics of the northwest Turkish blueschists. In: *The Geological of the eastern Mediterranean* (Ed A.H.F. Roberston), Geological Society, London, Special Publication **17:** 455-466.
Okay, A.I. 1989. Tectonic units and sutures in the Pontides, northern Turkey. In: *Tectonic evolution of Tethyan region* (Ed A.M.C. Şengör), Kluwer Academic Publications, Dordrecht: 109-115.
Okay, A.I. 2000. Was the Late Triassic orogeny in Turkey caused by the collision of an oceanic plateau ? In: *Tectonics and Magmatism in Turkey and the Surrounding area.* (Ed J.D.A. Piper), Geological Society, London, Special Publications., London, **173**: 25-41.
Okay, A.I. 2001. The tectonics of the Strandja Massif: late Variscan and mid-Mesozoic deformation and metamorphism in the northern Aegean. *International Journal of Earth Sciences* **90**: 217-233.
Okay, A.I., Demirbağ, E., Kurt, H., Okay, N. and Kusçu, I. 1999. An Active, deep marine strike-slip basin along the North Anatolian fault in Turkey. *Tectonics* **18**: 129-147.

Okay, A.I. and Şahintürk, Ö. 1997. Geology of the Eastern Pontides. In: *Regional and petroleum geology of the Black Sea and surrounding region* (Ed A.G. Robinson), AAPG, Tulsa, **68**: 291-311.
Okay, A.I., Şengör, A.M.C. and Görür, N. 1994. Kinematic history of the opening of the Black Sea and its effect on the surrounding regions. *Geology* **22**: 267-270.
Okay, A.I. and Kelley, S.P. 1994. Tectonic setting, petrology and geochronology of jadeite+glaucophane and chloritoid+glaucophane schists from northwest Turkey. *Journal of metamorphic geology* **12**: 455-466.
Okay, A.I., Monod, O. and Monié, P. 2001a. Triassic blueschists and eclogites from northwest Turkey: vestiges of Paleotethyan subduction. In: *Fourth International Turkish Geology Symposium*, Adana-Turkey.
Okay, A.I. and Özgül, N. 1984. HP/LT metamorphism and the structure of the Alanya Massif, southern Turkey. In: *The geological evolution of the eastern Mediterranean* (Ed A.H.F. Robertson), Geological Society, London, Special Publication **17**: 429-439.
Okay, A.I. and Satır, M. 2000a. Coeval plutonism and metamorphism in a latest Oligocene metamorphic core complex in northwest Turkey. *Geological magazine* **137**: 495-516.
Okay, A.I. and Satır, M. 2000b. Upper Cretaceous Eclogite-Facies Metamorphic Rocks from the Biga Peninsula, Northwest Turkey. *Turkish Journal of Earth Sciences* **9**: 47-56.
Okay, A.I., Satır, M., Maluski, H., Siyako, M., Monie, P., Metzger, R. and Akyüz, S. 1996. Paleo- and Neo-Tethyan events in northwestern Turkey: geologic and geochronologic constraints. In: *The tectonic evolution of Asia* (Ed T.M. Harrison), Cambridge University Press: 420-441.
Okay, A.I. and Sıyako, M. 1993. The new position of the Izmir-Ankara Neotethyan suture between Izmir and Balıkesir (in Turkish). In: *Tectonics and Hydrocarbon Potential of Anatolia and Surrounding Regions. Ozan Sungurlu symposium* (Ed S. Turgut), Ankara, Turkey, pp. 333-355
Okay, A.I. and Tansel, I. 1992. New data on the upper age of the Intra-Pontide ocean from north of **Ş**arkoy (Thrace). *Mineral Research Exploration Bulletin* **114**: 23-26.
Okay, A.I., Tansel, I. and Tüysüz, O. 2001b. Obduction, subduction and collision as reflected in the Upper Cretaceous-Lower Eocene sedimentary record of western Turkey. *Geological Magazine* **138**: 117-142.
Okay, A.I. and Tüyzüs, O. 1999. Tethyan Sutures of northern Turkey. In: *Mediterranean Basins: Tertiary extension within the Alpine Orogen* (Eds Durand, B, Jolivet, L., Horvath, F., Seranne, M.), Geological Society, London, Special Publication **156**: 475-515.
Okay, I.O. and Monié, P. 1997. Early Mesozoic subduction zone in the Eastern Mediterranean: evidence from Triassic eclogite in northwest Turkey. *Geology* **25**: 595-598.
Önen, A.P. and Hall, R. 1993. Ophiolites and related metamorphic rocks from the Kütahya region, north-west Turkey. *Geological Journal* **28**: 399-412.
Önen, P. & Hall, R. 2000. Sub-ophiolite metamorphic rocks from NW Anatolia, Turkey. *Journal of Metamorphic Geology* **18**(5), 483-495.
Özkaya, I. 1982. Origin and tectonic setting of some of the melange units in Turkey. *Journal of Geology* **90**: 269-278.
Page, B.M. and Suppe, J. 1981. The Pliocene Lichi melange of Taïwan : its plate-tectonic and olistostromal origin. *American Journal of Science* **281**: 193-227.
Pamic, J. 2002. The Sava-Vardar Zone of the Dinarides and Hellenides versus the Vardar Ocean. *Eclogae Geologicae Helvetiae* **95**: 99-113.
Papadopoulos, P., Arvanitidis, N. and Zanas, I. 1989. Some preliminary geological aspects

on the Makri Unit (Phyllites series), Peri-Rhodope Zone. *Geologica Rhodopica* 34-42.
Papanikolaou, D. 1984. The three metamorphic belts of the Hellenides: a review and a kinematic interpretation. *Geological Society, London, Special Publication* **17**: 551-561.
Papanikolaou, D. 1996-97. The Tectonostratigraphic Terranes of the Hellenides. In: *IGCP project No 276, Terrane maps and Terrane descriptions* (Ed D. Papanikolaou), *Annales Géologiques des Pays Helléniques*, Institute of Geology, Athens, **37**: 495-514.
Papanikolaou, D.J. 1989. Geotectonic map of Greece IGCP 276 edn. *Geological Society of Greece, Special Publication* 1, Athens.
Paréjas, E. 1940. La tectonique transversale de la Turquie. *Revue de la faculté des Sciences de l'Université d'Istanbul* **V**: 133-241.
Parlak, O. and Delaloye, M. 1999. Precise $^{40}Ar/^{39}Ar$ ages from the metamorphic sole of the Mersin ophiolite (southern Turkey). *Tectonophysics* **301**: 145-158.
Parlak, O., Delaloye, M. and Bingöl, E. 1995. Origin of sub-ophiolitic metamorphic rocks beneath the Mersin ophiolite, Southern Turkey. *Ofioliti* **20**: 97-110.
Parlak, O., Höck, V. and Delaloye, M. 2000. Supra-subduction zone origin of the Pozantı-Karşantı ophiolite (southern Turkey) deduced from whole-rock and mineral chemistry of the gabbros cumulates. In: *Tectonism and magmatism in Turkey and surrounding area* (Ed J.D.A. Piper), Geological Society, London, Special Publication **173**: 219-234.
Parrot, J.F. and Guernet, C. 1972. Le cortège ophiolitique de l'Eubée moyenne (Grèce): étude pétrographique des formations volcaniques et des roches métamorphiques associées dans les Monts Kandilis aux radiolarites. *Cahiers de l'ORSTOM, série Géologiques* **IV**: 153-161.
Pe-Piper, G. 1998. The nature of Triassic extension-related magmatism in Greece: evidence from Nd and Pb isotope geochemistry. *Geological Magazine* **135**: 331-348.
Pearce, J.A. 1983. Role of the sub-continental lithosphere in the magma genesis at active continental margins. In: *Continental basalts and mantle xenoliths* (Ed M.J. Norry), Nantwich, Shiva: 230-249.
Pearce, J.A. and Cann, J.R. 1973. Tectonic setting of basic volcanic rocks determined using trace element analyses. *Earth and Planetary Science Letters* **19**: 290-300.
Pearce, J.A., Harris, N.B.W. and Tindle, A.G. 1984. Trace Element Discrimination Diagrams for the Tectonic Interpretation of Granitic Rocks. *Journal of Petrology* **25**: 956-983.
Pfister, M., Rybach, L. and Şimşek, Ş. 1997. Geothermal reconnaissance of the Marmara sea region. In: *ActiveTectonics of Northwestern Anatolia - The Marmara Poly-Project* (Ed M. Pfister), vdf, Zürich: 504-535.
Philippson, A. 1898. La tectonique de l'Egeide. *Annales de Géographie, Paris.* 112-141.
Pickett, E.A. and Robertson, A.H.F. 1996. Formation of the late Paleozoic-Early Mesozoic Karakaya complex and related ophiolites in NW Turkey by Paleotethyan subduction-accretion. *Journal of the Geological Society of London* **153**: 995-1009.
Pickett, E.A.A., Robertson, A.H.F., Dixon, J.E. and Okay, A.I. 1992. Paleotethyan subduction - accretion: evidence from the Karakaya complex, NW Turkey. In: *6th Congress of the Geological Society of Greece* (Ed D.J. Papanikolaou), **Abstracts**, pp. 25-26. Geological Society of Greece, Athens.
Poisson, A. and Şahıncı, A. 1988. La série mésozoïque de Kemalpaşa et le flysch Paléocène d'Izmir au Nord-Ouest de Menderes (Anatolie ocidentale, Turquie). Un jalon du microcontinent taurique. *Comptes-Rendus de l'Académie des Sciences de Paris* **307**: 1075-1080.
Raymond, L.A. 1984. Classification of melanges. In: *Melanges : Their Nature, Origin and Significance* (Ed L.A. Raymond), Geological Society of America, Boulder, Colorado, **198**: 7-20.

Renz, C. 1940. Die Tektonik der griechischen Gebirge. *Pragm. Akad. Athinon* **8**: 171 p.
Renz, C. 1955. Die vorneogene Stratigraphie der normalsedimentären Formationen Griechenlands, Inst. Geol. Sub. Res. Athens, Athens.
Richter, D. and Müller, C. 1993. Der " Erste Flysch " in der Pindos-Zone (Griechenland). *Neues Jahrbuch für Geologie und Paläontologie, Monatshefte* **H. 4**: 209-226.
Richter, D., Müller, C., Hottinger, L. and Risch, H. 1995. Die Flysch-Zonen Griechenlands X. Neue Daten zur Stratigraphie und Paläogeographie des Flysches und seiner Unterlage im Giona-Parnass-Elikon-Gebirge (Parnass-Zone, Griechenland). *Neues Jahrbuch: Geologisch, Paläontologish Abhanlungen* **197**: 295 _ 329.
Richter, D., Müller, C. and Risch, H. 1996. Die Flysch-Zonen Griechenlands XI. Neue Daten zur Stratigraphie und Paläogeographie des Flysches und seiner Unterlage in der Pelagonischen Zone (Griechenland). *N. Jb. Geol. Paläont. Abh.* **201**: 327 - 366.
Ricou, L.-E., Burg, J.-P., Godfriaux, I. and Ivanov, Z. 1998. Rhodope and Vardar : the metamorphic and the olitostromic paired belts related to the Cretaceous subduction under Europe. *Geodinamica Acta* **11**: 285-309.
Ricou, L.E. 1994. Tethys reconstructed: plates, continental fragments and their boundaries since 260 Ma from Central America to South-eastern Asia. *Geodinamica Acta* **7**: 169-218.
Robertson, A.H.F. 1990. Origin and emplacement of an inferred Late Jurassic subduction-accretion complex, Euboea, Eastern Greece. *Geological Magazine* **128**: 27-41.
Robertson, A.H.F. 1994. Role of the tectonic facies concept in orogenic analysis and its application to Tethys in the Eastern Mediterranean region. *Earth-Science Reviews* **37**: 139-213.
Robertson, A.H.F. 2000. Formation of mélanges in the Indus Suture Zone, Ladakh Himalaya by successive subduction-related, collisional and post-collisional processes during Late Mesozoic-Late Tertiary time. In: *Tectonics of the Nanga Parbat Syntaxys and the Western Himalaya* (Ed M.Q. Jan), Geological Society, London, Special Publication **170**: 333-374.
Robertson, A.H.F. 2002. Overview of the genesis and emplacement of Mesozoic ophiolites in the Eastern Mediterranean tethyan region. *Lithos* **65**: 1-67.
Robertson, A.H.F., Clift, P.D., Degnan, P.J. and Jones, G. 1990. Tectonic evolution of the Mesozoic-Cenozoic Pindos Ocean; Greece. In: *5th Congress of the Geological Society of Greece*, Bulletin of the Geological Society of Greece **XXV**, Thessaloniki, Greece, pp. 55-64.
Robertson, A.H.F., Clift, P.D., Degnan, P.J. and Jones, G. 1991. Paleogeographic and paleotectonic evolution of the Eastern Mediterranean Neotethys. In: *Paleogeography and paleoceanography of Tethys* (Ed L.F. Jansa), *Palaeogeography, Palaeoclimatology, Palaeoecology* **87**: 289-343.
Robertson, A.H.F., Dixon, J.E., Brown, S., Collins, A., Morris, A., Pickett, E., Sharp, I. and Ustaömer, T. 1996. Alternative tectonic models for the Late Paleozoic-Early Tertiary development of Tethys in the Eastern Mediterranean region. In: *Palaeomagnetism and Tectonics of the Mediterranean Region* (Ed D.H. Tarling), Geological Society, London, Special Publication **105**: 239-263.
Robinson, A.G., Banks, C.J., Rutherford, M.M. and Hirst, J.P.P. 1995. Stratigraphic and structural development of the eastern Pontides, Turkey. *Journal of the Geological Society of London* **152**: 861-872.
Roddick, J.C., Cameron, W.E. and Smith, A.G. 1979. Permo-Triassic and Jurassic 40Ar-39Ar ages from Greek ophiolites and associated rocks. *Nature* **279**: 788-790.
Rollinson, H. 1993. *Using geochemical data : evaluation, presentation, interpretation*. Longman geochemistry series. John Wiley & Sons, Tottenham, 352 pp.

Saleeby, J.B. 1984. Tectonic significance of serpentinite mobility and ophiolitic melange. In: *Melanges : Their Nature, Origin and Significance* (Ed L.A. Raymond), *Geological Society of America*, Boulder, Colorado, **198**: 153-168.
Sarıbudak, M., Sanver, M. and Ponat, E. 1989. Location of the western Pontides, NW Turkey, during Triassic time: preliminary paleomagnetic results. *Geophysical Journal* **96**: 43-50.
Schermer, E.R., Howell, D.E. and Jones, D.L. 1984. The origin of allochtonous terranes: perspectives on the growth and shaping of continents. *Annual Review of Earth and Planetary Sciences* **12**: 107-131.
Schindler, C. 1997. Geology of Northwestern Turkey: Results of the Marmara Poly-Project. In: *Active Tectonics of Northwestern Anatolia - The Marmara Poly-Project* (Ed M. Pfister), vdf, Zürich: 330-373.
Seghedi, I., Szakacs, A. and Baltres, A. 1990. Relationships between sedimentary deposits and eruptive rocks in the Consul unit (North Dobrogea) - implications on tectonic interpretations. *Dari de Seama ale Sedintelor Institul Geologie Geofizica* **74**: 125-136.
Sherlock, S., Kelley, S.P., Inger, S., Harris, N. and Okay, A.I. 1999. ^{40}Ar-^{39}Ar and Rb-Sr geochronology of high-pressure metamorphism and exhumation history of the Tavşanlı Zone, NW Turkey. *Contribution to Mineralogy and Petrology* **137**: 46-58.
Silver, E.A. and Beutner, E.C. 1980. Melanges. *Geology* **8**: 32-34.
Simantov, J. and Bertrand, J. 1987. Major and trace element geochemistry of the central Euboea basaltic rocks (Greece). Possible geotectonic implications. *Ofioliti* **12**: 201-218.
Siyako, M., Bürkan, K.A. and Okay, A.I. 1989. Tertiary geology and hydrocarbon potential of the Biga and Gelibolu Peninsula. *TAPG Bulletin* **1/3**: 183-199.
Smith, A.G., Hynes, A.J., Menzies, M., Nisbet, E.G., Price, I., Welland, M.J. and Ferrière, J. 1975. The stratigraphy of the Othris Mountains, eastern central Greece: a deformed Mesozoic continental margin sequence. *Eclogae Geologicae Helvetiae* **68**: 463-481.
Spakman, W., van der Lee, S. and van der Hilst, R. 1993. Travel time tomography of the European Mediterranean-mantle down to 1400 km. *Physics of the Earth and Planetary Interiors* **79**: 3-74.
Spötl, C., Longstaffe, F.J., Ranseyer, K., Kunk, M.J. and Wiesheu, R. 1998. Fluid-rock reactions in an evaporitic mélange, Permian Haselgebirge, Austrian Alps. *Sedimentology* **45**: 1019-1044.
Spray, J.G., Bébien, J., Rex, D.C. and Roddick, J.C. 1984. Age constraint on the igneous and metamorphic evolution of the Hellenic-Dinaric ophiolites. In: *The Geological Evolution of the Eastern Mediterranean* (Ed A.H.F. Robertson), Geological Society, London, Special Publication **17**: 619-627 (824).
Spray, J.G. and Roddick, J.C. 1980. Petrology and Ar/Ar Geochronology of some Hellenic Sub-Ophiolite Metamorphic Rocks. *Contribution to Mineralogy and Petrology* **72**: 43-55.
Stais, A. and Ferriere, J. 1991. Nouvelles données sur la paléogéographie mésozoïque du domaine vardarien: les bassins d'Almopias et de Peonias (Macédoine, Hellenides internes septentrionales. *Bulletin de la Société Géologique de Grèce* **25**: 491-507.
Stais, A., Ferriere, J., Caridroit, M., De Wever, P., Clément, B. and Bertrand, J. 1990. Données nouvelles sur l'histoire anté-obduction (Trias-Jurassique) du domaine d'Almopias (Macédonie, Grèce). *Comptes-Rendus de l'Académie des Sciences de Paris* **310**, 1475-1480.
Stampfli, G., Marcoux, J. and Baud, A. 1991. Tethyan margins in space and time. In: *Paleogeography and paleoceanography of Tethys* (Ed L.F. Jansa), *Palaeogeography, Palaeoclimatology, Palaeoecology*, Elsevier, **87**: 373-410.

Stampfli, G. and Mosar, J. 1999. The making and becoming of Apulia. In: *3rd Workshop on Alpine Geological Studies* (Ed M.I. Spalla): 141-154.
Stampfli, G.M. 1996. The Intra-Alpine terrain: a Paleotethyan remnant in the Alpine Variscides. *Eclogae Geologicae Helvetiae* **89**: 13-42.
Stampfli, G.M. 2000. Tethyan oceans. In: *Tectonics and magmatism in Turkey and the Surrounding Area* (Ed J.D.A. Piper), Geological Society, London, Special Publications **173**: 1-23.
Stampfli, G.M., Mosar, J., De Bono, A. and Vavassis, I. 1998. Late Paleozoic, early Mesozoic plate tectonic of the western Tethys. In: *8th International Congress of the Geological Society of Greece, Bulletin of the Geological Society of Greece* **32**, Patra, Greece, pp. 113-120.
Stampfli, G.M. and Borel, G.D. 2002. A plate tectonic model for the Paleozoic and Mesozoic constrained by dynamic plate boundaries and restored synthetic oceanic isochrons. *Earth and Planetary Science Letters* **196**: 17-33.
Stampfli, G.M., Kozur, H. and Borel, G.D. 2003a. Europe from the Variscan to the Alpine cycles, in press.
Stampfli, G.M., Vavassis, I., De Bono, A., Rosselet, F., Matti, B. and Bellini, M. 2003b. Remnants of the Paleotethys oceanic suture-zone in the western Tethyan area. In: *Stratigraphic and Structural Evolution on the Late Carboniferous to Triassic Continental and Marine Successions in Tuscany (Italy): Regional Reports and General Correlation* (Ed F.A. Decandia), *Bolletino della Società Geologica Italiana*, Volume speciale, **2**: in press.
Steen, Ø. and Andresen, A. 1997. Deformational structures associated with gravitational block gliding : examples from sedimentary olistoliths in the Kalvag melange, western Norway. *American Journal of Science* **297**: 56-97.
Stöcklin, J. 1974. Possible ancient continental margin in Iran. In: *The geology of continental margins* (Ed C.L. Drake), Springer Verlag: 873-887.
Stöcklin, J. 1984. The Tethys paradox in plate tectonics. In: *Plate reconstruction from Paleozoic Paleomagnetism,* (Ed A.G. Union), Washinton DC, Geodynimical Series **12**: 27-28.
Straub, C., Kahle, H.-G. and Schindler, C. 1997. GPS and geologic estimates of the tectonic activity in the Marmara Sea region, NW Anatolia. *Journal of Geophysical Research* **102**: 27587-27601.
Şahıncı, A. 1976. La série de Boztepe au nord de Manisa (Anatolie-occidentale, Turquie). Norien supérieur néritique et Sénonien inférieur pélagique. *Comptes Rendus de l'Académie des Sciences de Paris* **283**: 1019-1020.
Şengör, A.M.C. 1979. Mid-Mezozoic closure of Permo-Triassic Tethys and its implications. *Nature* **279**: 590-593.
Şengör, A.M.C. 1984. The Cimmeride orogenic system and the tectonics of Eurasia. *Geological Society of America Special Paper* **195**: 82.
Şengör, A.M.C. 1985. The story of Tethys: how many wives did Okeanos have ? *Episodes* **8**: 3-12.
Şengör, A.M.C. 1989. The Tethyside orogenic system: an introduction. In: *Tectonic Evolution of the ethyan Region* (Ed A.M.C. Şengör), Kluwer Academic Publishers: 1-22.
Şengör, A.M.C. and Yılmaz, Y. 1981. Tethyan evolution of Turkey: a plate tectonic approach. *Tectonophysics* **75**: 181-241.
Şengör, A.M.C., Yılmaz, Y. and Sungurlu, O. 1984. Tectonics of the Mediterranean Cimmerides: nature and evolution of the western termination of Paleo-Tethys. In: *The geological evolution of the eastern Mediterranean* (Ed A.H.F. Robertson), Geological Society, London, Special Publication **17**: 77-112.

Şentürk, K. and Okay, A.I. 1984. Blueschists discovered east of Saros Bay in Thrace. *Bulletin of the Mineral Research and Exploration Institute of Turkey* **97/98**: 152-155.
Taira, A., Kiyokawa, S., Aoike, K. and Saito, S. 1997. Accretion tectonics of the Japanese Islands ans evolution of continental crust. *Comptes Rendus de l'Académie des Sciences de Paris* **325**: 467-478.
Tankut, A. 1984. Basic and ultrabasic rocks from the Ankara Melange, Turkey. In: *The geological evolution of the Eastern Mediterranean* (Ed A.H.F. Roberstson), Geological Society of London, Special Publication, London, **17**: 449-454.
Tankut, A., Dilek, Y. and Önen, P. 1998. Petrology and geochemistry of the Neo-Tethyan volcanism as revealed in the Ankara melange, Turkey. *Journal of volcanology and geothermal research* **85**: 265-284.
Taylor, S.R. and McLennan, S.M. 1981. The composition and evolution of the continental crust: rare earth element evidence from sedimentary rocks. *Philosophical Transactions of the Royal Society of London* **A301**: 381-399.
Tekeli, O. 1981. Subduction complex of pre-Jurassic age, northern Anatolia, Turkey. *Geology* **9**: 68-72.
Tekin, U.K., Göncuöglu, M.C. and Turhan, N. 2002. First evidence of Late Carnian radiolarians from the Izmir-Ankara suture complex, central Sakarya, Turkey : implications for the opening age of the Izmir-Ankara branch of Neo-Tethys. *Geobios* **35**: 127-135.
Tertiary Magmatism of the Rhodopian Region, **1998** (Ed G. Serri), *Acta Vulcanologica*, **10**.
Thiébault, F., Fleury, J.J., Clement, B. and Degardin, J.M. 1994. Paleogeographic and paleotectonic implications of clay mineral distribution in late Jurassic-early Cretaceous sediments of the Pindos-Olonos and Beotian Basins, Greece. *Palaeogeography, Palaeoclimatology, Palaeoecology* **108**: 23-40.
Thuizat, R., Montigny, R., Çakır, U. and Juteau, T. 1978. K-Ar investigations of two Turkish ophiolites. In: *Short paper pf the 4th International Conference Geochronology, Isotope Geology* (Ed R.E. Zartman), Geological Survey of America, **Open file repor t78+701**, pp. 430-432.
Thuizat, R., Whitechurch, H., Montigny, R. and Juteau, T. 1981. K-Ar dating of some infra-ophiolitic metamorphic soles from the Eastern Mediterranean: new evidence for oceanic thrustings before obduction. *Earth and Planetary Science Letter* **52**: 302-310.
Torelli, L., Sartori, R. and Zitellini, N. 1997. The giant chaotic body in the Atlantic Ocean off Gibraltar : new results from a deep seismic reflection survey. *Marine and Petroleum Geology* **14**: 125-138.
Trifanova, E. and Boyanov, I. 1986. late Permian foraminifers from rock fragments in the Mesozoic phyllitoid formation of the East Rhodopes, Bulgaria. *Geologica Balcanica* **16**: 25-30.
Trifonova, E. 1988. Early Jurassic Radiolarians from the Eastern Rhodopes: a revision of the age of Dolno-Lukovo Formation. *Geologica Balcanica* **18**: 58.
Tsikouras, B., Pe-Piper, G. and Hatzipanagiotou, K. 1990. A new date for an ophiolite on the northeastern margin of the Vardar Zone, Samothraki, Greece. *Neues Jahrbuch: Mineralogisch Monatshefte* **H. 11**: 521-527.
Tsujimori, T. 1998. Geology of the Osayama serpentinite melange in the central Chugoku Mountains, southwestern Japan ; 320 Ma blueschist-bearing serpentinite melange beneath the Oeyama Ophiolite. *Journal of the Geological Society of Japan* **104**: 213-231.
Tüysüz, O. 1990. Tectonic evolution of a part of the Tethys orogenic collage: the Kargi massif, northern Turkey. *Tectonics* **9**: 141-160.
Tüysüz, O. 1999. Geology of the Cretaceous sedimentary basins of the Western Pontides. *Geological Journal* **34**: 75-93.

Tüysüz, O., Dellaloğlu, A.A. and Terzioğlu, N. 1995. A magmatic belt within the Neo-Tethyan suture zone and its role in the tectonic evolution of northern Turkey. *Tectonophysics* **243**: 173-191.

Ucurum, A. 2000. Geology, Geochemistry and Evolution of the Divriği and Kuluncak Ophiolitic Mélanges, with References to serpentinites in the East-Central Turkey. *International Geology Review* **42**: 172-191.

Ujiie, K., Toshio, H. and Wonn, S. 2000. Magnetic and structural fabrics of the melange in the Shimanto accretionary complex, Okinawa Island ; implication for strian history during decollement-related deformation. *Journal of Geophysical Research, B* **105**: 25729-25741.

Ustaömer, T. and Roberstson, A.H.F. 1994. Late Palaeozoic maginal basin and subduction-accretion : the Palaeotethyan Küre Complex, Central Pontides, northern Turkey. *Journal of the Geological Society, London* **151**: 291-305.

Ustaömer, T. and Robertson, A. 1997. Tectonic-Sedimentary Evolution of the North Tethyan Margin in the Central Pontides of Northern Turkey. In: *Regional and petroleum geology of the Black sea and surrounding region* (Ed A.G. Robinson), AAPG Memoir, **68**: 255-290.

Vavassis, I. 2001. *Geology and Paleogeographic Evolution of the Pelagonian zone in Northern Evia Island, Greece. Constraints and geodynamic implications for the Hellenides.* Ph.D. Thesis, University of Lausanne, Lausanne, Switzerland.

Vavassis, I., De Bono, A., Stampfli, G.M., Giorgis, D., Valloton, A. and Amelin, Y. 2000. U-Pb and Ar-Ar geochronological data from the Pelagonian basement in Evia (Greece): geodynamic implications for the evolution of Paleotethys. *Schweizerische Mineralogische und Petrographische Mitteilungen* **80**: 21-43.

Vergely, P. and Mercier, J. 2000. Données nouvelles sur les chevauchements d'âge post-Crétacé supérieur dans le massif du Païkon (zone de l'Axios-Vardar, Macédoine, Grèce) : un nouveau modèle structural. *Comptes Rendus de l'Académie des Sciences de Paris* **330**: 555-561.

Vissers, G.L.M., Strating, E.H.H., Heijmans, M. and Krabbendam, M. 2001. Structures and micrustructures in a thrust-related, greenschist facies tectonic melange, Voltri Group (NW Italy). *Ofioliti* **26**: 33-46.

Vollmer, F.W. and Bosworth, W. 1984. Formation of melange in a foreland basin overthrust setting : Example from the Taconic Orogen. In: *Melanges : Their Nature, Origin and Significance* (Ed L.A. Raymond), Geological Society of America, Boulder, Colorado, **198**: 53-70.

Wakabayashi, J. 1999. The Franciscan ; California's classic subduction complex. In: *Classic Cordilleran concepts ; a view from California* (Ed D.L. Stout), Geological Society of America, Special Paper **338**: 111-121.

Wawrzenitz, N. and Krohe, A. 1998. Exhumation and doming of the Thasos metamorphic core complex (S Rhodope, Greece) : structural and geochronological constraints. *Tectonophysics* **285**: 301-332.

Wawrzenitz, N. and Mposkos, E. 1997. First evidence for Lower Cretaceous HP/HT-Metamorphism in the Easter Rhodope, North Aegean Region, North-East Greece. *European Journal of Mineralogy* **9**: 659-664.

Wedepohl, K.H. and Baumann, A. 1999. Central European Cenozoic plume volcanism with OIB characteristics and indications of a lower mantle source. *Contribution to Mineralogy and Petrology* **136**: 225-239.

Wiedmann, J., Kozur, H. and kaya, O. 1992. Fauna and age signifiance of the pre-Jurassic turbidite- olistostrome unit in the western part of Turkey. *Newsletters on stratigraphy* **26**: 133-144.

Wong, H.K., Lüdmann, T., Ulug , A. and Görür, N. 1995. The Sea of Marmara : a plate

boundary sea in an escape tectonic regime. *Tectonophysics* **244**: 231-250.
Wortel, M.J.R. and Spakman, W. 2000. Subduction and Slab Detachment in the Mediterranean-Carpathian Region. *Science* **290**: 1910-1917.
Yalınız, M.K., Floyd, P.A. and Göncuöglu, M.C. 1996. Supra-subduction zone ophiolites of Central Anatolia : geochemical evidence from the Sarıkaraman Ophiolite, Aksaray, Turkey. *Mineralogical Magazine* **60**: 697-710.
Yılmaz, P.O. and Maxwell, J.C. 1982. K-Ar investigations from the Antalya complex ophiolites, SW Turkey. *Ofioliti* **2**: 527-538.
Yılmaz, Y., Genç, S.C., Yigitbas, E., Bozcu, M. and Yılmaz, K. 1995. Geological evolution of the late Mesozoic continental margin of Northwestern Anatolia. *Tectonophysics* **243**: 155-171.
Yılmaz, Y., Gözübol, A.M. and Tüysüz, O. 1982. Geology of an area in and around the Northern Anatolian Transform Fault Zone between Bolu and Akyazı. In: *Multidisciplinary approach to Earthquacke Prediction* (Ed A. Vogel), Vieweg & Sohn, Braunschweig: 45-65.

Appendix 1 - Sample processing for microfossil extraction

Methods used to get preserved and age-diagnostic taxa, both for radiolarian and conodont.

Radiolarian extraction

The extracting methods are based on the dissolving of the sample using a specific acid, depending on the nature of the rock. During the thesis, I had to distinguish between carbonated and siliceous rocks.

Carbonaceous rock (mainly mudstone)
In this case, the radiolarian are most of time calcitized; a preliminary attack with low concentration hydrochloric acid is made to test the sample for its preservation potential for radiolarian. Few samples have been processed in this way and none of them yielded radiolarian.

Siliceous rock (mainly chert)
Due to the siliceous nature of radiolarian, siliceous rocks are the best candidates to get preserved radiolarian. A preliminary attack in 20 % fluoridric acid is made to check the preservation potential of the sample. Before this step, it is better to soak the sample for several hours into HCl acid, to remove all residual calcite (e.g. calcite veins) and thus to prevent crystallisation of fluorite (CaF_2) during the HF bath. If the sample shows an interesting preservation potential, it is dissolved using HF for about 10 hours; the HF concentrations used vary between 3 and 5 %. The residue is washed and filtered using a 62 μm sieve. HF acid must be handled with extreme care. After its drying, binocular observation and possible picking of the best preserved radiolarians (if present), SEM pictures allow the determination of the fauna. 45 samples have been processed in this way and only 10 yielded preserved and determinable taxa.

Conodont extraction

Because all the samples were carbonated, small pieces have been dissolved in formic acid at 10 % for 2-3 days. The residue has been washed using a 0.1 mm sieve. If there is too much residue, separation of conodont (specific weight of 2.8 to 3.1) with heavy liquid is done (bromoform, specific weight of 2.89). As for radiolarian, after drying of the residue, binocular observation and possible picking of the best preserved conodonts (if present), SEM pictures allow the determination of the fauna.

Appendix 2 - Whole-rock geochemistry of the magmatic rocks of the Çetmi mélange

Major elements

	SiO2	TiO2	Al2O3	Fe2O	FeO	MnO	MgO	CaO	Na2O	K2O	P2O5	H20	CO2	Somme	Fe2O3/FeO
Sple	%	%	%	%	%	%	%	%	%	%	%	%	%	%	
L14	45.41	0.81	15.77	5.64	3.21	0.17	3.85	7.19	2.01	3.24	0.19	2.62	9.29	99.42	1.76
L19	56.64	0.58	17.06	3.95	4.49	0.16	3.08	4.15	5.92	1.63	0.28	1.04	0.62	99.61	0.88
L36	50.00	1.20	14.19	6.88	3.23	0.16	5.33	4.26	5.04	1.68	0.40	2.32	4.59	99.29	2.13
L86	55.29	0.88	15.19	5.94	3.64	0.16	3.45	7.26	3.97	0.14	0.25	3.79	0.14	100.11	1.63
L96	55.21	0.51	17.69	3.17	0.94	0.12	3.89	7.98	4.69	0.67	0.34	3.81	0.93	99.98	3.37
L97	59.15	0.42	17.49	3.27	2.10	0.09	2.61	3.76	5.88	1.00	0.29	3.01	0.17	99.25	1.56
L107	50.43	0.91	17.70	4.06	3.73	0.13	2.46	5.37	6.26	1.10	0.22	2.83	3.92	99.12	1.09
L157	60.69	0.39	17.04	3.46	2.29	0.12	2.24	3.83	5.89	0.52	0.28	2.61	0.68	100.03	1.51
L177	56.93	0.68	16.00	5.94	1.75	0.11	4.58	7.53	2.90	2.79	0.27	0.29	0.24	100.05	3.39
L182	51.05	0.65	17.49	5.85	3.53	0.17	4.43	11.02	3.54	0.69	0.12	0.99	0.23	99.79	1.66
L204	60.22	0.69	16.74	3.48	3.59	0.15	1.48	6.18	5.60	0.29	0.21	0.72	0.46	99.80	0.97
L352	50.15	0.79	15.94	6.14	2.74	0.14	2.63	6.10	5.54	1.88	0.19	2.42	5.38	100.04	2.24
L16	46.86	2.34	15.70	4.27	7.12	0.14	3.53	6.12	4.22	0.35	0.41	3.29	5.23	99.57	0.60
L46	48.35	1.54	17.04	3.17	5.38	0.13	6.83	5.47	4.03	1.69	0.36	4.05	1.03	99.16	0.59
L82	51.79	1.58	14.03	2.94	4.50	0.08	2.15	8.84	6.82	0.25	0.30	1.36	4.66	99.32	0.65
L172	47.13	2.14	16.02	7.67	3.12	0.14	4.01	6.13	6.02	0.16	0.65	2.88	3.92	100.00	2.46
B5	46.25	1.50	15.58	4.04	5.26	0.19	7.09	16.16	1.85	0.52	0.29	1.05	0.27	100.12	0.77
B7	48.76	1.53	15.45	6.47	3.37	0.15	6.62	10.85	2.89	0.08	0.30	3.35	0.18	100.04	1.92
B54	50.14	0.74	15.42	3.26	4.12	0.15	7.47	12.20	0.17	0.01	0.20	5.62	0.46	100.00	0.79
B85	49.66	0.45	15.13	6.91	2.54	0.23	4.10	13.72	3.03	0.22	0.14	1.79	2.06	100.04	2.72

Major and Trace elements measured at the Centre d'Analyses Minérales, Lausanne University, by J-C Lavanchy; XRF spectrometry.

FeO measured with a photometer.

CO2 measured with a coulometer.

H2O recalculated from the LOI and FeO analyses.

Trace elements

	Nb	Zr	Y	Sr	U	Rb	Th	Pb	Ga	Zn	Cu	Ni	Co	Cr	V	Ce	Nd	Ba	La	S	Hf	Sc	As
Sple	ppm	ppm	ppm	ppm	ppm	ppm	ppm	ppm	ppm	ppm	ppm	ppm	ppm	ppm	ppm	ppm	ppm	ppm	ppm	ppm	ppm	ppm	ppm
L14	7	120	24	216	2	137	6	15	17	71	5	20	33	53	260	47	23	289	28	5	4	24	10
L19	6	62	23	438	<2<	41	3	13	16	99	63	5	49	11	193	30	10	641	9	<3<	3	24	5
L36	10	103	21	496	<2<	35	<2<	8	20	100	73	16	58	42	347	51	20	410	14	<3<	6	43	4
L86	8	92	25	89	4	6	6	12	13	89	109	12	55	47	280	23	10	190	7	<3<	3	43	7
L96	4	59	21	117	3	21	5	7	19	51	91	35	51	96	291	43	20	207	23	120	5	26	17
L97	11	66	16	98	2	28	6	6	16	59	22	13	37	12	124	30	8	147	14	<3<	5	14	7
L107	15	122	28	358	2	33	7	3	14	86	92	9	40	17	308	34	13	143	23	17	6	26	5
L157	13	69	15	123	3	17	6	7	14	79	19	25	52	13	121	30	14	152	11	<3<	5	18	5
L177	9	100	26	241	3	46	7	16	15	72	56	50	59	169	221	45	20	335	20	<3<	5	23	6
L182	11	72	18	115	3	19	4	13	15	65	35	31	84	73	246	22	11	94	12	<3<	5	24	6
L204	11	104	25	178	3	7	5	12	16	88	93	4	73	13	194	22	11	175	6	<3<	6	20	6
L352	8.5	100	22.6	281	<2<	75.6	4	4	16	102		21		35	220	25		156	14				
B54	8.4	52	14.6	33	<2<	<1.0<	4	3	15	81		75		200	267	12		25	9				
B85	4.4	61	21	267	<2<	1.6	7	7	16	62		63		268	241	24		53	23				
L16	40	181	26	413	<2<	8	4	<2<	20	100	18	10	46	32	507	33	14	213	10	2750	6	52	13
L46	37	155	27	311	<2<	43	5	2	14	78	43	186	49	416	276	54	18	820	23	<3<	5	37	5
L82	32	134	19	131	<2<	5	5	<2<	8	68	90	15	49	31	303	31	15	83	12	1160	5	17	5
L172	55	209	29	117	6	6	8	<2<	17	113	9	4	44	9	227	30	11	110	9	<3<	5	31	6
B5	28.3	131	25.4	405	<2<	5.8	4	4	18	104		219		397	243	27		87	17				
B7	41.8	105	23.5	243	<2<	1.3	6	<2<	16	87		69		238	271	30		64	23				

REE

	Y	La	Ce	Pr	Nd	Sm	Eu	Gd	Tb	Dy	Ho	Er	Tm	Yb	Lu	Th	U
Sple	ppm	ppm	ppm	ppm	ppm	ppm	ppm	ppm	ppm	ppm	ppm	ppm	ppm	ppm	ppm	ppm	ppm
L14	22.00	21.60	43.00	4.40	24.00	5.50	1.22	4.60	0.70	4.20	0.93	2.50	0.40	2.40	0.36	6.30	1.60
L19	22.00	17.30	31.70	3.20	17.80	4.00	1.04	3.80	0.60	3.70	0.84	2.30	0.40	2.40	0.35	3.40	1.00
L36	18.00	18.20	37.40	3.90	22.00	5.00	1.27	4.20	0.60	3.40	0.70	1.90	0.30	1.60	0.23	3.00	1.00
L86	26.00	13.90	28.10	2.90	16.30	3.90	0.95	4.20	0.70	4.60	1.07	3.00	0.50	2.80	0.41	5.10	1.30
L96	16.00	19.70	37.40	3.60	19.40	3.80	0.86	3.30	0.50	2.90	0.63	1.70	0.30	1.80	0.29	4.50	1.60
L97	12.00	17.80	33.20	3.10	15.20	2.60	0.70	2.20	0.30	2.10	0.47	1.30	0.20	1.40	0.22	5.30	1.60
L107	25.00	26.90	50.60	4.50	22.50	4.40	1.03	4.30	0.70	4.80	1.05	3.00	0.50	3.00	0.44	9.00	2.70
L157	11.00	18.90	30.30	3.10	15.30	2.60	0.69	2.30	0.30	1.90	0.43	1.30	0.20	1.40	0.22	6.70	1.90
L177	20.00	22.90	43.70	4.00	20.70	4.00	0.82	3.60	0.60	3.50	0.81	2.20	0.40	2.00	0.33	7.50	3.10
L182	15.00	15.90	28.90	2.70	13.90	2.80	0.69	2.80	0.50	3.00	0.67	1.80	0.30	2.00	0.28	4.10	0.90
L204	22.00	22.50	43.70	4.20	22.40	4.60	1.01	4.30	0.60	4.20	0.93	2.60	0.40	2.50	0.37	7.20	2.60
L352	21.20	16.50	31.60	3.69	14.80	3.30	0.90	3.56	0.59	3.70	0.79	2.35	0.37	2.40	0.39	4.40	0.51
B54	13.70	10.70	22.80	2.99	11.70	2.80	0.91	2.96	0.48	2.73	0.59	1.57	0.27	1.80	0.26	2.20	0.63
B85	19.60	24.40	34.80	4.61	17.00	3.20	0.86	3.45	0.52	3.18	0.73	2.23	0.31	2.10	0.38	5.40	0.75
L16	31.00	32.50	62.20	5.80	31.60	6.90	1.90	6.30	1.00	5.90	1.24	3.30	0.50	3.00	0.42	5.20	1.00
L46	23.00	29.30	53.20	4.80	25.30	5.00	1.45	4.50	0.70	4.30	0.93	2.40	0.40	2.20	0.32	5.30	1.10
L82	18.00	24.10	43.20	4.10	21.70	4.50	1.16	4.10	0.60	4.00	0.80	2.10	0.30	1.80	0.27	4.40	0.50
L172	27.00	36.50	69.10	6.60	34.50	6.70	1.66	5.90	0.90	5.60	1.20	3.20	0.50	2.70	0.42	7.40	4.90
B5	21.90	18.10	34.80	4.18	16.70	3.80	1.45	4.12	0.74	4.07	0.98	2.53	0.35	2.30	0.33	2.50	0.89
v	21.80	25.70	45.50	5.35	20.10	3.90	1.36	4.49	0.69	4.15	0.88	2.49	0.37	2.30	0.34	4.40	0.95

REE analyses done at XRAL Laboratories, Canada; ICP-MS.

Appendix 3 - Whole-rock geochemistry of the Elliayak eclogite (Çetmi mélange)

Major and Trace elements measured at the Centre d'Analyses Minérales, Lausanne University, by J-C Lavanchy; XRF spectrometry.

Major elements

	SiO2	TiO2	Al2O3	Fe2O3	MnO	MgO	CaO	Na2O	K2O	P2O5	LOI	Cr2O3	NiO	Somme
Sple	wt-%	wt-%	wt-%	wt-%	wt-%	wt-%	wt-%	wt-%	wt-%	wt-%	wt-%	wt-%	wt-%	wt-%
L61	69.40	0.66	15.31	5.52	0.08	1.00	0.27	1.13	2.57	0.08	3.55	0.04	0.01	99.60
L310	67.75	0.74	15.83	6.02	0.10	1.09	0.95	1.05	2.65	0.12	3.25	0.04	0.01	99.59
L311	64.89	0.77	17.16	6.53	0.13	1.54	0.82	1.31	3.11	0.13	3.43	0.04	0.01	99.86
L346	67.83	0.69	15.84	5.79	0.15	1.50	0.61	0.94	2.90	0.07	2.89	0.03	0.01	99.25
L52	47.49	1.52	17.20	10.85	0.17	6.59	8.68	3.43	1.01	0.11	2.78	0.06	0.02	99.90

Trace elements

	Nb	Zr	Y	Sr	U	Rb	Th	Pb	Ga	Zn	Ni	Cr	V	Ce	Ba	La
Sple	ppm	ppm	ppm	ppm	ppm	ppm	ppm	ppm	ppm	ppm	ppm	ppm	ppm	ppm	ppm	ppm
L61	13	169	15.5	147	<2<	120.5	11	24	19	97	56	237	119	50	389	20
L310	15.3	208	20.8	169	<2<	117	11	16	20	97	68	262	126	57	399	22
L311	16.2	199	22.8	113	<2<	134.2	13	23	21	101	66	240	130	84	508	16
L346	12.7	166	19.6	114	<2<	126	10	14	21	96	51	173	124	64	464	13
L52	4.3	129	26.2	188	<2<	19.9	2	<2<	16	108	173	374	201	4	92	<4<

REE analyses done at XRAL Laboratories, Canada; ICP-MS.

REE

	Y	La	Ce	Pr	Nd	Sm	Eu	Gd	Tb	Dy	Ho	Er	Tm	Yb	Lu	Th	U
Sple	ppm	ppm	ppm	ppm	ppm	ppm	ppm	ppm	ppm	ppm	ppm	ppm	ppm	ppm	ppm	ppm	ppm
L61	15	19.5	48	4.8	16.6	3.2	0.45	2.7	0.5	2.7	0.55	1.9	0.4	2.3	0.38	11.6	2
L310	21	21.5	56.2	5.6	18.8	3.5	0.53	3	0.6	3.5	0.83	2.5	0.4	3	0.5	12	1.9
L311	23	14.2	69.3	4	14.3	3.2	0.61	3.1	0.7	4.2	1.06	3	0.5	3.3	0.54	14.2	2.3
L346	19.9	12.5	53.2	3.21	11.9	2.6	0.63	2.79	0.57	3.63	0.79	2.22	0.35	2.2	0.33	12.1	1.18
L52	25.5	5.4	15.2	2.39	11.5	3.4	1.23	4.64	0.81	4.86	1.05	3.12	0.44	2.9	0.43	0.3	0.16

Appendix 4 - Whole-rock geochemistry of the greywacke-shale matrix of the Çetmi mélange

Major and Trace elements measured at the Centre d'Analyses Minérales (CAM), Lausanne University, by J-C Lavanchy; XRF spectrometry.

	SiO2	TiO2	Al2O3	Fe2O3	MnO	MgO	CaO	Na2O	K2O	P2O5	LOI	Cr2O3	NiO	Somme
Sple	wt-%	wt-%	wt-%	wt-%	wt-%	wt-%	wt-%	wt-%	wt-%	wt-%	wt-%	wt-%	wt-%	wt-%
L94	76.73	0.34	11.59	3.18	0.04	0.97	0.63	1.69	2.03	0.07	2.58	0.01	0.00	99.87
L100	73.67	0.44	9.29	5.96	0.09	1.17	2.62	1.09	1.05	0.15	4.32	0.02	0.00	99.87
L106	77.87	0.33	7.04	1.97	0.04	0.66	4.17	1.66	0.90	0.09	4.47	0.01	0.00	99.20
L132	75.75	0.59	12.01	3.77	0.04	0.93	0.20	2.13	1.81	0.10	2.42	0.02	0.00	99.75
L213	82.75	0.46	8.51	2.05	0.03	0.84	0.15	1.76	1.21	0.06	1.48	0.02	0.00	99.32
K6	83.11	0.31	6.82	2.33	0.09	0.60	1.92	1.07	0.96	0.04	2.78	0.02	0.00	100.06
L268	59.94	0.78	17.14	6.41	0.10	2.57	1.90	1.09	3.80	0.15	5.26	0.02	0.01	99.16
L282	56.38	0.79	18.56	7.46	0.12	3.06	2.12	1.74	3.29	0.14	5.41	0.02	0.01	99.11
L292	57.82	0.75	17.02	7.66	0.21	3.12	1.71	1.94	2.78	0.17	6.24	0.03	0.01	99.45

Trace elements

	Nb	Zr	Y	Sr	U	Rb	Th	Pb	Ga	Zn	Ni	Cr	V	Ce	Ba	La
Sple	ppm	ppm	ppm	ppm	ppm	ppm	ppm	ppm	ppm	ppm	ppm	ppm	ppm	ppm	ppm	ppm
L94	11.3	138	15.8	76	<2<	75.3	8	17	14	46	26	75	48	48	827	22
L100	9.1	222	18.9	75	<2<	42.2	8	24	12	99	28	110	53	43	209	22
L106	9.9	148	12.4	108	<2<	35.5	6	14	9	30	16	80	31	24	118	14
L132	12.1	218	20.4	66	<2<	78.6	9	13	14	64	32	114	66	37	302	20
L213	9.2	282	14.8	64	<2<	48.6	8	13	10	35	30	133	44	34	210	18
K6	6.3	143	10.8	50	<2<	39.6	6	17	9	44	18	104	31	28	180	16
L268	18	197	25.3	58	2	148.1	11	11	22	94	65	198	161	56	253	32
L282	17.9	175	25.3	124	<2<	130.5	12	17	23	109	88	156	162	66	476	32
L292	15.6	161	23.1	126	<2<	114.3	10	22	21	108	93	189	161	43	441	20

REE analyses done at the IMG, Lausanne University, by F. Bussy; ICP-MS.

REE

	Co	Dy	Er	Eu	Gd	Hf	Ho	La	Lu	Nd	Pr	Sc	Sm	Sr	Tb	U	Th	Yb
Sple	ppm	ppm	ppm	ppm	ppm	ppm	ppm	ppm	ppm	ppm	ppm	ppm	ppm	ppm	ppm	ppm	ppm	ppm
L94	7.839	2.242	1.374	0.545	3.101	3.699	0.509	21.61	0.244	15.7	4.216	7.814	2.698	66.46	0.397	2.066	6.923	1.309
L100	10.61	3.573	1.888	0.997	4.039	6.004	0.73	24.11	0.329	23.8	5.272	8.403	4.023	74.03	0.668	2.284	7.69	1.717
L106	4.947	1.898	1.067	0.513	2.353	3.371	0.447	14.57	0.2	13.9	3.442	4.565	2.379	102.9	0.37	1.422	4.754	1.224
L132	12.1	3.752	2.05	0.92	4.688	5.846	0.824	27.47	0.338	26.85	6.233	9.554	4.597	61.52	0.631	2.623	9.197	1.931
L213	7.278	2.401	1.48	0.725	3.44	7.326	0.531	20.82	0.264	19.37	4.874	6.325	3.993	54.56	0.461	2.037	6.507	1.359
K6	7.739	1.723	1.085	0.554	2.719	4.559	0.456	15.86	0.182	14.68	3.596	5.732	2.85	47.82	0.371		4.96	1.114
L268	16.9	4.983	2.682	1.242	5.149	5.286	0.926	33.52	0.462	30.48	7.192	17.4	5.973	55.62	0.893	3.043	13.85	2.682
L282	18.41	4.562	2.565	1.197	5.671	4.63	0.875	35.13	0.447	31.53	7.405	19.99	6.09	121.4	0.826	2.944	14.32	2.552
L292	27.17	4.47	2.337	1.41	5.515	4.124	0.863	34.06	0.424	31.82	7.338	18.41	6.315	124.8	0.839	2.914	12.08	2.393

Appendix 5 - Whole-rock geochemistry of the metamorphic sole from the Denizgören ophiolite, Ezine area

Major and Trace elements measured at the Centre d'Analyses Minérales (CAM), Lausanne University, by J-C Lavanchy; XRF spectrometry.

Major elements

	SiO2	TiO2	Al2O3	Fe2O3	FeO	MnO	MgO	CaO	Na2O	K2O	P2O5	H20	CO2	Cr2O	NiO	Somme
Sple	wt-%	wt-%	wt-%	wt-%	wt-%	wt-%	wt-%	wt-%	wt-%	wt-%	wt-%	wt-%	wt-%	wt-%	wt-%	wt-%
E14	48.49	2.41	13.77	9.15	4.34	0.18	4.82	7.73	4.17	0.15	0.34	3.43	0.22	0.02	0.00	99.22
E15	48.73	1.58	14.20	6.05	5.63	0.21	7.59	8.72	3.62	0.11	0.15	3.12	0.20	0.02	0.01	99.93
E28	47.59	1.83	15.79	5.86	5.37	0.17	6.05	9.50	3.53	0.26	0.19	3.21	0.19	0.04	0.01	99.6
E78	45.84	2.20	13.76	7.51	6.56	0.23	5.81	12.46	2.19	0.16	0.23	2.68	0.25	0.02	0.01	99.91
E115	48.97	1.43	14.82	4.97	4.79	0.15	5.82	12.60	3.58	0.08	0.17	2.02	0.47	0.04	0.01	99.92
E66	48.27	1.07	15.98	9.78	0.00	0.16	7.69	10.99	3.20	0.65	0.11	1.98	0.00	0.05	0.02	99.94
E70	49.12	1.16	14.75	10.18	0.00	0.21	7.85	9.95	2.52	1.71	0.12	2.05	0.00	0.05	0.02	99.67
E84	43.79	0.39	15.21	7.68	0.00	0.14	11.40	16.55	0.95	0.08	0.03	3.69	0.00	0.13	0.03	100.07
E90	48.35	0.52	18.73	7.28	0.00	0.13	7.90	10.77	3.03	1.12	0.03	2.01	0.00	0.07	0.03	99.95

Trace elements

	Nb	Zr	Y	Sr	U	Rb	Th	Pb	Ga	Zn	Ni	Cr	V	Ce	Ba
Sple	ppm	ppm	ppm	ppm	ppm	ppm	ppm	ppm	ppm	ppm	ppm	ppm	ppm	ppm	ppm
E14	14.7	261	60.4	149	<2<	1.7	3	<2<	21	137	38	105	258	16	35
E15	3.8	103	32.4	118	<2<	<1.0<	2	<2<	18	99	62	96	284	<3<	<9<
E28	7.5	154	37.8	179	<2<	4	3	<2<	20	100	73	240	238	7	43
E78	7	154	48.2	163	<2<	1.5	2	<2<	23	117	62	83	390	<3<	14
E115	6.6	115	27.8	289	<2<	1.1	3	<2<	19	73	72	245	241	5	9
E66	4.1	62	24.1	177	<2<	11	2	<2<	18	70	121	289	249	<3<	91
E70	3.2	72	26.6	199	<2<	35.5	<2<	3	17	123	120	327	259	3	282
E84	<1.0<	19	11.3	102	<2<	1.1	2	<2<	14	49	235	902	188	<3<	<9<
E90	1.2	41	11	142	<2<	24.6	<2<	<2<	15	53	206	496	143	<3<	38

REE analyses done at XRAl Laboratories, Canada; ICP-MS.

REE

	Ce	Dy	Er	Eu	Gd	Ho	La	Lu	Nd	Pr	Sm	Tb	Th	Tm	U	Y	Yb	Yb
Sple	ppm	ppm	ppm	ppm	ppm	ppm	ppm	ppm	ppm	ppm	ppm	ppm	ppm	ppm	ppm	ppm	ppm	ppm
E14	34.9	10.8	6.54	2.47	9.84	2.39	14.3	0.93	25.9	5.6	7.9	1.65	1.3	0.93	0.37	57.4	6	6
E15	10.8	5.82	3.56	1.34	5	1.26	3.6	0.56	10.6	1.88	3.5	0.92	0.2	0.56	0.58	31.6	3.3	3.3
E28	20.1	6.7	4.3	1.13	5.6	1.5	8.3	0.71	15.1	3.3	4.4	1.1	1.9	0.7	0.2	36	4.3	4.3
E78	18.4	8.83	5.61	1.94	7.23	2	6.3	0.8	15.9	3.23	5.5	1.36	0.6	0.82	0.45	49.2	5.8	5.8
E115	15.7	4.78	2.88	1.33	4.23	1.01	6.2	0.39	11.1	2.45	3.4	0.76	0.8	0.41	0.21	26.4	2.6	2.6
E66	9.2	4.15	2.61	1.04	3.47	0.97	4	0.39	7.3	1.48	2.5	0.64	0.3	0.43	0.09	22.3	2.5	2.5
E70	7.2	4.14	2.7	0.91	3.45	0.97	2.6	0.4	6.8	1.25	2.5	0.67	0.2	0.43	0.52	24.5	2.6	2.6
E84	1.6	1.76	1.32	0.4	1.29	0.45	0.5	0.18	1.6	0.27	0.8	0.28	<0.1	0.19	<0.05	10.4	1.2	1.2
E90	1.4	1.85	1.27	0.34	1.28	0.4	0.4	0.2	1.5	0.22	0.7	0.24	<0.1	0.2	<0.05	10.7	1.3	1.3

Appendix 6 - $^{40}Ar/^{39}Ar$ analytical data for in situ laser ablation analyses for the amphibolites of the metamorphic sole of the Denizgören ophiolite (Ezine area), and for the tuff of the upper member of the Küçükkuyu Fm

Analyses done at the ISTEEM, Montpellier University, by P. Monié.

Sample	40Ar*/39Ar	36Ar/40Ar x 1000 J=0.014283	39Ar/40Ar	37Ar/39Ar	% 39Ar	% Atm.	Age	error
E84								
Amphibole								
Amphibolite								
1	18,460	3,252	0,0021	15,626	2,1	96,1	422,2	92,8
2	9,212	2,879	0,0161	58,154	3,7	85,1	223,0	38,0
3	3,439	2,347	0,0890	16,692	22,1	69,3	86,5	5,2
4	3,074	1,484	0,1825	13,287	29,3	43,8	77,5	8,1
5	4,088	2,212	0,0846	28,800	32,6	65,3	102,4	9,3
6	4,196	2,017	0,0961	48,267	38,1	59,6	105,0	14,9
7	4,762	1,650	0,1075	59,658	57,5	48,7	118,7	5,5
8	4,882	1,057	0,1408	49,331	66,4	31,2	121,6	8,5
9	4,955	1,089	0,1367	49,582	72,9	32,1	123,4	7,1
10	4,844	1,531	0,1130	48,021	78,0	45,2	120,7	7,7
11	4,501	2,216	0,0766	52,580	83,8	65,4	112,4	11,8
12	4,511	1,603	0,1166	50,975	100,0	47,3	112,6	5,5
						Total age =	116.7	± 3.9
E94								
Amphibole								
Amphibolite								
1	5,660	2,574	0,0422	1,562	5,5	76,0	140,3	7,9
2	4,149	2,104	0,0911	9,329	13,7	62,1	103,9	5,3
3	3,618	0,557	0,2308	1,673	31,3	16,4	90,9	1,3
4	3,162	0,350	0,2834	2,113	39,8	10,3	79,7	2,1
5	3,296	0,548	0,2541	5,080	46,3	16,2	83,0	2,4
6	4,468	0,710	0,1768	14,935	55,0	21,0	111,6	3,9
7	4,916	0,855	0,1518	25,636	66,0	25,2	122,4	2,9
8	5,335	0,641	0,1518	27,224	71,1	18,9	132,5	6,3
9	4,975	0,702	0,1592	28,897	75,3	20,7	123,8	5,9
10	4,478	0,405	0,1965	15,318	100,0	11,9	111,9	2,2
						Total age =	107.2	± 1.6
L302								
Biotite								
Tuff								
	0,612	3,163	0,1063	0,291	4,1	93,4	15,7	14,1
2	1,177	2,731	0,1639	0,044	18,1	80,7	30,1	5,0
3	1,256	2,255	0,2655	0,015	29,0	66,6	32,1	4,8
4	1,362	2,015	0,2967	0,000	35,4	59,5	34,8	4,0
5	1,406	1,752	0,3428	0,000	40,4	51,7	35,9	3,7
6	1,418	1,735	0,3436	0,139	48,8	51,3	36,2	3,3
7	1,400	1,797	0,3349	0,139	58,3	53,1	35,7	3,5
8	1,367	1,925	0,3154	0,069	67,0	56,9	34,9	2,2
9	1,232	1,842	0,3696	0,155	73,9	54,4	31,5	2,6
10	1,268	1,710	0,3901	0,134	83,0	50,5	32,4	2,4
11	1,451	1,084	0,4683	0,163	92,7	32,1	37,0	2,4
12	1,419	1,599	0,3717	0,041	95,1	47,2	36,2	8,7
13	1,295	0,293	0,7056	0,051	100,0	8,6	33,1	4,7
						Total age =	32.7	± 1.4

Appendix 7 - U-Th-Pb microprobe analytical data for the granodiorite cut by the Şelale Detachment fault

Analyses done at the CRPG Nancy, by D. Bosch, Montpellier University.

Sample L326

Grain area	U ppm	Pb* ppm	Th ppm	Th/U	$^{206}Pb/^{204}Pb$	$^{208}Pb/^{206}Pb$	±	$^{206}Pb/^{238}U$	± (1s)	$^{207}Pb/^{235}U$	± (1s)	$^{207}Pb/^{206}Pb$	± (1s)
#1-1	425	1.9	494	1.16	334	0.271	0.063	0.00522	0.00021	0.0411	0.0074	0.0570	0.0100
#2-1	510	2.0	556	1.09	1623	0.264	0.018	0.00459	0.00006	0.0312	0.0012	0.0493	0.0019
#2-2	834	3.3	1363	1.63	1513	0.390	0.014	0.00467	0.00006	0.0305	0.0013	0.0474	0.0020
#3-1	444	1.8	484	1.09	1317	0.260	0.023	0.00474	0.00005	0.0302	0.0014	0.0461	0.0021
#4-1	633	2.5	928	1.47	1993	0.348	0.014	0.00463	0.00005	0.0324	0.0012	0.0508	0.0017
#5-1	795	3.5	572	0.72	49	0.180	0.411	0.00509	0.00072	0.0211	0.0221	0.0301	0.0312
#6-1	458	1.9	527	1.15	1573	0.272	0.017	0.00476	0.00005	0.0334	0.0011	0.0508	0.0015
#7-1	511	2.1	574	1.12	2071	0.270	0.019	0.00479	0.00006	0.0345	0.0013	0.0522	0.0019
#8-1	718	2.9	1008	1.40	2532	0.337	0.009	0.00472	0.00005	0.0315	0.0008	0.0484	0.0012
#8-2	477	2.0	501	1.05	3269	0.254	0.011	0.00479	0.00005	0.0347	0.0009	0.0526	0.0012
#9-1	612	2.5	858	1.40	2079	0.335	0.014	0.00470	0.00006	0.0328	0.0014	0.0507	0.0020
#10-1	563	2.2	847	1.50	1607	0.355	0.015	0.00463	0.00008	0.0314	0.0014	0.0492	0.0020
#11-1	403	1.6	434	1.08	1276	0.238	0.023	0.00458	0.00007	0.0307	0.0018	0.0486	0.0028
#12-1	422	1.6	441	1.04	1391	0.257	0.026	0.00452	0.00008	0.0324	0.0019	0.0520	0.0029
#13-1	1202	4.6	2143	1.78	5049	0.418	0.013	0.00446	0.00006	0.0300	0.0007	0.0487	0.0009
#14-1	753	2.9	1230	1.63	2763	0.386	0.009	0.00456	0.00006	0.0301	0.0007	0.0479	0.0009
#15-1	577	2.2	809	1.40	1442	0.332	0.012	0.00450	0.00006	0.0313	0.0014	0.0504	0.0021
#16-1	539	2.2	633	1.17	1578	0.238	0.041	0.00478	0.00013	0.0317	0.0020	0.0481	0.0027

Grain area	Rho	Apparent age $^{238}U/^{206}Pb$	± (1s)	$^{235}U/^{207}Pb$	± (1s)
#1-1	0.22	33.59	1.34	40.85	7.19
#2-1	0.31	29.52	0.36	31.22	1.22
#2-2	0.30	30.05	0.39	30.52	1.30
#3-1	0.24	30.48	0.35	30.16	1.42
#4-1	0.31	29.78	0.33	32.42	1.13
#5-1	0.35	32.73	4.61	21.20	21.73
#6-1	0.33	30.64	0.35	33.33	1.06
#7-1	0.40	30.79	0.39	34.40	1.31
#8-1	0.13	30.38	0.33	31.48	0.83
#8-2	0.43	30.83	0.35	34.68	0.89
#9-1	0.33	30.20	0.41	32.79	1.33
#10-1	0.38	29.79	0.49	31.42	1.35
#11-1	0.26	29.49	0.46	30.73	1.78
#12-1	0.31	29.10	0.52	32.40	1.85
#13-1	0.55	28.71	0.37	30.00	0.69
#14-1	0.59	29.34	0.39	30.13	0.68
#15-1	0.29	28.97	0.37	31.30	1.35
#16-1	0.44	30.75	0.85	31.68	1.98

MEB picture of selected zircon grains

Zr 4

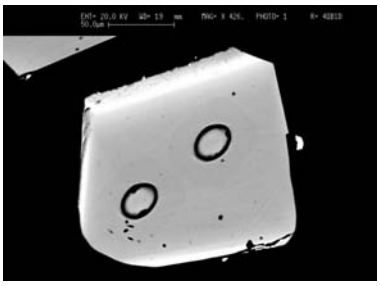

Zr 5

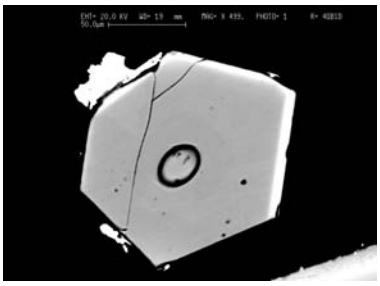

Zr 6

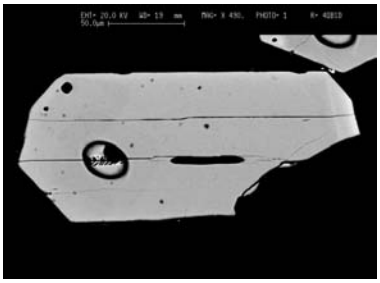

PLATE 1 - Lower-middle Triassic conodonts from the Çetmi mélange and the Ezine Group

Determination Dr. H. Kozur, Budapest (Hungaria)

Çetmi mélange

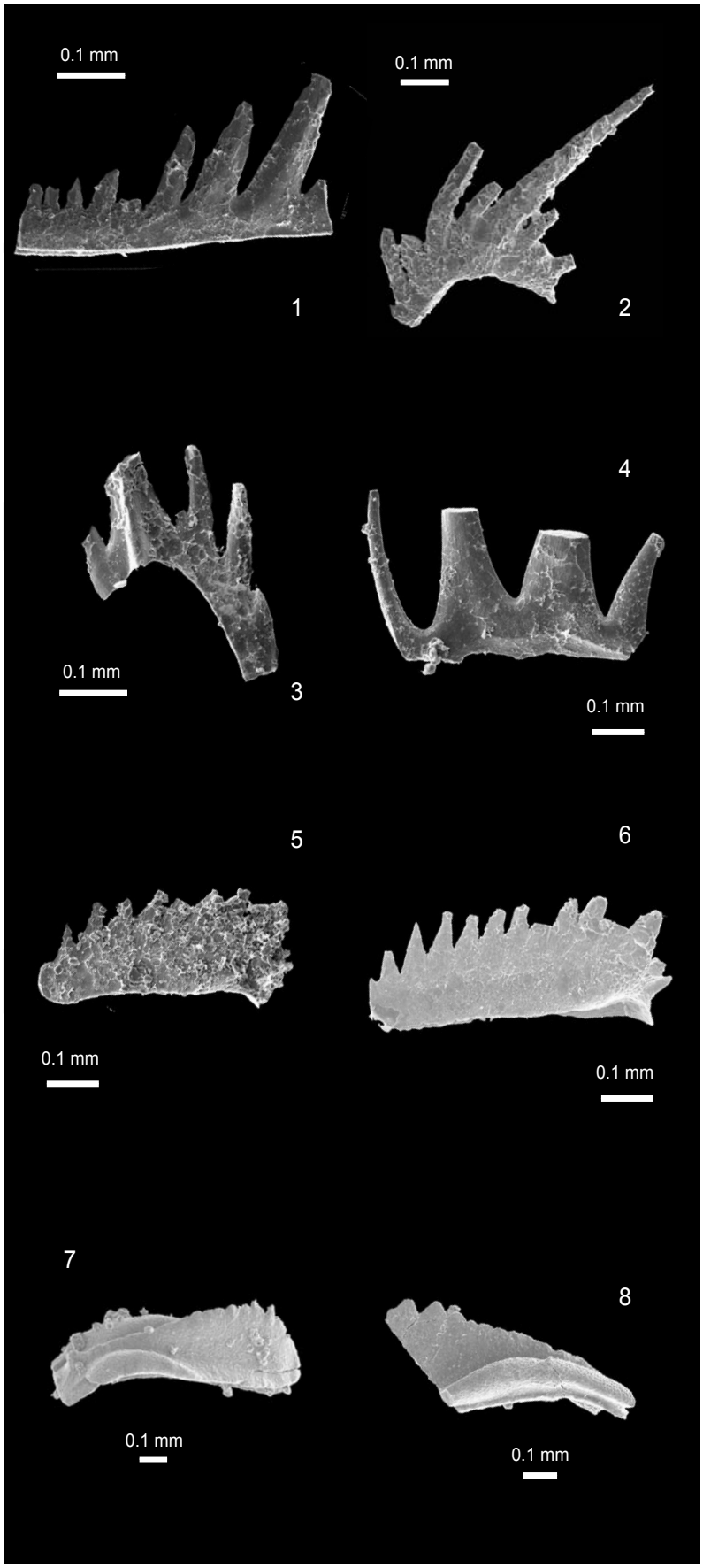

Ezine Group

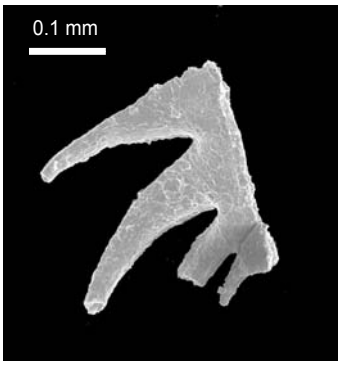

Gladigondollela sp. - E34

1- *Gladigondolella* sp., Sc element - sample L89

2- *Gladigondolella* sp., Sc element - L89

3- *Gladigondolella* sp., M element - L89

4- *Gladigondolella* sp., fragment of a Sb element - L89

5- *Nicoraella* cf. *kockeli* (Tatge) - L89

6- *Chiosella gondolelloides* (Banda) - L231

7- *Paragondolella fueloepi (Kovac)* - K13

8- *Paragondolella fueloepi (Kovac)* - K13

PLATE 2A - Upper Triassic foraminifers from the limestone blocks of the Çetmi mélange

Determination Dr. R. Martini and Pr. L. Zaninetti, University of Geneva (Switzerland)

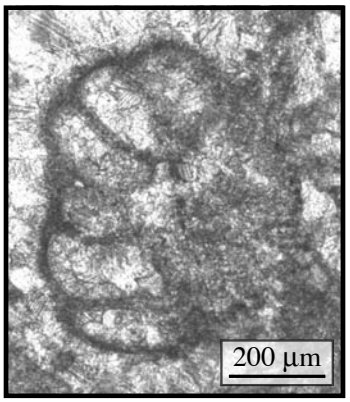

Duostominidae - sample L43

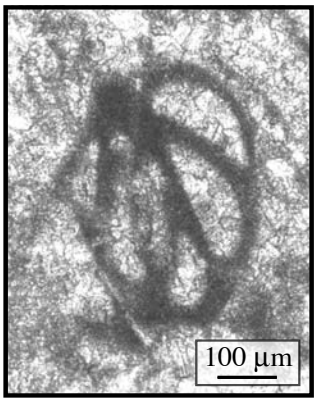

Miliolidae - L43

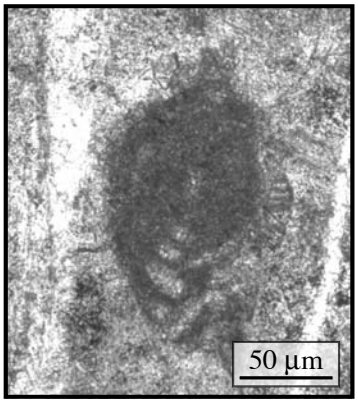

Ophtalmidium sp. - L44

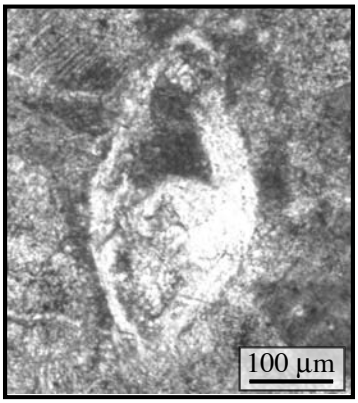

"*Lenticulina*" sp. - L44

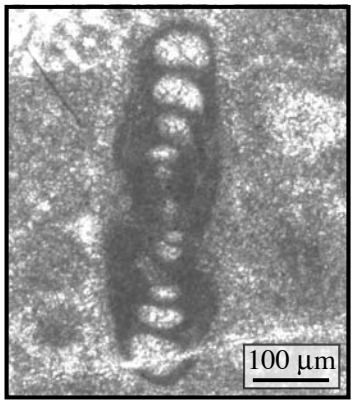

Ophtalmidium sp. - L54

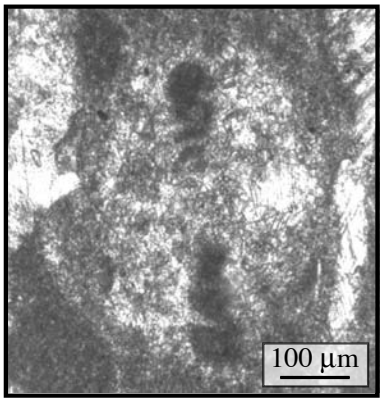

Aulotortus sp. - L54

Nodosariidae - L54

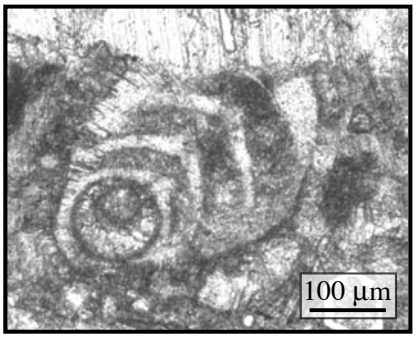

Frondicularia sp. - L54

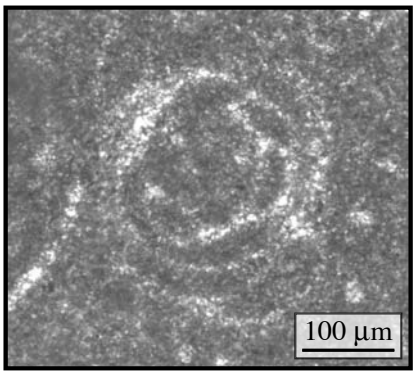

Aulotortus aff. *A. friedli*
(Kristan & Tollmann, 1962) - L55

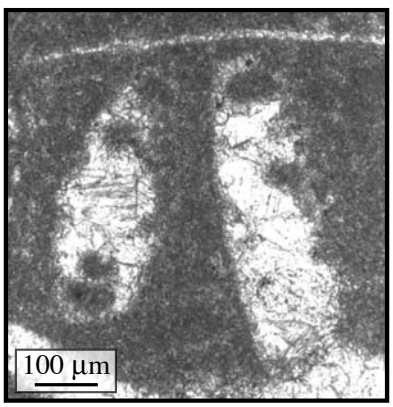

Aulotortus aff. communis
(Kristan, 1957) - L55

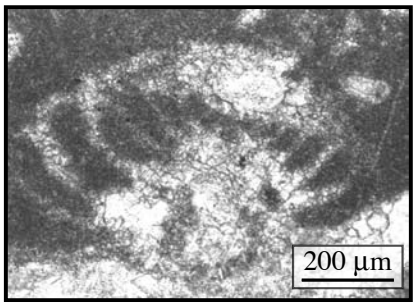

Auloconus permodiscoides
(Oberhauser, 1964) - L55

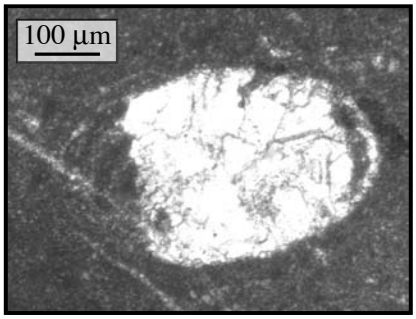

Aulotortus aff. A. communis
(Kristan, 1957) - L55

PLATE 2B - Upper Triassic foraminifers from the limestone blocks of the Çetmi mélange

Determination Dr. R. Martini and Pr. L. Zaninetti, University of Geneva (Switzerland)

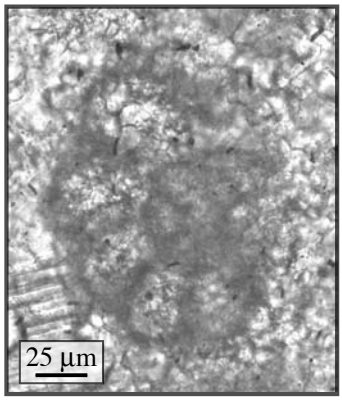

Endotriada sp. - L93

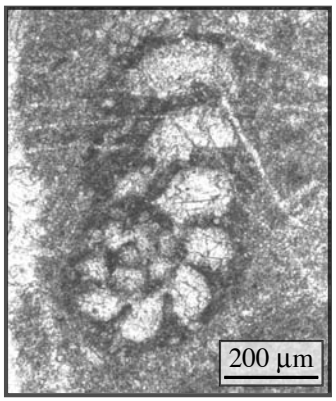

Endotebanella kocaeliensis (Dager, 1978a) - L175

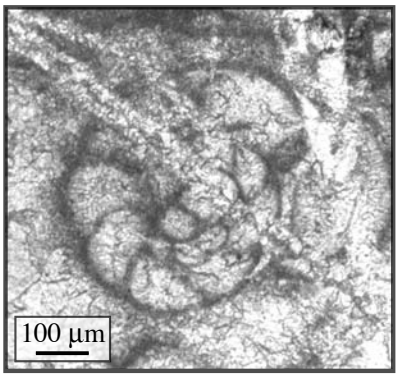

Endotriada tyrrhenica, Vachard, Martini, Rettori, Zaninetti, 1994 - L175

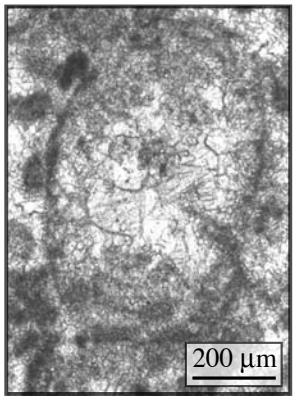

Aulotortus gr. sinuosus (Weanshenk, 1956) - L216

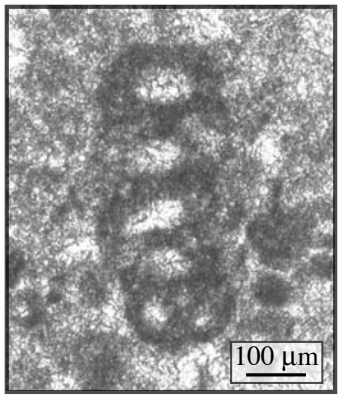

Endotebanella kocaeliensis (Dager, 1978a) - L216

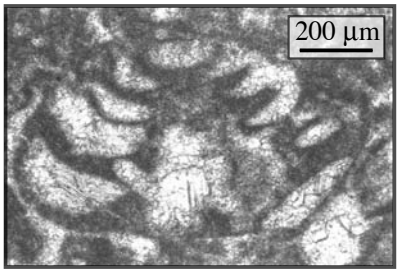

Auloconus permodiscoides (Oberhauser, 1964) - L216

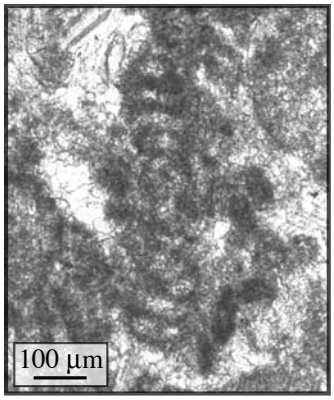

Glomospirella expansa (Kristan & Tollmann, 1964) - L216

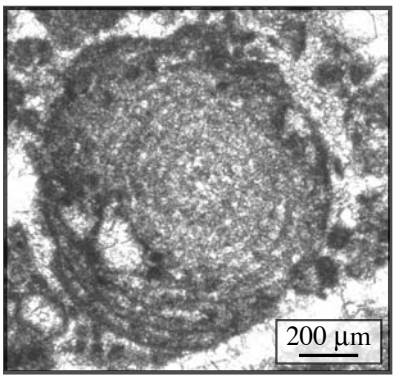

Triasina hantkeni, Majzon, 1954 - L216

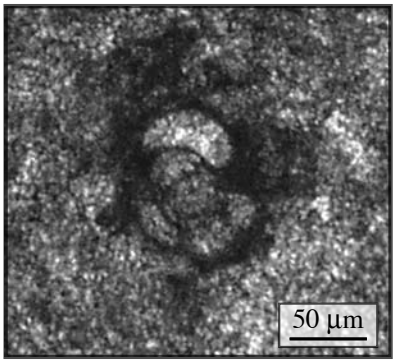

Hoyenella inconstans (Michalik, Jendredjakovac and Borza, 1979) - K16

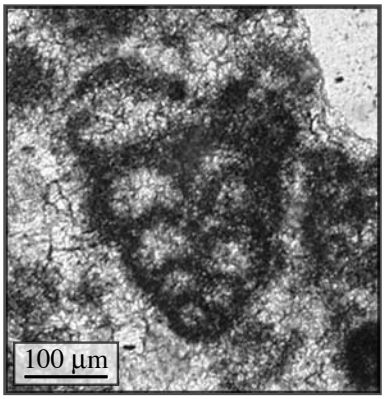

Duostomonidae - K16

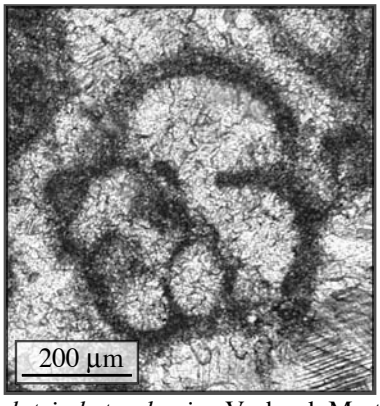

Endotriada tyrrhenica, Vachard, Martini, Rettori, Zaninetti, 1994 - K16

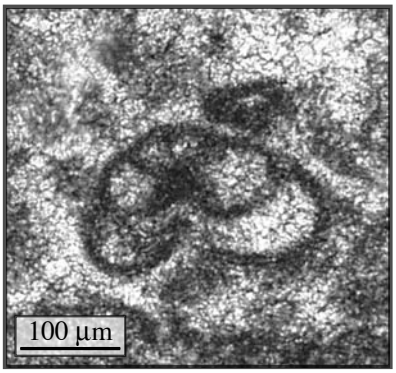

"*Trochamina*" aff. *almtatensis,* Khoen-Zaninetti, 1968 - K16

PLATE 2C - Upper Triassic foraminifers from the limestone blocks of the Çetmi mélange

Determination Dr. R. Martini and Pr. L. Zaninetti, University of Geneva (Switzerland)

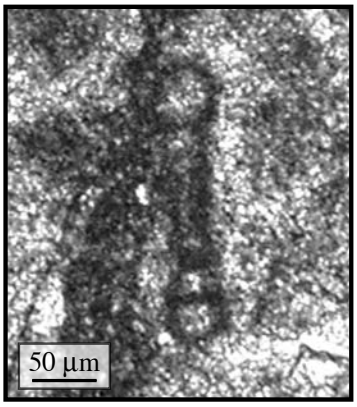

Cyclogira ? sp. - K16

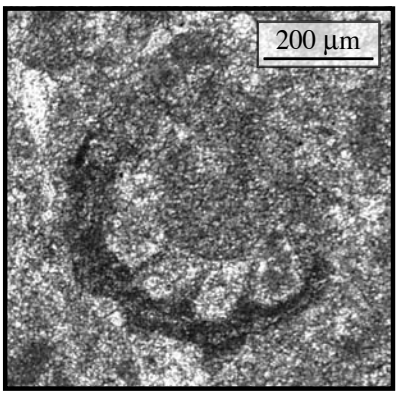

Duostominidae - B19

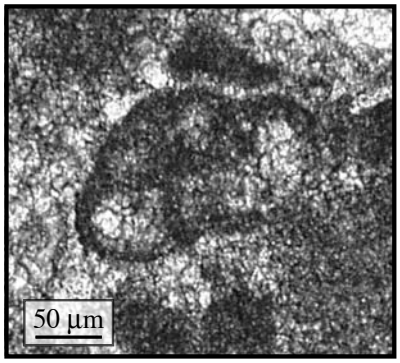

"*Trochamina*" aff. *almtatensis*, Khoen-Zaninetti, 1968 - B19

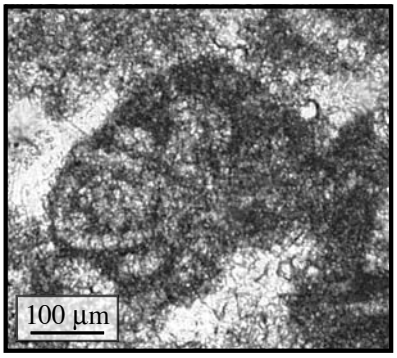

Glomospira ? sp. - B19

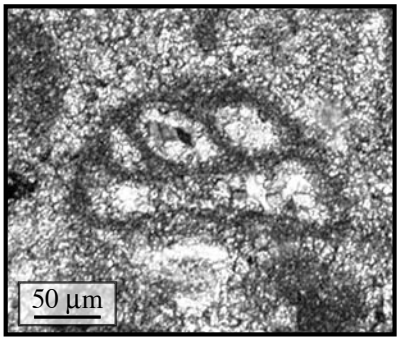

Duotaxis gr. *birmanica*, Zaninetti and Bronnimann, in Bronnimann, Whittaker and Zaninetti, 1975 - B19

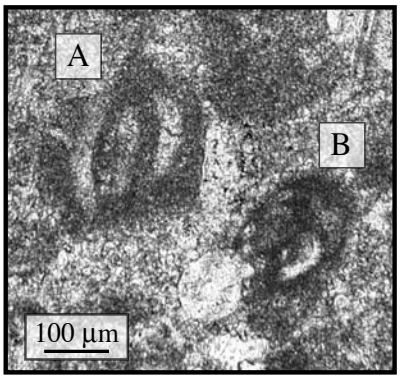

A: *Ophtalmidium* sp.; B: *Cucurbita* sp. - B19

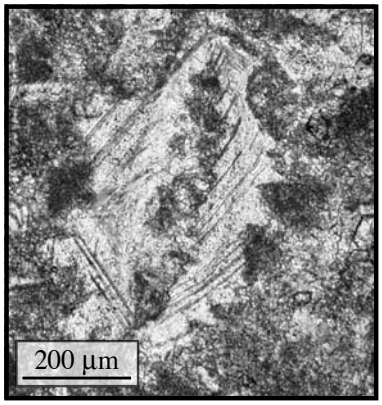

Triassic "Pakiphloya" - B19

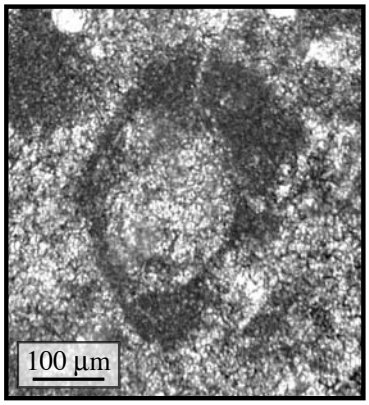

Aulotortus sp. - B19

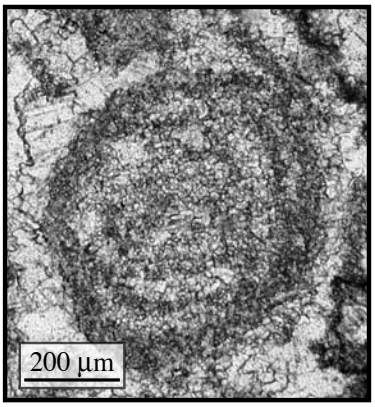

Pilammina sp. - B29

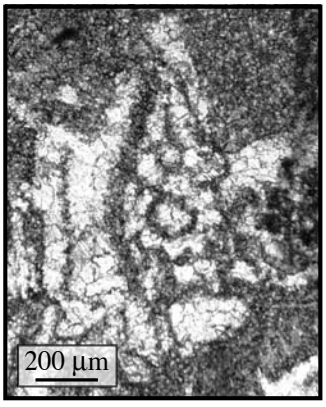

undet. Dasycladacae - B29

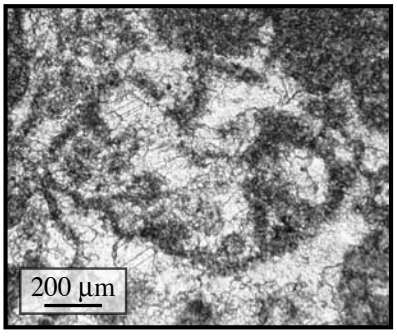

Duostominidae - B29

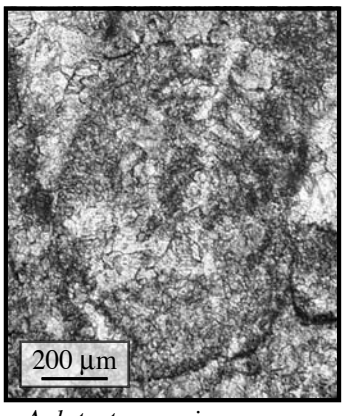

Aulotortus gr. *sinuosus* (Weynschenk, 1956) - B30

PLATE 2D - Upper Triassic foraminifers from the limestone blocks of the Çetmi mélange

Determination Dr. R. Martini and Pr. L. Zaninetti, University of Geneva (Switzerland)

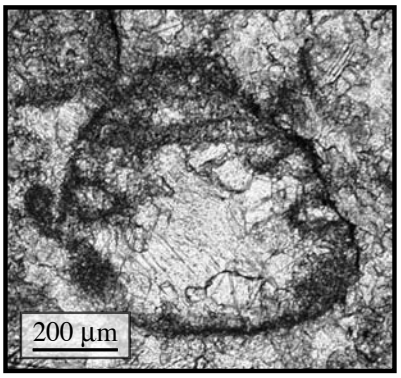

Auloconus permodiscoides (Oberhauser, 1964) - B30

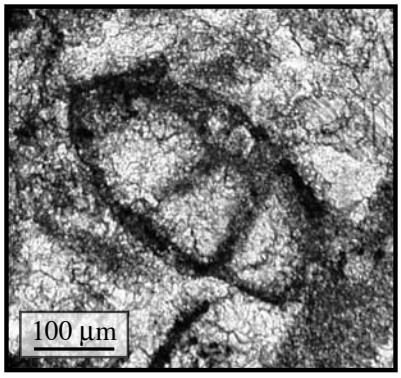

Duostominidae - B30

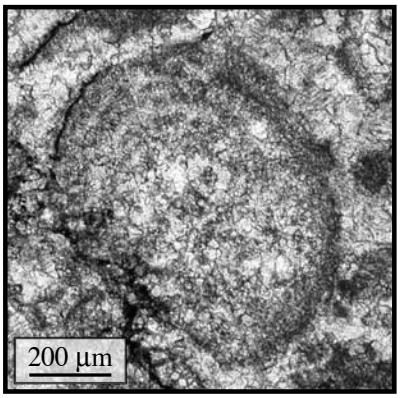

Triasina hantkeni, Majzon, 1954 - B30

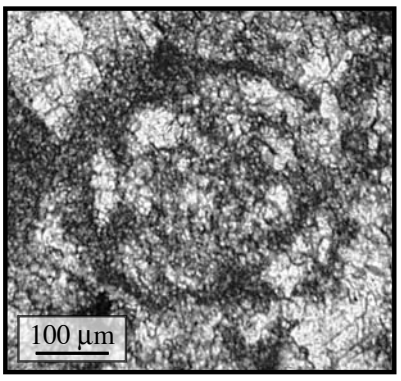

Gandinella falsofriedli (Salaj, Borza and Samuel, 1983) - B30

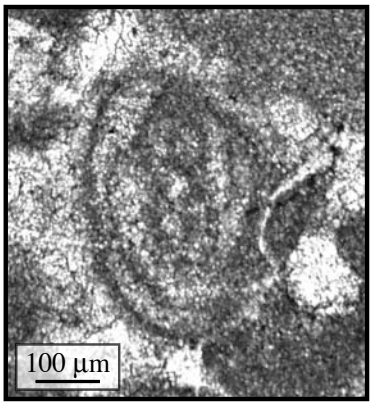

Ophtalmidium sp. - B35

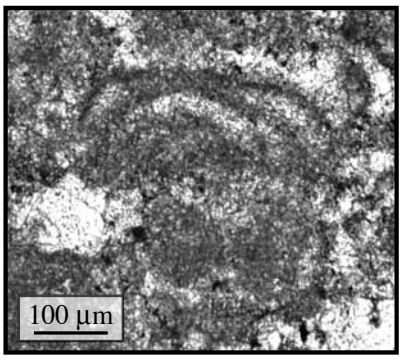

Glomospirella sp. - B35

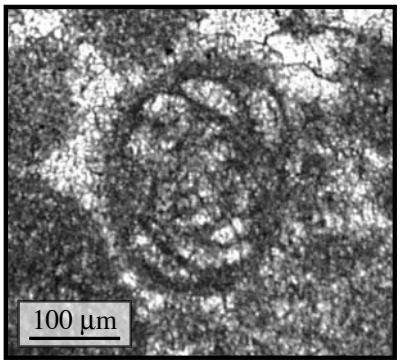

Gandinella falsofriedli (Salaj, Borza and Samuel, 1983) - B35

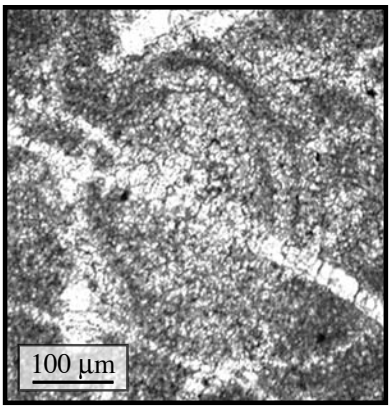

Aulotortus sp. - B35

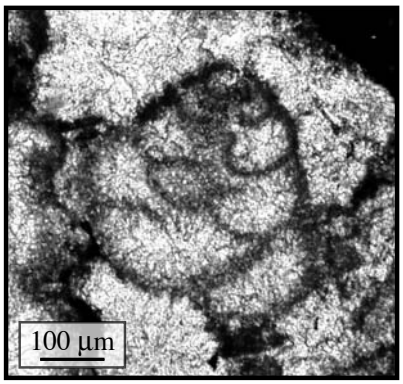

Duostominidae - B53

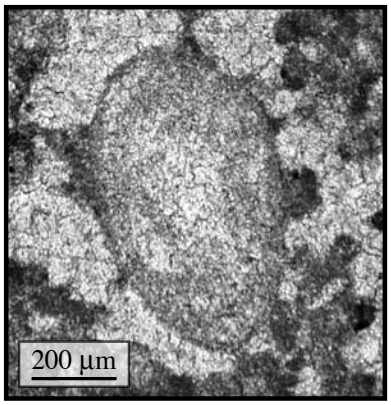

Aulotortus sp. - B53

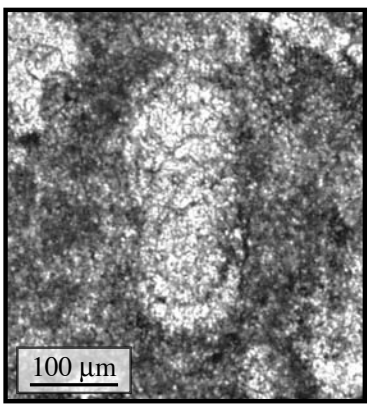

Glomospirella sp. - B53

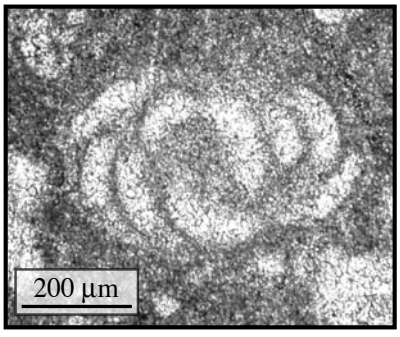

Hoyenella n. sp. - B98

PLATE 3A - Middle Jurassic-lower Cretaceous radiolarians from blocks of the Çetmi mélange
Determination Dr. A-C. Bartolini, University of Paris (France)

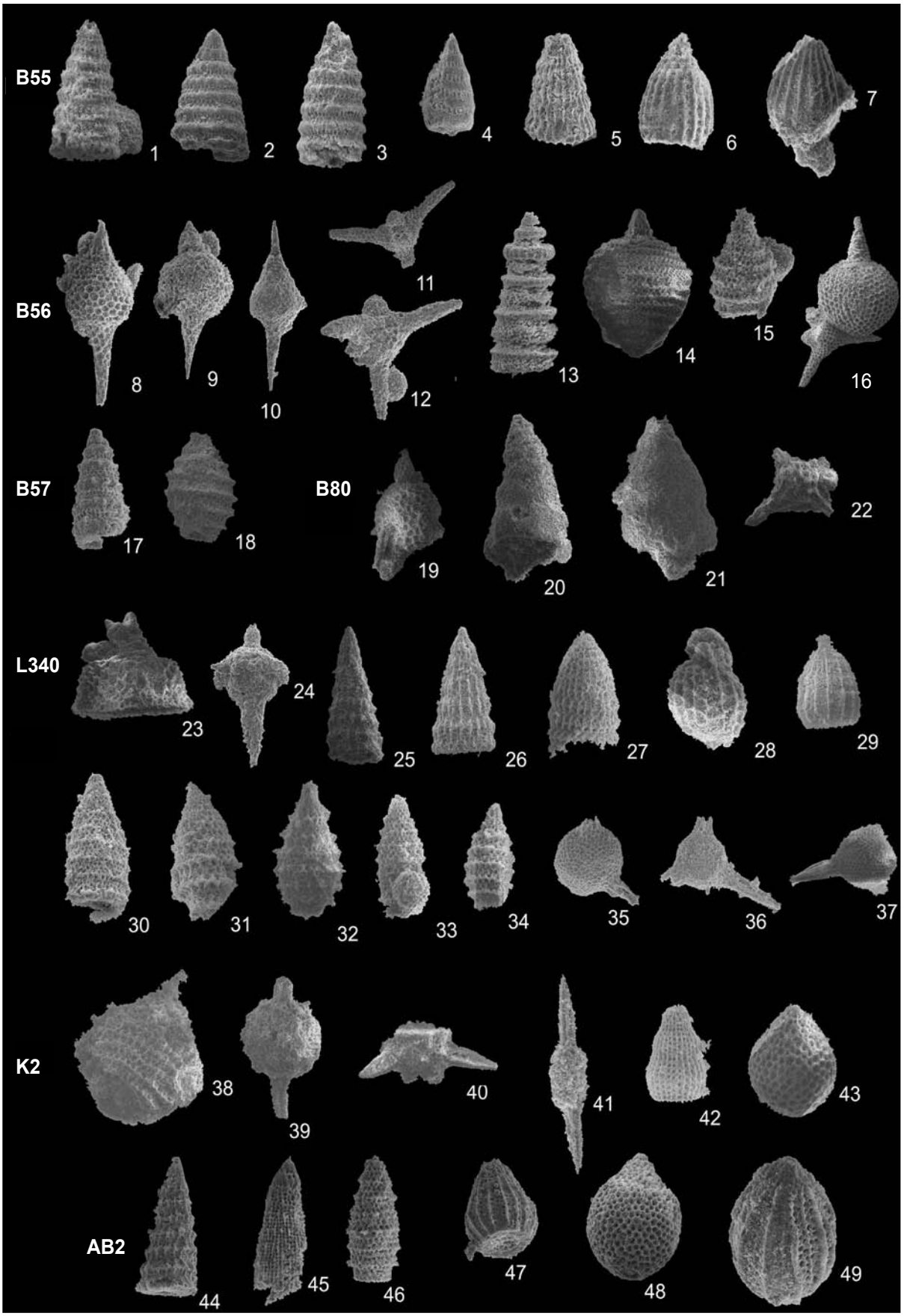

PLATE 3A - Caption

Determination Dr. A-C. Bartolini, University of Paris (France)

1 *Svinitzium depressum* (BAUMGARTNER), B55, x 300 ; **2** *Pseudodictyomitra carpatica* (LOZYNIAK), B55, x 300 ; **3** *Pseudodictyomitra carpatica* (LOZYNIAK), B55, x 300 ; **4** *Pseudodictyomitra nuda* SCHAAF, B55, x 300 ; **5** *Archeodictyomitra* cfr. *A. coniforma* DUMITRICA, B55, x 300 ; **6** *Archeodictyomitra mitra* DUMITRICA, B55, x 400 ; **7** *Archeodictyomitra* cfr. *A.* (?) *lacrimula* FOREMAN ; **8** *Podobursa* cfr. *P.* (?) *quadriaculeata* (STEIGER), B56, x 200 ; **9** *Podobursa* (?) sp., B56, x 200 ; **10** *Syringocapsa vicetina* (SQUINABOL), B56, x150 ; **11** *Parapodocapsa furcata* STEIGER, B56, x150 ; **12** *Podocapsa amphitreptera* FOREMAN, B56, x 200 ; **13** *Cinguloturris cylindrica* KEMKIN & RUDENKO, B56, x 300 ; **14** *Mirifusus dianae minor* BAUMGARTNER, B56, x 150 ; **15** *Tethysetta boesii* gr. (PARONA), B56, x 300 ; **16** *Sethocapsa dorysphaeroides* NEVIANI sensu SCHAAF, B56, x 120 ; **17** *Pseudodictyomitra lanceloti* SCHAAF, B57, x 300 ; 18 *Tethysetta boesii* gr. (PARONA), B57, x 300 ; **19** *Sethocapsa* (?) *sphaerica* (OZVOLDOVA), B80, x 200 ; **20** *Spongocapsula palmerae* PESSAGNO, B80, x 180 ; **21** *Spongocapsula perampla* (RÜST), B80, x 200 ; **22** *Emiluvia chica* s.l. FOREMAN, B80, x 200 ; **23** *Palinandromeda podbielensis* (OZVOLDOVA), L340, x 200 ; **24** *Podobursa helvetica* (RÜST), L340, x 200 ; **25** *Transhsuum brevicostatum* gr. (OZVOLDOVA), L340, x 250 ; **26** *Transhsuum maxwelli* gr. (PESSAGNO), L340, x 300 ; **27** *Parahsuum stanleyens* (PESSAGNO), L340 x 300 ; **28** *Tricolocapsa tetragona* MATSUOKA, L340, x 400 ; **29** *Archaeodictyomitra* (?) *amabilis* AITA, L340, x 400 ; **30** *Tethysetta* sp., L340, x 400 ; **31** *Tethysetta* sp., L340, x 400 ; **32** *Tethysetta dhimenaensis* ssp. A BAUMGARTNER, L340, x 400 ; **33** *Tethysetta dhimenaensis dhimenaensis* BAUMGARTNER, L340, x 300 ; **34** *Tethysetta spinata* (VINASSA), L340, x 400 ; **35** *Triactoma* sp., L340, x 200 ; **36** *Triactoma jonesi* (PESSAGNO), L340, x 200 ; **37** *Triactoma* sp., L340, x 200 ; **38** *Mirifusus* cfr. *M. dianae*, K2, x 200 ; **39** *Acaeniotyle umbilicata* (RÜST), K2, x 200 ; **40** *Acaeniotyle* sp., K2, x 200 ; **41** *Archaeospongoprunum*, K2, x 300 ; **42** *Archaeodictyomitra*, K2, x 400 ; **43** (?) *Zhamoidellum ovum* DUMITRICA, K2, x 400 ; **44** *Transhsuum brevicostatum* (OZVOLDOVA), AB2, x 300 ; **45** *Parahsuum*, AB2, x 300 ; **46** *Tethysetta dhimenaensis dhimenaensis* BAUMGARTNER, AB2, x 400 ; **47** *Archaeodictyomitra* (?) *amabilis* AITA, AB2, x 400 ; **48** *Stichocapsa robusta* MATSUOKA, AB2, x 400 ; **49** *Protunuma japonicus* MATSUOKA & YAO, AB2, x 600.

PLATE 3B - Middle Jurassic-lower Cretaceous radiolarians from blocks of the Çetmi mélange
Determination Dr. A-C. Bartolini, University of Paris (France)

Sample L35

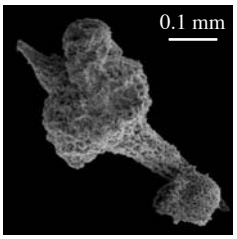

Syringocapsa spinellifera BAUMGARTNER

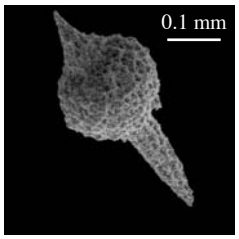

Syringocapsa sp.

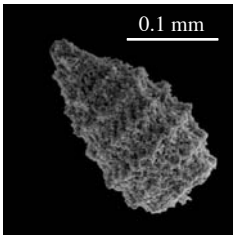

Parvicingula sp.

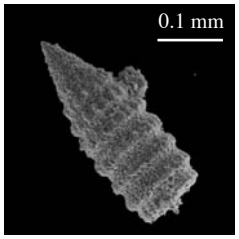

Pseudodictyomitra cfr. *P. carpatica* (LOZYNIAK)

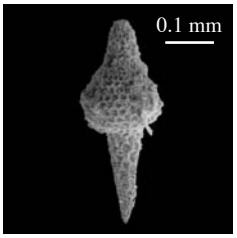

Podobursa sp.

Sample L70

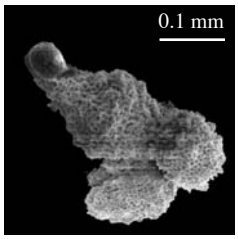

? *Mirifusus* cfr. *M. chenodes* (RENZ)

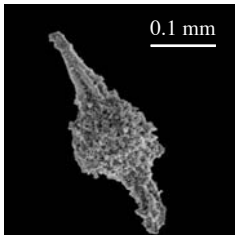

A*rchaeospongoprunum* sp.

Sample L139-2

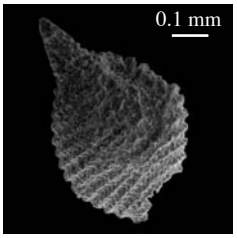

Mirifusus cfr. *M. guadalupensis* PESSAGNO

PLATE 4A - Palynomorph assemblage of the sample L153, belonging to the matrix of the Çetmi mélange
Determination Dr. P. Hochuli, ETH Zürich (Switzerland)

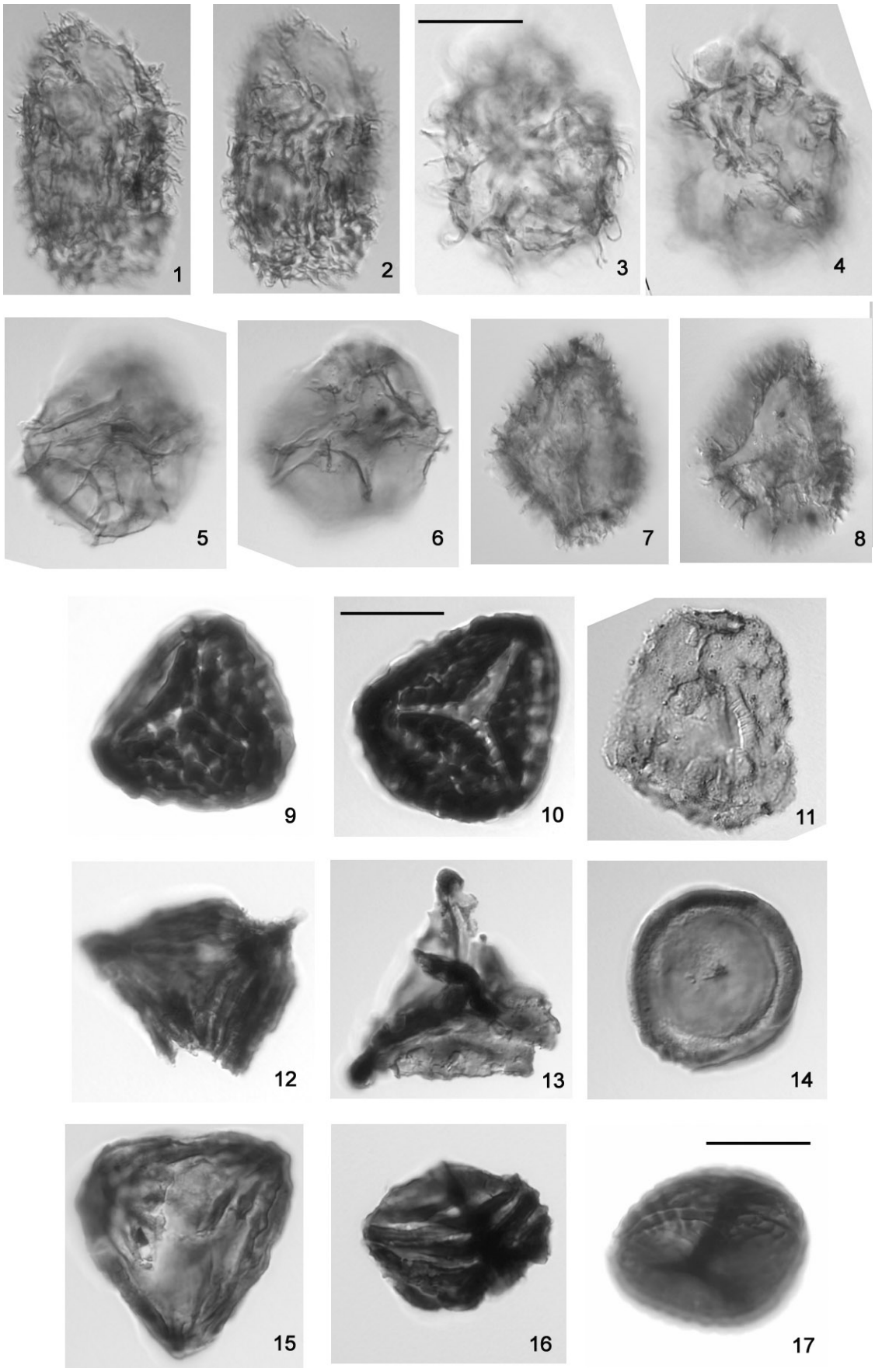

PLATE 4B - Palynomorph assemblage of the sample L153, belonging to the matrix of the Çetmi mélange
Determination Dr. P. Hochuli, ETH Zürich (Switzerland)

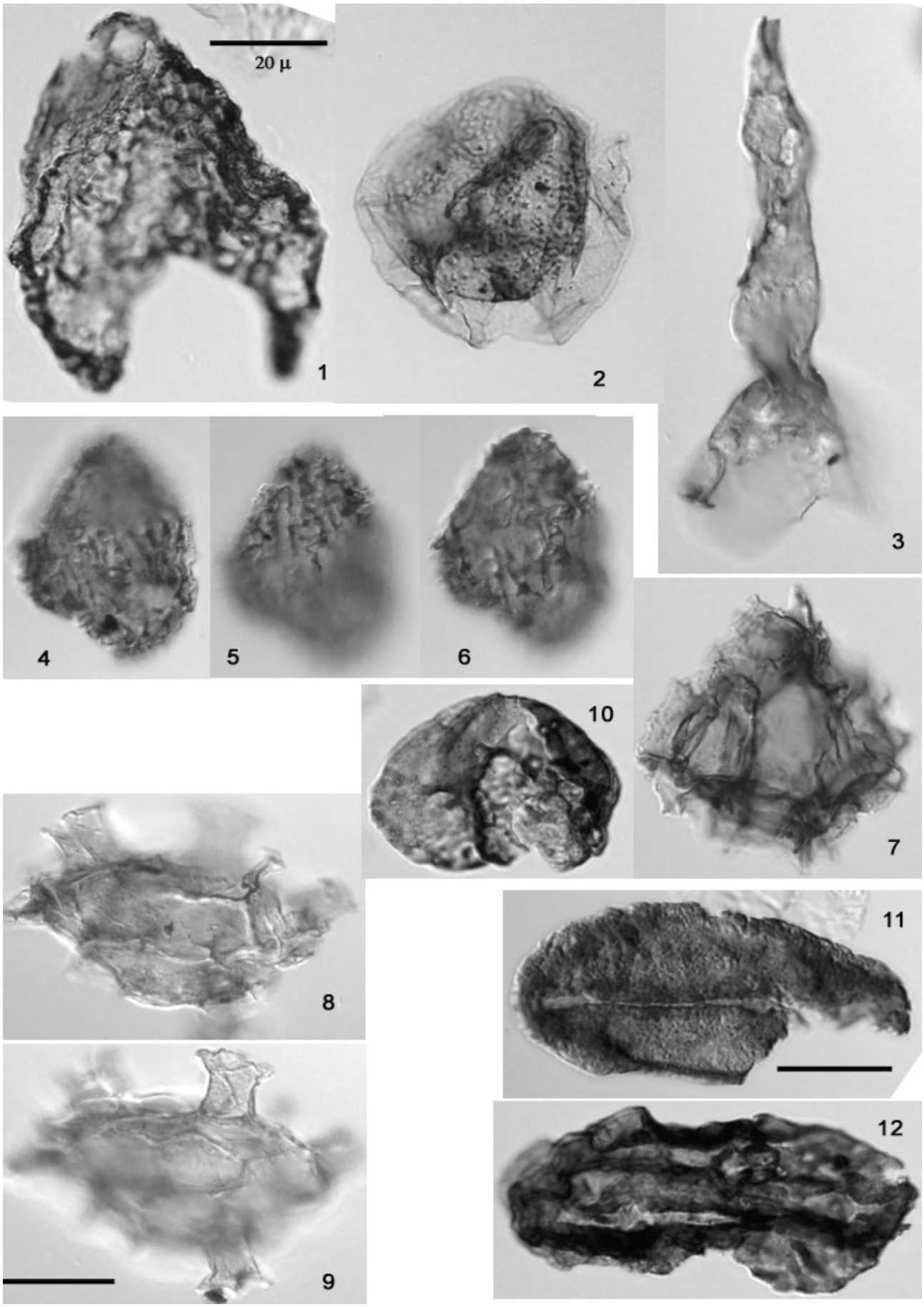

PLATE 4A and 4B - Caption

Determination Dr. P. Hochuli, ETH Zürich (Switzerland)

Plate 4A - Scale bars 20 μ_

1 - 2 *Protoellipsodinium spinocristatum* Davey & Verdier, 1971, (L 153-4)

3 - 4 *Protoellipsodinium spinosum* Davey & Verdier, 1971, (L 153-3)

5 – 6 *Pterodinium cingulatum* (O. Wetzel) Below 1981 (L 153-4)

7 – 8 *Protoellipsodinium* cf. *spinocristatum* Davey & Verdier, 1971, (L 153-4)

9 *Ischyosporites* sp. (L 153-4)

10 *Hamulatisporis* sp. (L 153-4)

11 *Cribroperidinium orthoceras* (Eisenack) Davey, 1969, Operculum (L 153-4)

12 *Plicatella* sp. (L 153-4)

13 *Gleicheniidites* sp. (L 153-3)

14 *Classopollis* sp. (L 153-4)

15-17 *Cicatricosisporites* div. spp. (L 153-4 (15), L 153-3 (16-17))

Plate 4B - Scale bars 20 μ_

1 *Nannoceratopsis spiculata* Stover, 1966 (L 153-4), reworked from late Early - early Middle Jurassic)

2 *Leberidocysta* cf. *chlamydata* (Cookson & Eisenack) Stover & Evitt, 1978 (L 153-3)

3 *Odontochitina operculata* (O. Wetzel) Deflandre & Cookson, 1955 (L 153-4)

4 – 6 *Ellipsodinium rugulatum* Clarke & Verdier, 1967 (L 153-4)

7 *Wrevittia helicoidea* (Eisenack & Cookson) Helenes & Lucas-Clark, 1997 (L 153-4)

8 - 9 *Callaiosphaeridium asymmetricum* (Deflandre & Courteville) Davey & Williams, 1966 (L 153-3)

10 *Triadispora* sp. (L 153-3), reworked from Middle – Late Triassic

11 *Ovalipollis* sp. (L 153-3), reworked from Middle – Late Triassic

12 Striate bisaccate pollen (L 153-3), reworked from Triassic

PLATE 5A - Uppermost Albian-lower middle Cenomanian foraminifers, belonging to an unconformable sequence overlying the Çetmi mélange (northern area)
Determination Pr. A. Arnaud-Vanneau, University of Grenoble (France)

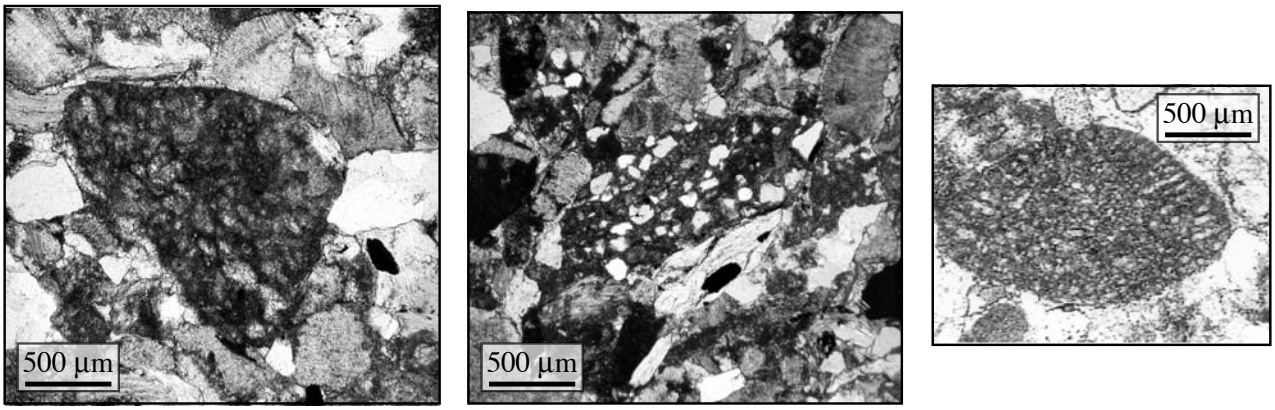

Orbitolina-Mesorbitolina (?)

PLATE 5B - Upper Cretaceous (upper Santonian) foraminifers, from a couche-rouge block of the Abant Complex, Intra-Pontide suture
Determination Pr. M. Caron, University of Fribourg (Switzerland)

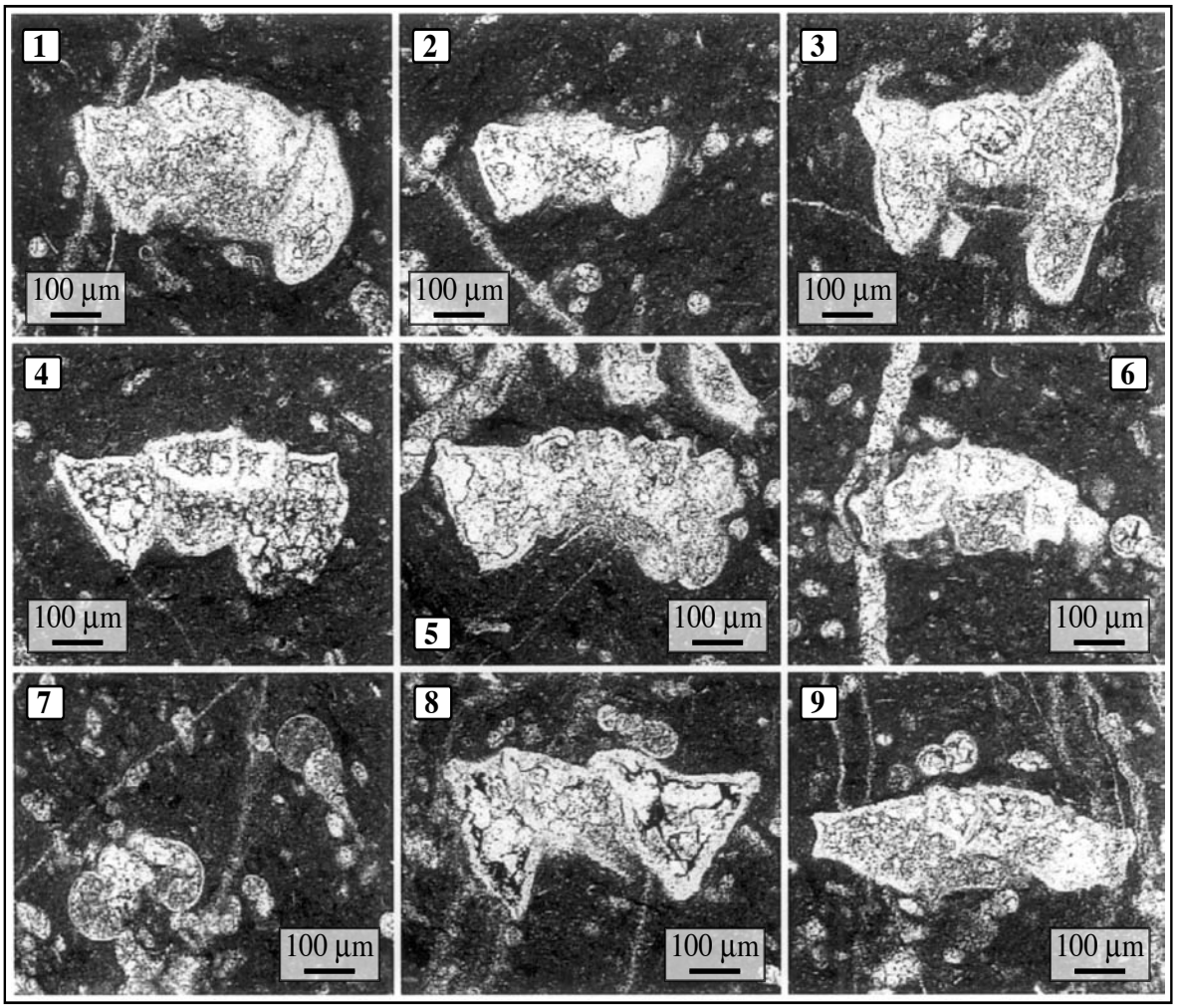

1: *Globotroncanita elevata*; 2: *Dicarinella concavata*; 3: *Dicarinella concavata*; 4: *Dicarinella* aff. *concavata*;
5: *Dicarinella asymetrica*; 6: *Marginotruncana pseudolinneiana;* 7: *Hedbergella* + heterohelix;
8: *Globotruncanita* sp.; 9: *Marginotruncana coronata*

PLATE 6 - Middle-upper Permian foraminifers and algae from the Ezine Group

Determination Dr. C. Jenny, Petit-Lancy (Switzerland)

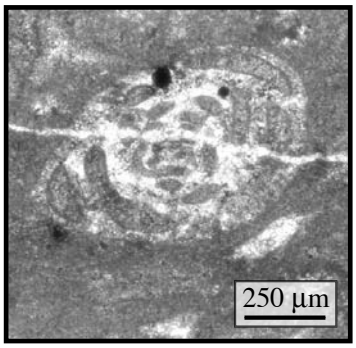

Hemigordius sp. - sample E96

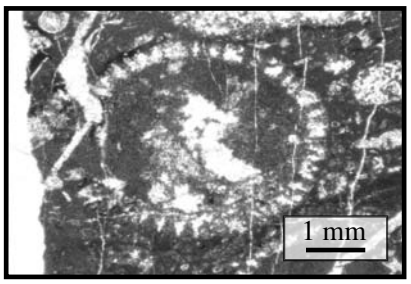

Gyroporella - E96

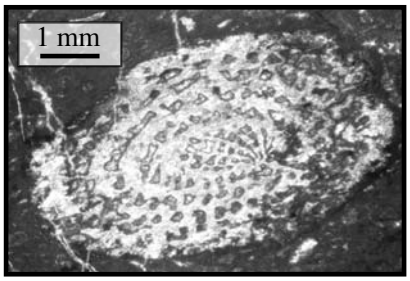

Staffella sp. - E96

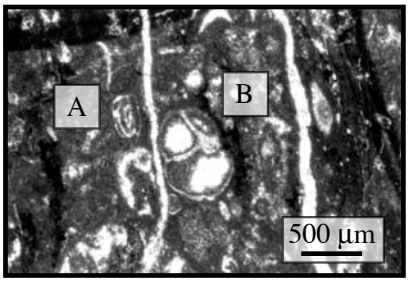

A: *Agathammina* sp.
and B: *Globivalvulina* sp. - E96

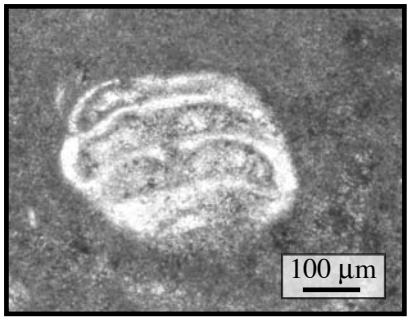

Geinitzina sp. - E96

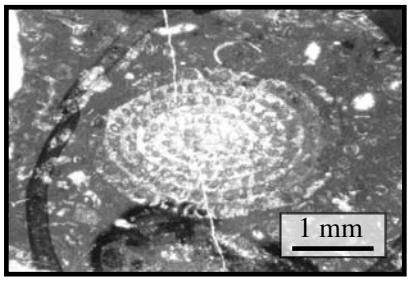

Staffella aff. *sphaerica* (ABICH) - E96

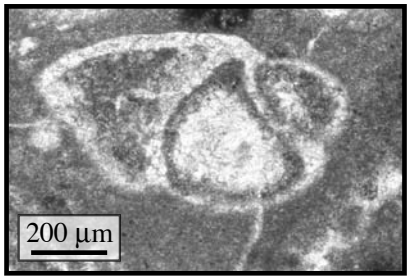

Globivalvulina sp. - E96

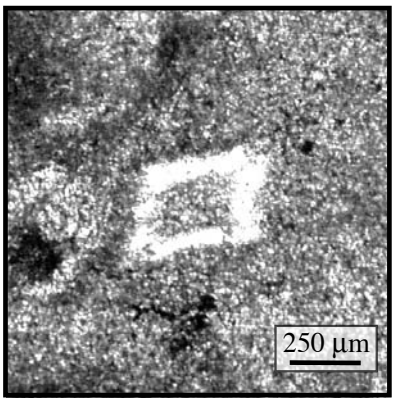

Rectostipulina quadrata
JENNY-DESHUSSES - E95

PLATE 7A - Field pictures of the Çetmi mélange (all pictures from the southern area)

Picture 2.1 - Han Bulog limestone block (Middle Anisian)

Picture 2.2 - Norian-Rhaetian limestone block (bn 19)

Picture 2.3 - Megalodontidae from a Norian-Rhaetian limestone block (bn 9)

Picture 2.4 - Recrystallized Megalodon from a Norian-Rhaetian recrystallized limestone block (bn 12)

Picture 2.5 - Red radiolarite (Late Kimmeridgian-Late Tithonian)

Picture 2.6 - Greywacke-shale matrix

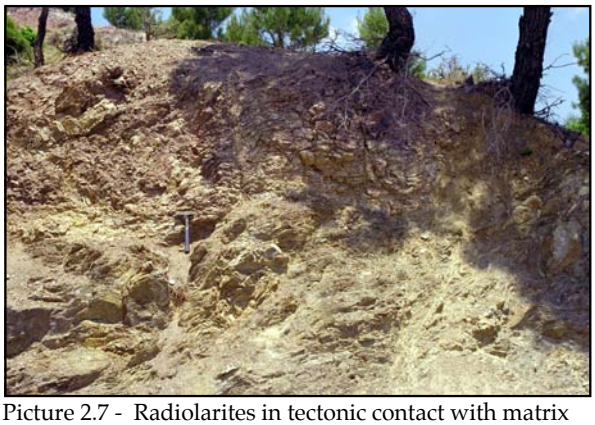

Picture 2.7 - Radiolarites in tectonic contact with matrix

Picture 2.8 - Matrix, detail of a discontinuous greywacke layer mold by silty shales

PLATE 7B - Field pictures of the Ezine area

Picture 3.1 - Stratigraphic contact between Geyikli Fm and Karadağ Fm

Picture 3.2 - First conglomeratic event, middle member of Karadağ Fm

Picture 3.3 - second conglomeratic event, middle member of Karadağ Fm

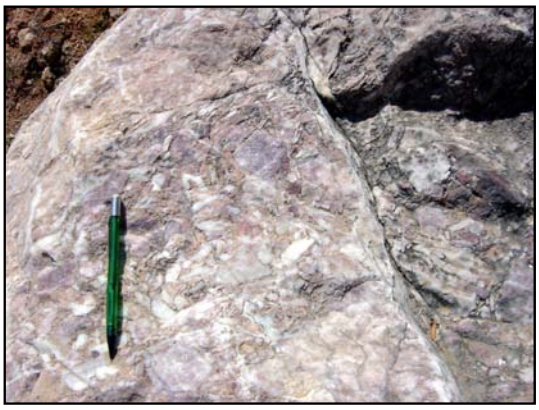

Picture 3.4 - Pink debris-flows, Çamkoÿ Fm

Picture 3.5 - Pink debris-flows, Çamkoÿ Fm

Picture 3.6 - Silty carbonated turbidite, Çamkoÿ Fm

Picture 3.7 - Karstic massive grey limestone, Çamkoÿ Fm

Picture 3.8 - Karstic massive grey limestone, Çamkoÿ Fm

PLATE 7C - Field pictures of the Küçükkuyu Fm, the Şelale Detachment Fault, the Alakeçi Mylonitic Zone, and the Kazdağ Massif

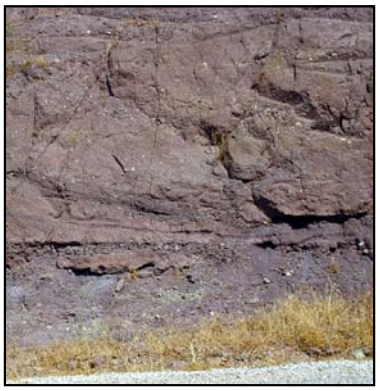

Picture 4.1 - Red volcanogenic conglomerate (lower member of Küçükkuyu Fm)

Picture 4.2 - lacustrine turbidites (intermediate member of Küçükkuyu Fm)

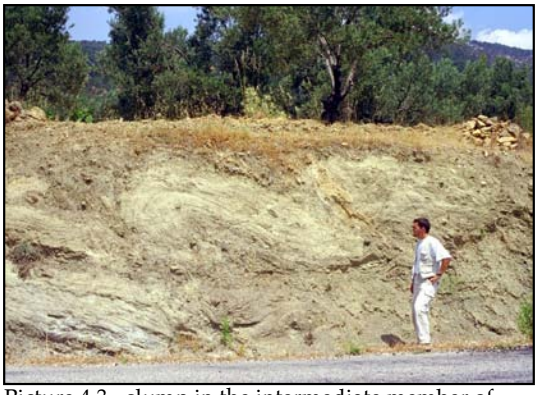

Picture 4.3 - slump in the intermediate member of Küçükkuyu Fm)

Picture 4.4 - Fault plane of the Şelale Detachment Fault

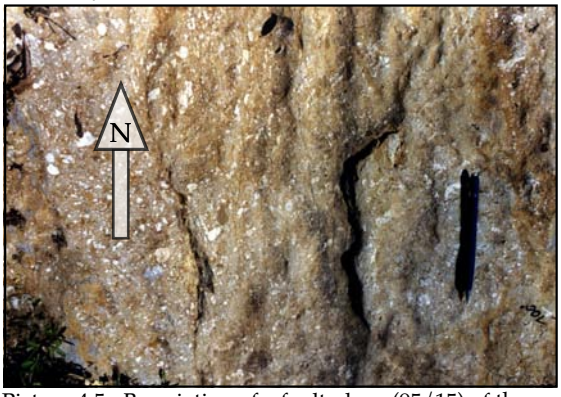

Picture 4.5 - Brecciation of a fault plane (95/15) of the Şelale Detachment Fault

Picture 4.6 - Ductile deformation in the Kazdağ Massif

Picture 4.7 - Alakeçi mylonites

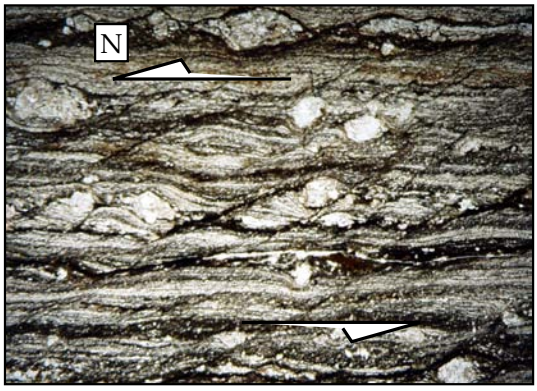

Picture 4.8 - C'-shear-band cleavage in a mylonite

PLATE 8 - Geological map of the Çetmi mélange, northern area

Key

Çetmi mélange

- Limestone (Late Triassic)
- Radiolarite (Late Jur.-Early Cret.)
- Undifferanciated mélange
- Spilite dominated
- Greywacke dominated
- Çamlıca micaschist
- Serpentinite
- Sandstone/shale

- Neogene sedimentary and volcanic rocks
- Granodiorite (Tertiary ?)
- 65/40 Bedding - strike/dip
- 130/30 Foliation - strike/dip

scale: 1/50'000

1 km

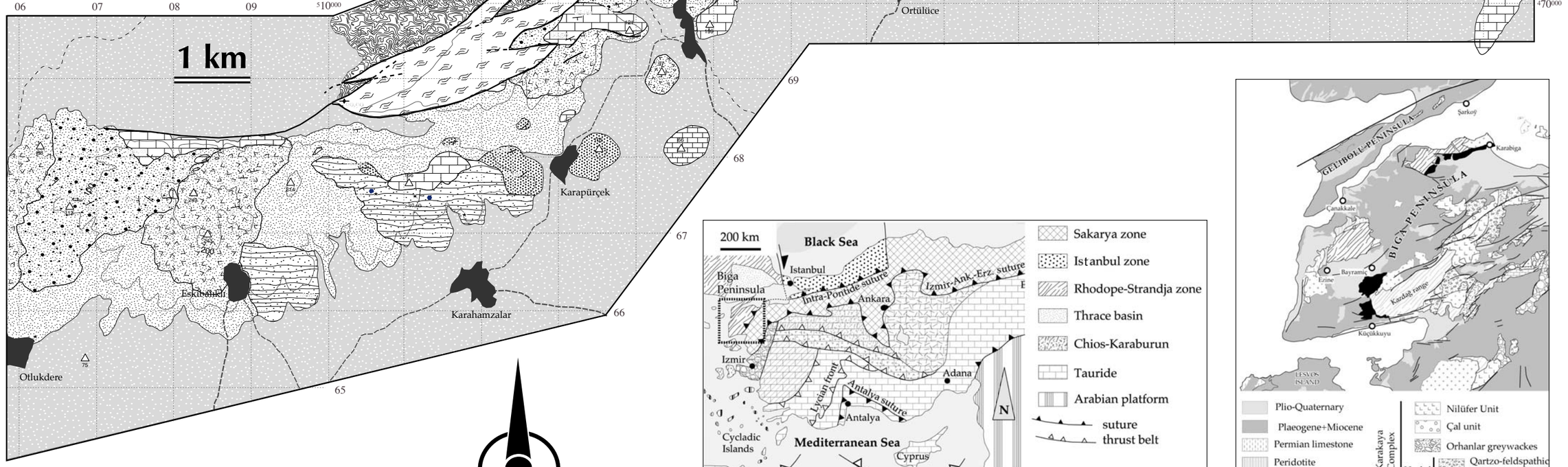

PLATE 9A - Geological map of the Çetmi mélange, southern area

Key

- Quaternary
- Undifferentiated Pliocene sandstone, conglomerate, limestone

Küçükkuyu Group

- Upper member: acidic tuff/tuffite
- Intermediate member (lower Miocene): Sandstone/shale alternations
- Lower member: Red clastics/volcanics

- Kazdağ metamorphic massif, amphibolite, gneiss, marble, PT conditions 5 kb / 640 °C, metamorphism in the latest Oligocene (Okay and Satır, 2000)
- Alakeçi Mylonite Zone protolith: Kasdağ massif and Çetmi mélange
- Evciler granodiorite 24 Ma (Okay and Satır, 2000)
- 65/40 Bedding - strike/dip
- 130/30 Foliation - strike/dip - azimut lineation
- Tectonic contact
- Detachment fault
- Fault

Çetmi mélange

- Undifferanciated mélange, mostly spilitic rocks, greywacke-shale association (matrix), minor smaller blocks (limestone, radiolarite, ...)
- Greywacke dominated mélange
- Spilite dominated mélange
- Limestone blocks, recrystallized or not (Norian-Rhaetian)
- ★ Red radiolarite blocks (Late Jurassic-Early Cretaceous)
- Gelinmezarı Sandstone sandstone/shale alternance (post Late Jurassic)
- Serpentinite
- Listvenite
- Elliayak eclogite, garnet-micaschist, eclogite PT conditions >10 kb / 480 °C Peak PT: before 100 Ma, (Okay and Satır, 2000 Lips, 1998)

scale: 1/50'000

- Scar
- Normal fault

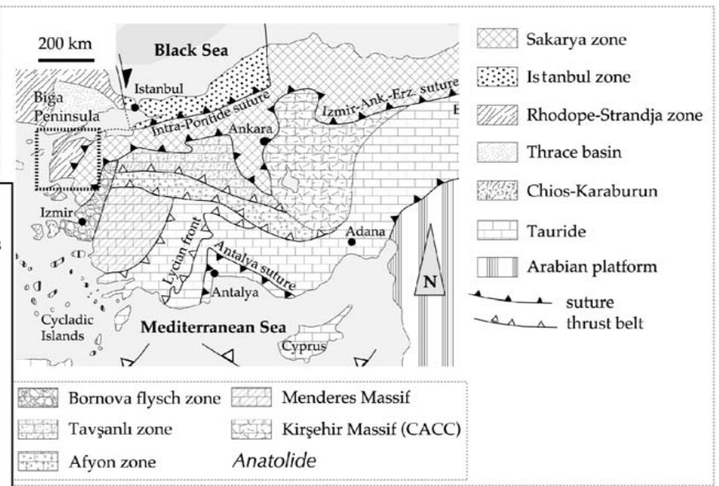

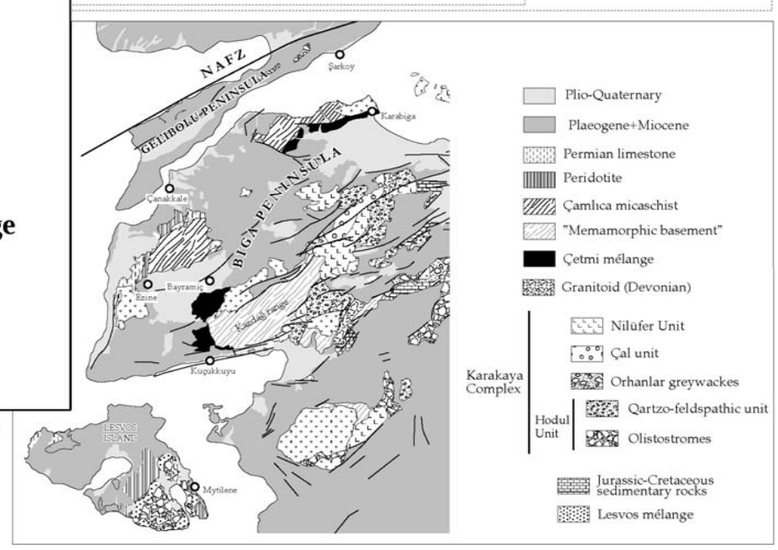

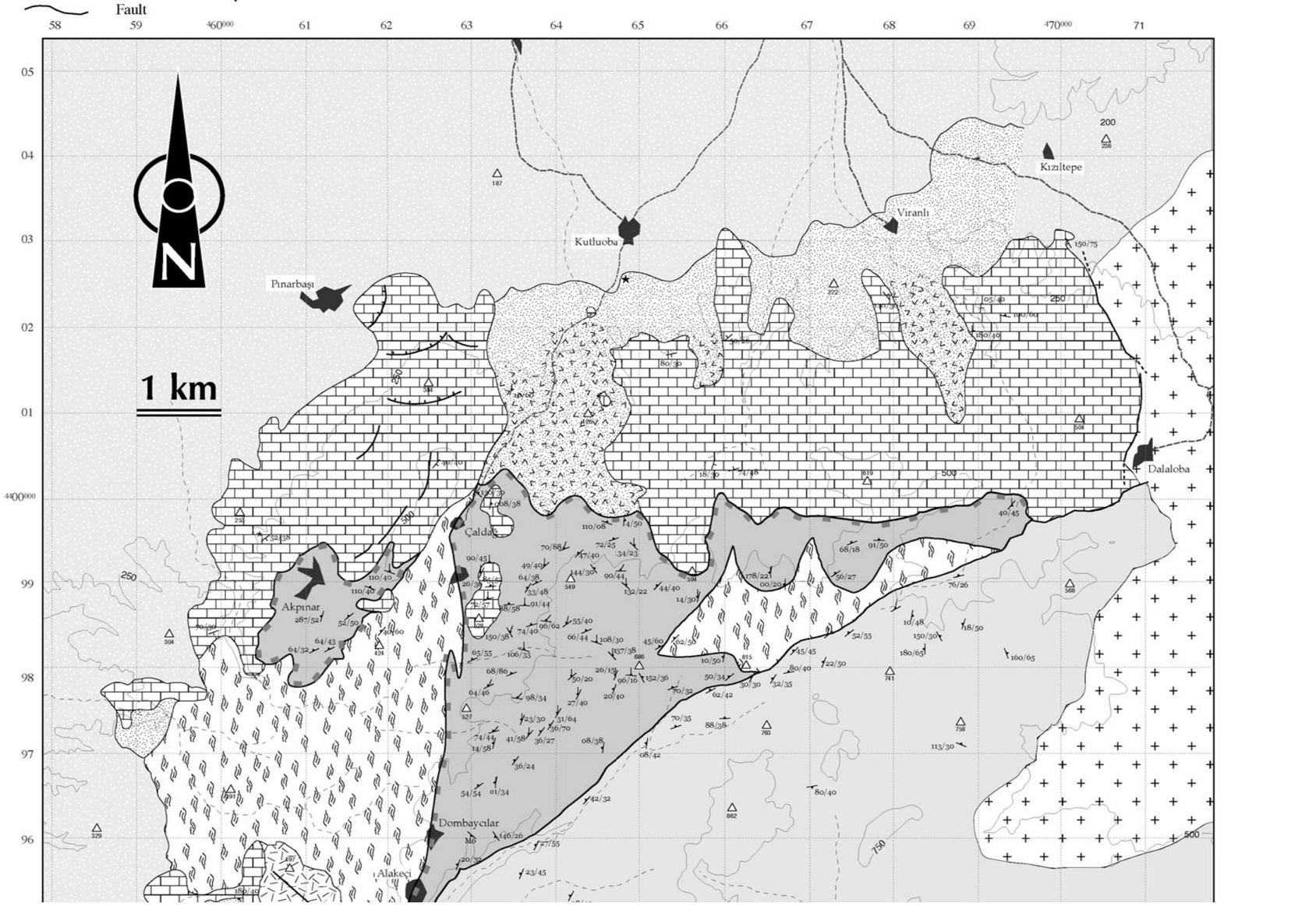

PLATE 9B - Geological map of the Çetmi mélange, southern area (followed)

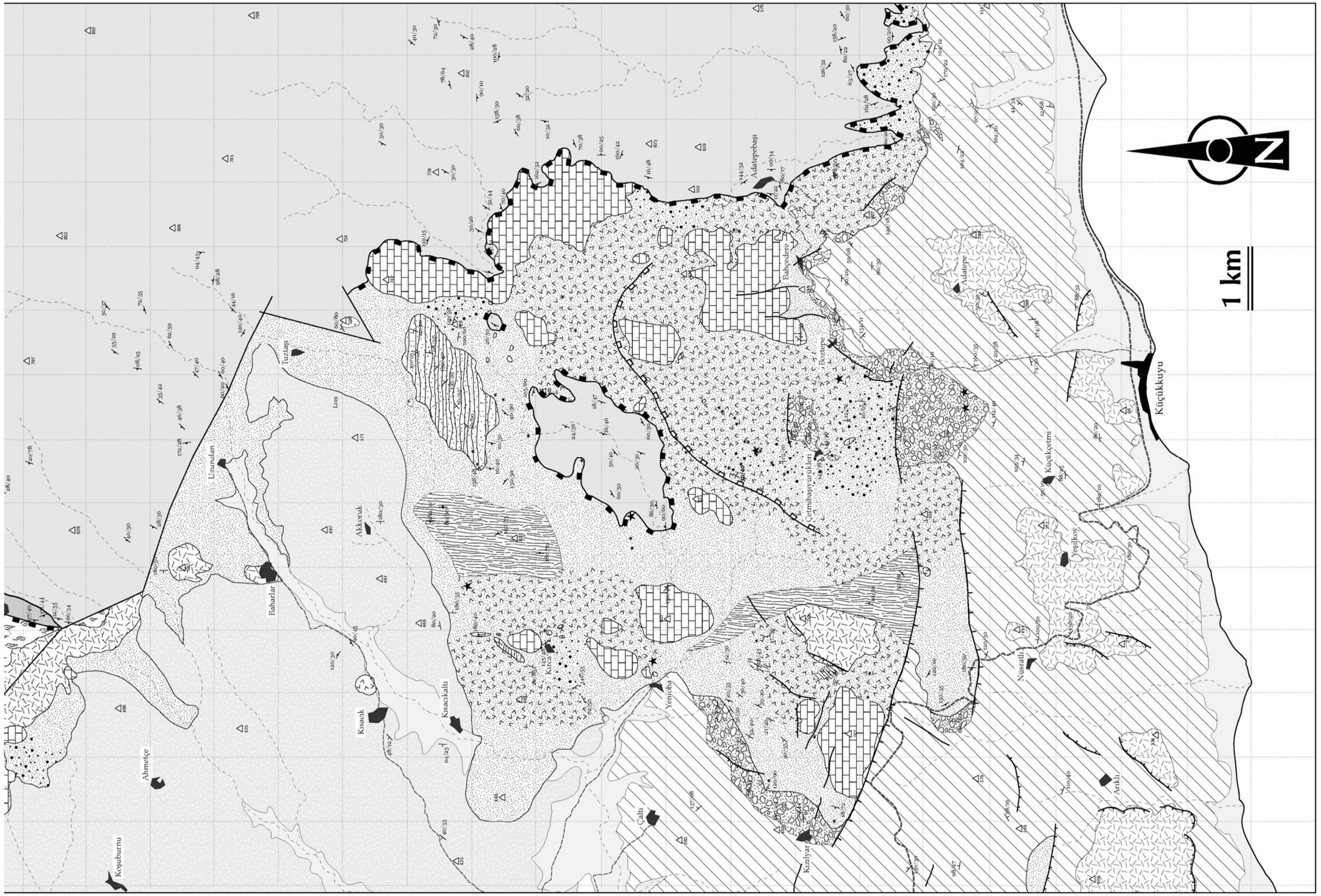

PLATE 10 - Geological map of the Ezine area

Key

- Undifferenciated Neogene
- Quaternary
- Kestanbol granodiorite
- Çamlıca micaschist
- silicified — Serpentinite
- prasinite amphibolite — Metamorphic sole
- Çamkoÿ Fm undifferenciated
- Massive limestone and "pink breccia"

Çamkoÿ Fm

Karadağ Fm

- upper member
- middle member
- lower member

Ezine Group

Geyikli Fm

- upper member
- shale / limestone olistolith — intermediate member 2
- intermediate member 1
- lower member

- 21/30 — Bedding - strike/dip
- 04/75 — Foliation - strike/dip
- Fault
- Thrust contact

scale: 1/50'000

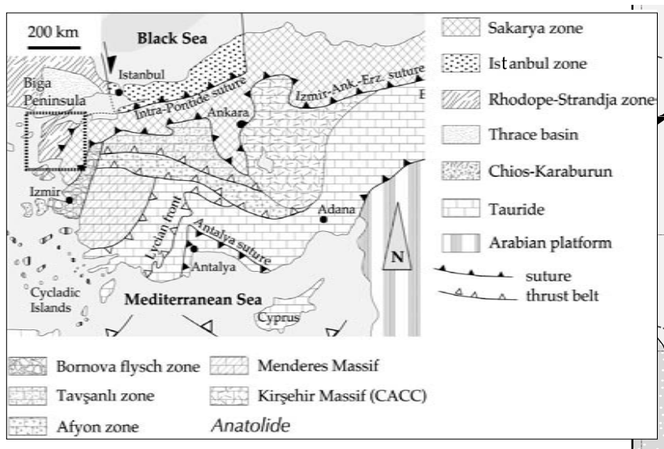

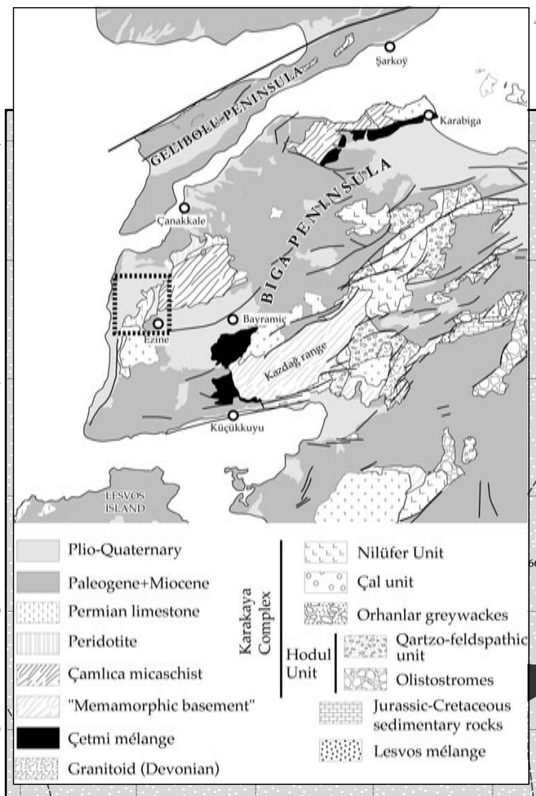

Taştepe
Pınarbaşı
Derbentbaşı
Bozalan
Ahlatoba
Çamköy
Mecidiye
Geyikli
Gökçebayır
Ezine

1 km

N

14 13 12 11 10 09 08 07 06 4405000 04

31 32 33 34 35 4436000 37 38 39 40 41 42 43

UTM coordinates